

2m4

CR-133484
134 184

C-5A/ORBITER WIND TUNNEL TESTING AND ANALYSIS

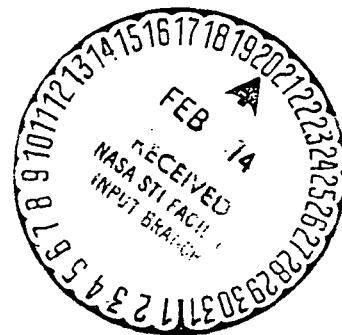
- PIGGYBACK FERRY -

(NASA-CR-~~133484~~) C-5A/ORBITER WIND TUNNEL TESTING AND ANALYSIS: PIGGYBACK FERRY
 Final Report (Lockheed-Georgia Co.)
 239 p HC \$14.00 CSCL 01C UNCLAS
 243 G3/02 28801

Final Report
 LG73ER0193
 December 1973

by

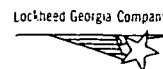
K. H. Tomlin
 W. T. Blackerby
 A. C. Hughes
 E. G. Husband
 J. H. Paterson



Prepared under Contract NAS9-13702
 for the
 NATIONAL AERONAUTICS AND SPACE ADMINISTRATION
 JOHNSON SPACECRAFT CENTER
 Houston, Texas

by the

LOCKHEED-GEORGIA COMPANY
 A Division of Lockheed Aircraft Corporation
 Marietta, Georgia 30063



C-5A/ORBITER WIND TUNNEL TESTING AND ANALYSIS

— PIGGYBACK FERRY —

Final Report
LG73ER0193
December 1973

by

K. H. Tomlin
W. T. Blackerby
A. C. Hughes
E. G. Husband
J. H. Paterson

Prepared under Contract NAS9-13702
for the
NATIONAL AERONAUTICS AND SPACE ADMINISTRATION
JOHNSON SPACECRAFT CENTER
Houston, Texas

by the

LOCKHEED-GEORGIA COMPANY
A Division of Lockheed Aircraft Corporation
Marietta, Georgia 30063



CONTENTS

<u>Section</u>	<u>Title</u>	<u>Page</u>
	LIST OF FIGURES	iv
	SUMMARY	vii
1.0	INTRODUCTION	1
2.0	ANALYSIS OF EXPERIMENTAL RESULTS	2
2.1	Stability and Control	2
2.1.1	Effects of Orbiter, Cruise Configuration	2
2.1.2	Effects of Orbiter Position, Cruise Configuration	3
2.1.3	Effect of Orbiter Incidence, Cruise Configuration	6
2.1.4	Effect of Afterbody Fairing, Cruise Configuration	6
2.1.5	Effect of Orbiter, Landing Configuration	7
2.1.6	Vertical Tail Development	8
2.1.7	Effect of Orbiter on Trim	9
2.2	Drag Characteristics	9
2.2.1	Effect of Orbiter	9
2.2.2	Effect of Orbiter Position	10
2.2.3	Effect of Afterbody Fairing	10
2.2.4	Effect of Orbiter Incidence	10
3.0	ASSESSMENT OF FULL SCALE FLIGHT FEASIBILITY	11
3.1	Stability and Control	11
3.1.1	Comparison of Wind Tunnel and Full Scale Directional Stability	11
3.1.2	Predicted Full Scale Directional Stability	11
3.2	Flying Qualities	12

CONTENTS (Continued)

<u>Section</u>	<u>Title</u>	<u>Page</u>
3.3	Performance	14
3.3.1	Full Scale Drag Characteristics	14
3.3.2	Airfield Performance	14
3.3.3	Climb and Cruise Performance	15
3.3.4	Orbiter Ferry Capability	16
3.4	Flight Restrictions	16
4.0	CONCLUSIONS AND RECOMMENDATIONS	18
Appendix A	WIND TUNNEL TEST DESCRIPTION AND PLOTTED DATA	A-1

LIST OF FIGURES

<u>Figure</u>	<u>Title</u>	<u>Page</u>
1	Effect of Orbiter on Longitudinal Stability - Cruise Configuration	20
2	Effect of Orbiter on Longitudinal Stability - Cruise Configuration, $C_L^{-\alpha}$, $C_L - C_M$	21
3	Effect of Orbiter on Directional Stability - Cruise Configuration	22
4	Effect of Orbiter on Lateral Stability - Cruise Configuration	23
5	Effect of Orbiter on Side Force - Cruise Configuration	24
6	Effect of Orbiter Position on Longitudinal Stability - Cruise Configuration, $C_M^{-\alpha}$	25
7	Effect of Orbiter Position on Longitudinal Stability - Cruise Configuration, $C_L^{-\alpha}$, $C_L - C_M$	26
8	Effect of Orbiter Position on Directional Stability - Cruise Configuration	27
9	Effect of Orbiter Position on Lateral Stability - Cruise Configuration	28
10	Effect of Orbiter Position on Sideforce - Cruise Configuration	29
11	Effect of Orbiter Incidence on Longitudinal Stability - Cruise Configuration, $C_M^{-\alpha}$	30
12	Effect of Orbiter Incidence on Longitudinal Stability - Cruise Configuration, $C_L^{-\alpha}$, $C_L - C_M$	31
13	Effect of Orbiter Incidence on Directional Stability - Cruise Configuration	32
14	Effect of Orbiter Incidence on Lateral Stability - Cruise Configuration	33
15	Effect of Orbiter Incidence on Sideforce - Cruise Configuration	34
16	Effect of Afterbody Fairing on Longitudinal Stability - Cruise Configuration	35
17	Effect of Afterbody Fairing on Directional Stability - Cruise Configuration	36
18	Effect of Orbiter on Longitudinal Stability - Landing Configuration, $C_M^{-\alpha}$	37

LIST OF FIGURES (Continued)

<u>Figure</u>	<u>Title</u>	<u>Page</u>
19	Effect of Orbiter on Longitudinal Stability - Landing Configuration, $C_L-\alpha$, C_L-C_M	38
20	Effect of Orbiter on Directional Stability - Landing Configuration	39
21	Effect of Orbiter on Lateral Stability - Landing Configuration	40
22	Vertical Tail Development - Cruise Configuration, $C_N-\beta$	41
23	Vertical Tail Development - Cruise Configuration, $C_Y-\beta$	42
24	Vertical Tail Development - Landing Configuration, $C_N-\beta$	43
25	Vertical Tail Development - Landing Configuration, $C_Y-\beta$	44
26	Vertical Tail Development - Landing Configuration, Orbiter Off, $C_N-\beta$	45
27	Vertical Tail Development - Landing Configuration, Orbiter Off, $C_Y-\beta$	46
28	Effects of Orbiter on Longitudinal Trim	47
29	Rudder Effectiveness, $\delta_R = 10^\circ$	48
30	Effect of Orbiter on Drag - Cruise Configuration	49
31	Effect of Orbiter Position on Drag - Cruise Configuration	50
32	Effect of Afterbody Fairing Shape on Drag - Cruise Configuration	51
33	Effect of Orbiter Incidence on Drag - Cruise Configuration	52
34	Comparison of Wind Tunnel and Full Scale Directional Stability - Cruise Configuration, Orbiter Off	53
35	Comparison of Wind Tunnel and Full Scale Directional Stability - Landing Configuration, Orbiter Off	54
36	Predicted Full Scale Directional Stability - Cruise Configuration	55
37	Predicted Full Scale Directional Stability - Landing Configuration	56
38	C-5A/Orbiter Piggyback Flight Vehicle Lateral-Directional Data	57
39	Lateral-Directional Response Mode Data	58
40	C-5A Stability Augmentation and Autopilot Systems Approximations	59
41	Flight Vehicle Lateral Response Comparison for a 30 KTAS Side-Gust Disturbance (SAS on)	60
42	Flight Vehicle Response Comparison for a Control Wheel Input of 10.0 Degrees (SAS on)	61

LIST OF FIGURES (Continued)

<u>Figure</u>	<u>Title</u>	<u>Page</u>
43	Flight Vehicle Lateral Response Comparison for a 30 KTAS Side-Gust Disturbance (SAS and Autopilot on)	62
44	Comparison of Estimated and Wind Tunnel Test Drag Polars - Cruise Configuration	63
45	Comparison of L/D for the C-5 and C-5/Orbiter Piggyback	64
46	Comparison of Estimated and Wind Tunnel Test Drag Polars - Landing Configuration	65
47	Takeoff Distances	66
48	Landing Distances	67
49	One Engine Inoperative Climb Gradient	68
50	Cruise Ceilings	69
51	Altitude Speed Capability	70
52	Ferry Performance Summary	71
53	Flight Restrictions	72
54	Flight Restrictions Compared with Super Guppy	73



SUMMARY

Wind tunnel testing and analytical studies of the feasibility of ferrying the NASA Shuttle Orbiter on the C-5A in a piggyback mode have been accomplished by the Lockheed-Georgia Company in response to NASA contract NAS9-13702. The study was managed by J. H. Paterson of the Flight Sciences Division. Testing was conducted in the Lockheed-California Company 8 x 12 foot low speed wind tunnel using an existing Air Force 0.0399 scale C-5A model in conjunction with a NASA 0.0405 scale Orbiter model. Six component force and moment data were measured over a range of pitch and yaw angles to determine lift and drag characteristics, lateral/directional stability characteristics and longitudinal and directional control powers.

Appendix A contains a description of the wind tunnel test program with a run schedule and the complete plotted data for all the test runs. Initial emphasis was given to determining the effects of the Orbiter above the C-5A and the optimum location for minimum interference on C-5A characteristics. A comprehensive series of cruise configurations were tested including a range of Orbiter longitudinal and vertical locations, incidences, and afterbody fairings. Subsequently, a series of configurations were devised during the test program to determine means of recovering directional stability degradation due to Orbiter interference.

Extensions to the present C-5 vertical stabilizer were designed as were twin fins to be located at the tips of the horizontal stabilizer. Analytical studies subsequent to the test and based on test results indicate that these exterior changes should not be necessary as automatic flight controls provide satisfactory flying qualities.

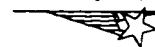
Performance studies of the C-5A/Orbiter Piggyback show that the drag penalty of the Orbiter on the C-5A does not preclude non-stop, unrefueled ferry missions up to 2500 nautical miles. Some flight restrictions for the Piggyback are unavoidable; however these are not considered unreasonable for the special nature of the mission. In short, ferrying the Shuttle Orbiter in a Piggyback mode on top of a C-5A appears feasible with minimum modifications to the basic C-5A.



1.0 INTRODUCTION

Recent interest by NASA and Rockwell International in alternatives to the present Orbiter Airbreathing Propulsion System for ferry and flight test of the Space Shuttle Orbiter has led to a series of proposals, analytical studies and wind tunnel tests to determine the feasibility of alternate systems. The Lockheed-Georgia Company has actively participated in these studies because of the suitability of Lockheed's C-5A as a carrier system for the Orbiter and in an attempt to apply Lockheed's "big airplane" talents and knowledge to this program.

In response to NASA RFP 9-BC451-M6-4-4P, regarding the feasibility of ferrying the Orbiter piggyback on top of a C-5A, Lockheed-Georgia submitted a proposal and subsequently was awarded NASA contract NAS9-13702 for a low speed wind tunnel test and analytical study of a C-5A/Orbiter Piggyback configuration. This report constitutes the final report for this contract work. Analysis of the wind tunnel test results and the feasibility of the C-5A Piggyback concept are contained in the main part of the report. Appendix A contains the final plotted results from the wind tunnel test.



2.0 ANALYSIS OF EXPERIMENTAL RESULTS

2.1 STABILITY AND CONTROL

2.1.1 Effects of Orbiter, Cruise Configuration

The small effect of the Orbiter on the C-5 longitudinal stability is demonstrated in Figure 1. These data are for the forward, low position of the Orbiter where maximum interaction of the two wings should occur. A negative shift in C_M of 0.04 occurs at all angles of attack. Minor modifications of the medium angle of attack pitching moment, in the destabilizing sense, is apparent for the Orbiter configuration without a fairing due to wake impingement on the horizontal tail. At high angles of attack, beyond stall, the typical C-5 initial pitch up followed by a strong nose down pitch is modified by both Orbiter configurations in such a manner that the net result should be almost imperceptible to the pilot.

An increase in lift curve slope due to the presence of the Orbiter, as well as a small increase in C_{LMAX} , is demonstrated in Figure 2. A small further improvement in C_{LMAX} due to the aft fairing is shown. The C_M-C_L curves demonstrate the negative C_{M0} shift and negligible change in neutral point due to the Orbiter. The C_{M0} shift is the equivalent of less than one degree of stabilizer angle.

The effect of the higher vertical center of gravity due to the Orbiter, approximately 60 inches, will result in a slight decrease in speed stability that will be most apparent in the landing approach mode. It is anticipated that this effect will require little more than pilot familiarization with the new pitch response to engine power since the current aircraft already has a vertical c.g. range of 51 inches.

The major effect of the Orbiter on the C-5 aerodynamic data is the reduction of weathercock stability as reflected by $C_{N\beta}$. Figure 3 demonstrates this effect for the most critical configuration forward and low with a negative shuttle incidence. This loss of directional stability is primarily a result of the Orbiter's influence on the air flow at the C-5 vertical tail. There is also a secondary destabilizing effect with



this Orbiter location due to Orbiter side area that is ahead of the C-5 center of gravity. The prime effect, however, occurs because of the flow bending, caused by the Orbiter body. As a result, the C-5 vertical tail does not experience the full yaw angle seen by the forward fuselage. This reduction in yaw angle, as seen by the fin is approximately 30% of the nominal value. As shown in Figure 3, the afterbody fairing resulted in an improvement in stability at high sideslip angles but delayed the turnover point.

Lateral stability, represented by dihedral effect, is little affected by the Orbiter as shown in Figure 4. A small reduction in $C_{l\beta}$ occurs through 15° of sideslip accompanied by a linearization of the higher sideslip angle data due to the Orbiter wing configuration effect on the C-5 wing. The aft fairing causes further increases in $C_{l\beta}$ at high sideslip angles due to the fin effectiveness.

Figure 5 shows that a large increase in $C_{Y\beta}$ occurs due to the presence of the Orbiter as a result of the side area increase, as would be expected. The aft fairing causes a small increase in sideforce at sideslip angles greater than 15° and no effect at lesser angles. It is somewhat surprising that more sideforce does not result from the added side area of the fairing. Apparently this area is not effective in sideforce due to the very thick boundary layer or there is a compensating flow change at the fin, or both.

2.1.2 Effect of Orbiter Position, Cruise Configuration

The effect on longitudinal stability of Orbiter fore and aft and vertical position relative to the C-5 is demonstrated in Figure 6. This comparison is made with the Gelac fairing No. 1 on the Orbiter and with the Orbiter at an incidence of 0.5 degrees. The destabilizing effect of the Orbiter in the forward high position is due to the combined effect of the Orbiter lifting moment and the interference with the flow at the C-5 horizontal stabilizer. The aft low position represents a significant improvement; showing a small negative ΔC_M shift that remains constant until the stall is reached. The pitch down tendency beyond stall of the basic C-5 has been reduced slightly. A small reduction in stability occurs in the aft high position with more pitch up at the

still than that for the low position due to the increased stabilizer interference: however, the stability change relative to the basic C-5, below stall is negligible.

Figure 7 shows that Orbiter position has little effect on the lift curve slope and only a small effect on C_{LMAX} : the highest C_{LMAX} occurs with the Orbiter in the aft high position. From a longitudinal stability point of view it is apparent that the aft low position would be the best with the aft high position a second choice.

The effect of Orbiter position on directional stability is very pronounced as shown in Figure 8. The major change that occurs with aft movement is due to the tail-off stability increase as the body side area is moved aft of the reference c.g. A small stabilizing change in fin effectiveness occurs with aft movement of the Orbiter. Again these data demonstrate the ability of the Orbiter body to reduce the local flow angle at the fin relative to the free stream angle through ± 15 degrees. The sensitivity of the C-5 weathercock stability to the presence of the Orbiter is largely due to the equal magnitudes of tail-off instability and tail-on stability. Thus, a 50 percent loss of fin effectiveness will cause a 100 percent loss of stability. The aft, high position of the Orbiter has the best directional stability characteristic but is still slightly unstable through small sideslip angles.

A significant change in dihedral effect occurs as a function of Orbiter position as shown in Figure 9. The major effect is due to Orbiter height above the C-5, showing larger $C_{\dot{\gamma}\beta}$ for increased height. Fore and aft position does not appear to have much influence, showing a small increase in $C_{\dot{\gamma}\beta}$ for aft movement of the Orbiter. It would appear that the major effect on $C_{\dot{\gamma}\beta}$ is probably due to the freeing effect of moving the wings apart thus allowing full development of the normal lift change due to sideslip on both wings.

Orbiter position has a negligible effect on the net sideforce due to sideslip as shown in Figure 10. A large increase in $C_{Y\beta}$ is, of course, present due to the side area of the Orbiter configuration.

Page intentionally left blank

2.1.3 Effect of Orbiter Incidence, Cruise Configuration

The effect of Orbiter incidence on the C-5 pitching moment is shown in Figure 11 for the aft, high position of the Orbiter with the aft fairing (Test Fairing No. 3). Increasing the Orbiter incidence relative to the C-5 reduced the pitching moment shift through nominal angles of attack, and at high angles of attack, increased the pitch up with a slightly less stable pitch out.

Small shifts in α_{OL} with no change in lift curve slope due to Orbiter incidence are shown in Figure 12. Increasing Orbiter incidence results in small increases in net C_{LMAX} . The $C_M - C_L$ data reflect the expected shift in C_{MO} with essentially no change in neutral point.

Insignificant changes in directional stability resulted from Orbiter incidence variation as shown in Figure 13. The basic configuration for the Orbiter was the aft, high position with the No. 3 fairing.

Only minor changes in $C_{Y\beta}$ occur due to Orbiter incidence as shown in Figure 14. A small increase in $C_{Y\beta}$ at the higher sideslip angles, as Orbiter incidence increases, is apparent.

No change in $C_{Y\beta}$ due to Orbiter incidence is apparent, as shown in Figure 15.

2.1.4 Effect of After-body Fairing, Cruise Configuration

The effect of various after-body fairing changes on pitching moment is shown in Figure 16. These fairing modifications were aimed at improving directional stability characteristics and have little direct influence on longitudinal stability other than through the drag changes.

$C_{N\beta}$ is unstable through small angles for C-5 Orbiter combinations with both the Gelac No. 1 fairing and the Rockwell fairing. Attempts to reshape the aft fairing to improve the flow field at the vertical tail are shown in Figure 17. Small improvements

were obtained with fairing No. 2 and 3 but are not sufficient in themselves to cure the problem.

The effects of after-body shape on $C_{u\beta}$ and $C_{Y\beta}$ are negligible, demonstrating the lack of load producing area in the aft body region.

2.1.5 Effect of Orbiter, Landing Configuration

The effect of the Orbiter on the longitudinal characteristics of the C-5A in the landing mode is similar to that of the clean configuration. A larger negative pitching moment shift due to the Orbiter is apparent - Figure 18. (The Orbiter is in high aft position.) A slight increase in stability is also noted.

Little or no change in lift curve slope occurs, as shown in Figure 19. A small neutral point shift in the stable sense is predictable from the $C_M - C_L$ curves of this figure. These data were obtained without the uprigged spoilers normally used for the C-5 landing configuration, however, little or no influence is expected.

In the landing configuration, the airflow at the C-5 vertical tail is not as restricted as in the clean configuration due to the large downflow, away from the fin, caused by the flaps. As shown in Figure 20, the net result is a more stable $C_{N\beta}$ level than for the clean airplane even though a small "flat spot" still occurs at small sideslip angles. The shape of the basic C-5 curve is predicated by fin stall at large sideslip angles. Since the air flow at the fin is restricted by the Orbiter in the Piggyback mode, the fin never experiences stall in the tested sideslip range, hence the more linear yawing moment at large angles.

The major effect of the Orbiter on $C_{Y\beta}$ is to delay the fin stall at high sideslip angles so that an increase in rolling moment occurs. This effect is shown in Figure 21. Little or no effect on $C_{L\beta}$ in the small sideslip angle range is noted.

The effect of the Orbiter on $C_{Y\beta}$ parallels that obtained in the clean configuration and the levels at each sideslip angle are almost identical.

2.1.6 Vertical Tail Development

The effects of the addition of a central fin to the C-5 horizontal tail bullet and the addition of tip fins to the horizontal tail are demonstrated in Figure 22. The Orbiter position is aft and high with the #3 aft fairing. This position results in a negligible change in tail-off $C_{N\beta}$ except at the higher sideslip angles, since the Orbiter fin-body area is well aft of the c.g.

The addition of a center fin above the C-5 tail produces sufficient stability beyond 5° of sideslip but is influenced by the Orbiter body effect at smaller angles. The addition of twin fins at the horizontal stabilizer tips successfully achieves the same stability level as the basic C-5 throughout the small angle range, and a much increased level at the higher sideslip angles.

The additional sideforce developed in sideslip by tip and center fins required for directional stability is shown in Figure 23. These large values are not desirable because of gust response and turn coordination, especially in light of the already large increase in sideforce due to the Orbiter.

As shown earlier, the directional stability in the landing configuration in the presence of the Orbiter, is better than that for the clean configuration. As a result the fins, as sized, represent an excess capability as shown in Figure 24.

The sideforce due to sideslip is approximately the same as for the clean configuration shown in Figure 25.

The effectiveness of the center and tip fins, without the Orbiter, are shown in Figure 26. The center fin retains its effectiveness at high sideslip angles to a higher degree than the tip fins. They are equally effective at small angles.

Similar data for the sideforce characteristics are shown in Figure 27.

2.1.7 Effect of Orbiter on Longitudinal Trim

The Orbiter, in the aft high position, has a negligible influence on the dynamic pressure of the airflow at the C-5 horizontal stabilizer and only a minor influence on the downwash. The net effect is shown in Figure 28 for the cruise configuration. It may be noted that the "Orbiter on" data of this figure also have the vertical center fin whereas the "Orbiter-off" data do not. Although not shown here, the data in the appendix demonstrates that there is no effect in pitch due to the center fin, thus the comparison is valid.

Data are not available for the landing configuration. The influence of the Orbiter on trim effectiveness is anticipated to be even less than that for the cruise configuration because of the downward depression of the wing wake, away from the tail, caused by the flaps.

A small loss in dynamic pressure at the fin occurs due to the presence of the Orbiter and a reduction of local yaw angle relative to the free stream yaw in steady sideslip, as previously demonstrated. The net effect on rudder power for trim is shown in Figure 29. The Orbiter on data also include the effects of a center fin extension as discussed in 2.1.6.

The incremental effectiveness of the rudder in yaw is not anticipated to be affected by flap deflection.

2.2 DRAG CHARACTERISTICS

2.2.1 Effect of Orbiter

Figure 30 illustrates the magnitude of the effect of the Orbiter on C-5 drag. At a cruise C_L of 0.5, the drag of the Piggyback configuration is 70% greater than the basic C-5 level. By enclosing the bluff aft end of the Orbiter, the drag level of the



Piggyback is reduced to a level about 40% above that of the C-5 at $C_L = 0.5$. Undoubtedly, the skin friction drag of this very long fairing offsets some of the potential reduction in Orbiter base drag.

2.2.2 Effect of Orbiter Position

The effect on Piggyback cruise configuration drag of Orbiter location is shown by Figure 31. In general, the drag is seen to be insensitive to position for the locations tested, except for the aft - low position, which carries slightly lower drag up to a C_L of 0.6. The drag of the aft high position is about the same as that of the forward positions at all C_L 's. These results indicate that interference drag is a very small contributor to total drag.

2.2.3 Effect of Afterbody Fairing

Figure 32 compares drag for the various afterbodies tested. Not a great deal of significance can be attached to these results. As expected, the increased afterbody fineness ratio of Gelac fairing #1 improved the flow relative to a blunter Rockwell fairing, however, the increased skin friction drag due to additional wetted area almost negates this as the decrease in cruise drag is only about 2 percent.

2.2.4 Effect of Orbiter Incidence

Figure compares drag results for the two Orbiter incidence angles and substantiates no change in Piggyback drag due to incidence over the range from -1.5° to 0.5° .

3.0 ASSESSMENT OF FULL SCALE FLIGHT FEASIBILITY

3.1 STABILITY AND CONTROL

3.1.1 Comparison of Wind Tunnel and Full Scale Directional Stability

The wind tunnel data, obtained from this test, are compared with the published, full-scale, levels for the C-5A to establish the base for the incremental data obtained in the presence of the Orbiter. The full-scale data are based upon the correlation of flight test data, obtained during the C-5A development program and the design wind tunnel data.

The cruise data for yaw due to sideslip are shown in Figure 34. The major change from the wind tunnel data is an extension of the fin sideforce capability to a higher yaw angle and a slightly more effective fin. There is also a more linear continuation of the tail-off yawing moment through high sideslip angles.

The landing flap data, shown in Figure 35, demonstrate further differences from the wind tunnel data. These differences are largely due to a change in the aft body interference with flaps down, that resulted in a less stable airplane than predicted by the wind tunnel. As may be noted, the net fin effectiveness, full scale, is considerably less than the wind tunnel level. These data are for landing flaps with the gear up. When the gear is down a higher $C_{N_{\beta}}$ is realized due to the effect of the gear on the afterbody interference.

3.1.2 Predicted Full-Scale Directional Stability

Using incremental tail-off and tail-on data for the effect of the Orbiter, the full-scale predicted levels of weathercock stability are shown in Figure 36 compared with the basic C-5 in the cruise configuration. As may be noted, the Orbiter/C-5 combination is neutrally stable through ± 15 degrees of sideslip.

The full-scale prediction for the landing configuration, gear up, is shown in Figure 37.

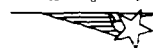
These data reflect the low full-scale fin effectiveness discussed in the previous paragraph. The configuration is predicted to be neutrally stable through $\pm 2^\circ$ of sideslip and lightly stable at higher angles. Although not shown here, the gear-down landing configuration will be more stable.

3.2 FLYING QUALITIES

The wind tunnel test results have shown that the present C-5A longitudinal aerodynamic characteristics would not be critically affected by the piggyback shuttle installation. Evidently such would not be the case for the lateral-directional characteristics, particularly in the cruise configuration. The C-5A with the Orbiter in position exhibits an increase in sideforce due to sideslip, $C_{Y\beta} = -1.39/\text{radian}$ compared to $-0.80/\text{radian}$ for the C-5A. The directional stability level is reduced to nil, $C_{n\beta} = 0$ composed with $0.0728/\text{radian}$ for the basic airplane. These predicted characteristics pertain to the $M=0.52$ at 20,000 feet flight condition. A cursory analysis was completed to assess the impact of these aerodynamic changes on C-5A flying qualities.

Pertinent flight vehicle data are tabulated in Figure 38. The reference gross weight is 704,626 pounds, which represents a 550,000 -pound airplane (no payload) with either a 154,626-pound cargo or the present design piggyback installation of the Orbiter vehicle. The Orbiter center of mass is considered to be 11.55 feet behind and 28.02 feet above the C-5A mass center.

Modal response data are presented in Figure 39. The aerodynamic changes due to the Orbiter installation result in a re-distribution of the total airplane damping due to $C_{Y\beta}$, C_{Lp} and C_{nr} . The spiral mode is more stable, now characterized by a 15.2 second time constant. The dutch roll mode is now unstable and the period of these oscillations is doubled, $\zeta_d = -.023$ and $T_d = 18.3$ seconds. The C-5A airplane incorporates a full-time stability augmentation system (SAS) on roll and yaw axes, and thus this unstable condition would not be experienced in flight. The Orbiter ferry mission may be completed with the autopilot also operative in cruise.



Flight vehicle response data were obtained using a digital computer program to evaluate responses to a 30KTAS lateral gust disturbance and a 10.0-degree lateral control wheel input. The program considers the solution of the three lateral equations of motion with respect to the usual linear assumptions. SAS and pertinent autopilot functions were included on a simple gain basis. The various high-order filters and the 0.25-second servo time constants were neglected such that the problem reduced to the control loop closures indicated in Figure 40. It is noted that the autopilot control command loops are excluded. The lateral stability functions have been included to enable an evaluation of flight vehicle response to external gust disturbances. Bank angles are presumed to be less than 7.0 degrees and thus the heading stability elements of the autopilot may also be excluded.

Figure 41 presents sideslip and bank angle responses to a continuous step gust of 30 KTAS. The lack of directional stability with the piggyback Orbiter installation results in a reluctance of the flight vehicle to naturally crab into the wind. Figure 42 provides a comparison of flight vehicle responses to control wheel throw. The excellent turn coordination characteristics of the basic C-5A airplane are somewhat degraded by the Orbiter installation. It is evident from the foregoing material that the aerodynamic changes associated with Orbiter installation may require a re-tuning of the basic C-5A stability augmentation system gains for cruise flight. The autopilot will probably be activated for the cruise condition of the Orbiter ferry mission. These would be an associated tightening of the lateral stability loop for the autopilot operative mode. The data presented in Figure 43 indicate that the flight vehicle responses to lateral gust disturbances would be stabilized, although still greater than for the basic C-5A airplane.

As stated earlier, the present analysis was of a cursory nature. The guarded conclusion is that the ferry cruise of the piggyback C-5A/Orbiter flight vehicle may not require significant C-5A flight control modifications. A continuation of studies to a greater depth than those described herein is recommended. The effects of flight vehicle vertical center of gravity location should receive attention. It is acknowledged that

an upward shift of the flight vehicle mass center will result in a reduction of the effective dihedral. The impact of c.g position on longitudinal characteristics should also be evaluated. Low speed, flaps-down, flight should also receive analytical attention.

3.3 PERFORMANCE

3.3.1 Full-Scale Drag Characteristics

Figure 44 compares estimated and wind tunnel drag for the C-5/Orbiter Piggyback. Test results on the isolated C-5 have been summed with wind tunnel data for an isolated Orbiter at the same test Reynolds number. The addition was accomplished at constant angle of attack. The excellent agreement between these two drag polars implies an absence of any net interference drag in the cruise configuration. Therefore, for purposes of this analysis, full-scale drag at flight Reynolds number for the Piggyback configuration has been defined by summing the estimated full-scale drag of an isolated Orbiter with C-5 flight test correlated drag. Resulting lift-to-drag ratios for the Piggyback at a typical cruise Mach number of 0.6 are shown compared with the C-5 in Figure 45.

Figure 46 shows a drag comparison, similar to Figure 44, for the landing configuration. The net interference drag in this case is seen to be equal to about 75% of the isolated Orbiter drag. Therefore, the low-speed, flaps-down drag data used for airport performance analyses reported herein have been increased to account for this effect.

3.3.2 Airfield Performance

Figures 47 and 48 show the takeoff and landing distances for the C-5/Orbiter Piggyback at varying gross weights. These data represent standard C-5 takeoff and land distances increased slightly to account for drag due to the Orbiter. Runway conditions for an airfield pressure altitude of 2000 feet and standard-day temperatures have been used for these as well as all other airfield performance data presented.



Takeoff flap setting for the C-5A is 16 degrees with a takeoff speed of $1.2 V_{STALL}$.

For a long-range ferry mission takeoff gross weight of 700,000 pounds, takeoff ground roll is seen to be 7230 feet with a total distance of 8640 feet to clear a 50-foot obstacle. Engine-out climb capability of the C-5 Piggyback configuration may restrict operations at these conditions such that increased takeoff speeds and distances may be required. However, operation from airfields with runway lengths of 10,000 feet should not be prohibited.

Landing flaps for the C-5A are set at 40 degrees and approach speeds are normally $1.3 V_{STALL}$. For an aborted mission after takeoff at 700,000 pounds, a landing ground roll of 3250 feet is indicated by Figure 48. Normal ferry mission landing weights would be approximately 550,000 pounds, for which a landing ground roll of 2200 feet and total landing distance from a 50-foot obstacle of 3580 feet would be expected.

3.3.3 Climb and Cruise Performance

One-engine-inoperative climb gradients for the C-5 Piggyback at several takeoff speeds and with the landing gear retracted are shown in Figure 49 for standard-day, 2000-foot pressure altitude conditions. Since Piggyback climb gradients are reduced relative to those of the basic C-5A, consideration has been given to increasing the takeoff speeds to improve climbout performance. As can be seen, an increase from $1.2 V_{STALL}$ to $1.3 V_{STALL}$ increases the gradient by about 0.35 percent, or for a constant climb gradient, the takeoff weight is increased by about 23,000 pounds. This amounts to approximately a 10 percent increase in fuel for long-range ferry missions.

Cruise ceilings for the C-5 Piggyback are shown in Figure 50 for several rates of climb. Long-range cruise performance calculated for the ferry mission is based on the altitudes for the 300-feet-per-minute ceiling shown for normal rated thrust (NRT). The cruise ceilings with military rated thrust (MRT) are useful for determining maximum speed-altitude capability of the C-5 Piggyback.

Figure 51 summarizes the speed-altitude capability at MRT of the Piggyback for weights corresponding to both an empty and fully loaded Orbiter. Also shown are data for the case of an Orbiter configuration without an afterbody fairing. At 25,000 feet, the maximum speed attainable is 259 KEAS with a faired afterbody, fully loaded Orbiter and 266.5 KEAS with an empty Orbiter.

3.3.4 Orbiter Ferry Capability

Figure 52 summarizes the capability of the C-5A to ferry the Orbiter in the Piggyback mode as a function of military critical field length and takeoff ground roll. These data are shown for takeoff speeds of 1.2, 1.25 and 1.3 times the stall speed and for three values of one-engine inoperative climb gradient. A climb gradient of 2.3% is the current minimum allowable gradient for the C-5A. Reducing the climb gradient to 1.8% improves the range by 240 miles while increasing takeoff distance by less than 1000 feet. Similarly, increasing takeoff speed from 1.2 to 1.3 V_{STALL} increases range by 160 miles but increases takeoff distance by 2500 feet.

For a special-purpose airplane it appears quite reasonable to accept lower climb gradients as a means of increasing range, provided there are no obstacles in the take-off path. Alternately, it is not necessary to resort to lower climb gradients, since the C-5A's inflight refueling capabilities make its range essentially unlimited.

3.4 FLIGHT RESTRICTIONS

Flight restrictions for the Piggyback are summarized in Figure 53 for two configurations, the C-5 with and without tail modifications. As discussed previously in subsection 3.2, ferry flight without any extension modifications to the C-5 tail can be accomplished with reliance on automatic flight controls, and flight restrictions listed here are given only as a matter of interest.

These restrictions have been established such that no structural modification to the C-5A is necessary other than that required to mount the Orbiter. The "fuselage fuel"

included in the weights breakdown represents an amount of ballast required for the Orbiter mounted in the aft position. This position is 10 feet aft relative to the baseline location, and the ballast is required to bring the c.g. within the current aft limit of the C-5A. The operating weights shown include the weight of the fuselage fuel tank.

Flight restrictions for the C-5/Orbiter Piggyback are compared with those of the Super Guppy in Figure 54. As can be seen, they are quite comparable. The only condition in which the C-5A is restricted more than the Super Guppy is in touchdown rate of sink. This is insignificant, since the design weights can be lowered somewhat and still allow the ferry-range performance shown in subsection 3.3.4. Design speeds and gust weights are naturally considerably greater for the C-5A as represented by the 300 KCAS level-flight maximum speed for the C-5A/Orbiter Piggyback, compared with 219 KCAS for the Super Guppy, and a maximum gross weight of 865,000 pounds for the Piggyback compared with 162,000 pounds for the Super Guppy. Maneuver-load factors for cruise are about the same: 2.0 for the Piggyback and 2.2 for the Super Guppy.

4.0 CONCLUSIONS AND RECOMMENDATIONS

Wind tunnel testing of the C-5A/Orbiter Piggyback configuration has demonstrated that the major effect of the Orbiter on the aerodynamics of the C-5A is a loss of directional stability due primarily to airflow losses at the vertical tail, and to an increase in overall side area and side forces. The effects of the Orbiter on longitudinal stability are almost negligible as evidenced by a C_{m_0} shift due to the Orbiter equivalent to less than one degree of horizontal stabilizer incidence. The effect on drag, as expected, is significant, but the drag level of the Piggyback configuration can be reduced to a level about 40% above C-5A cruise configuration drag with an Orbiter afterbody fairing. Interference effects from a drag standpoint appear from the test results to be insignificant for the ferry cruise configuration.

Variations in Orbiter longitudinal and vertical locations showed that the aft high position was the best, primarily because the losses in directional stability were minimized by moving the side areas aft of the reference c.g. The effects of varying the Orbiter incidence relative to the C-5A were, from any viewpoint, inconsequential for the range tested (-1.5° and 0.5°). A Lockheed-Georgia afterbody designed for the Orbiter to improve the flow at the empennage and the directional stability proved insufficient, although a slight drag reduction was noticed for the Lockheed-Georgia fairing.

During the wind tunnel test, several empennage modifications were designed and tested to remedy the directional stability problems. These modifications included a control fin addition above the present horizontal stabilizer, and twin fin additions to the horizontal stabilizer tip.

These were successful in restoring the stability level of the Piggyback to that of the basic C-5A so that, if desired, external modifications could be defined that would provide satisfactory flying qualities. cursory analytical studies indicate that the C-5A automatic controls can be modified to fly the Piggyback configuration in a ferry operation without external modifications and with only minor modifications to the flight control systems.

Performance analyses revealed the feasibility of trans-continental unrefueled distances for the C-5A ferrying the Shuttle Orbiter. Airfield performance assures operation from fields of less than 10,000 feet where minimum takeoff climbout gradients can be tolerated. In total, the feasibility of the C-5A/Orbiter Piggyback ferry concept appears excellent and the following recommendations are respectfully submitted:

- o Development of the C-5A ferry vehicle should be initiated as soon as possible.
- o A wind tunnel test program of the airlaunch configuration should be initiated.
- o Studies of airlaunch concepts and separation trajectory analyses should be made in conjunction with the wind tunnel program.
- o More detailed, flying-qualities studies of the C-5/Orbiter Piggyback configuration should be conducted to identify potential modifications of the C-5A automatic flight control systems.



C-5/ORBITER PIGGYBACK

EFFECT OF ORBITER ON LONGITUDINAL STABILITY CRUISE CONFIGURATION

C_M	SYM	RUN	CONFIGURATION
.3	O	57	C-5A
.1	△	26	C-5A + ORBITER
-.1	□	31	C-5A + ORBITER + A/B FAIRING (GELAC)

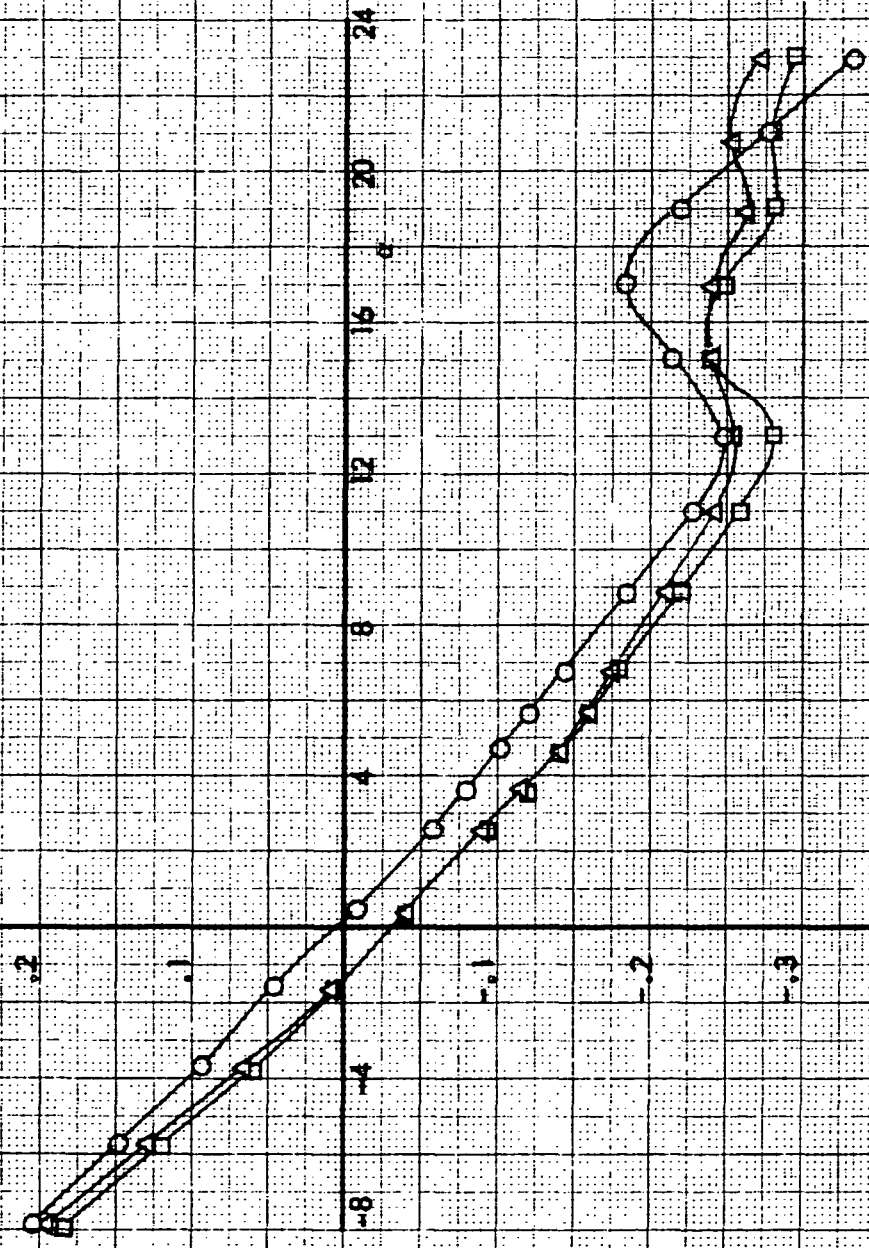


FIGURE 1

EFFECT OF ORBITER ON LONGITUDINAL STABILITY CRUISE CONFIGURATION

SYM	RUN	CONFIGURATION
○	57	C-5A
△	26	C-5A + ORBITER
□	31	C-5A + ORBITER+ A/B Fairing (GELAC)

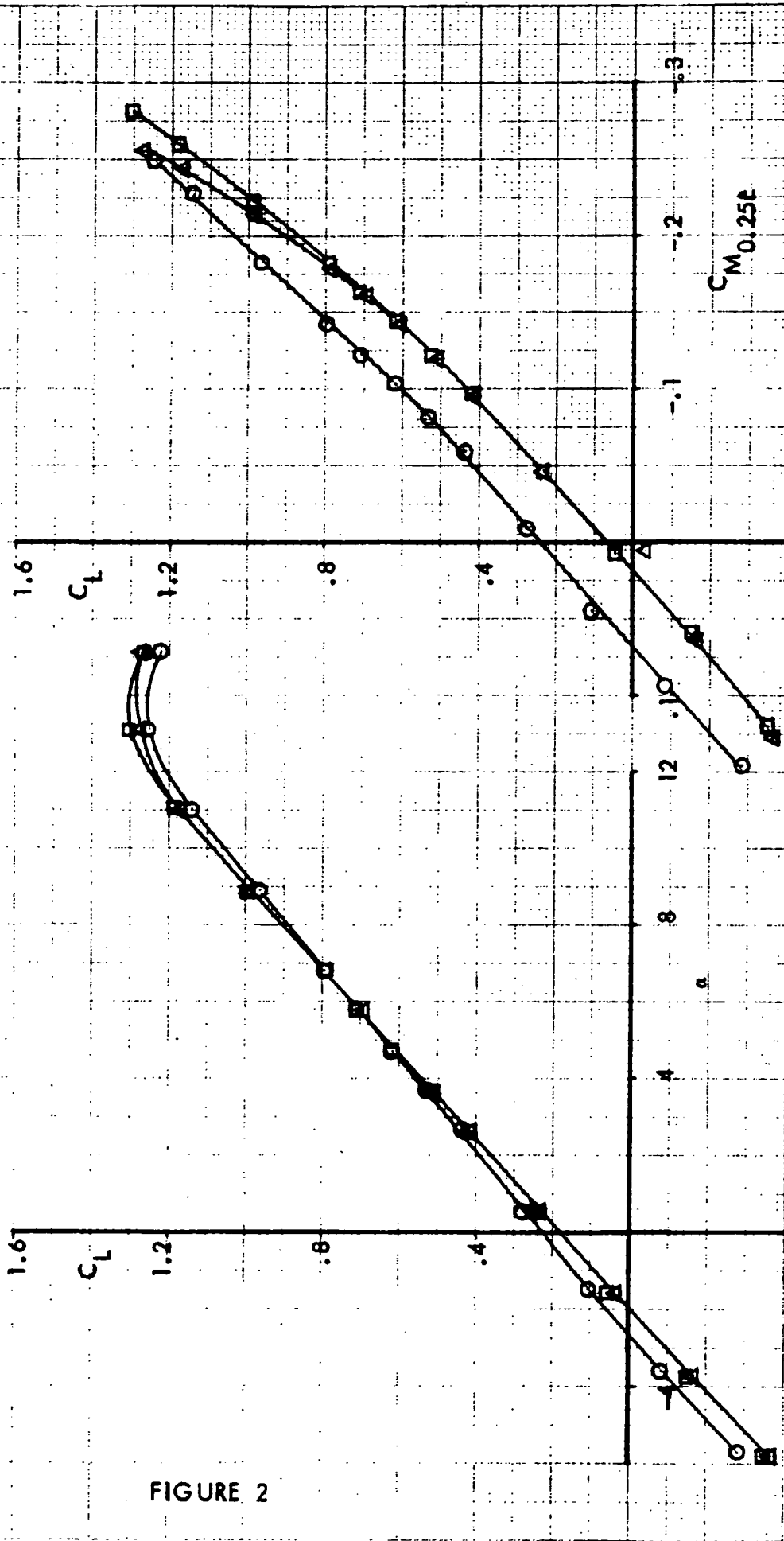


FIGURE 2

C-5/ORBITER PIGGYBACK

EFFECT OF ORBITER ON DIRECTIONAL STABILITY CRUISE CONFIGURATION

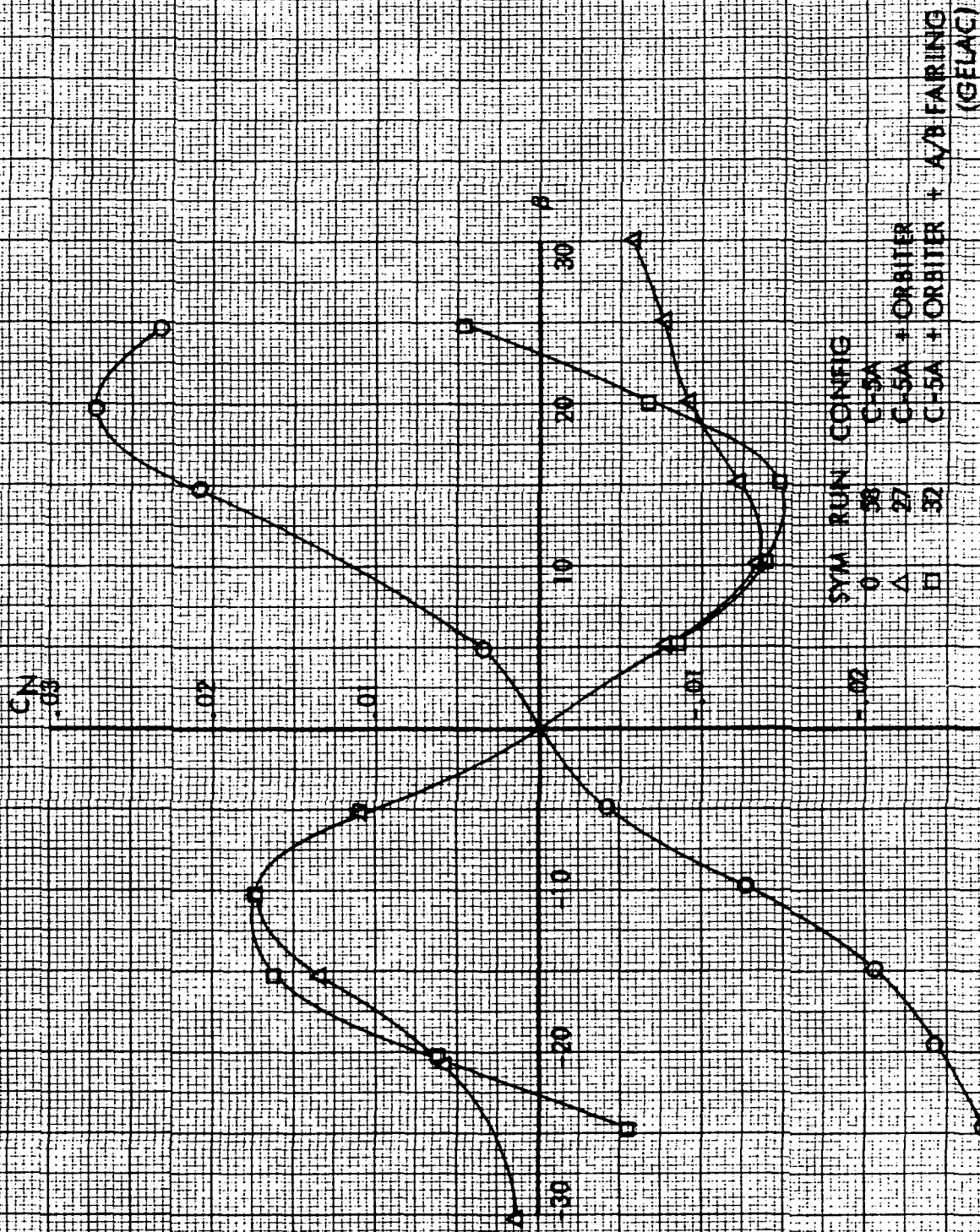


FIGURE 3

EFFECT OF ORBITER ON LATERAL STABILITY CRUISE CONFIGURATION

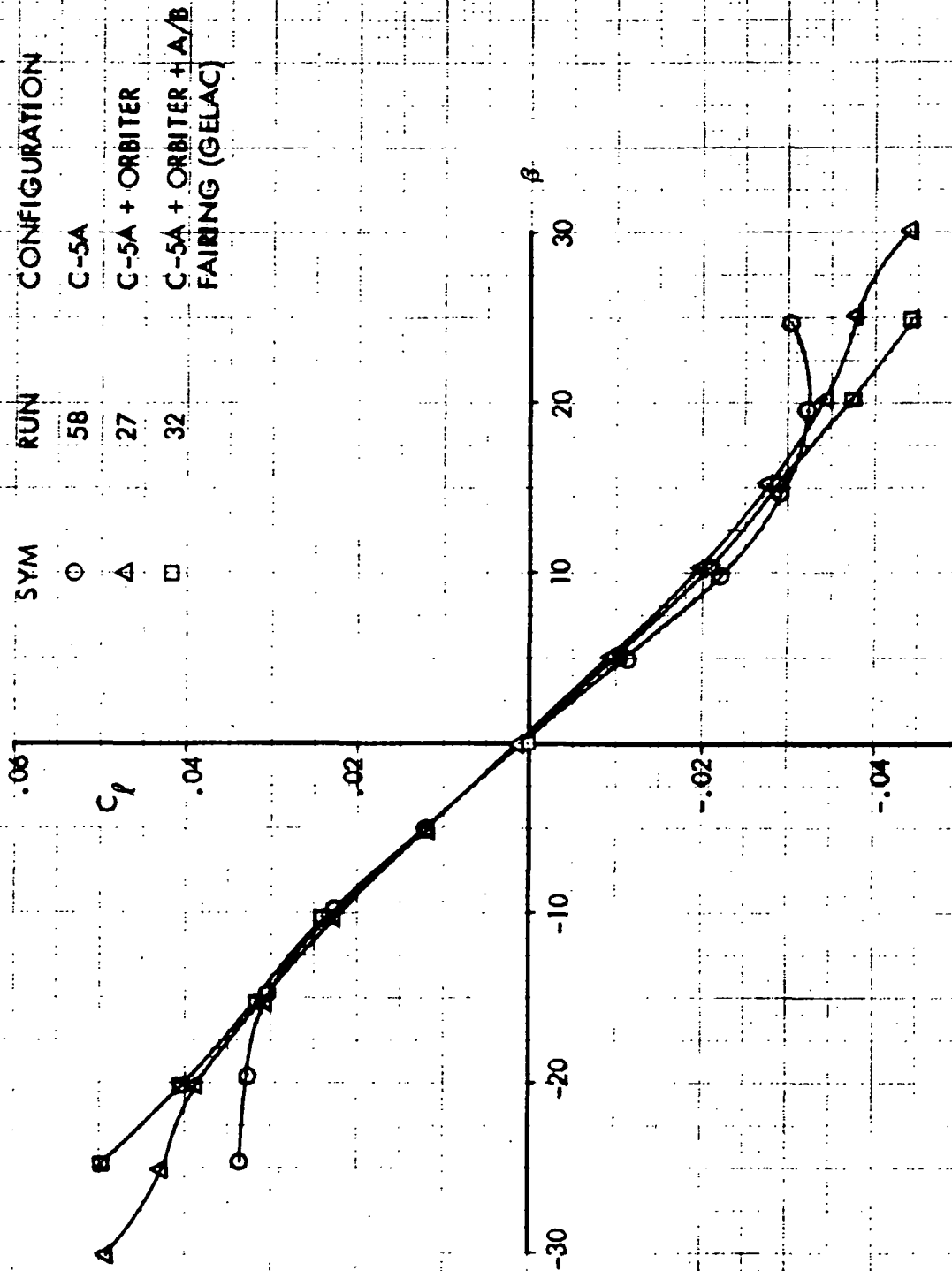


FIGURE 4

C-5A/ORBITER PIGGYBACK

EFFECT OF ORBITER ON SIDEFORCE CRUISE CONFIGURATION

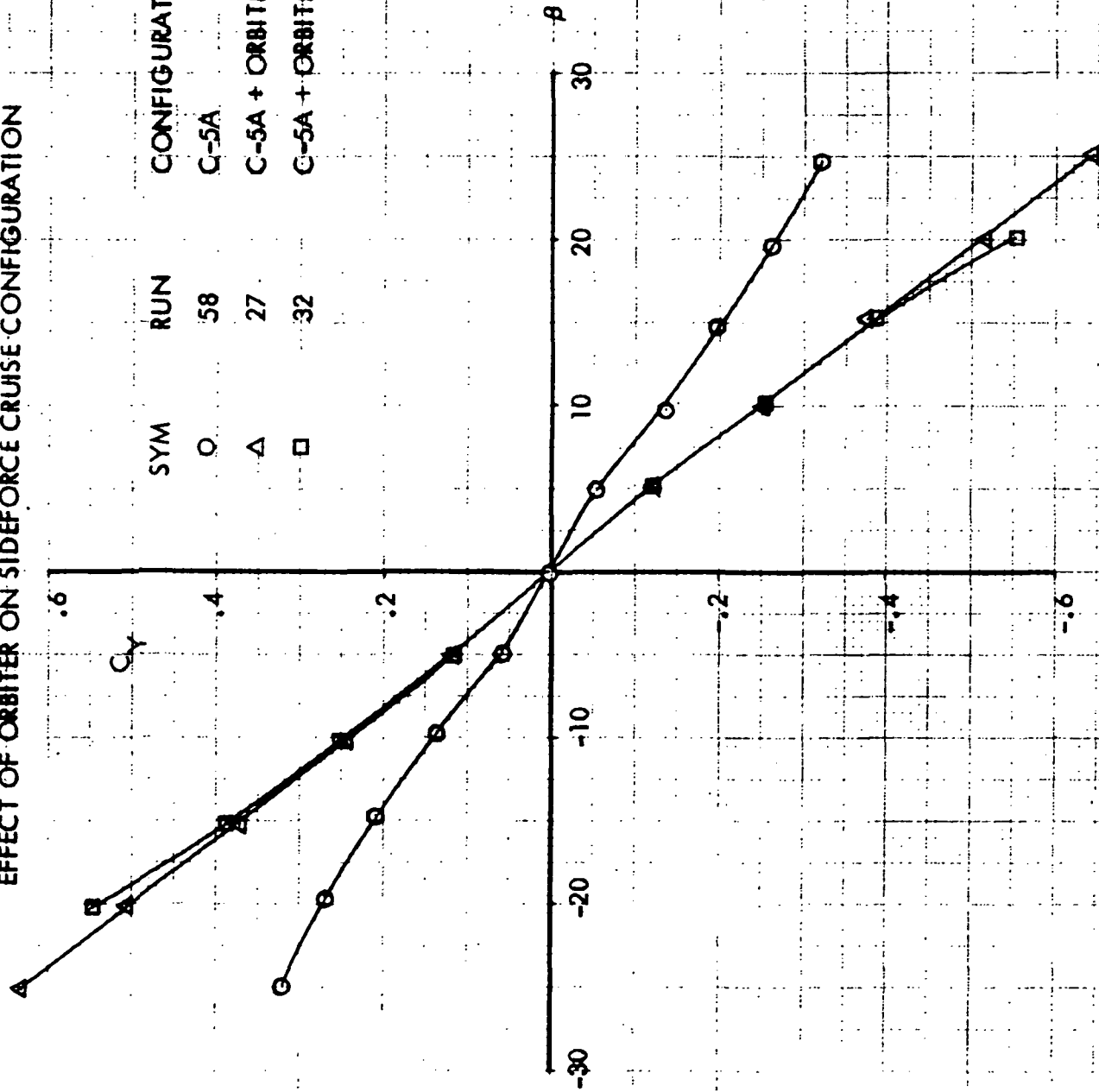


FIGURE 5

C-5/ORBITER PIGGYBACK

EFFECT OF ORBITER POSITION ON LONGITUDINAL STABILITY CRUISE CONFIGURATION

GILAC A/B FAIRING #1

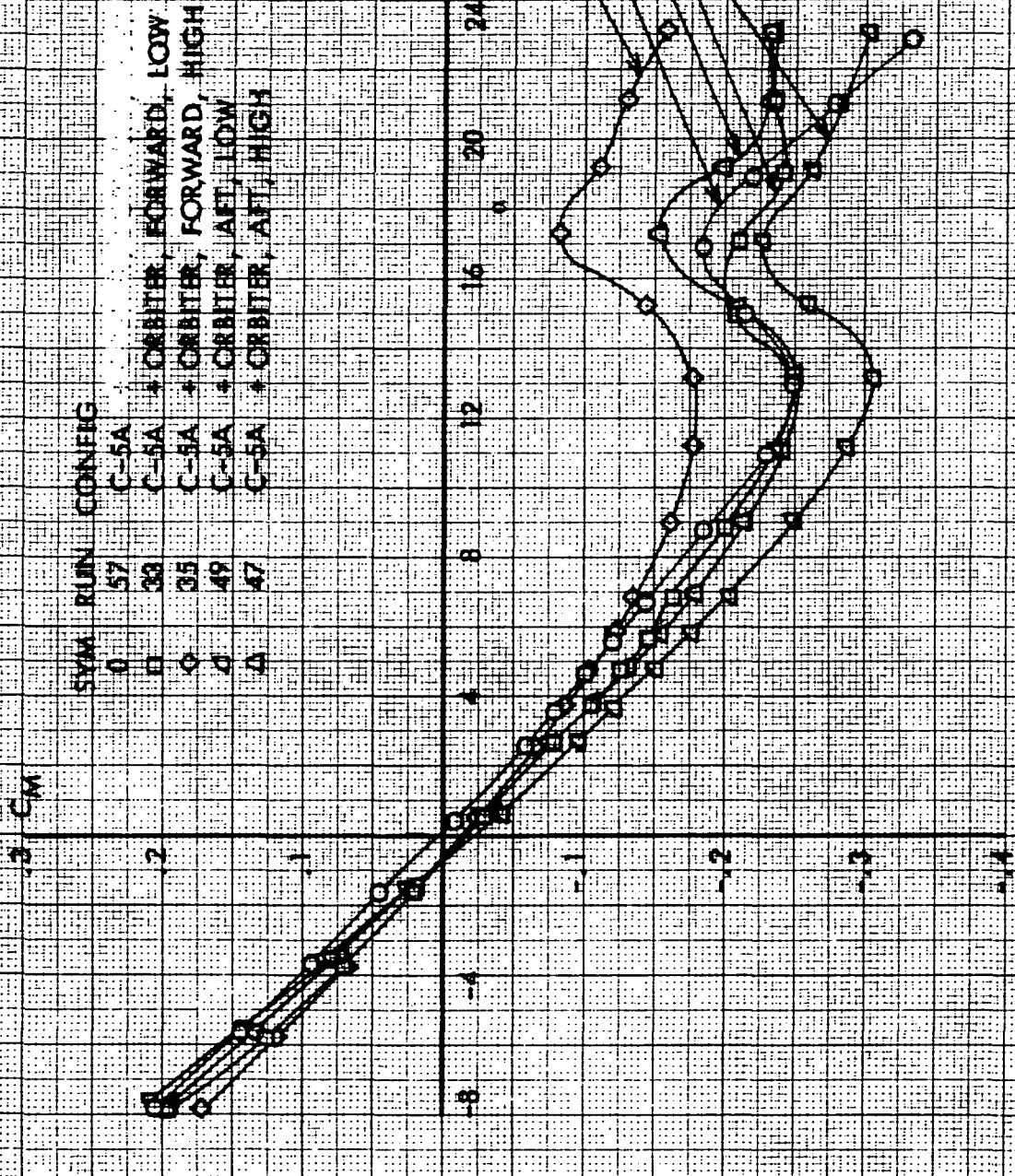


FIGURE 6

EFFECT OF ORBITER POSITION ON LONGITUDINAL STABILITY CRUISE CONFIGURATION

GELAC A/B FAIRING # 1

SYM	RUN	CONFIGURATION
○	57	C-5A
□	33	C-5A + ORBITER, FWD LOW
△	35	C-5A + ORBITER, FWD HIGH
◇	49	C-5A + ORBITER, AFT LOW
△	47	C-5A + ORBITER, AFT HIGH

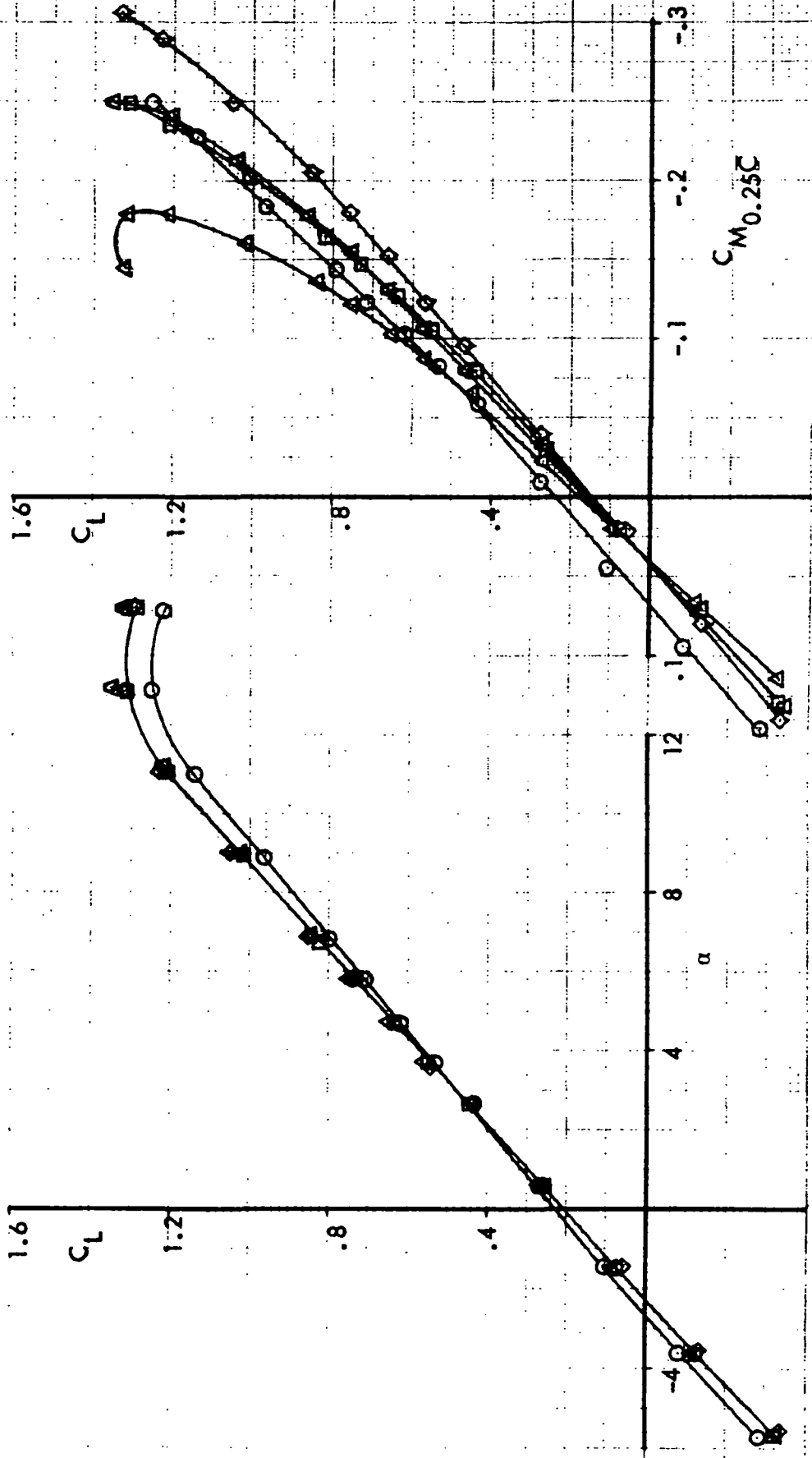


FIGURE 7

C-5/ORBITER PIGGYBACK

EFFECT OF ORBITER POSITION ON DIRECTIONAL STABILITY

SYM RUN CONFIG

- 0 C-5A
- 34 C-5A + ORBITER, FORWARD, LOW
- 36 C-5A + ORBITER, FORWARD, HIGH
- 50 C-5A + ORBITER, AFT, LOW
- 48 C-5A + ORBITER, AFT, HIGH

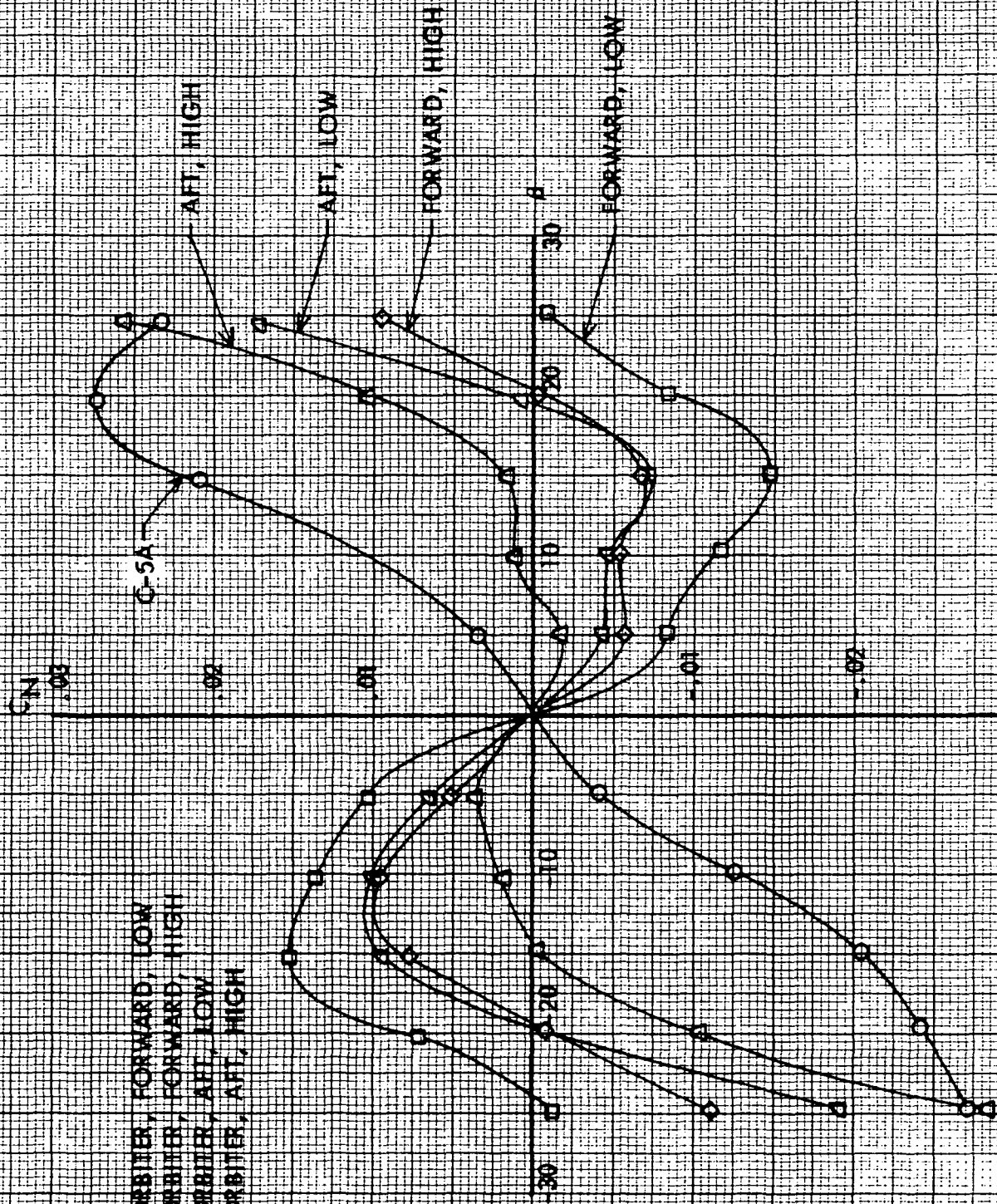


FIGURE 8

EFFECT OF ORBITER POSITION ON LATERAL STABILITY CRUISE CONFIGURATION

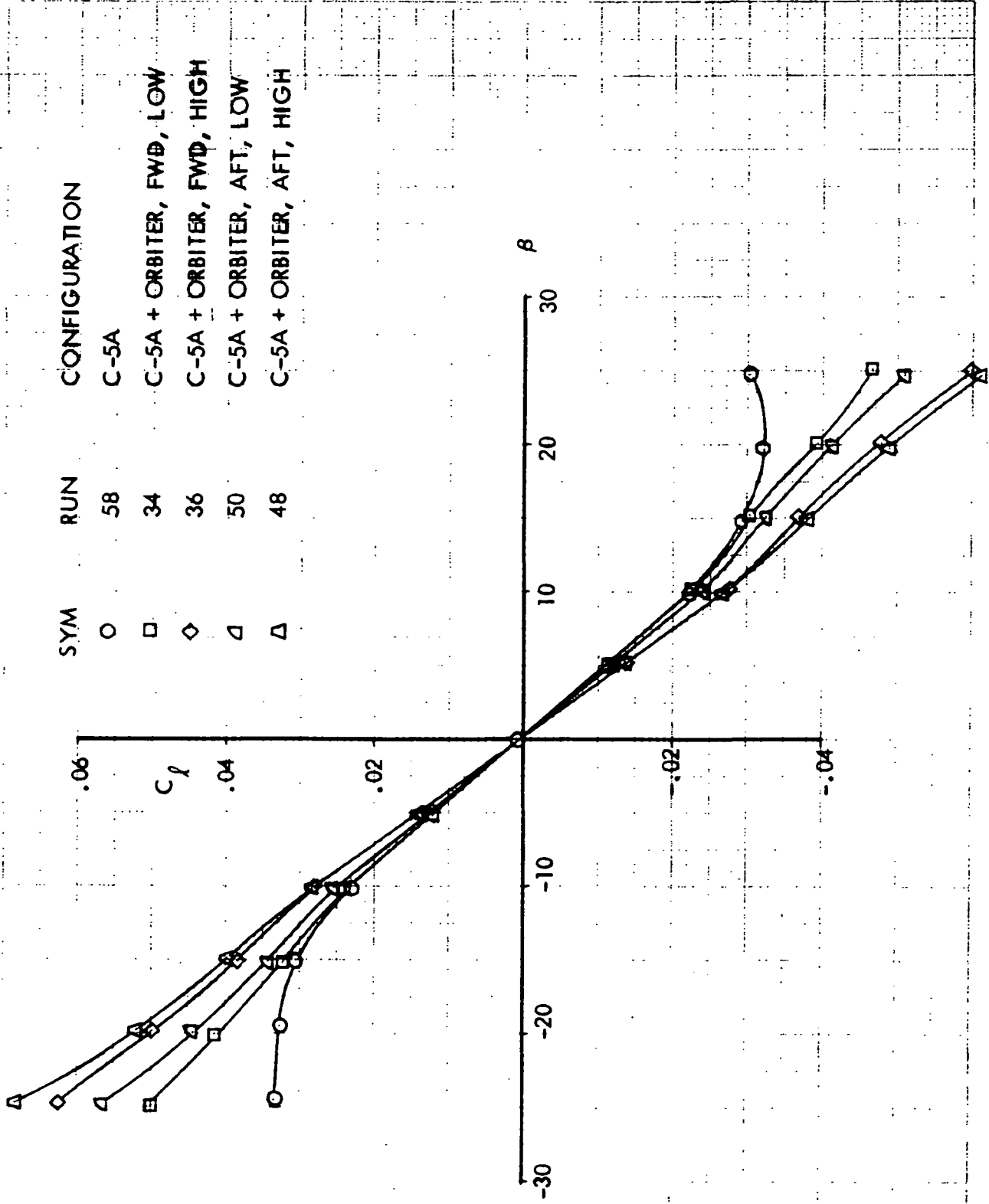


FIGURE 9

C-5A/ORBITER PIGGYBACK

EFFECT OF ORBITER POSITION ON SIDEFORCE
CRUISE CONFIGURATION

SYM	RUN	CONFIGURATION
○	58	C-5A
□	34	C-5A + ORBITER, FWD, LOW
◇	36	C-5A + ORBITER, FWD, HIGH
△	50	C-5A + ORBITER, AFT, LOW
△	48	C-5A + ORBITER, AFT, HIGH

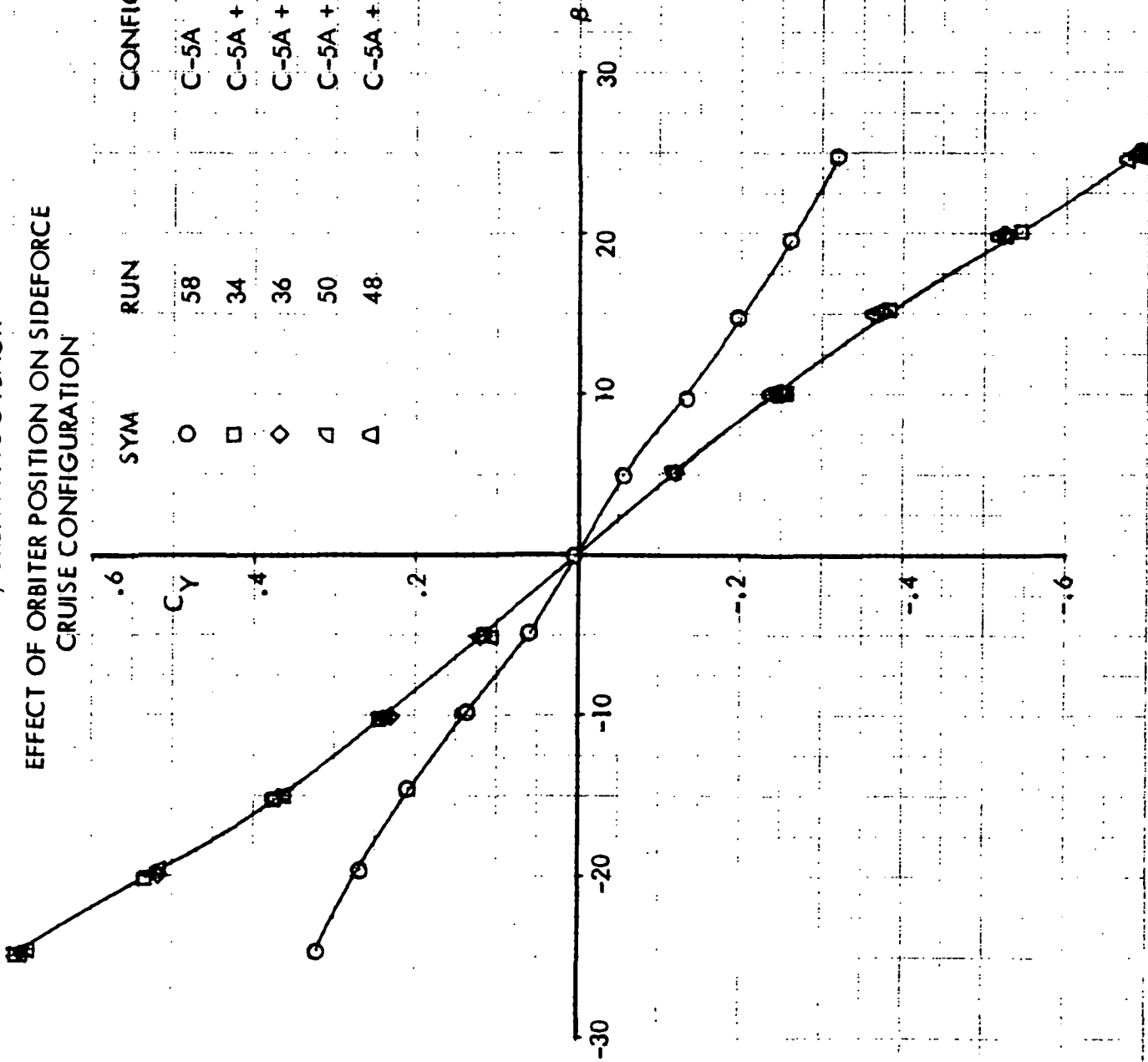


FIGURE 10

C-5/ORBITER FIGGYBACK

EFFECT OF ORBITER INCIDENCE ON LONGITUDINAL STABILITY
CRUISE CONFIGURATION

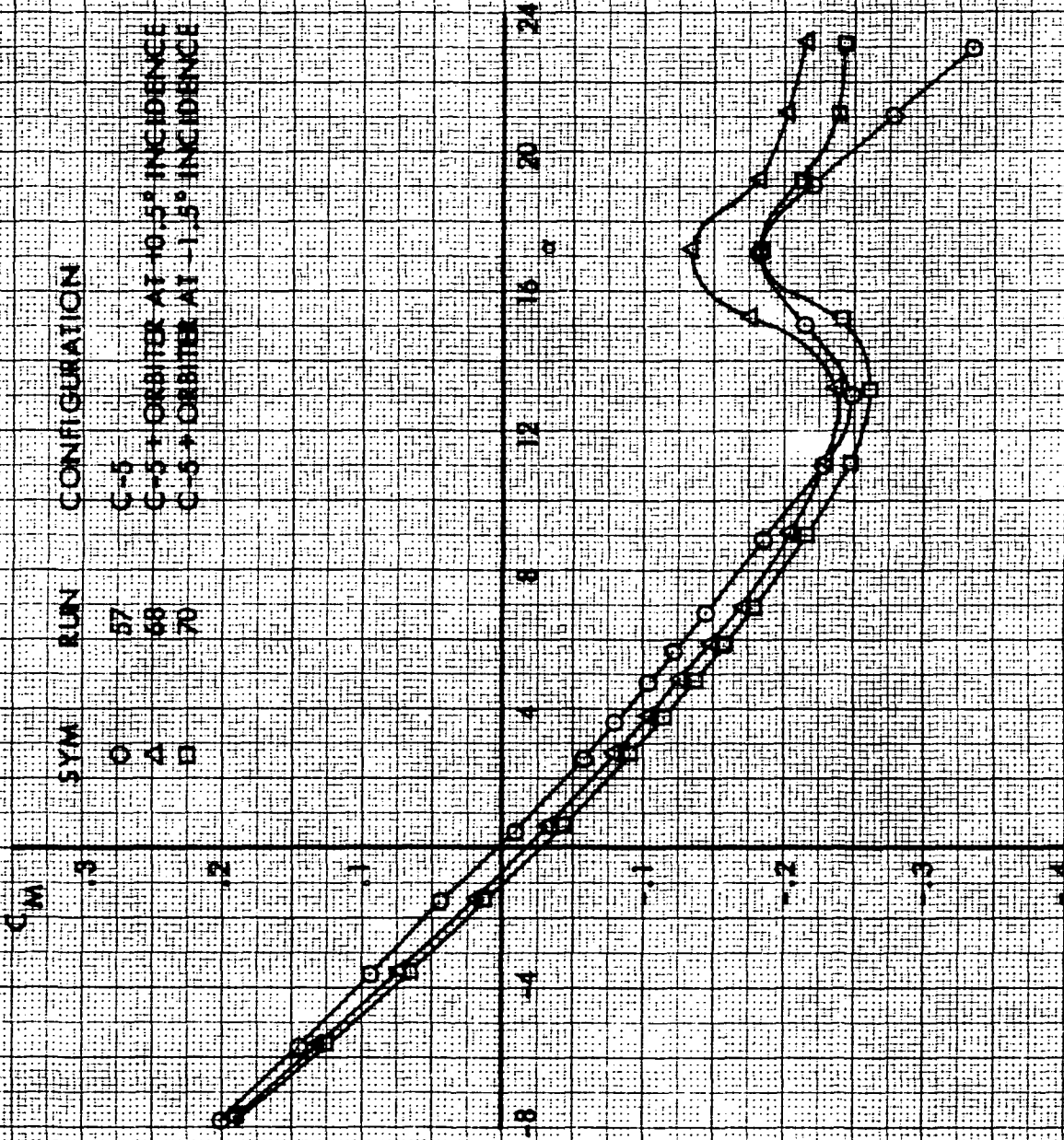


FIGURE 11

EFFECT OF ORBITER INCIDENCE ON LONGITUDINAL STABILITY CRUISE CONFIGURATION

SYM	RUN	CONFIGURATION
O	57	C-5A
Δ	68	C-5A + ORBITER AT 0.5° INCIDENCE
□	70	C-5A + ORBITER AT -1.5° INCIDENCE

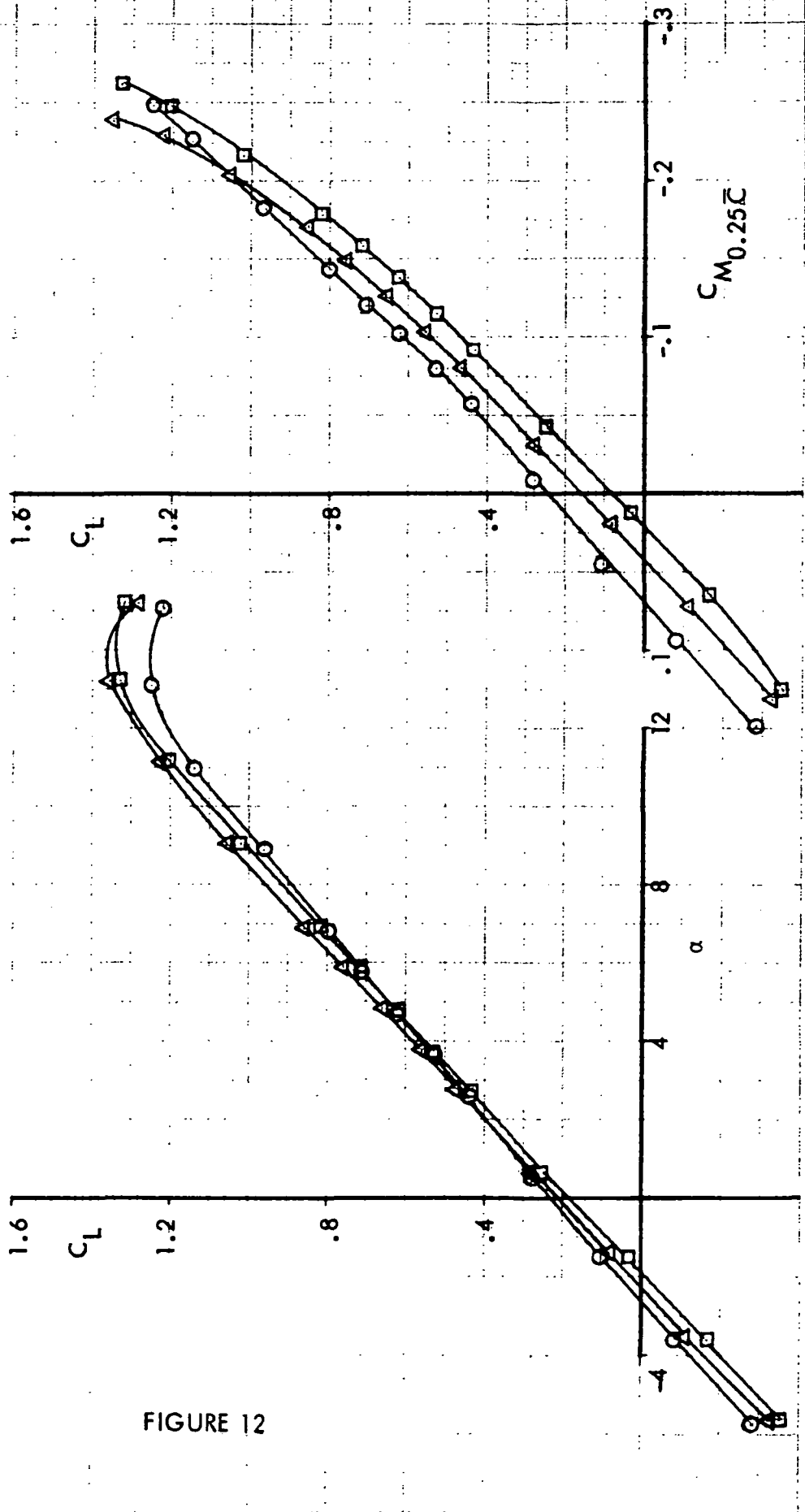
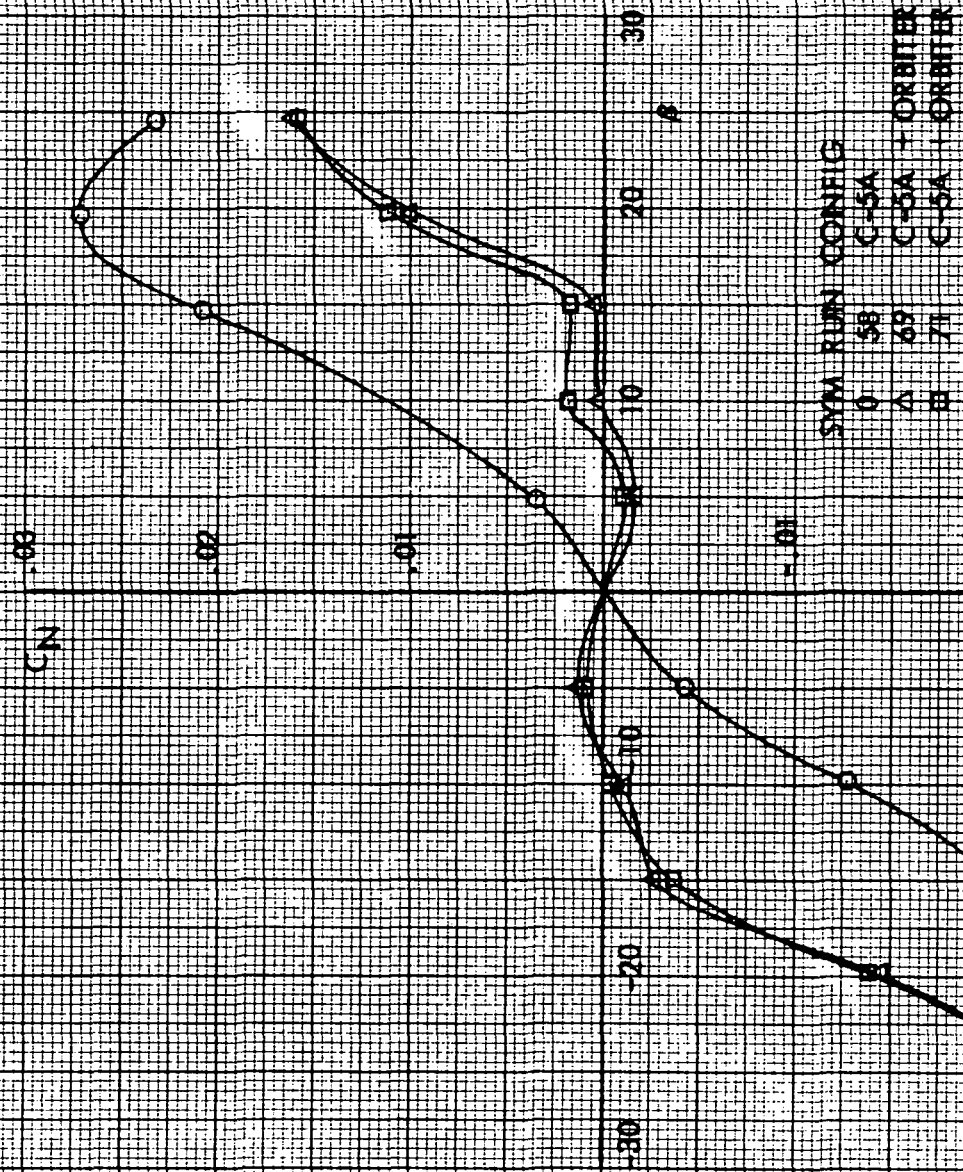


FIGURE 12

C-5/ORBITER PIGGYBACK
EFFECT OF ORBITER INCIDENCE ON
DIRECTIONAL STABILITY
CRUISE CONFIGURATION



SYN RUNN CONFIG
 0 C-5A
 Δ C-5A + ORBITER AT 0.5° INCIDENCE
 B C-5A + ORBITER AT 1.5° INCIDENCE

FIGURE 13

EFFECT OF ORBITER INCIDENCE ON LATERAL STABILITY CRUISE CONFIGURATION

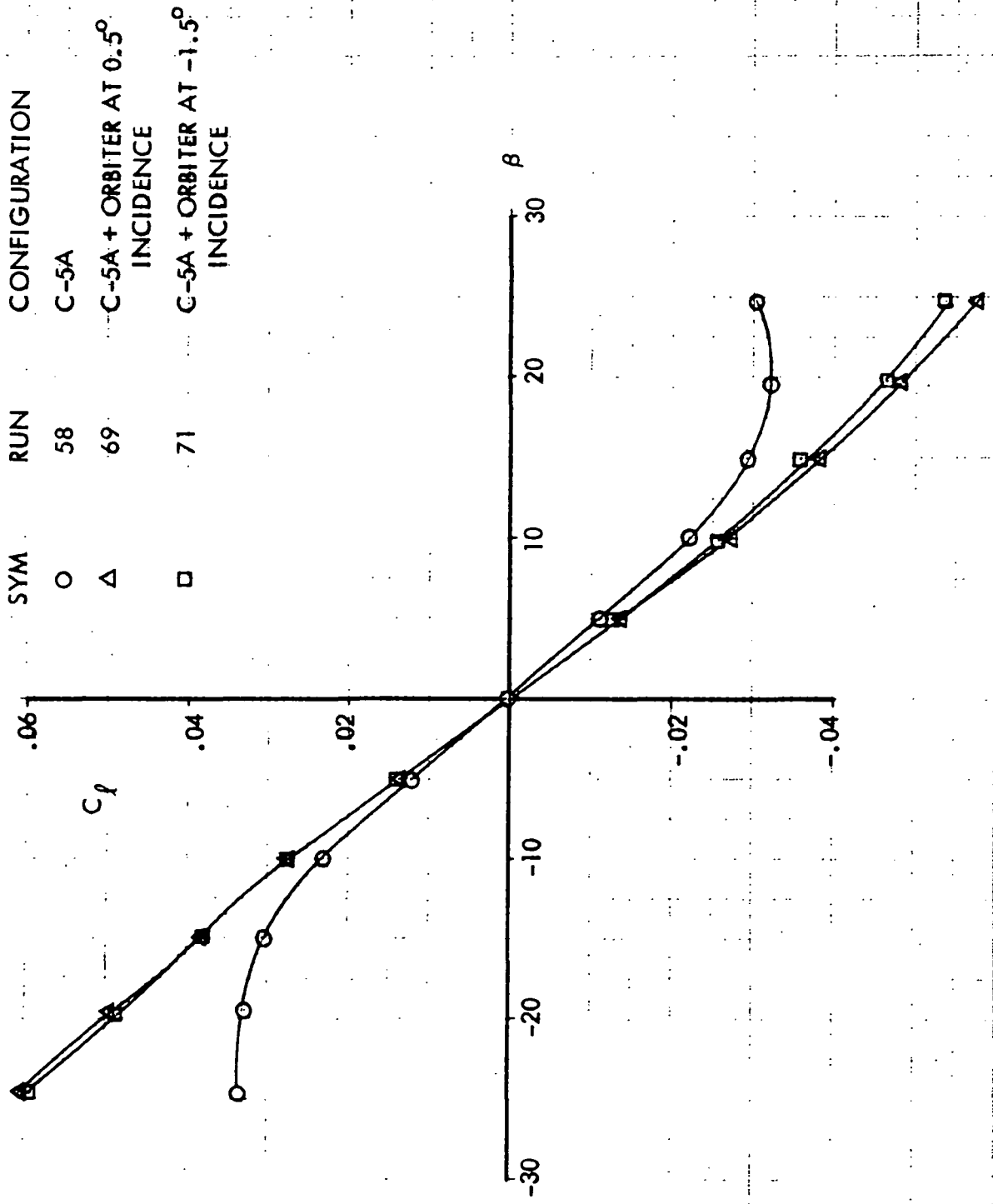


FIGURE 14

EFFECT OF ORBITER INCIDENCE ON SIDEFORCE
CRUISE CONFIGURATION

SYM	RUN	CONFIGURATION
○	58	C-5A
△	69	C-5A + ORBITER AT 0.5° INCIDENCE
□	71	C-5A + ORBITER AT -1.5° INCIDENCE

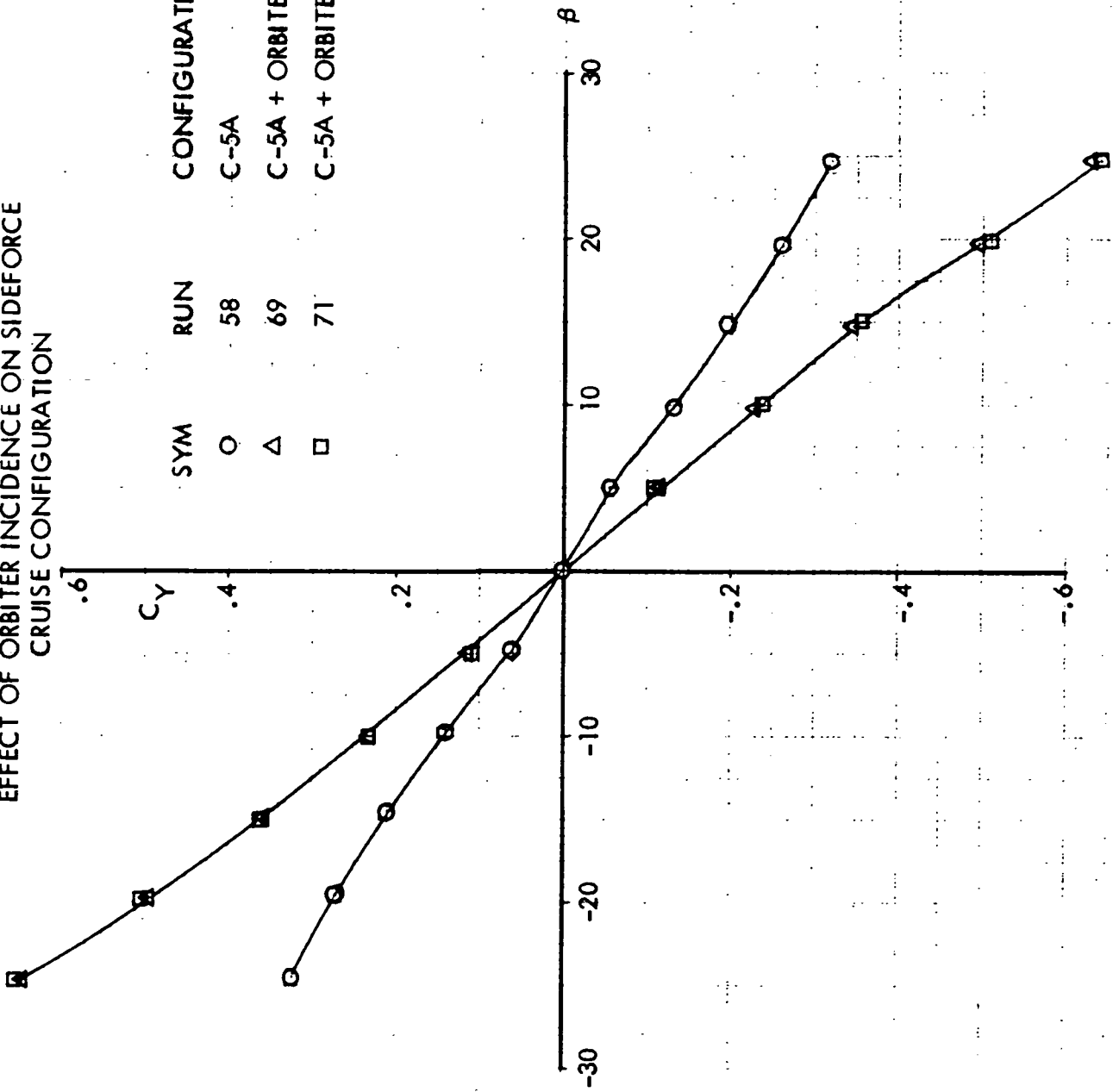


FIGURE 15

C-5/ORBITER PIGGYBACK

EFFECT OF AFTERBODY FAIRING SHAPE ON LONGITUDINAL STABILITY
CRUISE CONFIGURATION

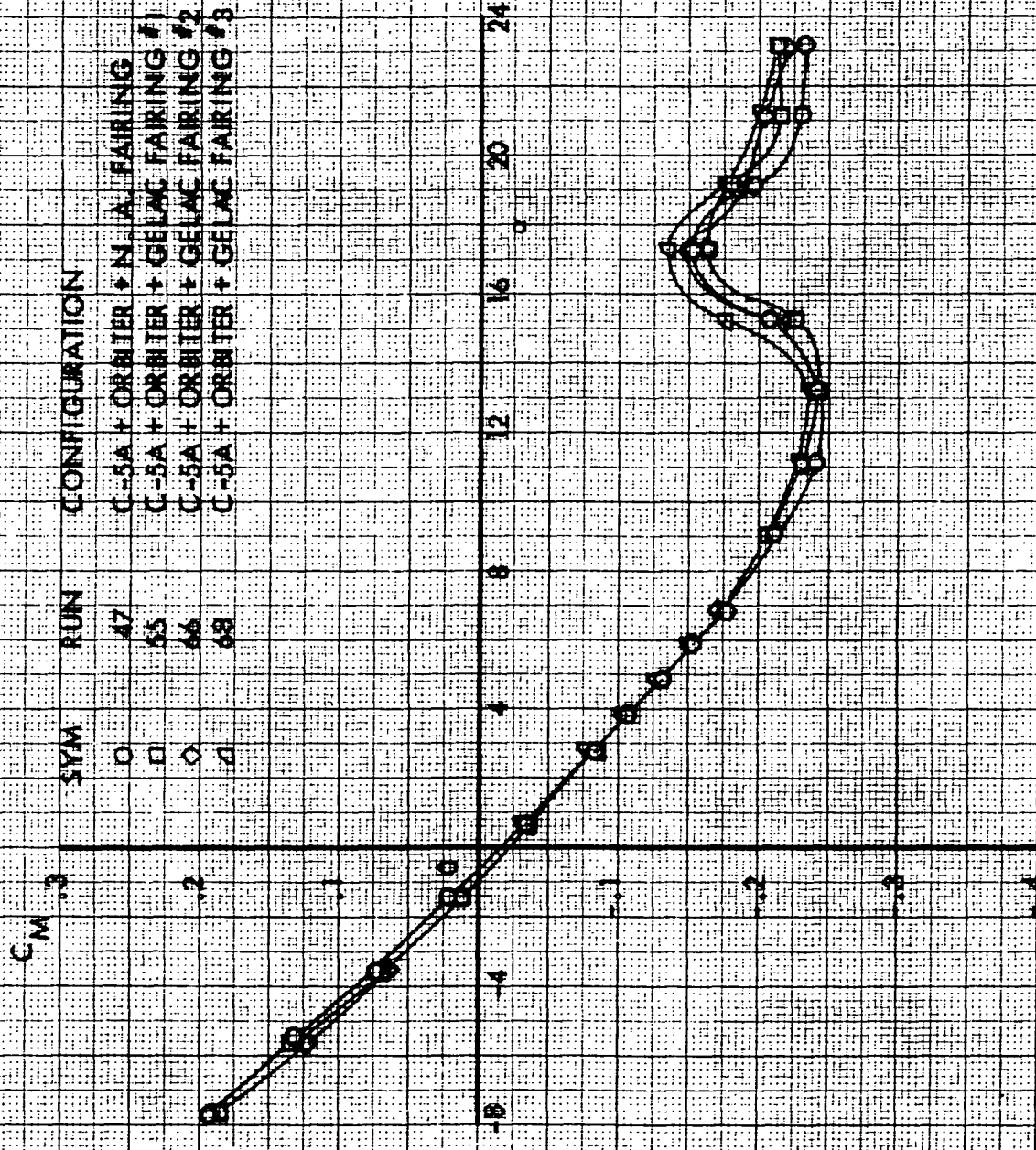
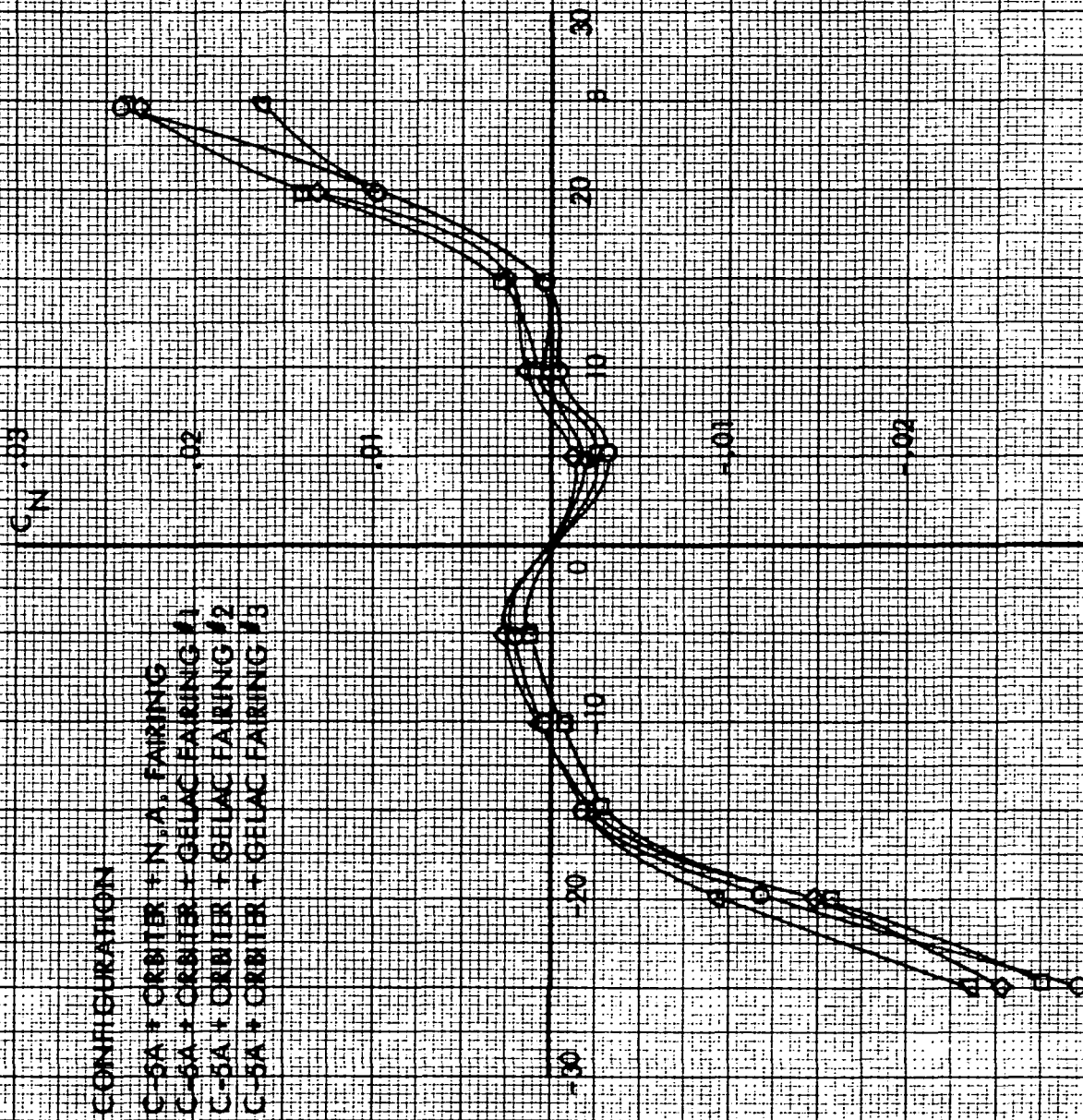


FIGURE 16

C-5A/ORBITER PIGGYBACK

EFFECT OF AFTERBODY FAIRING SHAPE ON DIRECTIONAL STABILITY
CRUISE CONFIGURATION



SYM	CONFIGURATION
□	C-5A + ORBITER + N.A. FAIRING
○	C-5A + ORBITER + GELAC FAIRING #1
◇	C-5A + ORBITER + GELAC FAIRING #2
△	C-5A + ORBITER + GELAC FAIRING #3

FIGURE 17

EFFECT OF ORBITER ON LONGITUDINAL STABILITY
LANDING CONFIGURATION

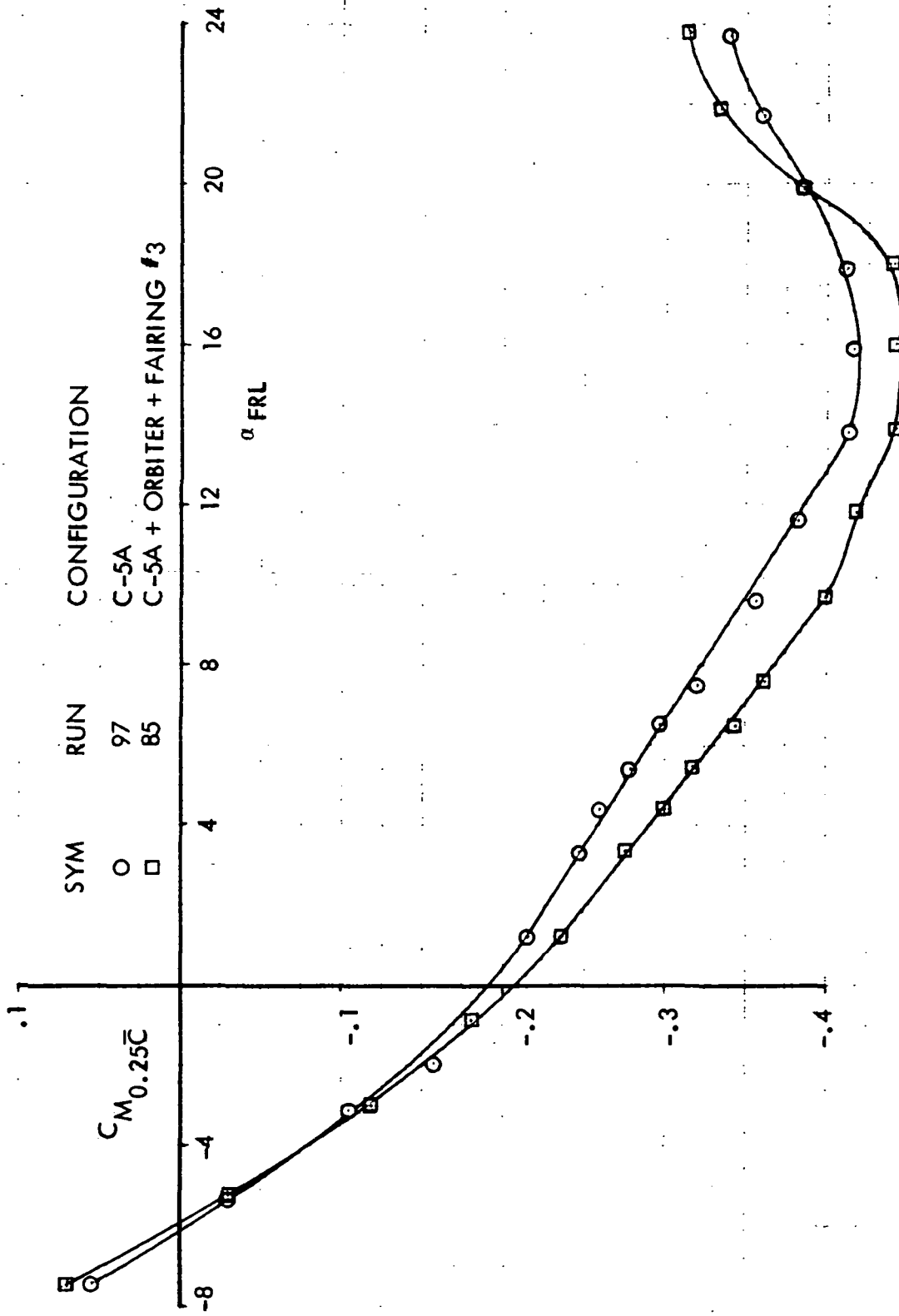


FIGURE 18

EFFECT OF ORBITER ON LONGITUDINAL STABILITY
LANDING CONFIGURATION

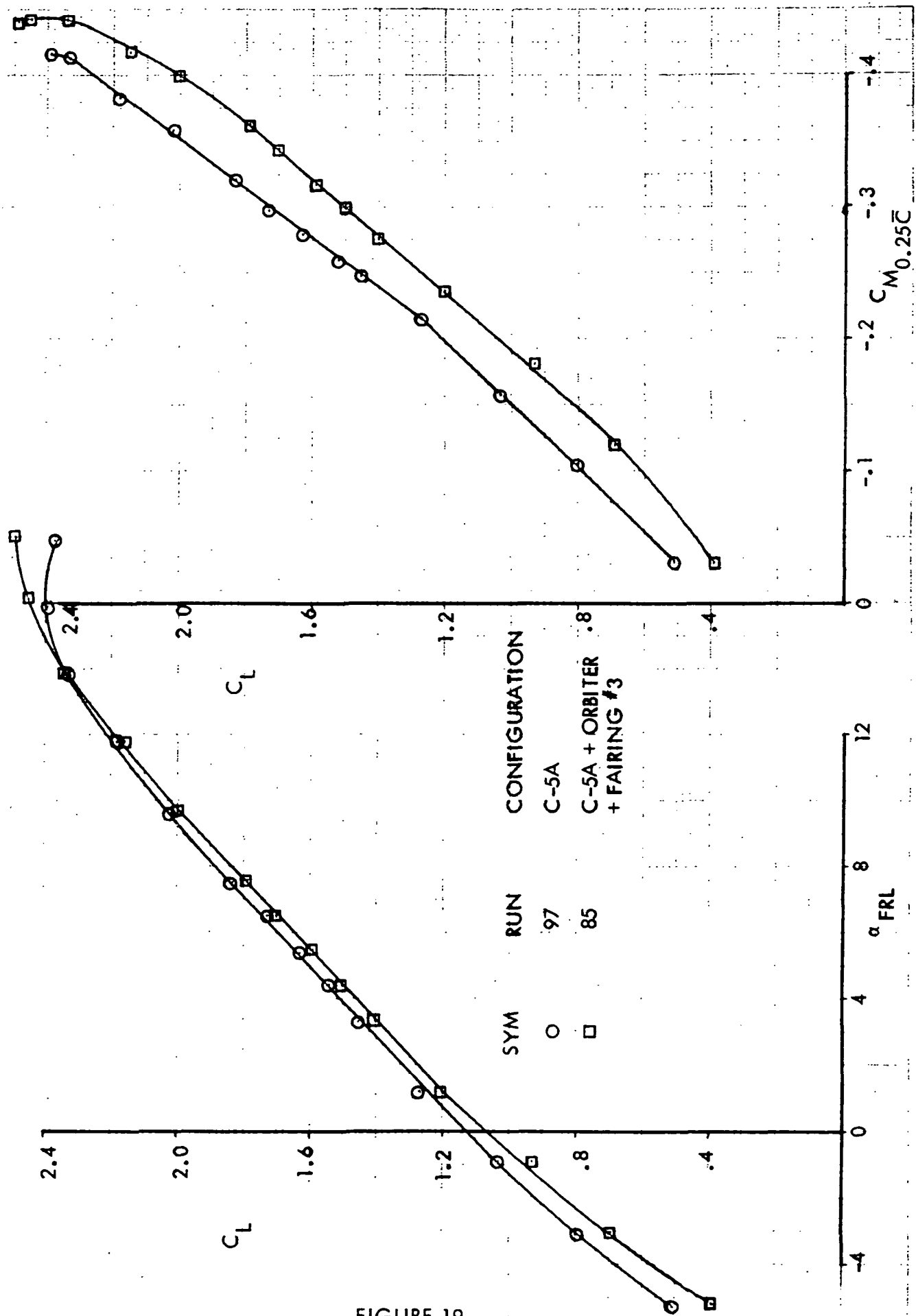


FIGURE 19

C-5A/PIGGYBACK ORBITER

EFFECT OF ORBITER ON DIRECTIONAL STABILITY
LANDING CONFIGURATION

SYM	RUN	CONFIGURATION
○	92	C-5A
□	91	C-5A + ORBITER + FAIRING #3

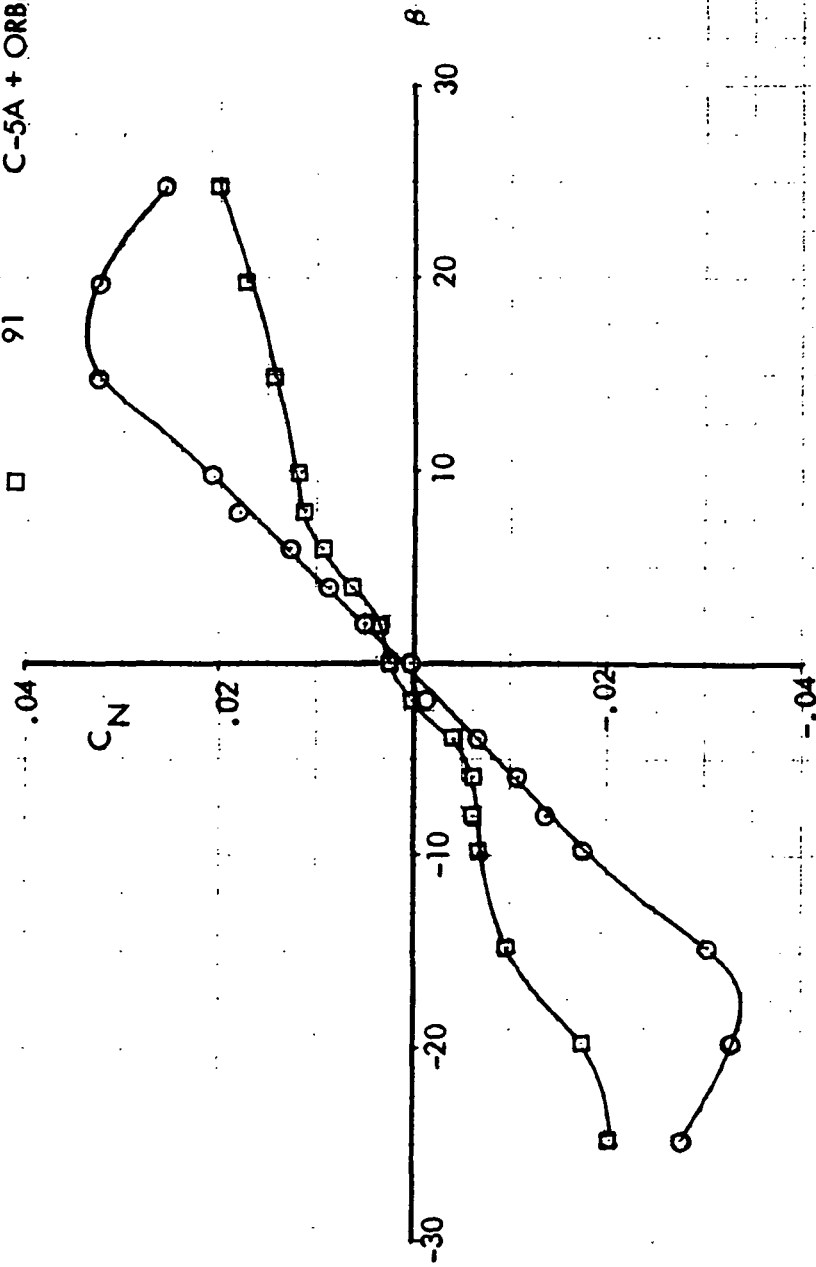


FIGURE 20

EFFECT OF ORBITER ON LATERAL STABILITY
LANDING CONFIGURATION

SYM	RUN	CONFIGURATION
O	92	C-5A
□	91	C-5A + ORBITER + FAIRING #3

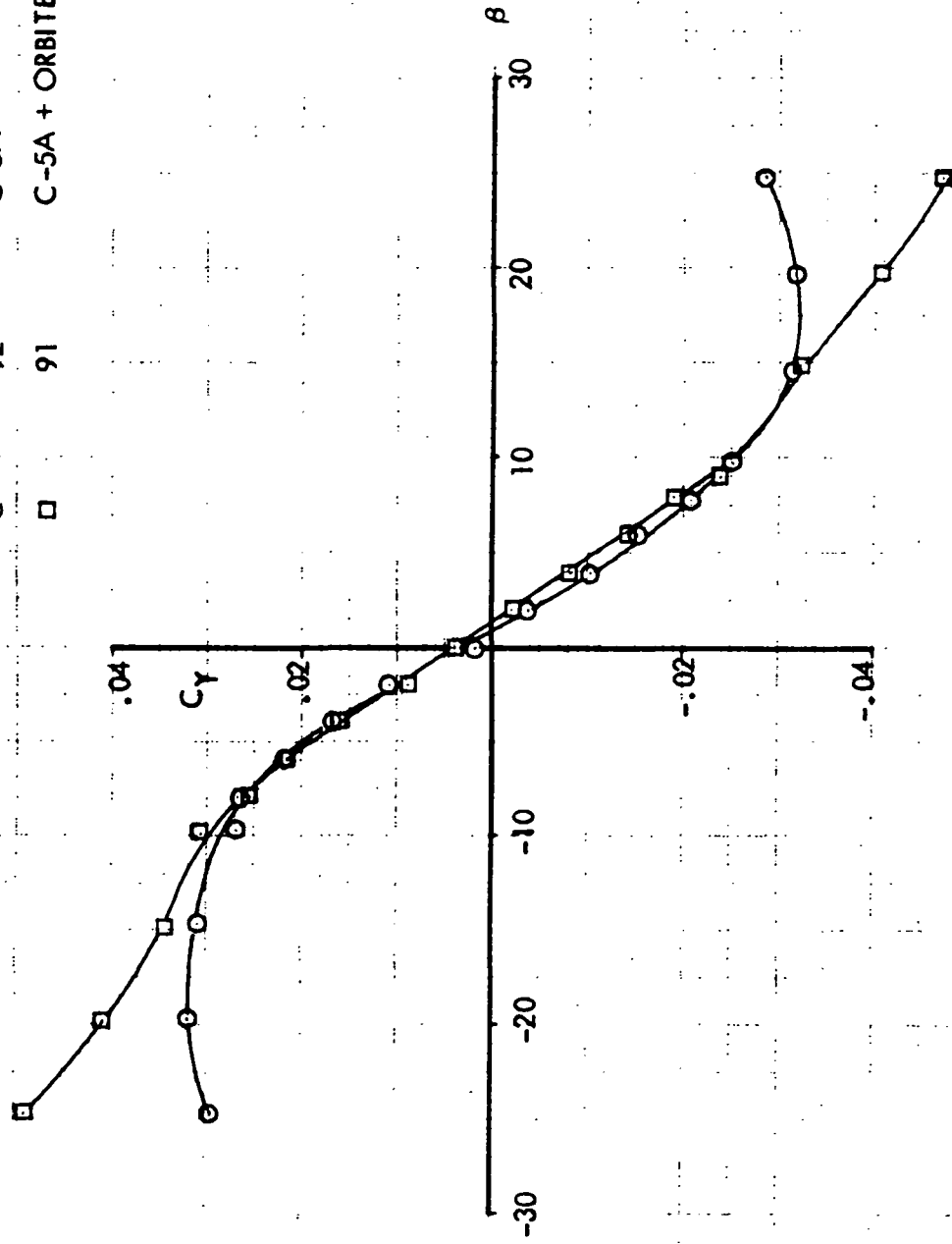


FIGURE 21

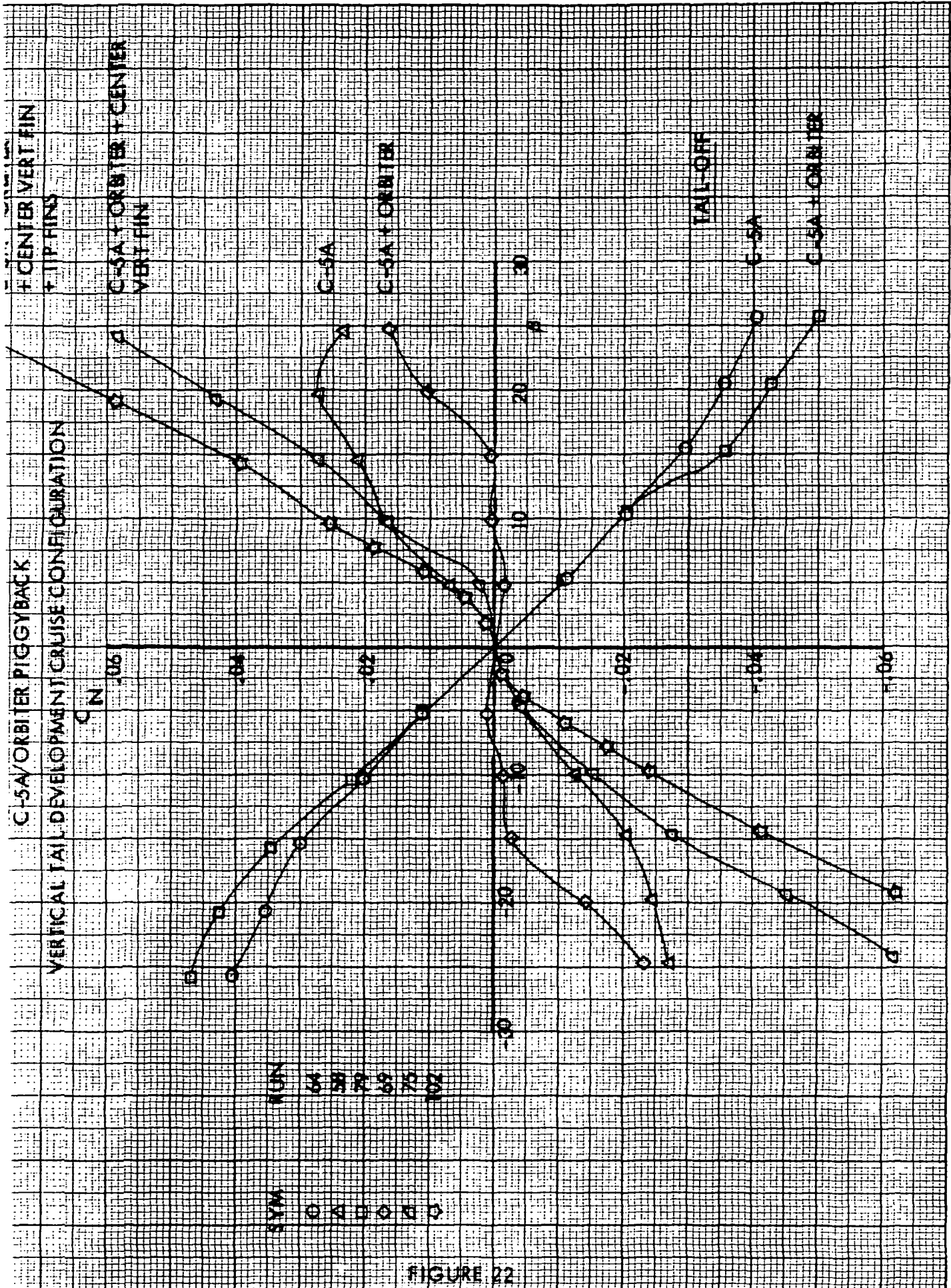


FIGURE 22

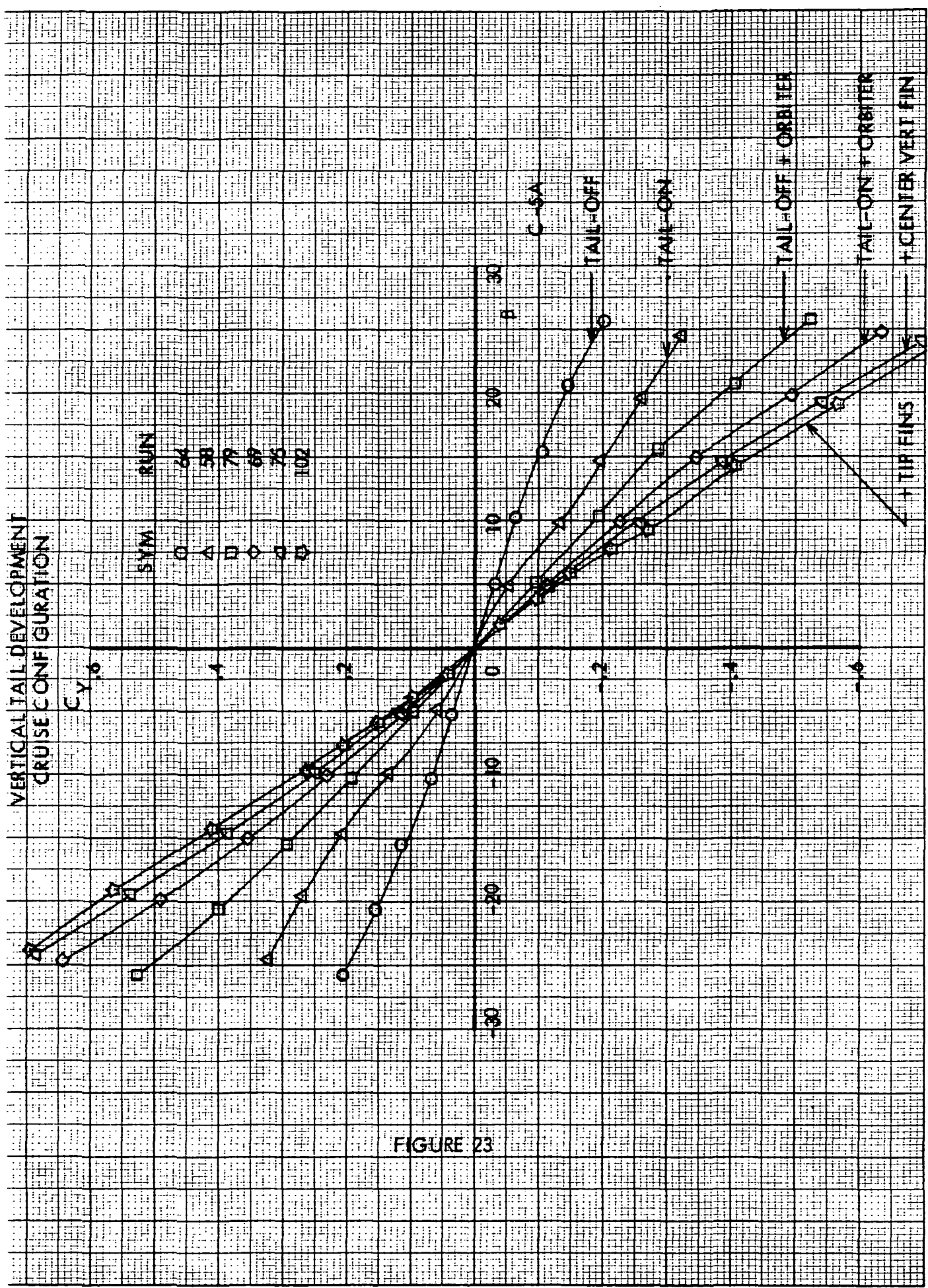


FIGURE 23

16-7

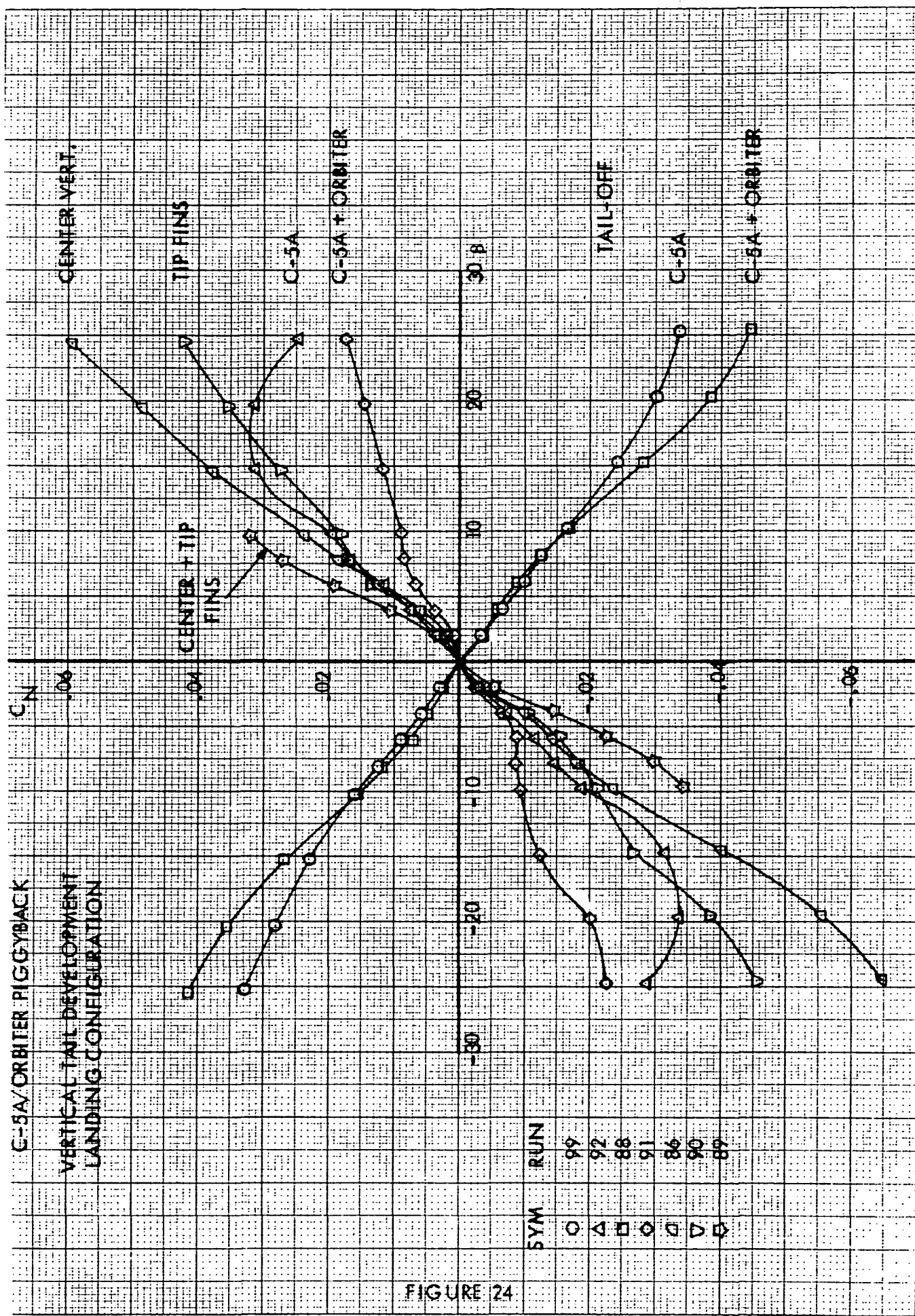


FIGURE 24

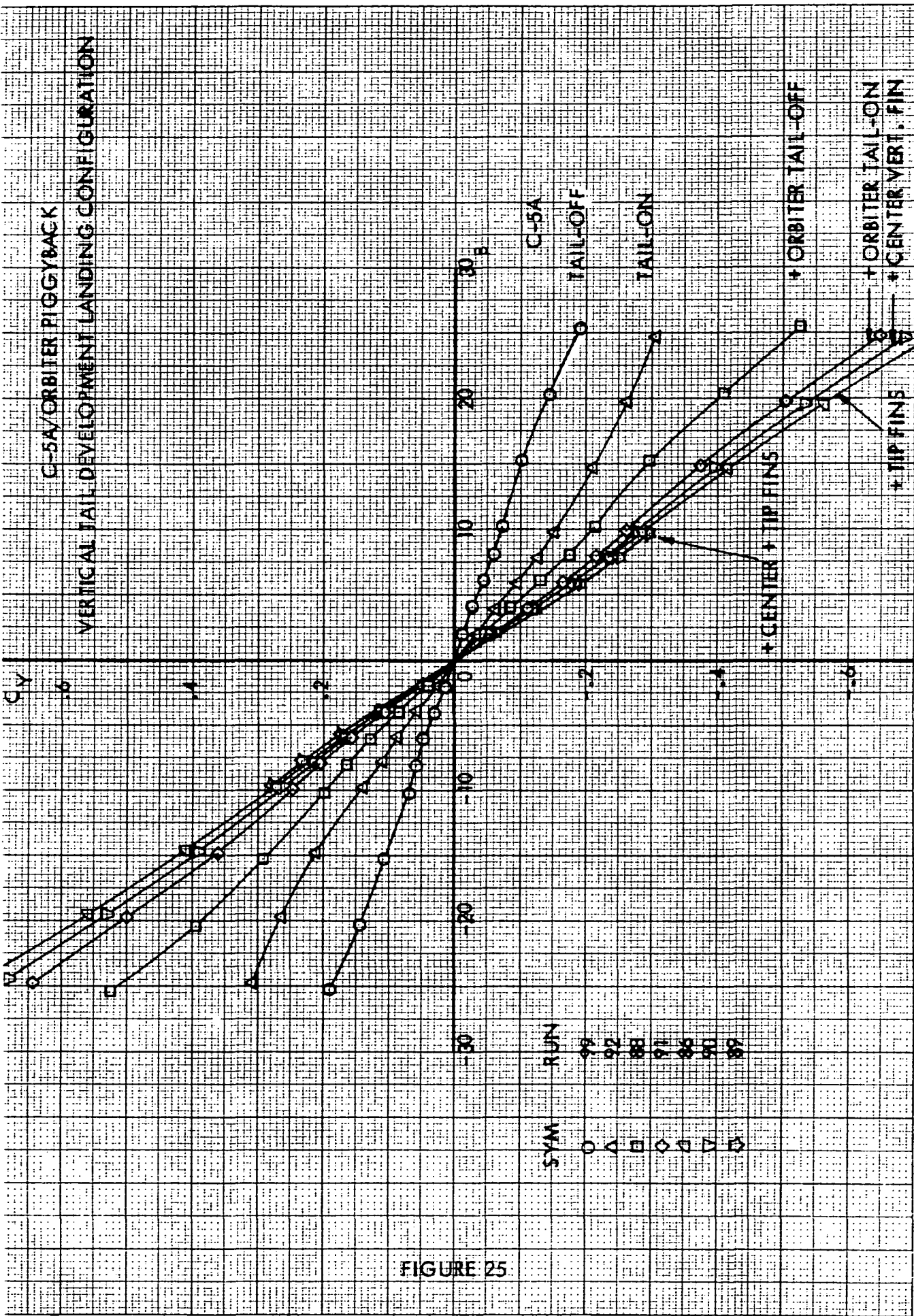


FIGURE 25

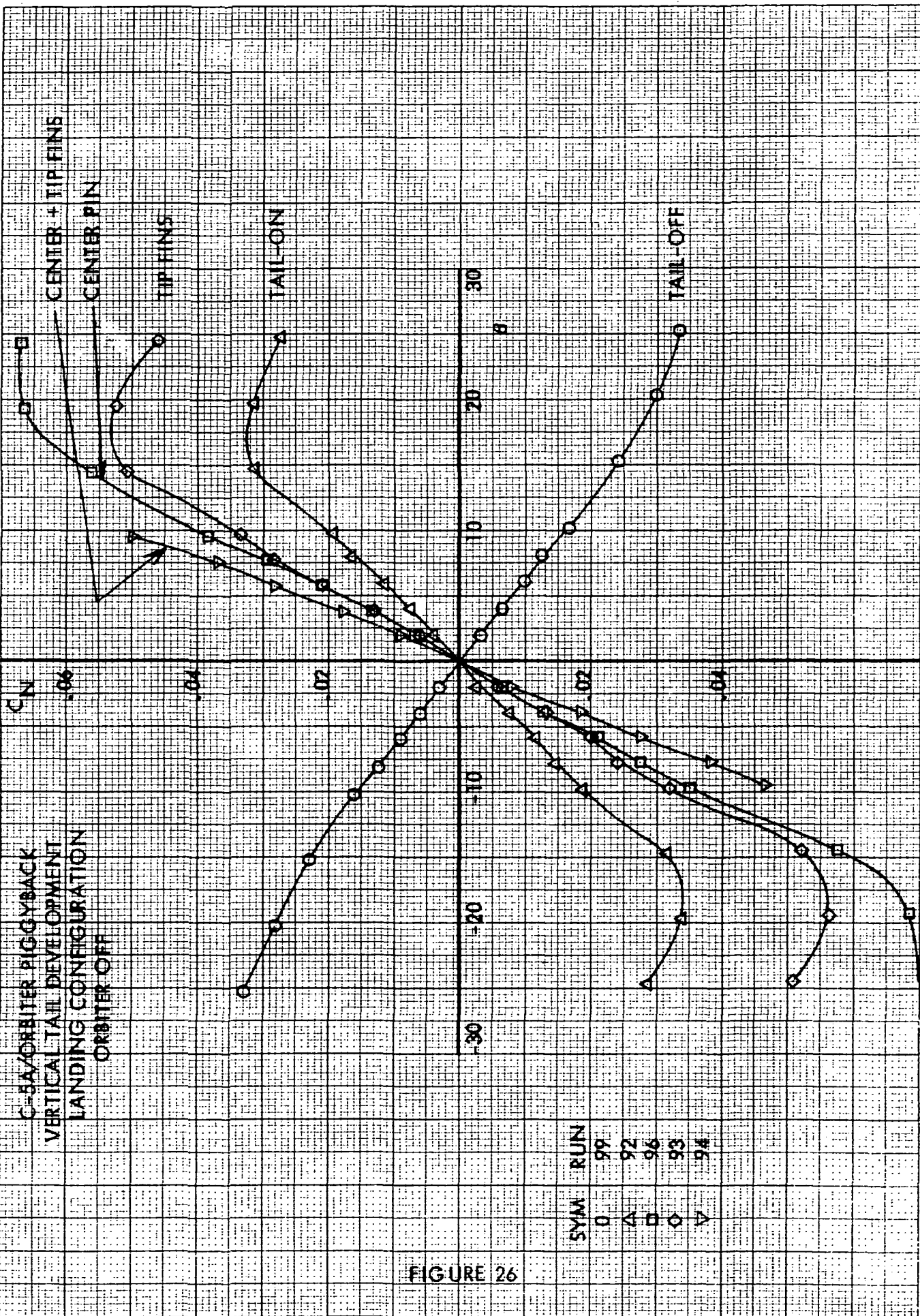


FIGURE 26

C-5A/ORBITER PIGGYBACK
 VERTICAL TAIL DEVELOPMENT
 LANDING CONFIGURATION
 ORBITER OFF

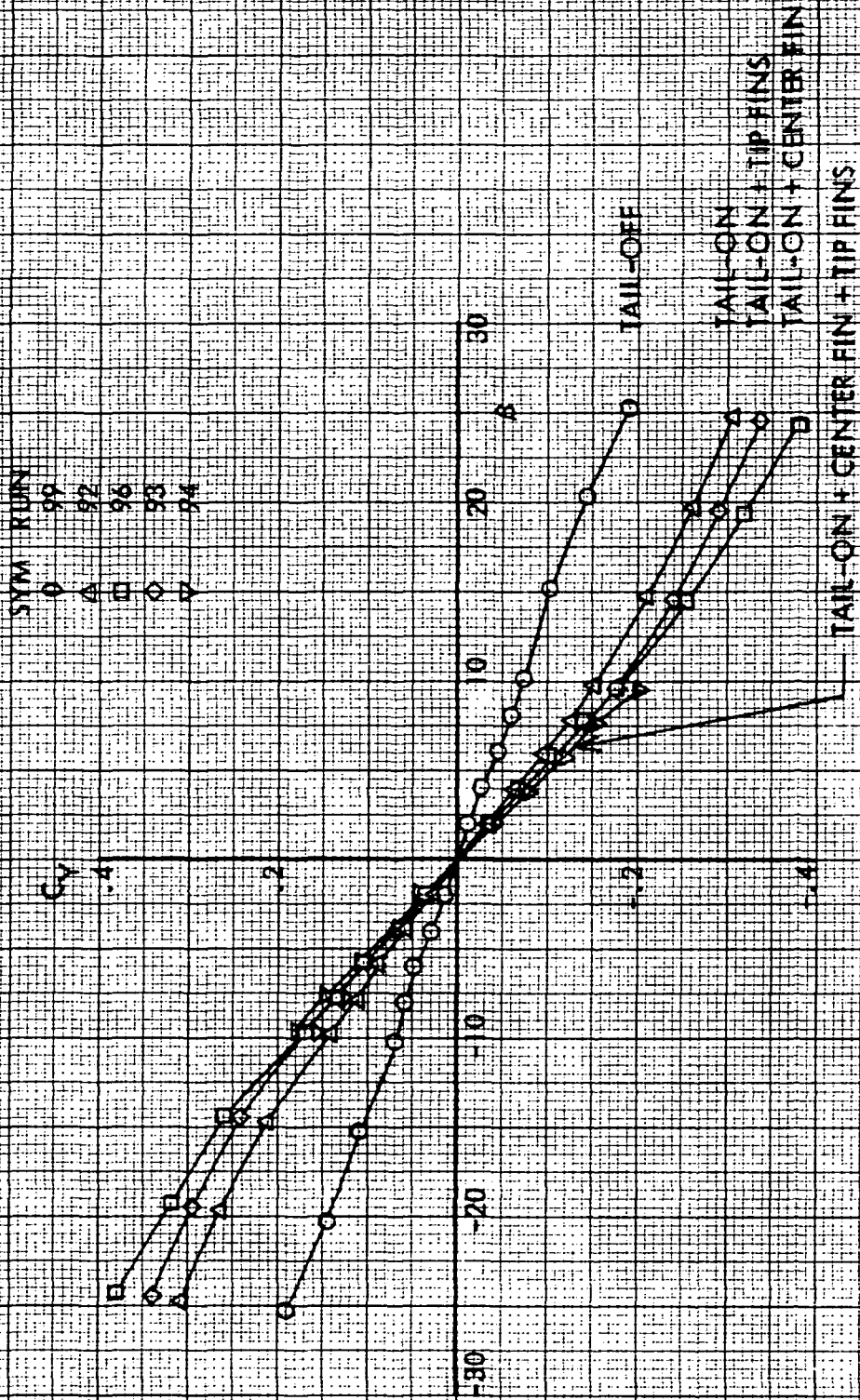


FIGURE 27

C-5A/ORBITER PIGGYBACK

EFFECT OF ORBITER ON LONGITUDINAL TRIM

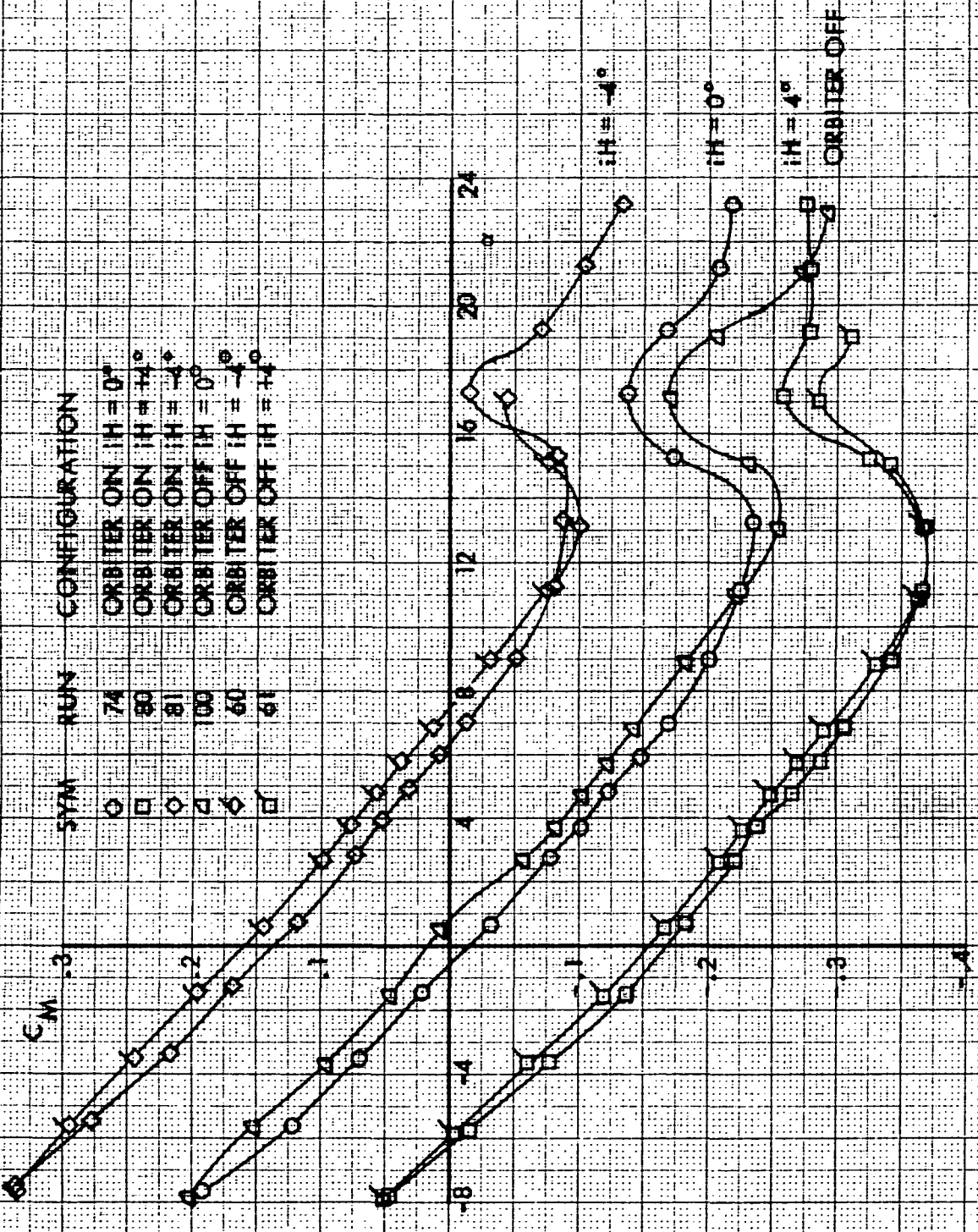


FIGURE 28

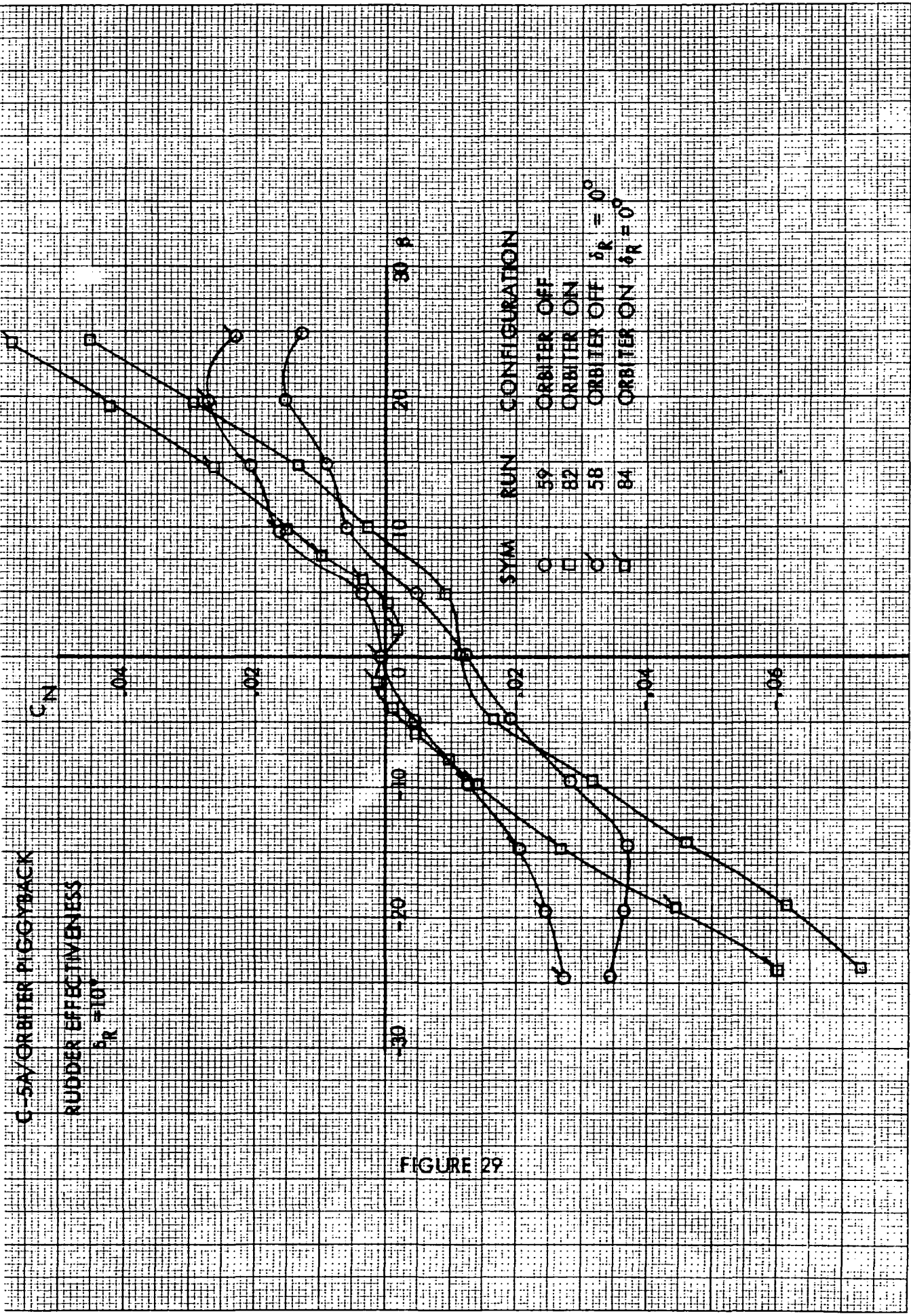
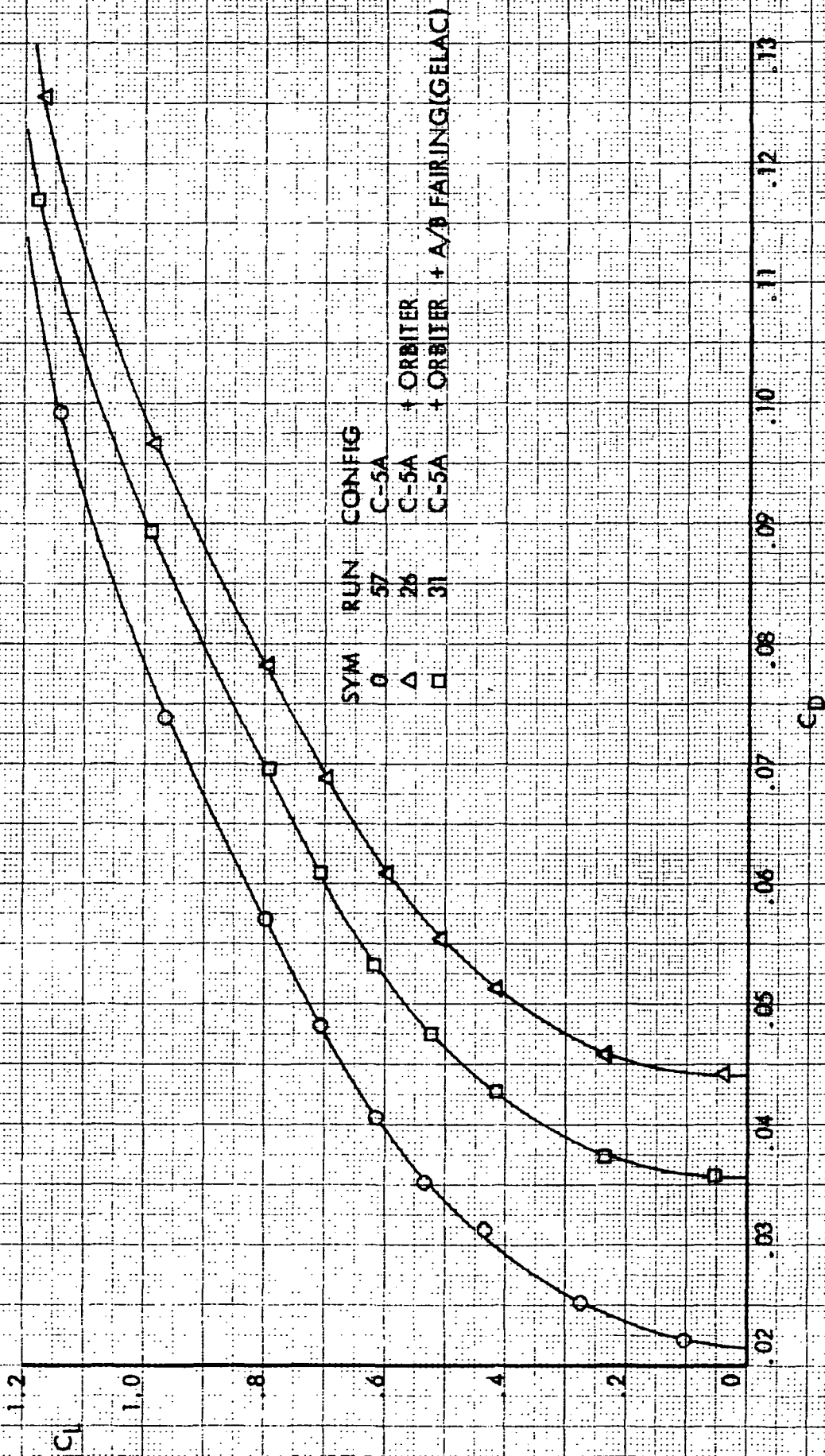


FIGURE 29

C-5/ORBITER PIGGYBACK

EFFECT OF ORBITER ON DRAG

CRUISE CONFIGURATION



SYM	RUN	CONFIG
○	57	C-5A
△	26	C-5A + ORBITER
□	31	C-5A + ORBITER + A/B FAIRING(GELAC)

FIGURE 30

C-5 ORBITER PIGGYBACK

EFFECT OF ORBITER POSITION ON DRAG-CRUISE CONFIGURATION

GELAC A/B FAIRING #1

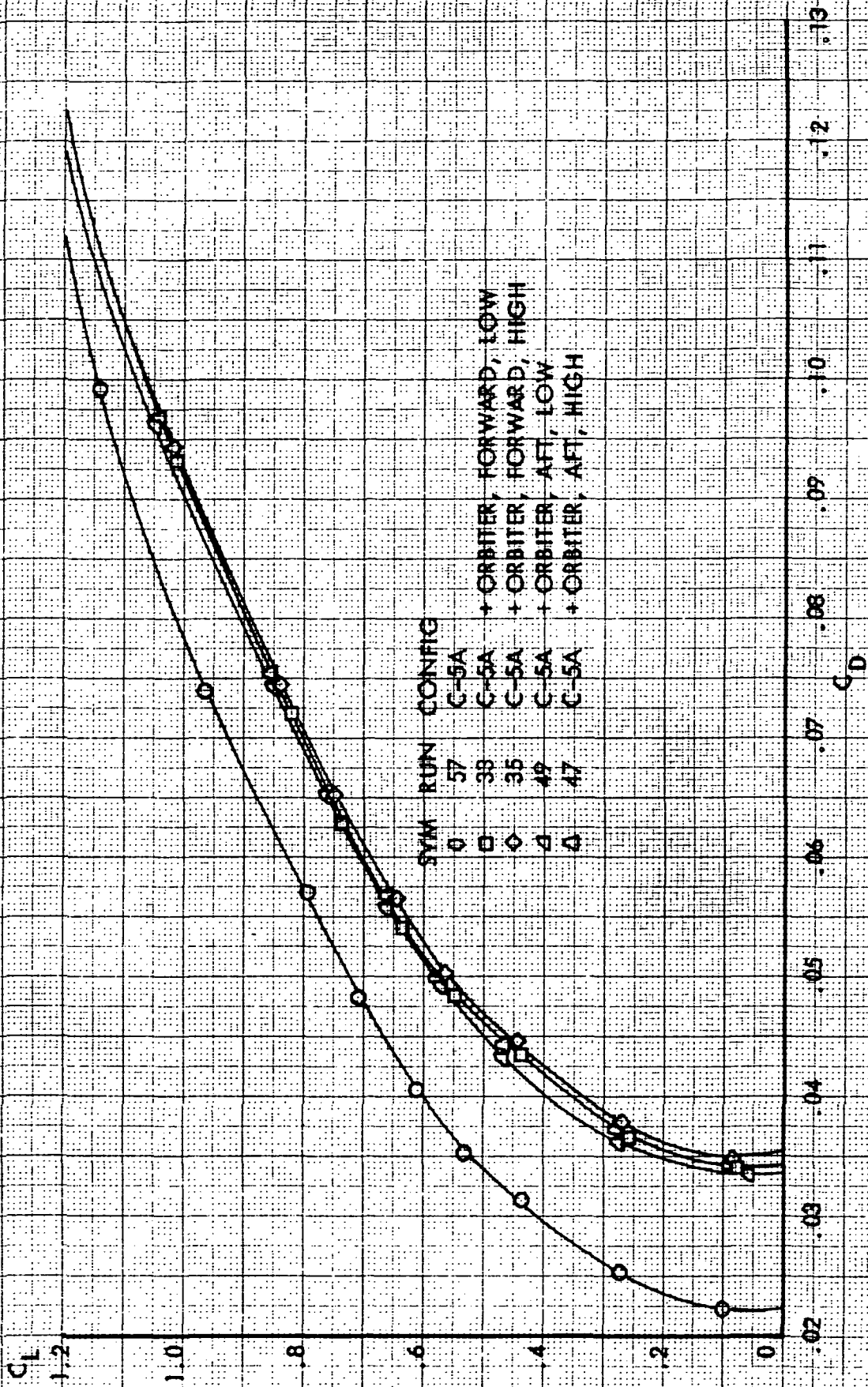


FIGURE 31

C-5/ORBITER PIGGYBACK

EFFECT OF AFTERBODY FAIRING SHAPE ON DRAG-CRUISE CONFIGURATION

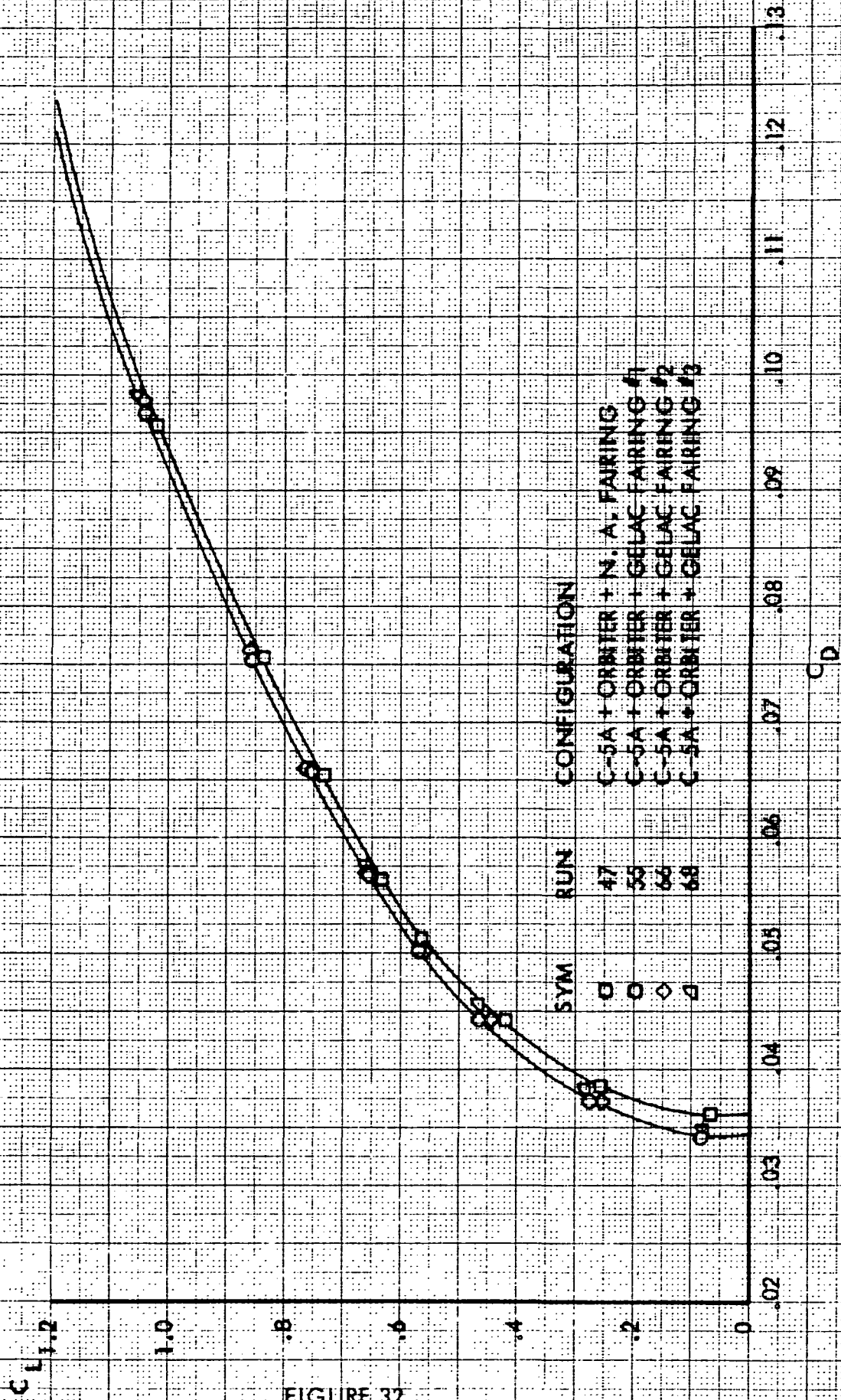


FIGURE 32

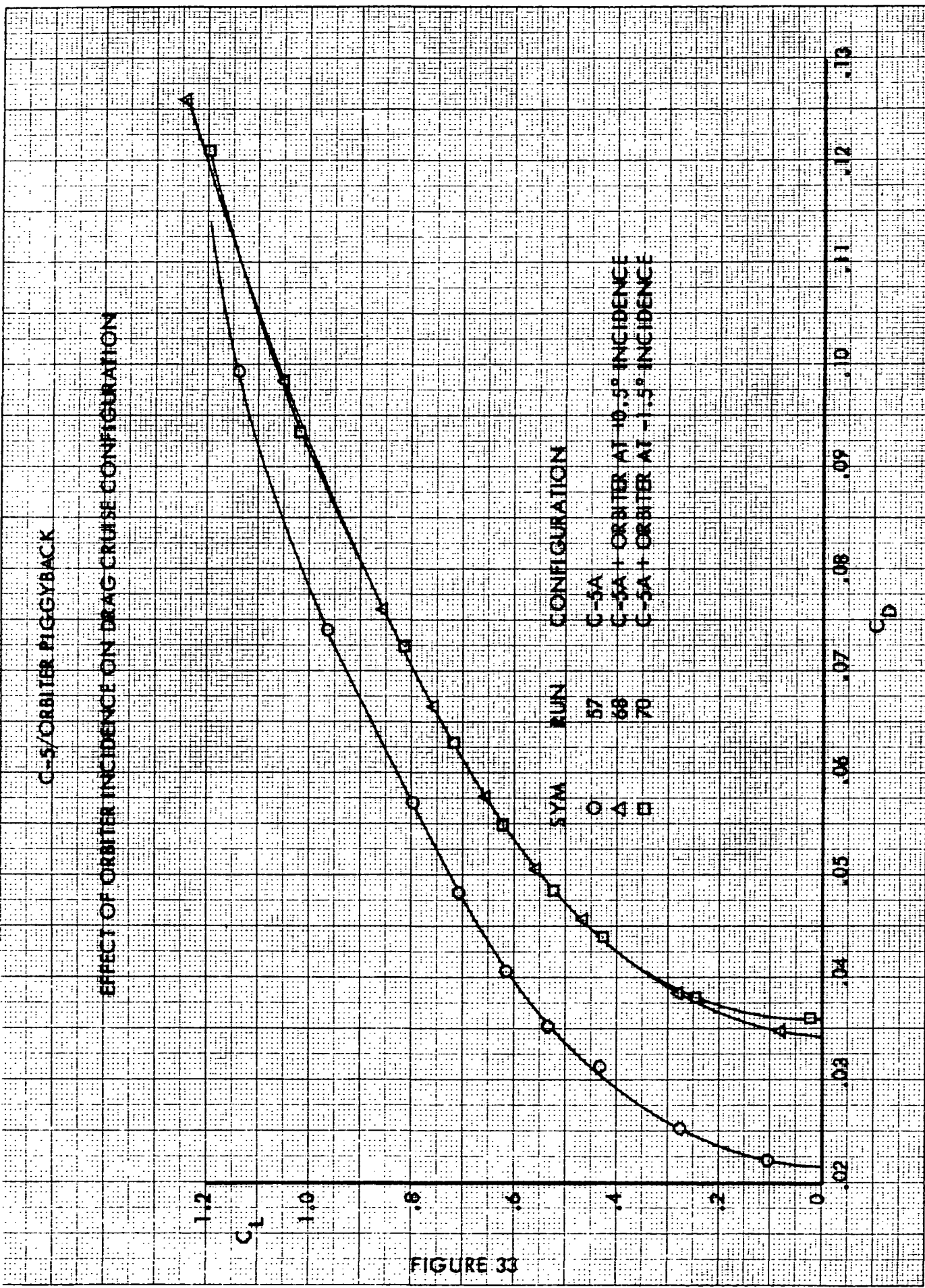


FIGURE 33

COMPARISON OF WIND TUNNEL AND FULL SCALE DIRECTIONAL STABILITY
CRUISE CONFIGURATION, ORBITER OFF

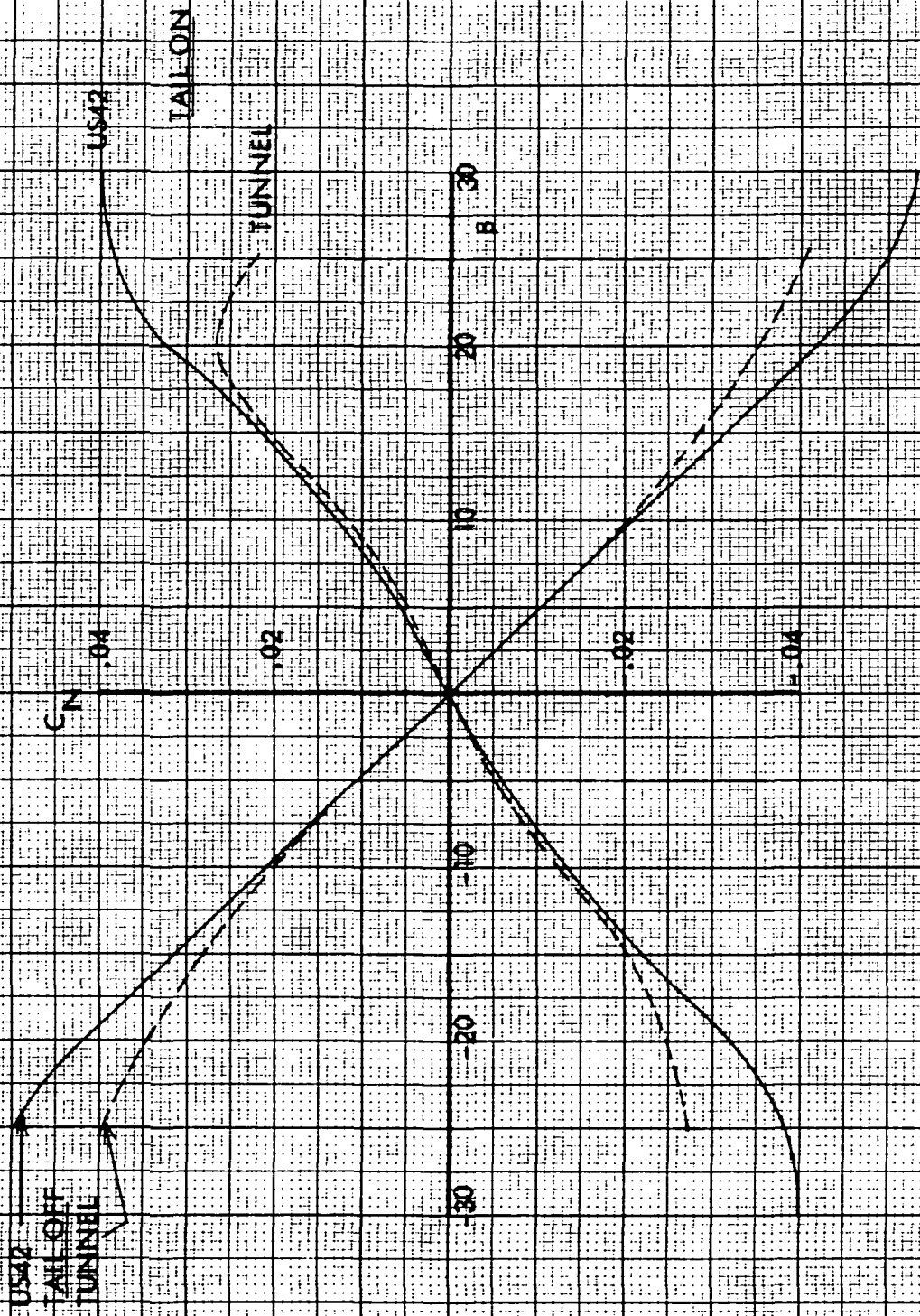


FIGURE 34

COMPARISON OF WIND TUNNEL AND FULL SCALE DIRECTIONAL STABILITY
LANDING CONFIGURATION, ORBITER OFF

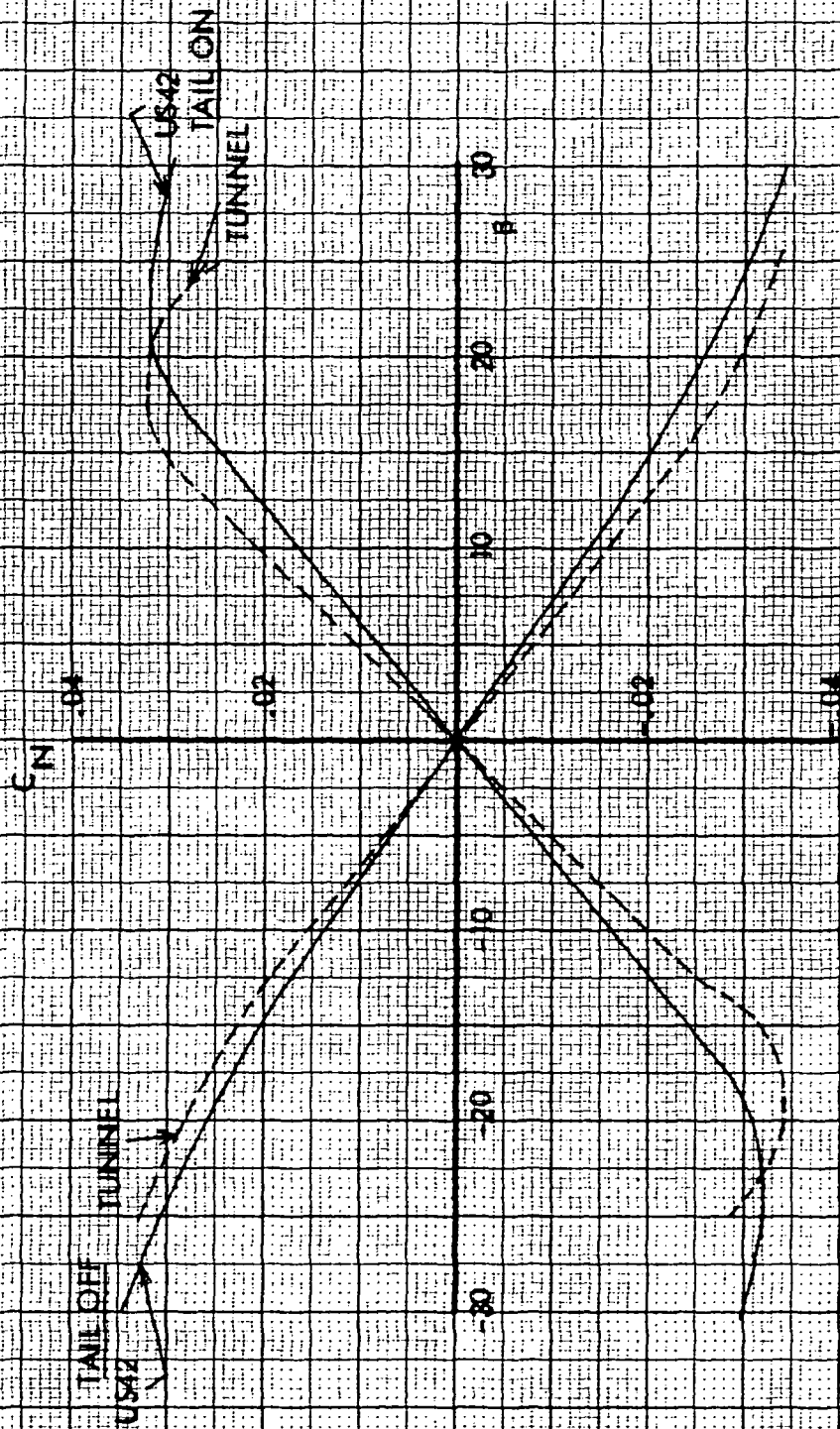


FIGURE 35

C-5A ORBITER PIGGYBACK

PREDICTED FULL SCALE DIRECTIONAL STABILITY

CRUISE CONFIGURATION

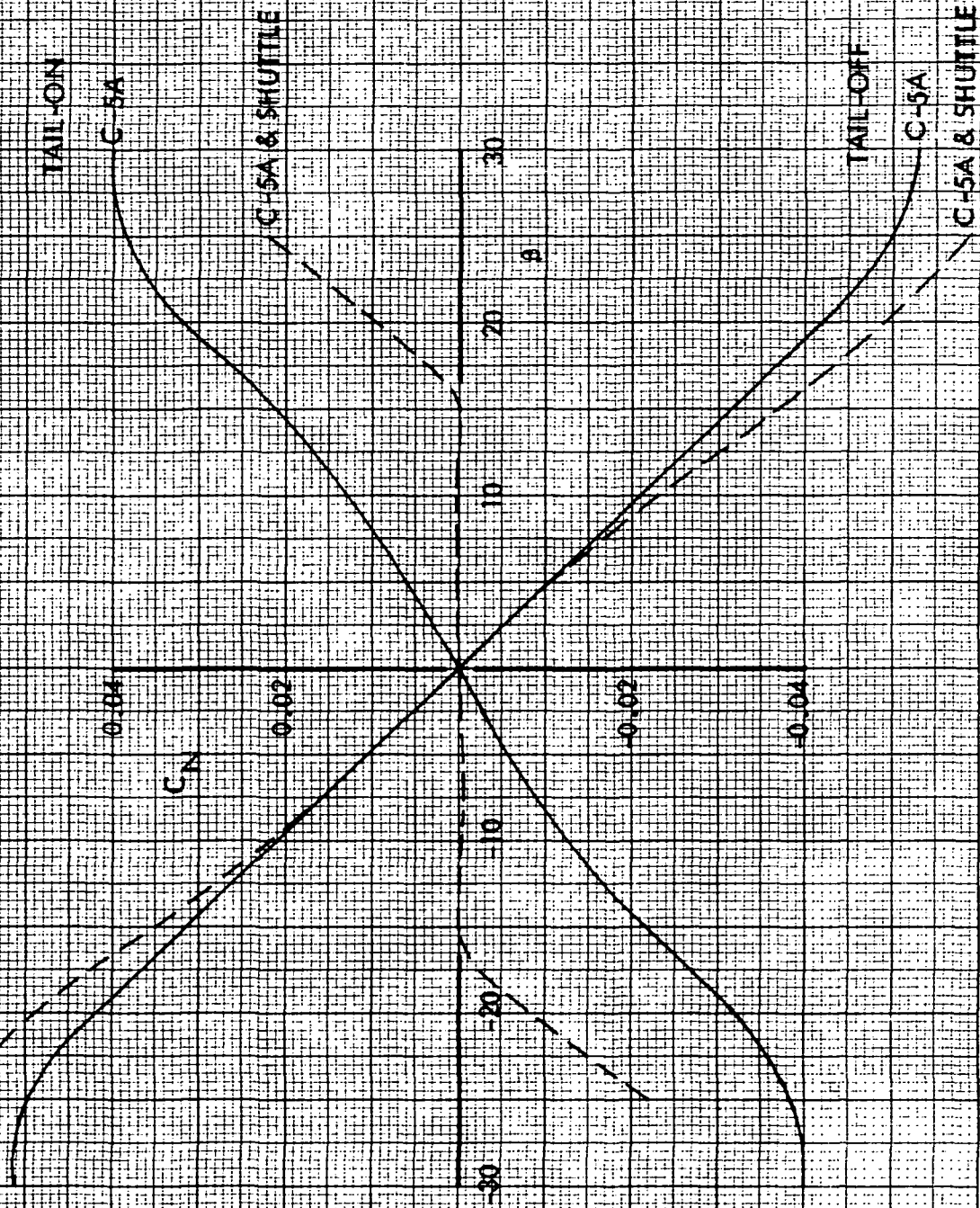


FIGURE 36

C-5A/ORBITER FIGGYBACK

PREDICTED FULL SCALE DIRECTIONAL STABILITY

LANDING CONFIGURATION

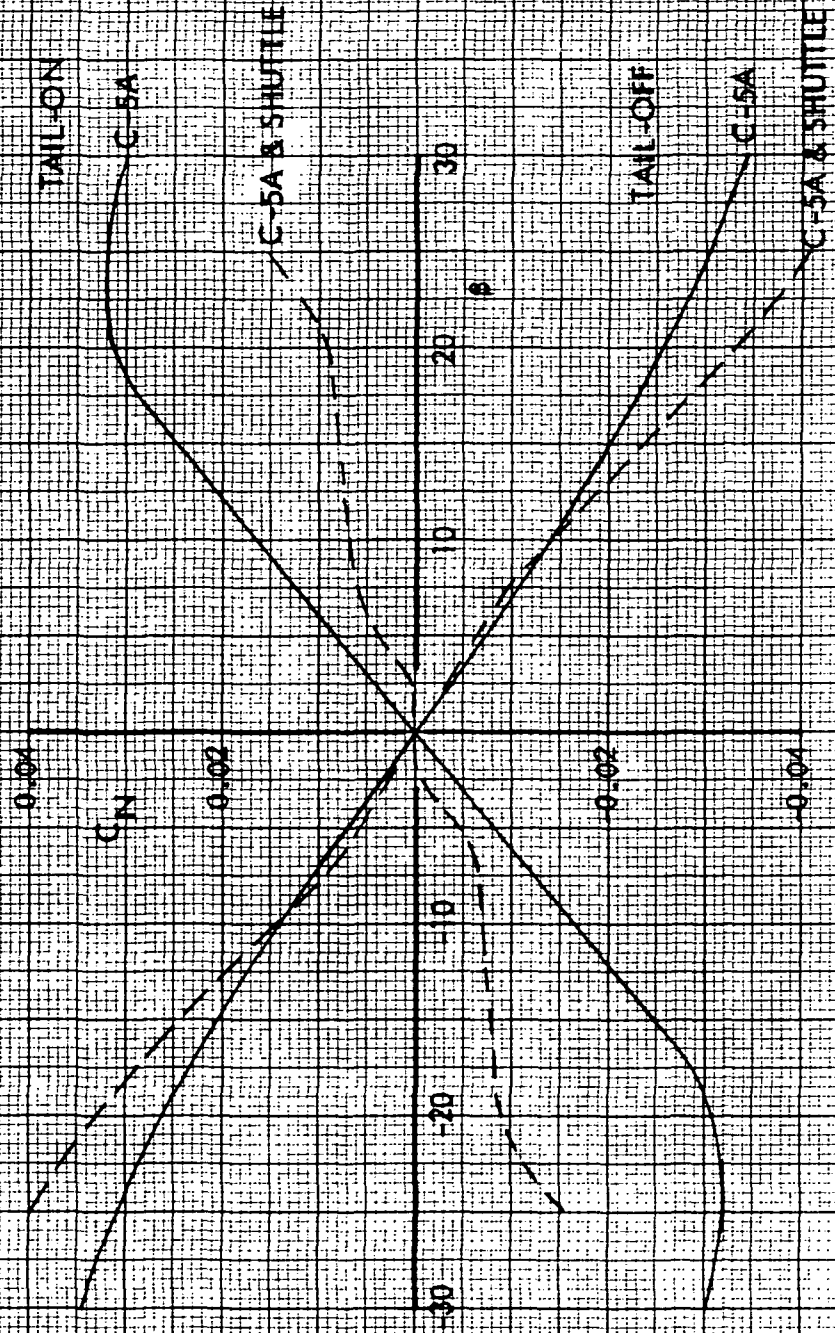


FIGURE 37

C-5A/ORBITER PIGGYBACK FLIGHT VEHICLE DATA

M = 0.52 @ 20,000 ft

$V_T = 319$ KTAS

Wing area, S = 6200 ft²

Wing span, b = 219 ft

FLIGHT CASE		#1	#2	#3
Gross Weight ~ lbs		550,000	704,626	704,626
$I_{xx} \sim \text{slugs ft}^2 \times 10^{-6}$		3.43	3.45	3.89
$I_{zz} \sim \text{slugs ft}^2 \times 10^{-6}$		5.48	6.07	6.11
$I_{xz} \sim \text{slugs ft}^2 \times 10^{-6}$		2.20	2.42	3.97
Stability and Control Derivatives				
Sideslip	$C_{y\beta} \sim /rad.$	-.802	-.802	-1.34
	$C_{l\beta} \sim /rad.$	-.0771	-.0997	-.0997
	$C_{n\beta} \sim /rad.$.0728	.0728	0
Roll rate	$C_{lp} \sim /rad.$	-.390	-.390	-.390
	$C_{np} \sim /rad.$	-.081	-.081	-.081
Yaw rate	$C_{yr} \sim /rad.$.510	.500	.500
	$C_{lr} \sim /rad.$.177	.199	.199
	$C_{nr} \sim /rad.$	-.180	-.180	-.180
Aileron angle	$C_{l\delta_a} \sim /rad.$	-.0319	-.0319	-.0319
	$C_{n\delta_a} \sim /rad.$	0	0	0
Rudder angle	$C_{y\delta_r} \sim /rad.$.2006	.2006	.2006
	$C_{l\delta_r} \sim /rad.$.0210	.0181	.0181
	$C_{n\delta_r} \sim /rad.$	-.1031	-.1031	-.1031
Spoiler angle	$C_{y\delta_s} \sim /rad.$	-.0573	-.0573	-.0573
	$C_{l\delta_s} \sim /rad.$.0268	.0268	.0268
	$C_{n\delta_s} \sim /rad.$.0057	.0057	.0057

FIGURE 38

LATERAL-DIRECTIONAL RESPONSE MODE DATA

Characteristic Equation:

$$(s^2 + 2\zeta_d w_d s + w_d^2) (s + 1/\tau_R) (s + 1/\tau_s) = 0$$

Item or Parameter	Case #1	Case #2	Case #3
G.W. (no payload)	550,000#	550,000#	550,000#
cargo weight	-	154,626#	-
orbiter weight	-	-	154,626#
gross weight	550,000#	704,626#	704,626#
Dutch Roll Mode			
frequency, w_d - rad/sec.	.634	.620	.344
damping ratio, ζ_d	.118	.076	-.023
period, T_d - secs.	9.98	10.2	18.3
time to 1/2-ampl, $t_{1/2}$ - secs.	9.18	14.6	-89
cycles 1/2-ampl, $C_{1/2}$.92	1.44	-4.9
Roll Convergence Mode			
time constant, τ_R - secs	1.45	1.42	1.35
time to 1/2-ampl, $t_{1/2}$ - secs	1.0	.98	.93
Spiral Mode			
time constant, τ_s - secs	694	216	15.2
time to 1/2-ampl, $t_{1/2}$ - secs	479	149	10.5

NOTE: Negative values signify an unstable dutch roll mode.

FIGURE 39

C-5A STABILITY AUGMENTATION &
AUTOPILOT SYSTEMS APPROXIMATIONS

Stability Augmentation Elements

Aileron: $\delta_a = 0.055 (\phi)$

Spoiler: $\delta_s = 0$

Rudder: $\delta_r = -.482(p) - .101(\phi) + 1.0 (r)$

Incremental Elements for Autopilot Operative*

Aileron: $\Delta \delta_a = 2.25 (p) + 3.22 (\phi)$

Spoiler: $\Delta \delta_s = -.786 (\phi)$

Rudder: $\Delta \delta_r = 0$

* Control command and heading stability ($\phi < 7^\circ$) elements are excluded.

FIGURE 40

C-5/ORBITER PIGGYBACK

FLIGHT VEHICLE LATERAL RESPONSE COMPARISON
FOR A 30 KTAS SIDE-GUST DISTURBANCE (SAS ON)

GW = 704,626 LB

M = 0.52

ALT = 20,000 FT

————— BASIC C-5A

————— C-5A + ORBITER

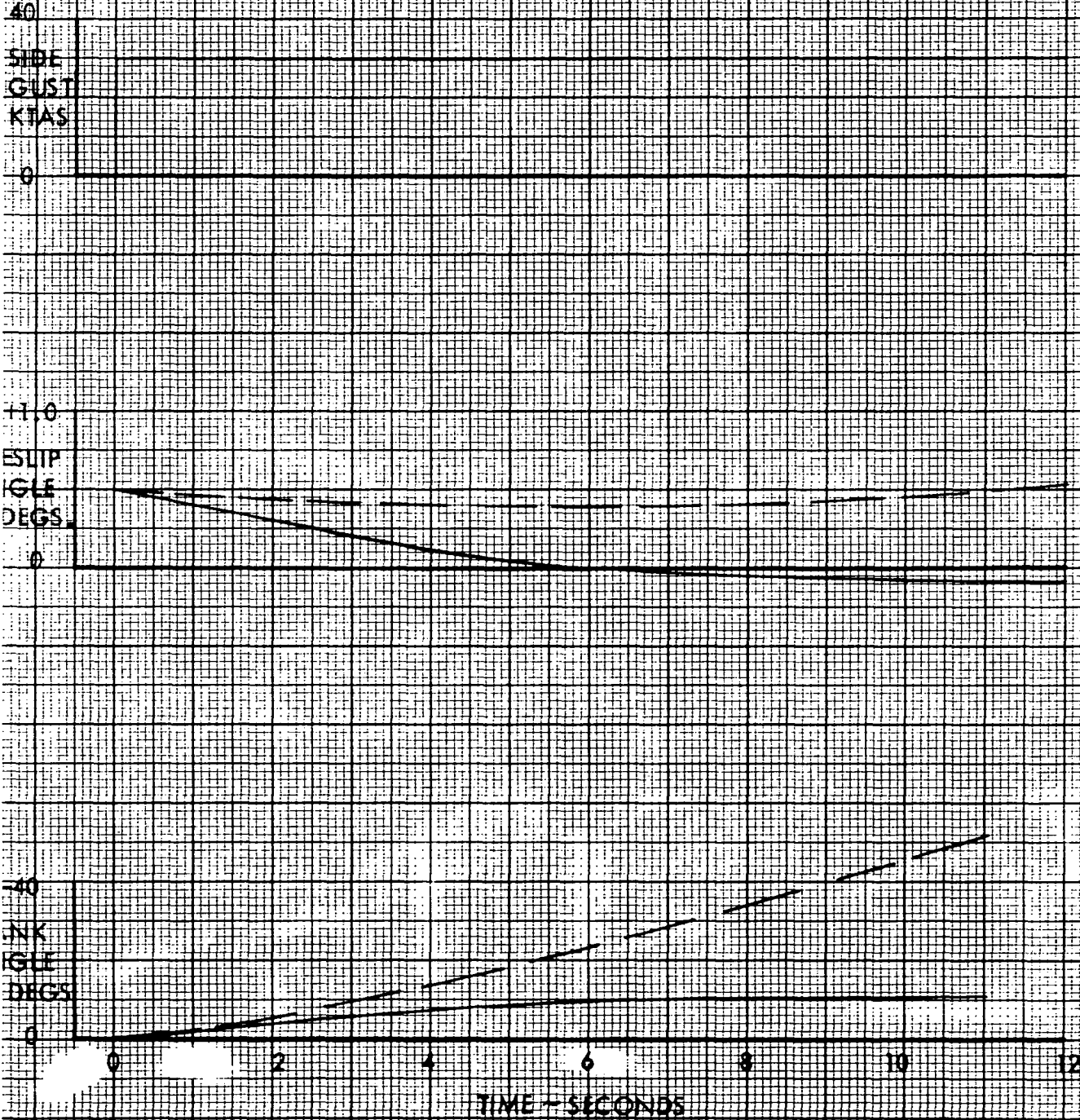


FIGURE 41

C-5A/ORBITER PIGGYBACK

FLIGHT VEHICLE RESPONSE COMPARISON FOR CONTROL WHEEL INPUT OF 10 DEGREES (SAS ON)

G.W. = 704,526 LB.

M = 0.52

ALT = 20,000 FT.

— BASIC C-5A

— C-5A + ORBITER

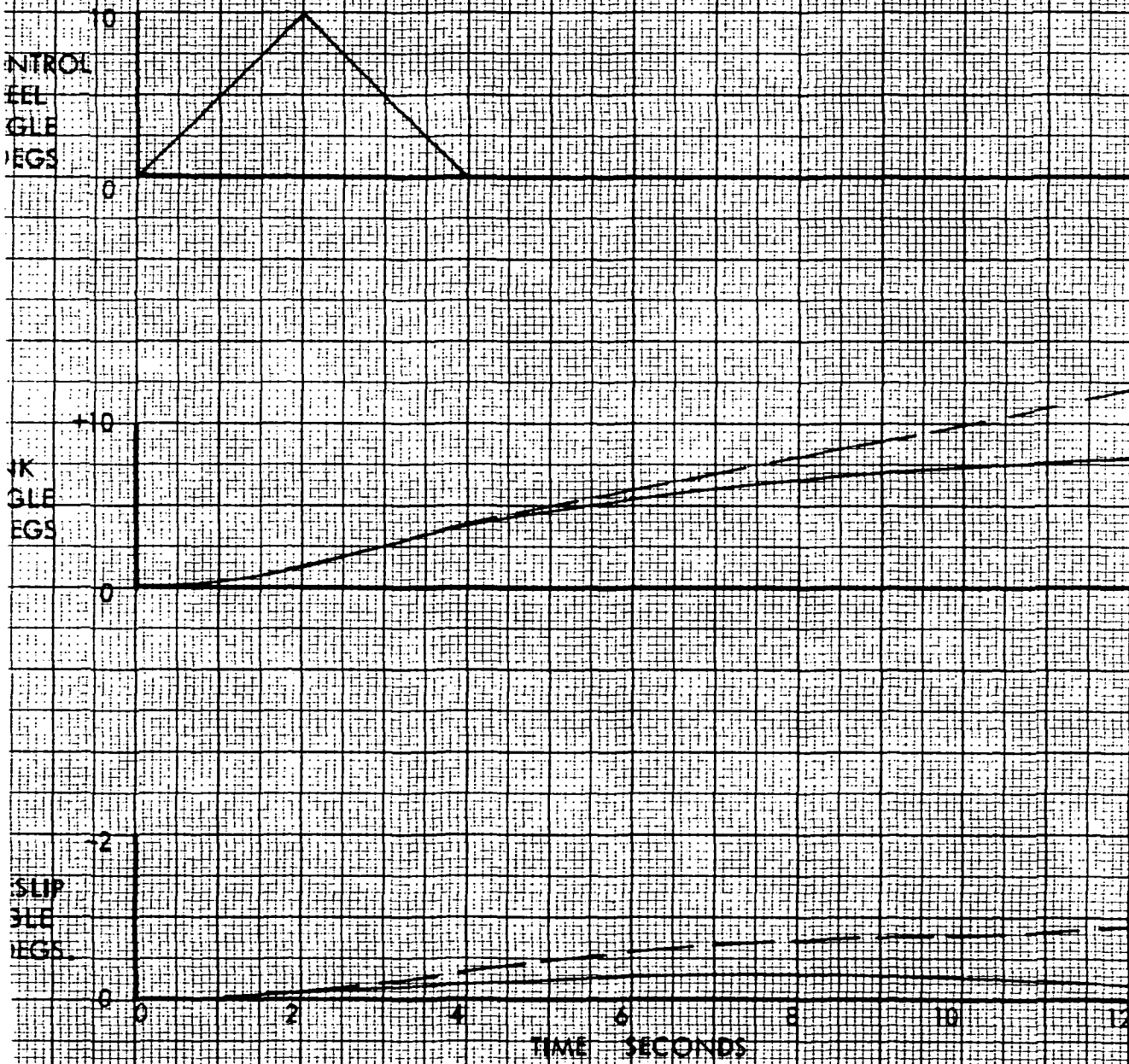


FIGURE 42

C-5A/ORBITER RIGGYBACK

FLIGHT VEHICLE LATERAL RESPONSE COMPARISON
FOR A 30 KTAS SIDE-GUST DISTURBANCE (SAS AND AUTORILIOT ON)

G.W. = 704,826 LB.

M = 0.52

ALT = 20,000 FT

— BASIC C-5A

— C-5A + ORBITER

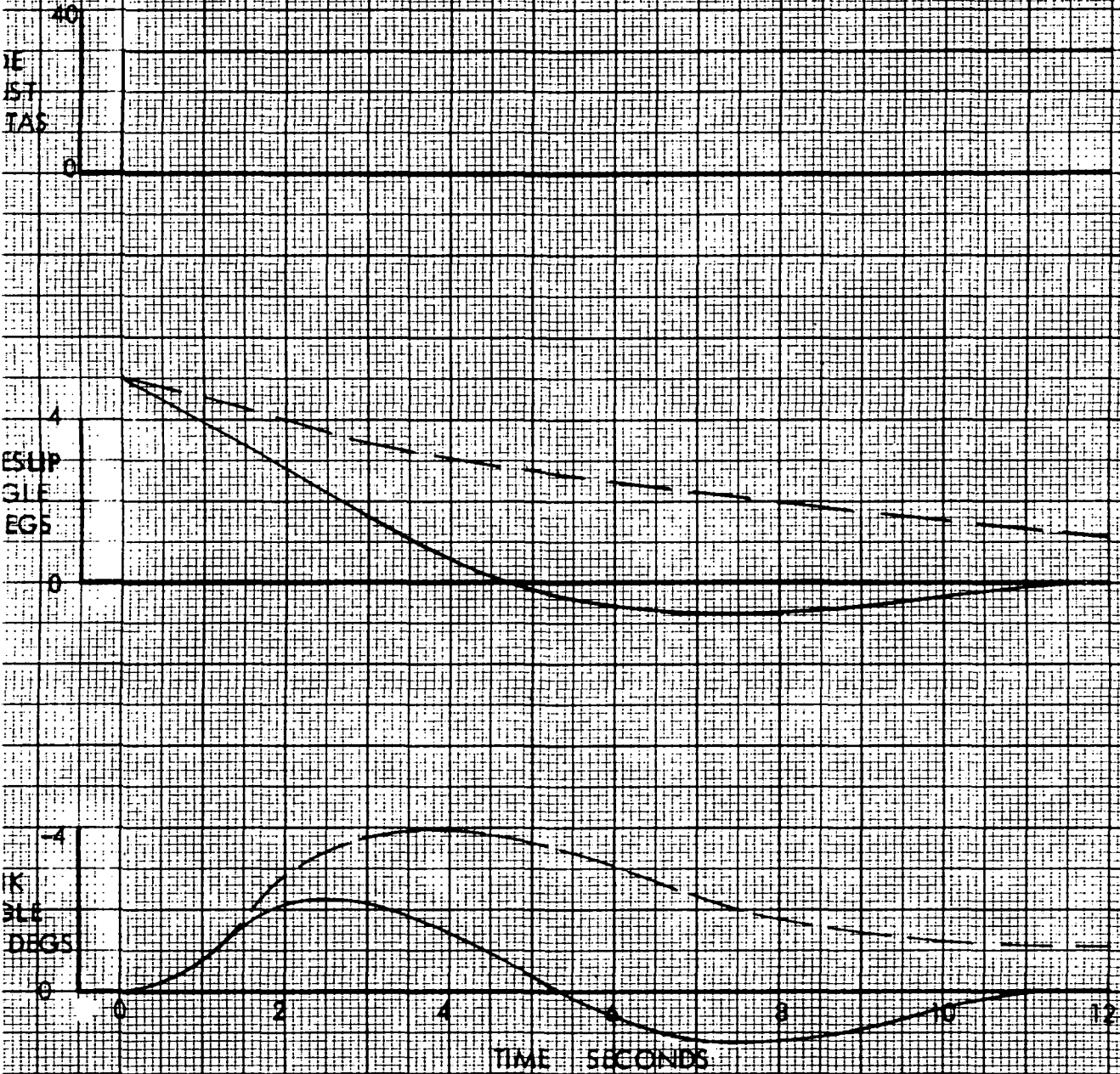


FIGURE 43

C-5/ORBITER FIGGYBACK

COMPARISON OF ESTIMATED AND WIND TUNNEL TEST DRAG POLARS

CRUISE CONFIGURATION

TEST $R_{\infty} = 1.4 \times 10^5$ / FT

- RUN 57, CLEAN CONFIGURATION C-5
- RUN 31, C-5 PLUS ORBITER
- ESTIMATED C-5 PLUS ORBITER

NOTE: ESTIMATED DRAG = RUN 57 DATA PLUS $\Delta C_{D, ORB}$ FROM PUBLISHED ORBITER ALONE TEST DATA

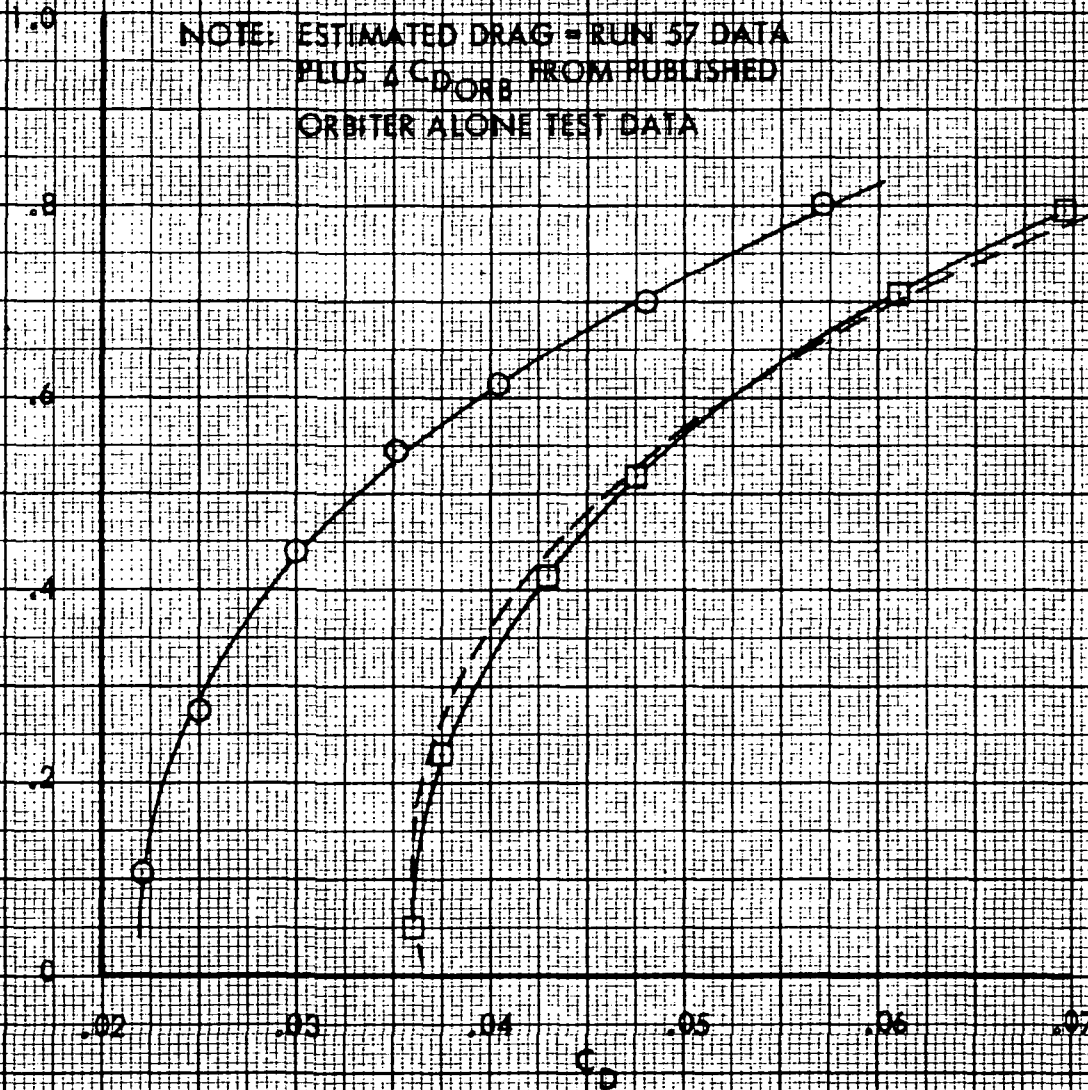


FIGURE 44

C-5/ORBITER PIGGYBACK

COMPARISON OF L/D FOR THE C-5 AND C-5/ORBITER PIGGYBACK

$M = 0.6$

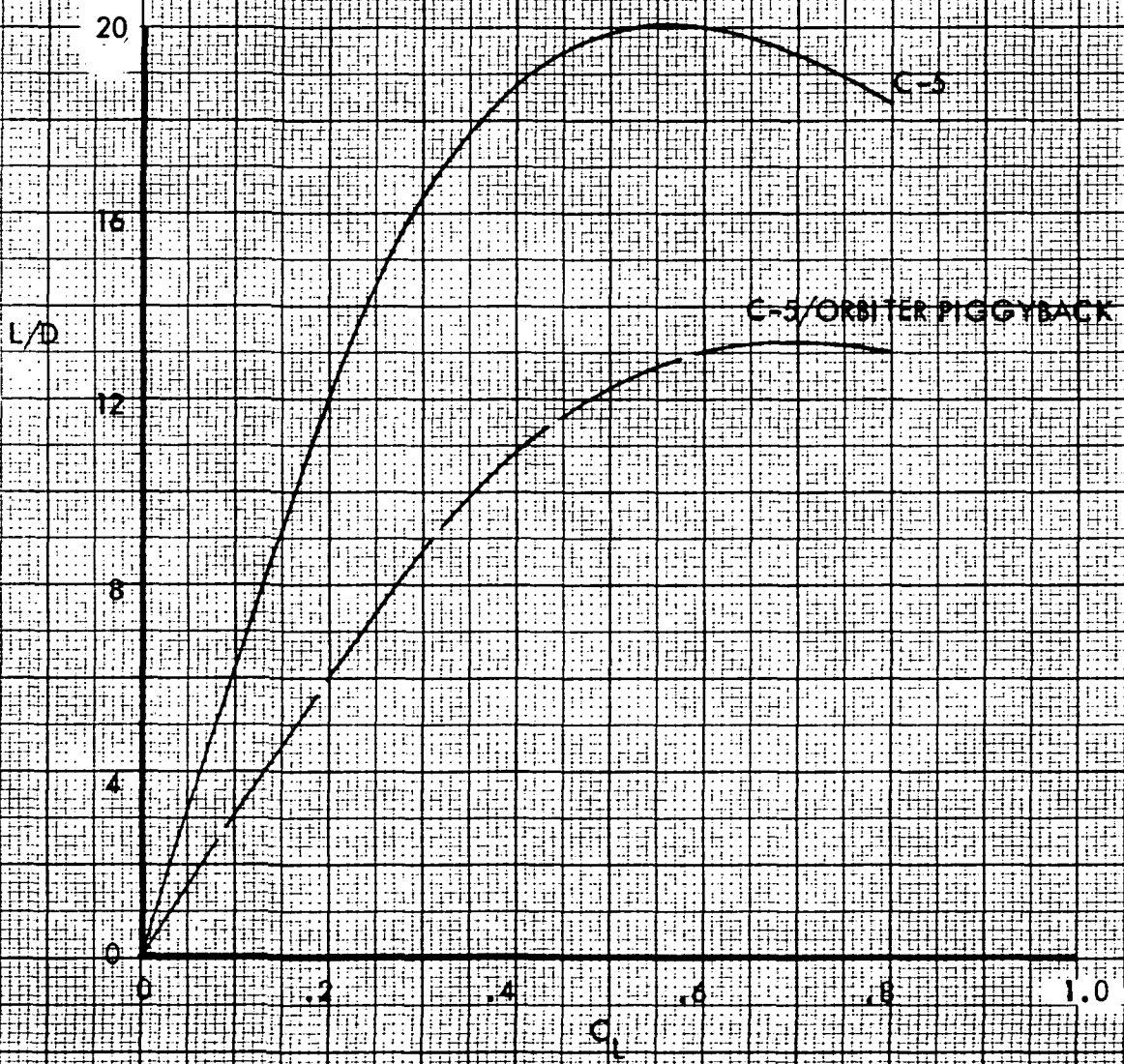


FIGURE 45

C-5/ORBITER PIGGYBACK

COMPARISON OF ESTIMATED AND WIND TUNNEL TEST DRAG POLARS LANDING CONFIGURATION

FLAPS = 40°

TEST $R_N = 1.4 \times 10^6 / FT$

- RUN 95 - C-5
- RUN 85 - C-5 PLUS ORBITER
- ESTIMATED C-5 PLUS ORBITER

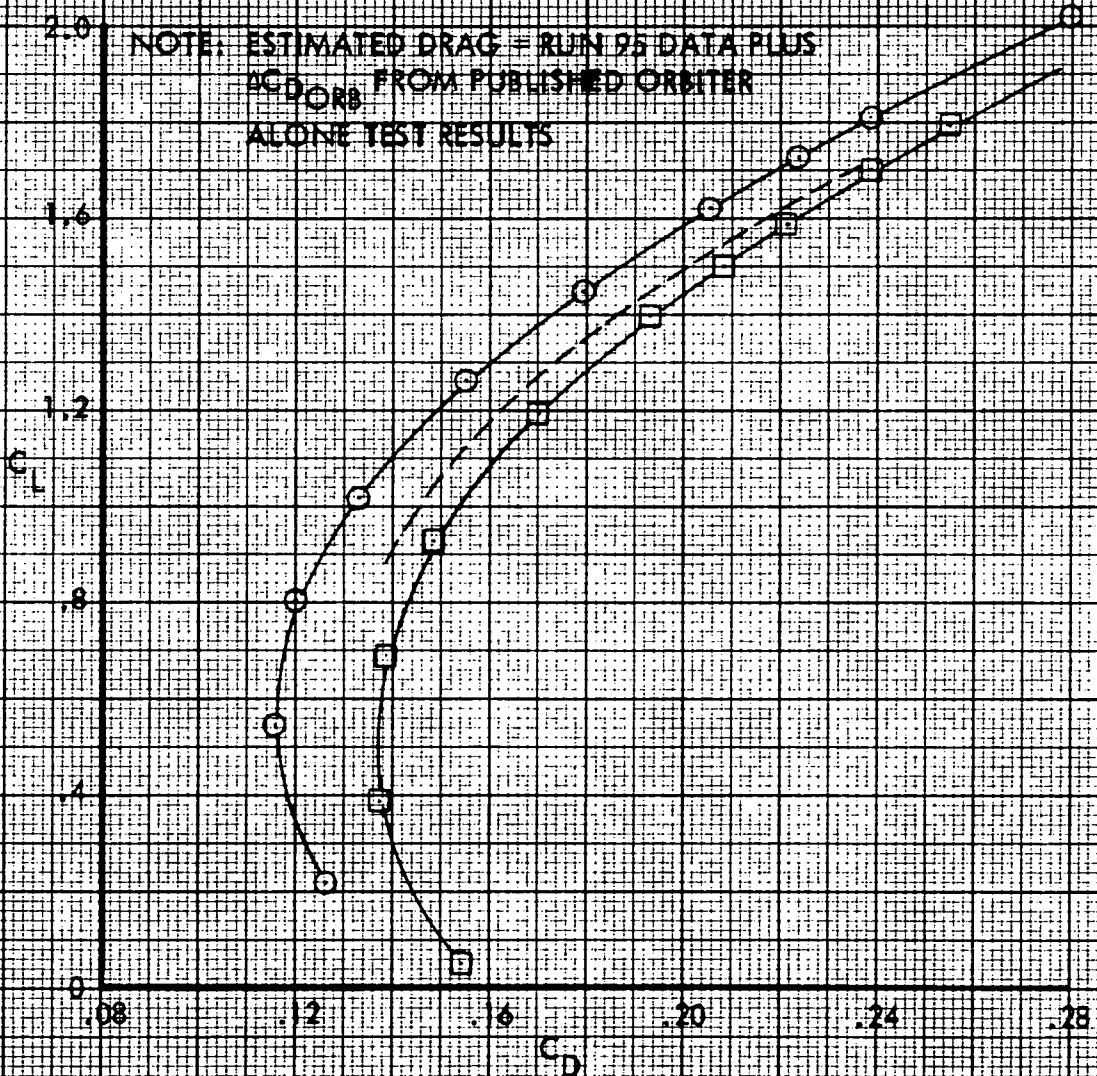


FIGURE 46

FIGURE 46

C-5/ORBITER PIGGYBACK
TAKEOFF DISTANCES

STD DAY

2000 FT

FLAPS - 16°

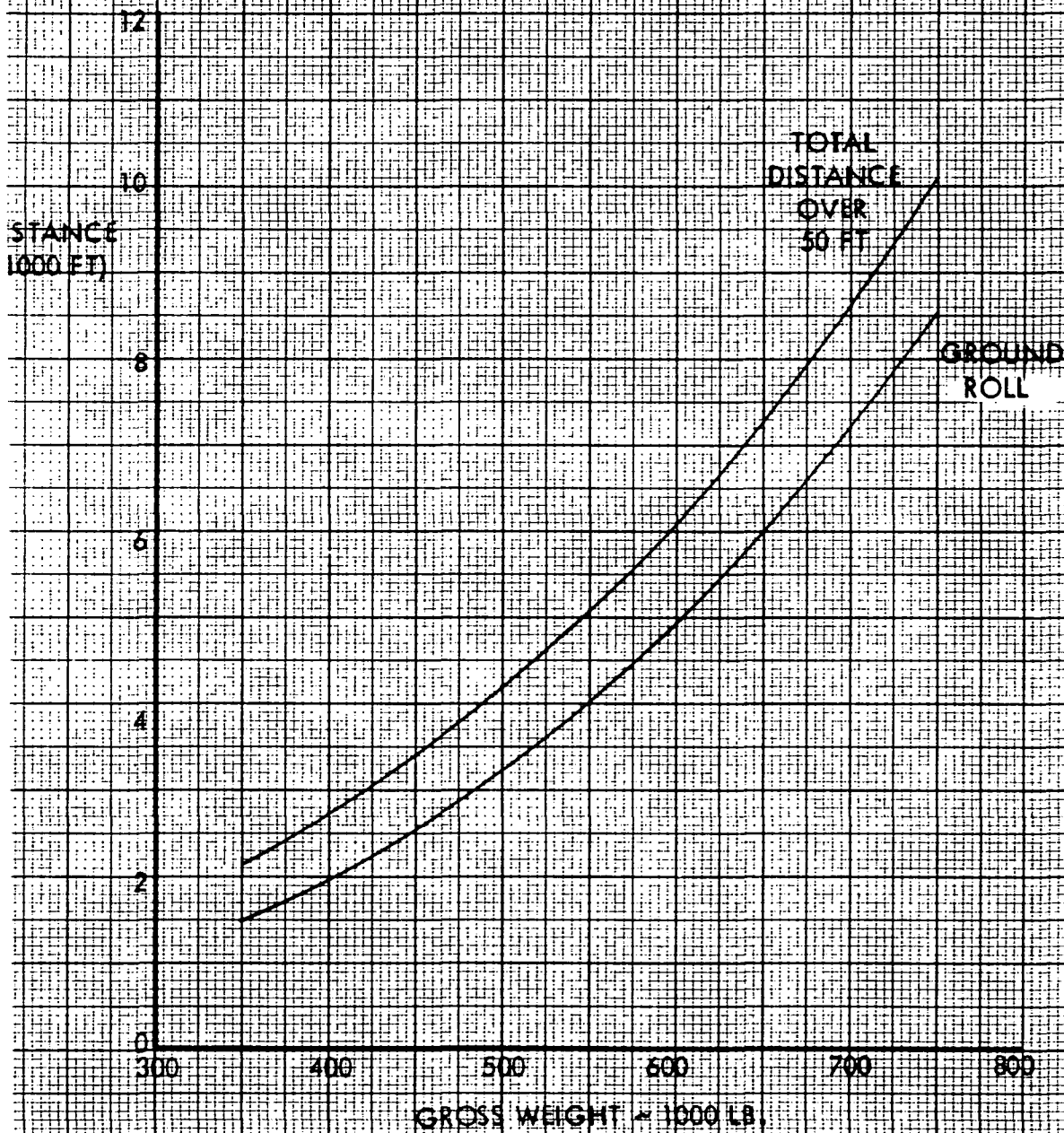


FIGURE 47

C-5/ORBITER PIGGYBACK LANDING DISTANCES

STD DAY
2000 FT.
FLAPS = 40°

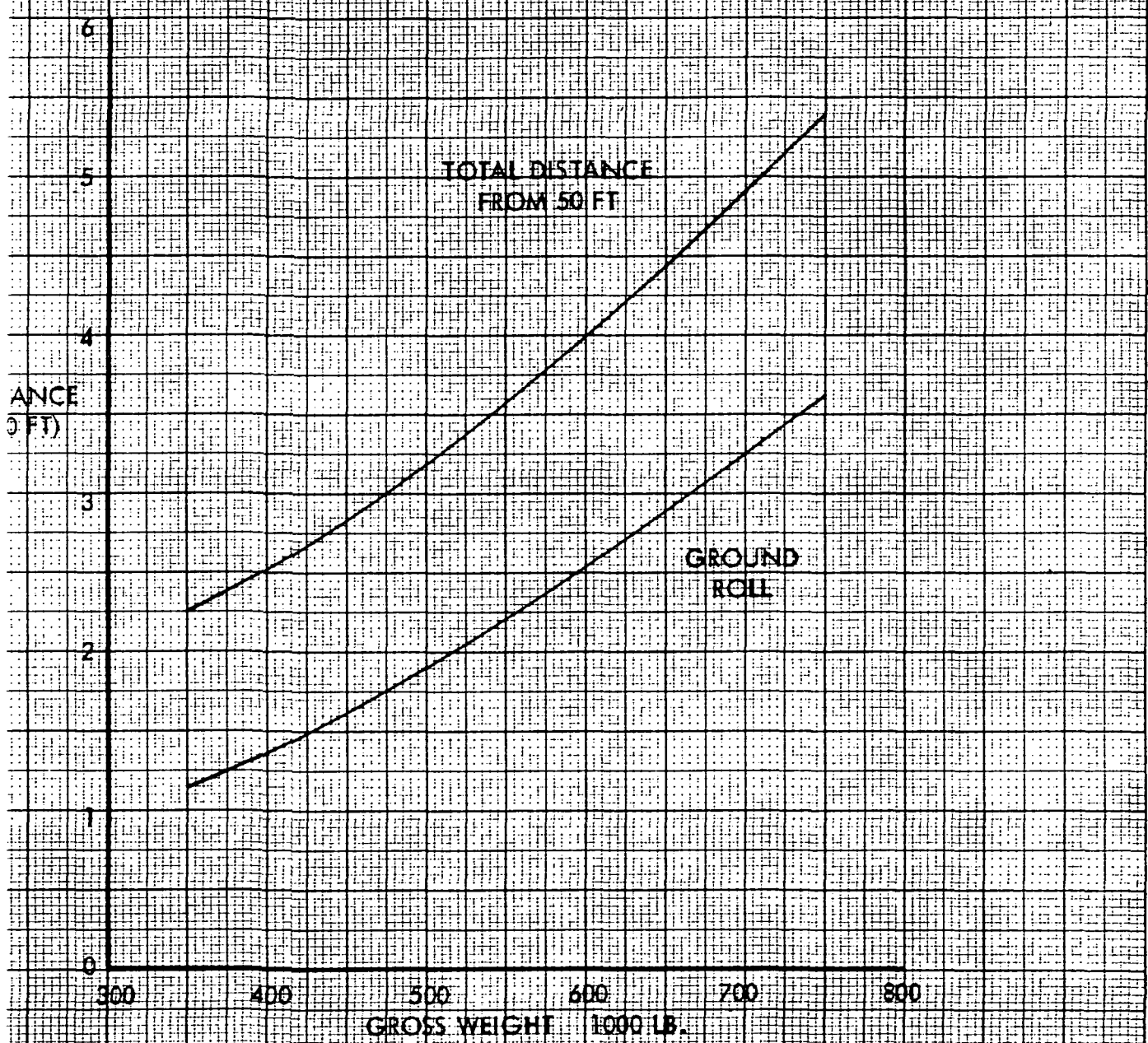


FIGURE 46

C-5/ORBITER PIGGYBACK

ONE ENGINE INOPERATIVE CLIMB GRADIENT

STD DAY

2000 FT

FLAPS = 16°

GEAR UP

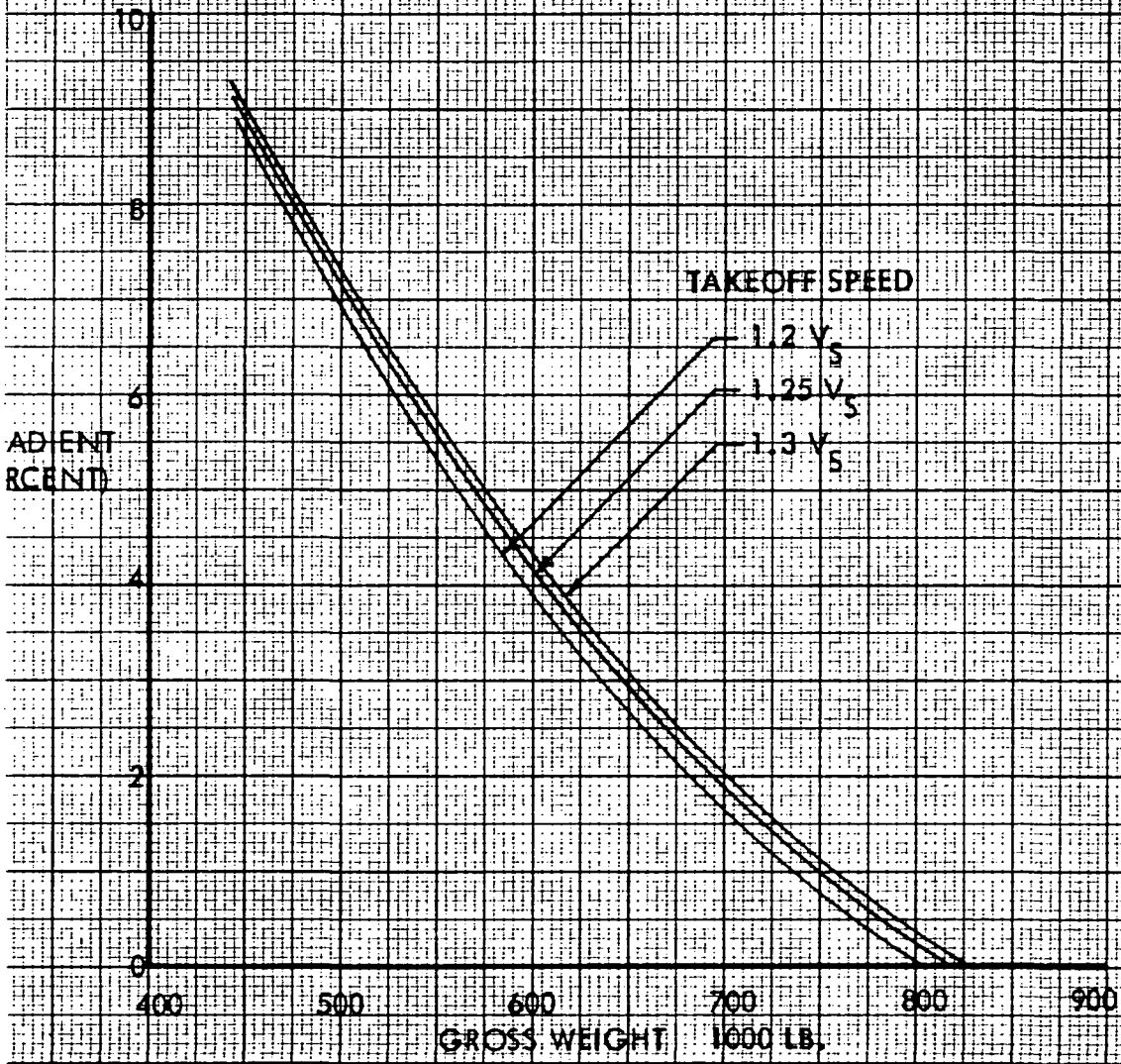


FIGURE 49

C-5/GRITER PIGGYBACK
CRUISE CEILINGS

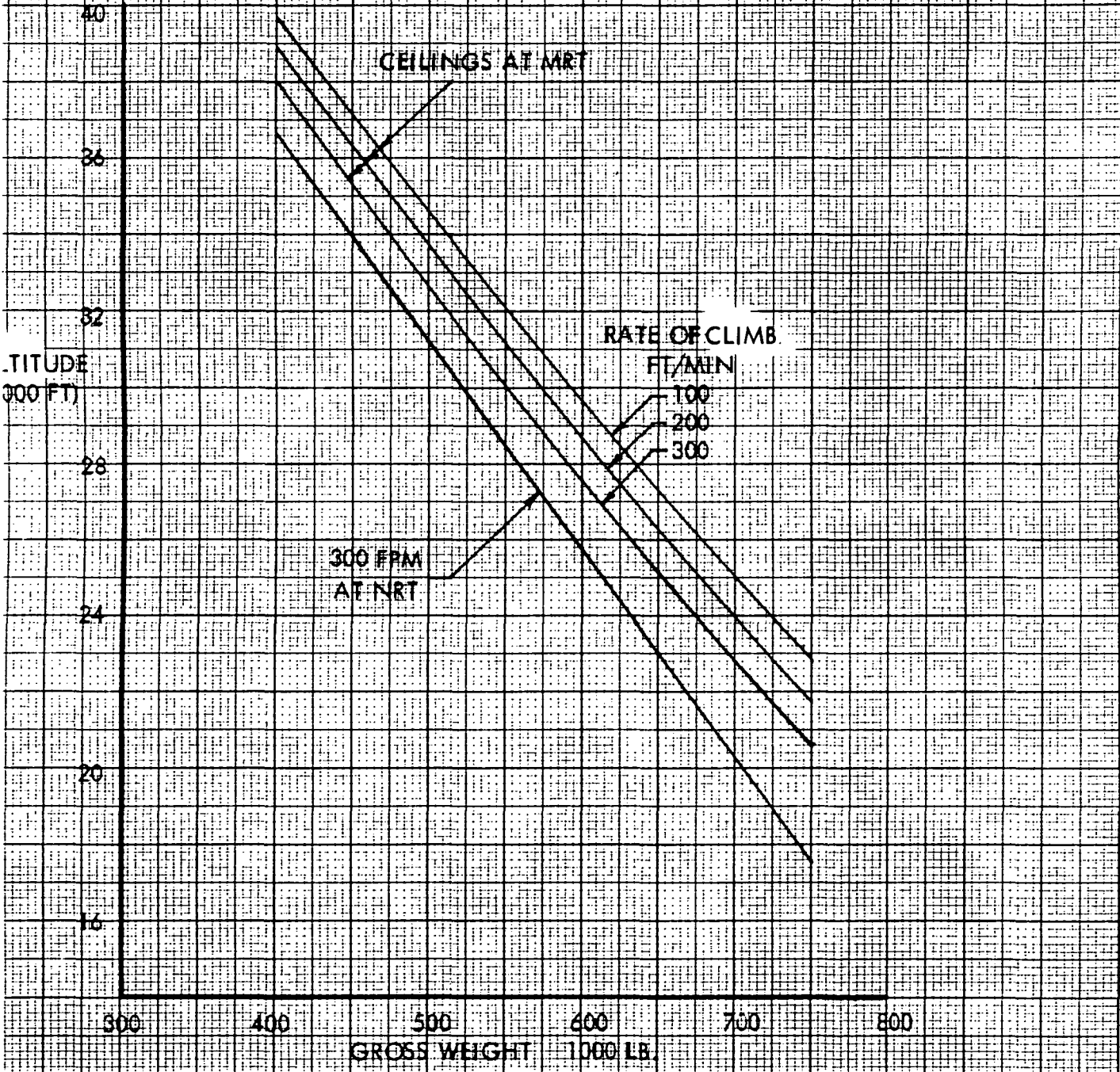


FIGURE 50

C-5/ORBITER PIGGYBACK
 ALTITUDE SPEED CAPABILITY

MAXIMUM LEVEL FLIGHT SPEEDS AT MILITARY RATED THRUST

CONFIGURATION: C-5 WITH 4 TF-39 ENGINES
 SPACE SHUTTLE ORBITER WITH
 AND WITHOUT FAIRED
 AFTERBODY

RATE OF CLIMB
 AVAILABLE AT
 BEST CLIMB SPEEDS
 SHOWN IN FT/MIN

ALTITUDE
 (100 FT)

FAIRED AFTERBODY

150,000 LB. ORBITER
 230,000 LB. ORBITER

NO FAIRED AFTERBODY

150,000 LB. ORBITER
 230,000 LB. ORBITER

AIR SPEED (KIAS)

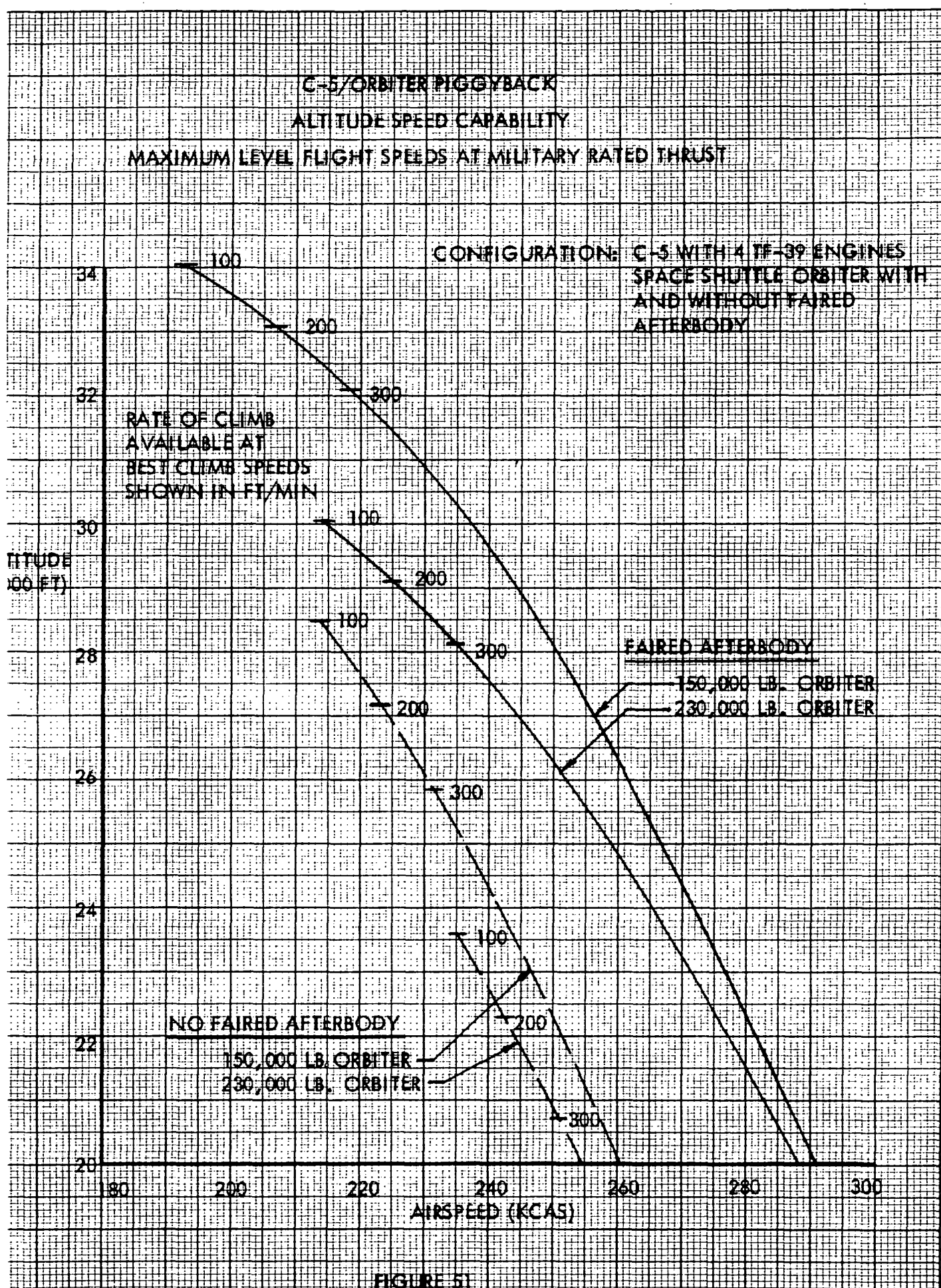
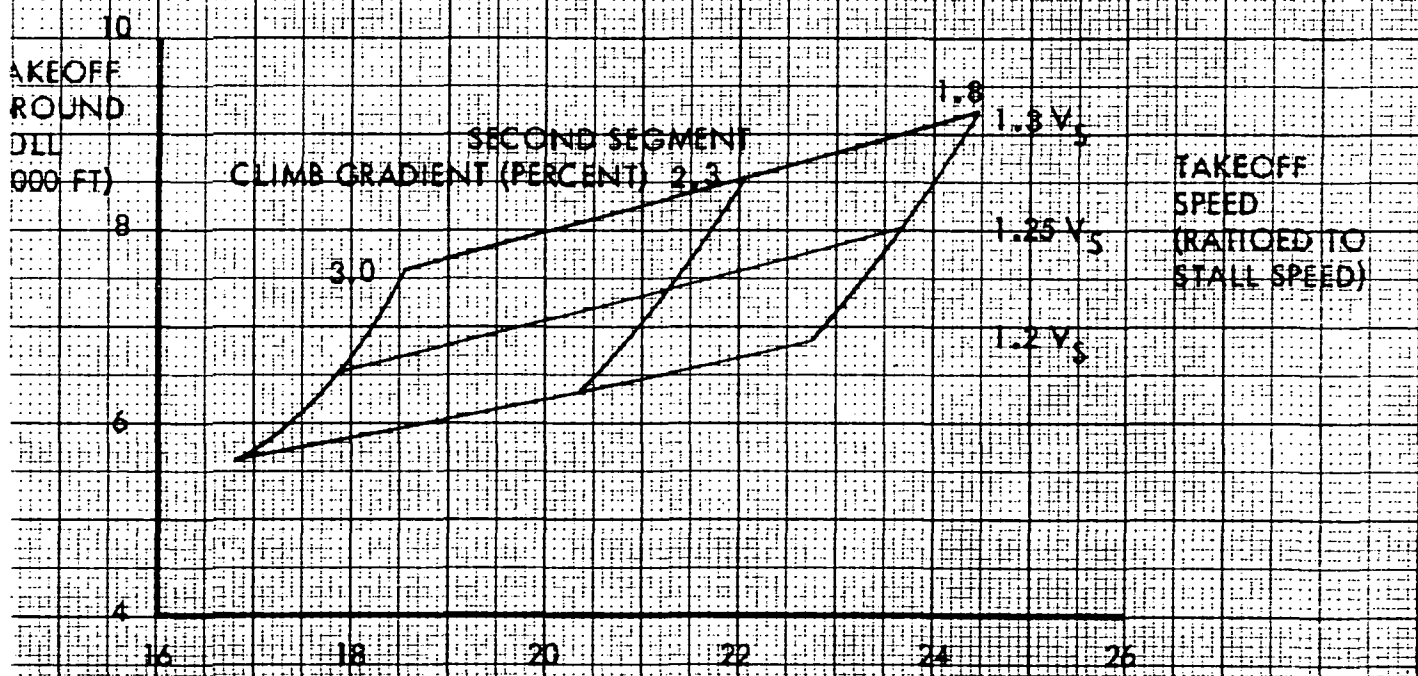
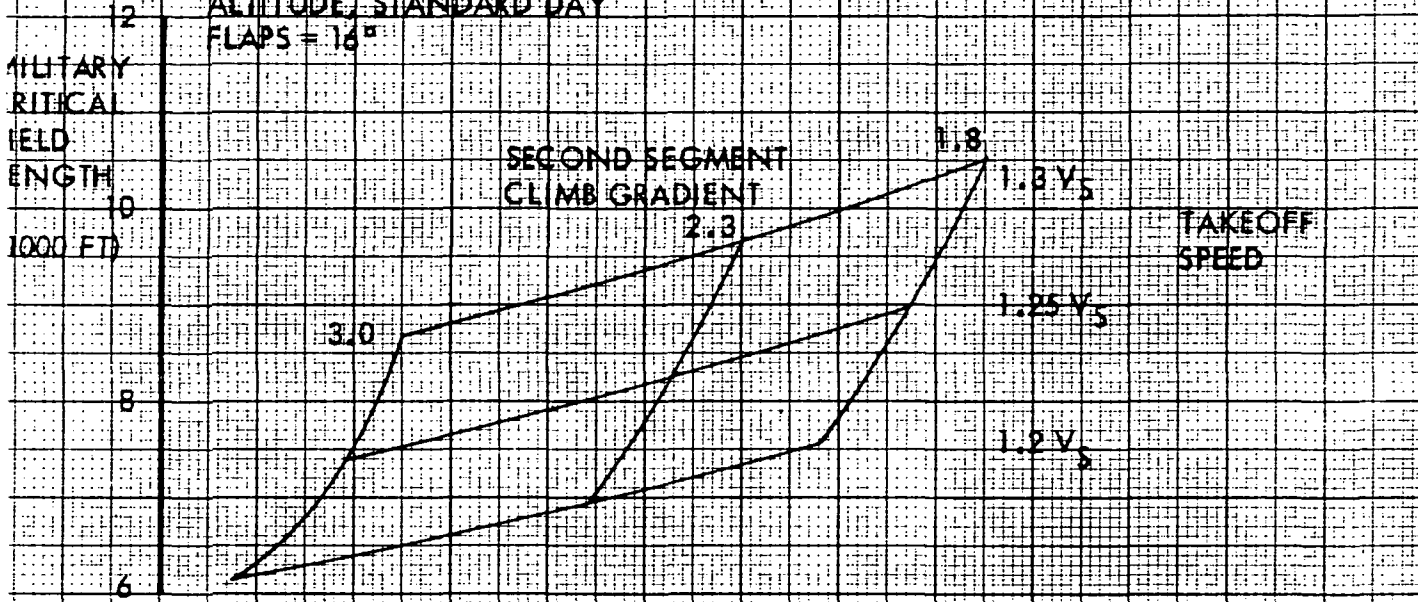


FIGURE 51

C-5/OMIBER PIGGYBACK

FERRY PERFORMANCE SUMMARY

AIRPORT PERFORMANCE DATA
 FOR OPERATIONS FROM 2300 FT
 ALTITUDE, STANDARD DAY
 FLAPS = 16°



FERRY RANGE - 100 NAUTICAL MILES

FIGURE 52

FLIGHT RESTRICTIONS

	A	B
LEVEL FLIGHT MAXIMUM SPEED, V_{HR}/M_H , KCAS	300/.775	280/.75
LIMIT SPEED, V_L/M_L , KCAS	360/.85	350/.8
SPEED FOR MAXIMUM GUST INTENSITY, V_G/M_H , KCAS	240/.775	210/.75
MANEUVER LOAD FACTOR, G	+2.0, -0.0	+2.0, -0.0
DESIGN SINK SPEED, F. P. S.	6.0	6.0
NO ABRUPT MANEUVERS	x	x
SIDE LOAD FACTOR DURING TURNS, G	.2	.2
WEIGHTS FOR STRUCTURAL DESIGN		
OPERATING WEIGHT, LB	334,900	336,310
MAXIMUM ZERO WING FUEL WEIGHT, LB	598,204 *	
MAXIMUM WING FUEL, LB	318,500	
MAXIMUM FUSELAGE FUEL, LB	11,300	13,525
MAXIMUM GROSS WEIGHT, LB	865,000	
MAXIMUM LANDING WEIGHT, LB	635,850	

* INCLUDES FUSELAGE FUEL

A = NO INCREASE IN VERTICAL STABILIZER AREA.

B = INCREASED VERTICAL STABILIZER AREA.

FIGURE 53

FLIGHT RESTRICTIONS

	A	SUPER GUPPY
LEVEL FLIGHT MAXIMUM SPEED, V_{HR}/M_H , KCAS	300/.775	219
LIMIT SPEED, V_L/M_L , KCAS	360/.85	219/.58
SPEED FOR MAXIMUM GUST INTENSITY, V_G/M_H , KCAS	240/.775	180-198
MANEUVER LOAD FACTOR, G	+2.0, -0.0	2.2 FLAPS UP 2.0 FLAPS DOWN
DESIGN SINK SPEED, F.P.S.	6.0	7.5
NO ABRUPT MANEUVERS	x	x
SIDE LOAD FACTOR DURING TURNS, G	.2	NO BRAKES
MAXIMUM GROSS WEIGHT, LB	865,000	162,000

FIGURE 54

APPENDIX A

WIND TUNNEL TEST DESCRIPTION AND PLOTTED DATA

CONTENTS

<u>Section</u>	<u>Title</u>	<u>Page</u>
I	MODEL DESCRIPTION	A-2
II	TEST FACILITY	A-3
III	TEST CONDITIONS	A-4
IV	DATA REDUCTION	A-5
V	REFERENCES	A-6
VI	MODEL CONFIGURATION SYMBOLS	A-7
VII	MODEL DIMENSIONAL DATA	A-10
VIII	RUN SCHEDULE	A-31

LIST OF FIGURES

<u>Figure</u>	<u>Title</u>	<u>Page</u>
A-1	Stabilizer Effectiveness, Orbiter Off	A-35
A-2	Effect of Orbiter Position, Tail On and Tail Off	A-39
A-3	Effect of Orbiter Afterbody Fairing Shape	A-43
A-4	Effect of Orbiter - Afterbody Fairing On and Off	A-47
A-5	Effect of Orbiter Incidence Angle and Position	A-51
A-6	Effect of Orbiter Position and Afterbody Fairing Shape	A-55
A-7	Spoiler Effectiveness, Orbiter On and Off	A-59
A-8	Effect of Center Vertical Stabilizer Extensions	A-63
A-9	Effect of Orbiter Incidence Angle - Orbiter in Aft High Position	A-67
A-10	Stabilizer Effectiveness - Orbiter On	A-71
A-11	Effect of Orbiter Incidence and Position	A-75
A-12	Rudder Effectiveness - Orbiter Off	A-79
A-13	Effect of Orbiter Afterbody Fairing	A-83
A-14	Effect of Orbiter - Tail On and Tail Off	A-85
A-15	Vertical Tail Effectiveness with Center Vertical Extension	A-90
A-16	Effect of Vertical Tail Modifications - Orbiter Off - Flaps Extended	A-94
A-17	Vertical Tail Effectiveness with Center and Stabilizer Tip Vertical Extensions - Flaps Extended	A-99
A-18	Effect of Orbiter Tail On and Off - Flaps Extended	A-103
A-19	Rudder Effectiveness with Center Vertical Tail Extension	A-108
A-20	Effect of Orbiter Position and Incidence	A-112
A-21	Effect of Orbiter Incidence and Fairing Shape	A-116
A-22	Vertical Tail Center Extension Effectiveness, Flaps Extended, Orbiter Off	A-120
A-23	Vertical Tail Center Extension Effectiveness, Flaps Extended, Orbiter On	A-124
A-24	Effect of Fairing Shape and Orbiter Location	A-128
A-25	Effect of Orbiter, Tail On and Tail Off	A-132

LIST OF FIGURES (Continued)

<u>Figure</u>	<u>Title</u>	<u>Page</u>
A-26	Effect of Orbiter Location	A-136
A-27	Effect of Orbiter Afterbody Fairing On and Off	A-140
A-28	Effect of Center Vertical Tail Extension, Flaps Extended, Orbiter Off	A-142
A-29	Effect of Center Vertical Tail Extension, Flaps Retracted, Orbiter Off	A-146
A-30	Effect of Center Vertical Tail Extension, Flaps Retracted, Orbiter Off	A-151
A-31	Effect of Vertical Tail Extensions at Stabilizer Tips	A-156



I - MODEL DESCRIPTION

The C-5A Piggyback model is a combination of the Rockwell International 0.0405 Shuttle Orbiter model and the Lockheed-Georgia 0.0399-scale low speed C-5A model joined with suitable attach fittings.

The Orbiter model is fabricated from wood and metal and incorporates adjustable control surfaces. Provision was made for the installation of various afterbody fairings. Five afterbody fairing shapes were available for test. The basic Rockwell International fairing is denoted by a superscript 1. The original Lockheed-Georgia fairing, denoted by a superscript 2, was designed to minimize the afterbody drag. Fairings 3, 4, and 5 were fabricated by cutting away various portions of the fairing in an attempt to improve the flow at the C-5A tail.

The 0.0399-scale, low speed C-5A model is assembled from numerous components that allow the simulation of configurations encompassing the entire flight regime of the aircraft. The model is fabricated primarily from aluminum with some steel and plastic parts. All control surfaces are adjustable, and the landing gears and cargo doors may be positioned in increments from fully retracted to fully extended.

A symbol list of all the model components used in this test is presented in Section VI.



II - TEST FACILITY

The C-5A - Orbiter Piggyback combination tests were conducted in the Lockheed-California Company 8 X 12 - Foot Low Speed Wind Tunnel. The tunnel is a conventional, low speed, single-return type with the test section vented to atmospheric pressure. Details of the facility are presented in Reference 1.

The model is supported in the upright position by a three-support fork. The fork is connected to an external, six-component, pyramidal-type balance located below the floor of the test section. The balance transmits loads from the model and support to an electrical readout system. Raw data are converted to punched cards using an IBM 1442 card reader punch. The raw data cards are input to the IBM 1131 Processor computer, which converts these data into coefficient form for output as tabulated data and provides the input for the Calcomp 565 plotter which produced the finished data plots presented in this appendix.

III - TEST CONDITIONS

All runs with flaps deflected were made at a dynamic pressure of 40 P.S.F. Flaps up runs were made at a dynamic pressure of 60 P.S.F. These dynamic pressures correspond to Mach Numbers of 0.165 and 0.201, and Reynolds Numbers of 1.436×10^6 and 1.758×10^6 , respectively. Reynolds Numbers are based on the C-5A model M.A.C.



IV - DATA REDUCTION

Six-component force data were measured during all runs. The data were reduced to coefficient form and transferred to the stability axis system coincident at the reference moment center (F.S. 53.762, W.L. 10.578, BL 0.000). Corrections applied to the six-component data include tunnel wall corrections, blockage, buoyancy drag, and support tare and interference corrections.

The support tare and interference were obtained in a previous test of a similar model (Reference 2). The correction values applied to the longitudinal components data were taken from faired plots of the tare and interference corrections, whereas the values applied to the lateral component data were taken directly from the computed results.

The six-component data reduction constants are listed below.

Wing Area, square feet		9.878
Wing Span, inches		104.997
Wing Mean Aerodynamic Chord, inches		14.817
Wing Mean Aerodynamic Chord Location	F.S.	53.762
	W.L.	12.577
	B.L.	21.654
Front Trunnion Location	F.S.	53.742
	W.L.	4.328
Moment Reference Center	F.S.	53.762
	W.L.	10.578

V - REFERENCES

1. "Wind Tunnel Computing Handbook," Lockheed California Company Report LALI, 15 June 1955.
2. "C-141: Investigation of the Low Speed Characteristics of the Production Airplane Configuration Using a 0.044 Scale Model in the Lockheed-California Company 8 X 12-Foot Wind Tunnel," Tests L-45-I, II, and III; Report No. ER 5071, June 1963.



VI - MODEL CONFIGURATION SYMBOLS

a¹⁰ Aileron, Simple hinge, sealed. Deflection range $\pm 25^\circ$, denoted by subscripts. angles set with protractor. 07-C5A-0197-110

A Orbiter, Shuttle - 0.0405 Scale Rockwell International Model. with/without aft fairing; capability of being located at 4 position on C-5A model, 3 angles of attack (ref. Orbiter FRL; $-1\ 1/2^\circ$, $+1/2^\circ$, $+2\ 1/2^\circ$)

Superscripts: Afterbody fairing shape and Orbiter location are denoted by number and letter superscripts, respectively. Lack of a number superscript indicates afterbody fairing removed.

- 1 Rockwell International fairing
- 2 Lockheed-Georgia fairing
- 3 Lockheed-Georgia fairing modified to lower surface upsweep
- 4 Lockheed-Georgia fairing modified to upper surface downsweep.
- 5 Lockheed-Georgia fairing modified to shorter fairing with horizontal knife edge Orbiter c.g. locations in terms of C-5 Fuselage Stations

	<u>Longitudinal Position</u>	<u>Vertical Position</u>
A (BASE)	54.424"	Base
B	56.819"	Base
C	59.235"	Base
D	54.424"	Base + 2.395"
E	56.819"	Base + 2.395"
F	59.235"	Base + 2.395"

Subscripts: Orbiter incidence in degrees referenced to C-5A FRL is denoted by a subscript

(i.e. $A_{1.5}^{1A}$ - Orbiter with Rockwell International afterbody fairing located in the base position at 1.5° incidence)

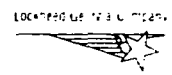
B^{22}	<u>Fuselage</u>		07-C5A-0181-200
b^{16}	<u>Bullet</u>		07-C5A-0182-403
$D^{8\text{ MOD}}$	<u>Dorsal</u>		07-C5A-0181-402A
e^{12}	<u>Elevator</u>	Inboard. Simple hinge, hinge line gap sealed. Deflection range -25° $+15^\circ$; denoted by subscripts. Set with protractor.	07-C5A-0198-401
e^{13}	<u>Elevator</u>	Outboard. Simple hinge, hinge line gap sealed. Deflections range -25° 15° , denoted by subscripts. Set with protractor.	07-C5A-0198-401
f^{37}	<u>Flaps, T.E. Fowler.</u>	Six sections/side, 0° and 40° (ldg.) to be tested.	07-C5A-0198-105
H^8	<u>Horizontal Stabilizer.</u>	Incidence settings capability. 0° , $\pm 4^\circ$, $\pm 6^\circ$, -8° , -12° ; set with pin in push rod in vertical.	07-C5A-0198-401- -0195-400
$K^{24A} N^{20A}$	<u>Pylon/Nacelles</u>		07-C5A-0197-300
Q^{13}	<u>Slats, Leading Edge.</u>	$14\% C_W$, 3 section/side. Inboard 2 section sealed to wing and pylon, outboard section $1.25\% C_W$ T.E. gap and sealed to pylons. Deflection 20° inboard sections, 20° outboard; denoted by subscript "20".	07-C5A-0197-109



r ⁷⁸	<u>Rudders</u> , lower and upper, respectively. Simple hinge, hinge line gap sealed; deflections $\pm 30^\circ$.	07-C5A-0192-402
V ⁹	<u>Vertical Stabilizer</u>	07-C5A-0182-402
W ^{11A}	<u>Wing</u>	07-C5A-0197-100
Z ^{f6}	<u>Flap Track Fairing</u>	07-C5A-0197-106
Z ^{g27}	<u>Nose Landing Gear Fairing</u>	07-C5A-0197-201
Z ^{g23}	<u>Main Landing Gear Fairing</u>	07-C5A-0151-204
Z ^{w27}	<u>Wing - Fuselage Fillet</u> - Alum. and Plastic; Composed of Z ^{w26} fwd. fillet and Z ^{w22} aft. fillet.	07-C5A-0197-200

S¹ = B²² W^{11A} A^{w27} K^{24A} N^{20A} Z^{f6} Z^{g27} Z^{g23}

V ¹	<u>Center Vertical Fin Extension</u> - Alum. plate, cut to match L.E - T.E vertical stabilizer sweep and tip chord of vertical (V ⁹), span 6", attached to top of horizontal bullet fairing.
h ¹	<u>Horizontal Stab. Fins.</u> - end plates on tips of horizontal stabilizer 1" inbd. from horizontal tips, 4" chord, 8" span (or height).

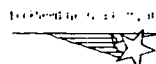


VII - MODEL DIMENSIONAL DATA

<u>Aileron, (a¹⁰)</u>		<u>0.039916 Scale</u>
Area per side, square feet		0.188
Span, inches		10.651
Chord lengths, inches		
Inboard		2.978
Outboard		2.337
Mean (RMS, streamwise)		
Sweep of hinge line, degrees		20.417
Deflection limits, degrees		<u>+25</u>

<u>Fuselage, (B²²)</u>		
Length, inches		110.487 (9.207')
Maximum frontal area, square inches		126.60
Equivalent maximum diameter, inches		12.69
Fuselage reference line	W.L.	7.983
Nose location	F.S.	6.387
Wetted area, square feet (imprints not removed)		25.223
Volume, Cu. Ft.		5.379

<u>Bullet, (b¹⁶)</u>		
Length, inches		21.44
Maximum frontal area, square inches		3.22
Equivalent diameter, inches		2.03
Wetted area, square feet (Exposed Only)		0.541



MODEL DIMENSIONAL DATA (CONT.)

Dorsal, (D⁸ mod.)

Wetted area, square feet	0.129
Imprint area, square feet (On fuselage)	0.075

Elevator, Inboard (e¹²)

Area per side, square feet	0.1434
Root chord, inches	3.227
Tip chord, inches	2.228
Mean chord length (RMS), inches	2.773
Span per side, inches	7.569
Hinge line, % horizontal chord	66.000
Deflections, degrees	<u>+ 30.000</u>

Elevator, Outboard (e¹³)

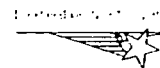
Area per side, square feet	0.0624
Root chord, inches	2.228
Tip chord, inches	1.609
Mean chord length (RMS), inches	1.943
Span per side, inches	4.684
Hinge line, % horizontal chord	66.000
Deflections, degrees	<u>+ 33.000</u>

Trailing Edge Fowler Flaps, (f³⁷)*

Panel 1 (Inboard)

Area per side, square feet	0.214
----------------------------	-------

*All dimensions given in Wing Reference Plane.



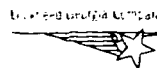
MODEL DIMENSIONAL DATA (CONT.)

Trailing Edge Fowler Flaps, (Cont.)

Span, inches		7.085
Sweep of leading edge, degrees		9.832
Chord lengths, inches		
Root		4.410
Tip		4.410
Average		4.410
Mean (RMS)		4.410
Chord locations, inches		
Root	W.S.	5.620
Tip	W.S.	12.705
Average	W.S.	9.163
Mean (RMS)	W.S.	9.163
Maximum deflection, degrees		40.000

Panel 2

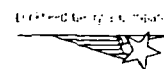
Area per side, square feet		0.173
Span, inches		5.718
Sweep of leading edge, degrees		9.832
Chord lengths, inches		
Root		4.410
Tip		4.410
Average		4.410
Mean (RMS)		4.410
Chord locations, inches		
Root	W.S.	13.344
Tip	W.S.	19.062
Average	W.S.	16.203



MODEL DIMENSIONAL DATA (CONT.)

Trailing Edge Fowler Flaps, (Cont.)

Mean (RMS	W.S.	16.203
Maximum deflection, degrees		40.000
Panel 3		
Area per side, square feet		0.125
Span, inches		4.845
Sweep of leading edge, degrees		12.364
Chord lengths, inches		
Root		3.804
Tip		3.804
Average		3.804
Mean (RMS)		3.804
Chord locations, inches		
Root	W.S.	19.701
Tip	W.S.	24.546
Average	W.S.	22.123
Mean (RMS)	W.S.	22.123
Maximum deflection		40.000
Panel 4		
Area per side, square feet		0.094
Span, inches		4.497
Sweep of leading edge, degrees		17.033
Chord lengths, inches		
Root		3.133
Tip		3.133
Average		3.133
Mean (RMS)		3.133



MODEL DIMENSIONAL DATA (CONT.)

Trailing Edge Fowler Flaps (Cont.)

Chord locations, inches

Root	W.S.	25.184
Tip	W.S.	29.681
Average	W.S.	27.433
Mean (RMS)	W.S.	27.433

Maximum deflection, degrees 40.000

Panel 5

Area per side, square feet 0.079

Span, inches 3.802

Sweep of leading edge, degrees 17.033

Chord lengths, inches

Root	3.133
Tip	3.133
Average	3.133
Mean (RMS)	3.133

Chord locations, inches

Root	W.S.	30.321
Tip	W.S.	34.135
Average	W.S.	32.222
Mean (RMS)	W.S.	32.222

Maximum deflection, degrees 40.000

Panel 6

Area per side, square feet 0.082

Span, inches 3.938

Sweep of leading edge, degrees 17.033



C-2

16

MODEL DIMENSIONAL DATA (CONT.)

Trailing Edge Fowler Flaps (Cont.)

Chord lengths, inches

Root		3.133
Tip		3.133
Average		3.133
Mean (RMS)		3.133

Chord locations, inches

Root	W.S.	34.773
Tip	W.S.	38.712
Average	W.S.	36.742
Mean (RMS)	W.S.	36.742

Maximum deflection, degrees 40.000

Horizontal Stabilizer, (H⁸)

Airfoil Section NACA
0010.5-0.833-0.40/1.432
(modified)

Area - projected square feet 1.539

- wetted, square feet (Exposed only) 2.910

Span 32.397

Chord lengths - MAC, inches 7.322

Root, inches 9.985

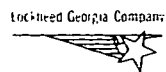
Tip, inches 3.695

Aspect ratio 4.736

Taper ratio 0.370

Sweep of 25% chord line, degrees 24.583

25% MAC Location F.S. 115.533



MODEL DIMENSIONAL DATA (CONT.)

Horizontal Stabilizer, (Cont.)

B.L. 6.858

Volume coefficient 0.629

Tail length, inches 60.028

Pylon, (K^{24A})

Sweep of L.E., degrees 71.504

Chord length, inches 13.073

Taper ratio 0.876

Airfoil section NACA
0008-1.100-0.335/1.575
(modified)

Wing intersection,
% wing chord 1.4

Toe-in, degrees 1.0

Wing intersection,
inboard B.L. 19.122

Wing intersection,
outboard B.L. 29.781

Nacelle, (N^{20A})

Length, inches 9.228

Maximum diameter,
inches 4.091

Duct diameter, inches 3.409

Fineness ratio 2.256

Area, square feet

Maximum frontal
area 0.091

Inlet area 0.075

Side area 0.249

Toe-in angle, degrees 1.0

Incidence, degrees 2.0



16

MODEL DIMENSIONAL DATA (CONT.)

Nacelle (Cont.)

Inlet location

Inboard nacelle	F.S.	41.970
	W.L.	8.864
	B.L.	18.999
Outboard nacelle	F.S.	47.490
	W.L.	7.891
	B.L.	29.658

Leading Edge Slat, (Q¹³)

Section I (outboard)

1-1/4% C_w gap

Area, square feet		0.191
Span, inches		19.556
Chord length - root, inches		1.698
tip, inches		1.135
average, inches		1.417
Chord location - root	B.L.	29.291
tip	B.L.	48.788
Angle from stowed position, degrees		22.0

Section II (mid section),
sealed

Area, square feet		0.079
Span, inches		6.336
Chord length - root, inches		1.881
tip, inches		1.698
average, inches		1.790



MODEL DIMENSIONAL DATA (CONT.)

Leading Edge Slat (Cont.)

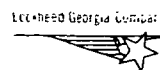
Chord location - root	B. L.	22.974
tip	B. L.	29.291
Angle from stowed position, degrees		20.0

Section III (inboard),
sealed

Area, square feet		0.261
Span		16.377
Chord length - root, inches		2.714
tip, inches		1.881
average, inches		2.298
Chord location - root	B. L.	6.646
tip	B. L.	22.974
Angle from stowed position, degrees		20.0

Rudder, (r^7 , r^8)

	r^8 (Upper)	r^7 (Lower)
Area, square feet	0.161	0.203
Location		
Lower end	W. L. 22.924	15.793
Upper end	W. L. 29.119	22.924
Hinge line, percent vertical chord	71	71
Span, inches	6.195	7.133
Deflection limits, degrees	<u>+30</u>	<u>+30</u>
Root chord, inches	3.097	4.278
Tip chord, inches	3.585	3.907



16

MODEL DIMENSIONAL DATA (CONT.)

Rudder, (Cont.)

Mean chord length (RMS), inches	3.750	4.097
Mean chord location	W.L. 25.949	19.272
Percent of vertical tail	10.5	13.1

Spoiler, (a²²)*

Panel 1 (Inboard Section)

Area per side, square feet		0.0514
Span, inches		3.606
Sweep of hinge line, degrees		9.832
Chord lengths, inches		
Root		2.206
Tip		2.026
Average		
Mean (RMS)		
Chord locations, inches		
Root	W.S.	5.550
Tip	W.S.	9.157
Average	W.S.	
Mean (RMS)	W.S.	
Maximum deflection, degrees		60.000

Panel 2

Area per side, square feet		0.0508
Span, inches		3.610
Sweep of hinge line, degrees		9.832
Chord lengths, inches		
Root		2.026

*All dimensions given in wing reference plane.



MODEL DIMENSIONAL DATA (CONT.)

Spoiler, (Cont.)

Tip		2.026
Average		2.026
Mean (RMS)		2.026

Chord locations, inches

Root	W.S.	9.169
Tip	W.S.	12.779
Average	W.S.	
Mean (RMS)	W.S.	

Maximum deflection, degrees		60.000
--------------------------------	--	--------

Panel 3

Area per side, square feet		0.0412
Span, inches		2.927
Sweep of hinge line, degrees		9.832

Chord lengths, inches

Root		2.026
Tip		2.026
Average		2.026
Mean (RMS)		2.026

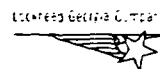
Chord locations, inches

Root	W.S.	13.270
Tip	W.S.	16.197
Average	W.S.	
Mean (RMS)	W.S.	

Maximum deflection, degrees		60.000
-----------------------------	--	--------

Panel 4

Area per side, square feet		0.0412
Span, inches		2.927
Sweep of hinge line, degrees		9.832



16

MODEL DIMENSIONAL DATA (CONT.)

Spoiler (Cont.)

Chord lengths, inches

Root	2.026
Tip	2.026
Average	2.026
Mean (RMS)	2.026

Chord locations, inches

Root	W.S.	16.209
Tip	W.S.	19.136
Average	W.S.	
Mean (RMS)	W.S.	

Maximum deflection, degrees	60.000
--------------------------------	--------

Panel 5

Area per side, square feet	0.0272
Span, inches	2.490
Sweep of hinge line, degrees	12.347
Distance hinge line forward of leading edge, inches	0.336

Chord lengths, inches

Root	1.910
Tip	1.910
Average	1.910
Reference**	2.247

**Reference chord is defined as twice the distance from the hinge line to spoiler t.e. minus the average chord.



MODEL DIMENSIONAL DATA (CONT.)

Spoiler (Cont.)

Chord locations, inches

Root	W.S.	19.627
Tip	W.S.	22.117
Average	W.S.	
Reference	W.S.	

Maximum deflection, degrees 60.000

Panel 6

Area per side, square feet 0.0272

Span, inches 2.490

Sweep of hinge line, degrees 12.347

Distance hinge line forward of leading edge, inches 0.336

Chord lengths, inches

Root	1.910
Tip	1.910
Average	1.910
References**	2.247

Chord locations, inches

Root	W.S.	22.129
Tip	W.S.	24.620
Average	W.S.	
Reference	W.S.	

Maximum deflection, degrees 60.000

**Reference chord is defined as twice the distance from the hinge line to spoiler t.e. minus the average chord.



16

MODEL DIMENSIONAL DATA (CONT.)

Spoiler (Cont.)

Panel 7

Area per side, square feet		0.0399
Span, inches		4.645
Distance hinge line forward of leading edge, inches		0.260
Sweep of hinge line, degrees		17.033
Chord lengths, inches		
Root		1.236
Tip		1.236
Average		1.236
Reference**		1.757
Chord locations, inches		
Root	W.S.	25.111
Tip	W.S.	29.756
Average	W.S.	
Reference	W.S.	
Maximum deflection, degrees		60.000

Panel 8

Area per side, square feet		0.0340
Span, inches		3.962
Sweep of hinge line, degrees		17.033
Distance hinge line forward of leading edge, inches		0.260
Chord lengths, inches		
Root		1.236
Tip		1.236
Average		1.236
Reference**		1.757

**Reference chord is defined as twice the distance from the hinge line to spoiler t.e. minus the average chord.



16

MODEL DIMENSIONAL DATA (CONT.)

Spoiler (Cont.)

Chord locations, inches

Root	W.S.	30.247
Tip	W.S.	34.209
Average	W.S.	
Reference	W.S.	

Maximum deflection, degrees 60.000

Panel 9

Area per side, square feet 0.0336

Span, inches 4.086

Sweep of hinge line, degrees 17.033

Distance hinge line forward
of leading edge, inches 0.247

Chord lengths, inches

Root	1.184
Tip	1.184
Average	1.184
Reference**	1.679

Chord locations, inches

Root	W.S.	34.700
Tip	W.S.	38.785
Average	W.S.	
Reference	W.S.	

Maximum deflection, degrees 60.000

**Reference chord is defined as twice the distance from the hinge line to spoiler t.e. minus the average chord.



MODEL DIMENSIONAL DATA (CONT.)

Vortex Generator, (U^2)

Height, inches

Superscript A 0.08

Superscript B 0.10

Superscript C 0.12

Width, inches

Superscript A 0.16

Superscript B 0.20

Superscript C 0.24

Angle to freestream, degrees 15.00

Chordwise location (centerline
of generator), % of t.e. flap 15.00

Spanwise location, inches from
flap tip chord

Subscript 1 0.18

Subscript 2 0.23

Subscript 3 0.28

Subscript 4 0.33

Subscript 5 0.38

Vertical Stabilizer, (V^9)

Airfoil section NACA

0013-1.1-0.40/1.575 (modified)

Areas (theoretical), square feet

Projected 1.531

Wetted (exposed only) 2.848

Span, inches 16.535

Chord lengths, MAC, inches 13.390

Root, inches 14.817

Tip, inches 11.853

Aspect ratio 1.240



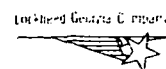
MODEL DIMENSIONAL DATA (CONT.)

Vertical Stabilizer (Cont.)

Taper ratio		0.800
Sweep of 25% chord line, degrees		34.931
25% MAC location	F.S.	107.992
	W.L.	23.388
Volume coefficient		0.079
Tail length, inches		53.246

Wing, (W^{11A}) (6204.601 ft² Full Scale)

Area, square feet			<u>Data Reduction</u>
Planform, theoretical		9.8857	9.878
Planform, exposed (Outboard of B.L.)		8.4930	
Wetted, exposed (Outboard of B.L.)		16.504	
Volume, Cu. Ft.			0.770
Span, inches	(8.749')	104.997	104.997
MAC chord length, inches		14.826	14.817
Location of 0.25 chord MAC	F.S.	53.765	
	W.L.	12.557	
	B.L.	21.658	
Aspect ratio		7.744	
Taper ratio, theoretical		0.371	
Taper ratio, exposed		0.401	
Dihedral (0.25 chord), degrees		3.500	
Sweep angle, degrees			
Panel I (Inboard)			
Leading edge		28.449	
0.25 chord		24.268	
Trailing edge		10.046	



1 6

MODEL DIMENSIONAL DATA (CONT.)

Wing (Cont.)

Panel 2

Leading edge	28.449
0.25 chord	24.803
Trailing edge	12.581

Panel 3

Leading edge	27.382
0.25 chord	23.954
Trailing edge	12.581

Panel 4

Leading edge	27.382
0.25 chord	25.001
Trailing edge	17.298

Chord length, inches

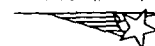
Root	21.806
Break station, inboard	14.826
Break Station, Mid	13.606
Break Station, Outboard	13.018
Tip	7.332

Chord location, inches

Root	B.L.	0
Break Station, Inboard	B.L.	19.144
Break Station, Mid	B.L.	22.973
Break Station, Outboard	B.L.	24.970
Tip	B.L.	52.498

Geometric twist, degrees

Root	0
Break Station, Inboard	1.132
Break Station, Mid	1.500
Break Station, Outboard	1.576



MODEL DIMENSIONAL DATA (CONT.)

Wing (Cont.)

Tip 3.500

Flap Track Fairing, Z^{f6}

Centerline locations W.S.
 W.S.
 W.S.
 W.S.
 W.S.
 W.S.
 W.S.

Nose Landing Gear Fairing (Z^{G27})

Maximum length, inches 11.30
 Maximum frontal area, square inches 6.06
 Wetted area, square feet 0.6311
 Imprint area on fuselage, square feet 0.5886

Main Landing Gear Fairing, (Z^{G28})

Maximum length, inches	33.290	(Z ^{G23}) 35.36
Maximum frontal area, square feet	0.125	0.135
Wetted area, square feet	4.364	4.366
Imprint area on fuselage, square feet	3.513	
Maximum width, inches	14.078	14.18

Wing - Fuselage Fillet, (Z^{W27})

Maximum length 41.71
 Wetted area 3.638
 Imprint area of fuselage and fillet on Wing 3.582
 Side area 1.10



MODEL DIMENSIONAL DATA (CONT.)

Wing - Fuselage Fillet (Cont.)

Imprint area of wing and fillet on fuselage 3.013

Location:

Most forward point F.S. 32.13

Most aft point F.S. 73.84

Main Landing Gear Outer Door (FWD), (d^{m3})

Length, inches 6.63

Reference area, square feet 0.1932

Span, inches 4.19

Deflections, % Open 0, 10, 25, 50, 75, 100

Main Landing Gear Outer Door (AFT), (d^{m4})

Length, inches 6.63

Reference area, square feet 0.1932

Span, inches 4.19

Deflections, % Open 0, 10, 25, 50, 75, 100

Main Landing Gear Inner Door (FWD), (d^{m5})

Length, inches 4.23

Reference area, square feet 0.0311

Span, inches 1.06

Deflections, degrees 0, 3, 6, 29, 75, 95

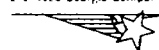
Main Landing Gear Inner Door (AFT), (d^{m6})

Length, inches 4.23

Reference area, square feet 0.0311

Span, inches 1.06

Deflections, degrees 0, 3, 6, 29, 75, 95



16

MODEL DIMENSIONAL DATA (CONT.)

Nose Landing Gear Inner Door, (dⁿ³)

Length, inches	5.35
Reference area, square feet	0.0884
Span, inches	2.37
Deflections, % Open	0, 10, 25, 50, 75, 100

Nose Landing Gear Outer Door, (dⁿ⁴)

Length, inches	4.18
Reference area, square feet	0.0371
Span, inches	1.28
Deflections, % Open	0, 10, 25, 50, 75, 100

Ref. Moment Center:

F.S.	53.762
W.L.	10.578
B.L.	0.000



VIII - RUN SCHEDULE

The following three pages present the run schedule for the wind tunnel test program.

S1 - B22 W11A ZW27 N20A Zf6 ZG27 ZG23

TEST NO.
LOCATION

RUN NO.	CONFIGURATION														TYPE RUN	REMARKS	PLOTTED FIG. NO.
	ASSY	AIL	L SLATS	E T. E. ORB	FLAP	ITER	DOR SAL	BUL LET	VERT	HOR.	ELEV.	RUD DER	SPOI LER	VERT EXT			
26	S1	a10	q13	f37	A-1.5	D8	b16	v9	H8	e12,13	r7,8				Pitch	60	
27					A-1.5										Yaw		A13, A27
31					A-1.5										Pitch		A5
32					A0.5										Yaw		A13, A27
33					A0.5										Pitch		A5
34					A0.5										Yaw		A26
35					A0.5										Pitch		A2
36															Yaw		A26
39															Pitch		A2
40															Yaw		
43					A0.5										Pitch		A2
44					A0.5										Yaw		A25
47						D8	b16	v9	H8	e12,13	r7,8				Pitch		A2
48															Yaw		A21, A24, A25
49					A0.5										Pitch		A6
50					A0.5										Yaw		A24
53					A0.5										Pitch		A6
54															Yaw		A24
55					A0.5										Pitch		A6
56															Yaw		A24
57															Pitch		A6
58															Yaw		A24
59															Pitch		A1, A7, A8
60															Yaw		A12, A13, A26
61															Yaw		A12
63															Pitch		A1
64															Pitch		A1
65	S1	a10	q13	f37		D8	b16	v9	H8	e12,13	r7,8				Yaw	60	A12
															Pitch		A7

S1 - B 22.11A Z W27 N 20A Z f6 G27 Z G23

TEST NO.
LOCATION

RUN NO.	CONFIGURATION													TYPE RUN	REMARKS	PLOTTED FIG. NO.	
	ASSY	AIL	L. E. SLATS	T. E. FLAP	ORB INTER	DOR SAL	BUL DET	VERT HOR.	ELEV	RUD DER	SPOI DER	VERT EXT	TIP FLNS				
66	S1	a10	q13	f37	5F A0.5	D8	b16	v9	H8	e12,13	r7,8			Pitch	60		
67					5F A0.5									Yaw			A21
68					A0.5									Pitch			A5
69														Yaw			A20, A21
70					5F A-1.5									Pitch			A5, A8
71														Yaw			A21
72											v1			Pitch			A8, A9, A11
73														Yaw			A20
74					5F A0.5									Pitch			A7, A9, A10
75														Yaw			
76					5A A0.5									Pitch			A11
77														Yaw			A20
78					5F A0.5									Pitch			A10
79														Yaw			A15
80						D8	b16	v9	H+4	e12,13	r7,8	v1		Pitch			A10
81									H84					Pitch			A10
82									H8					Yaw			A19
83														Pitch			A7
84														Yaw	60		A15, A9, A20
85														Pitch	40		
86														Yaw			A17
87														Pitch			
88														Yaw			
89						D8	b16	v9	H8	e12,13	r7,8	v1	h1	Yaw			A17
90														Yaw			A17
91					5F A0.5									Yaw			A17
92														Yaw			
93	S1	a10	q20	f27		D8	b16	v9	H8	e12,13	r7,8		h1	Yaw			

11-7

STABILIZER EFFECTIVENESS
ORBITER OFF

LR: UFL-353
PAGE: FIG.

SYM RUN CONFIG

+	63	S ¹ a ¹ Q ¹ T ¹
X	57	b ⁰ O ⁰ V ⁰ H ⁰ e ^{0,12,13,16,17,8} r ^{0,8}
▽	60	H ^{0,4}
◇	61	H ^{0,4}

SIM	RUN	CONFIGURATION
+	63	S ¹ a ¹ Q ¹ T ¹
X	57	b ⁰ O ⁰ V ⁰ H ⁰ e ^{0,12,13,16,17,8} r ^{0,8}
▽	60	H ^{0,4}
◇	61	H ^{0,4}

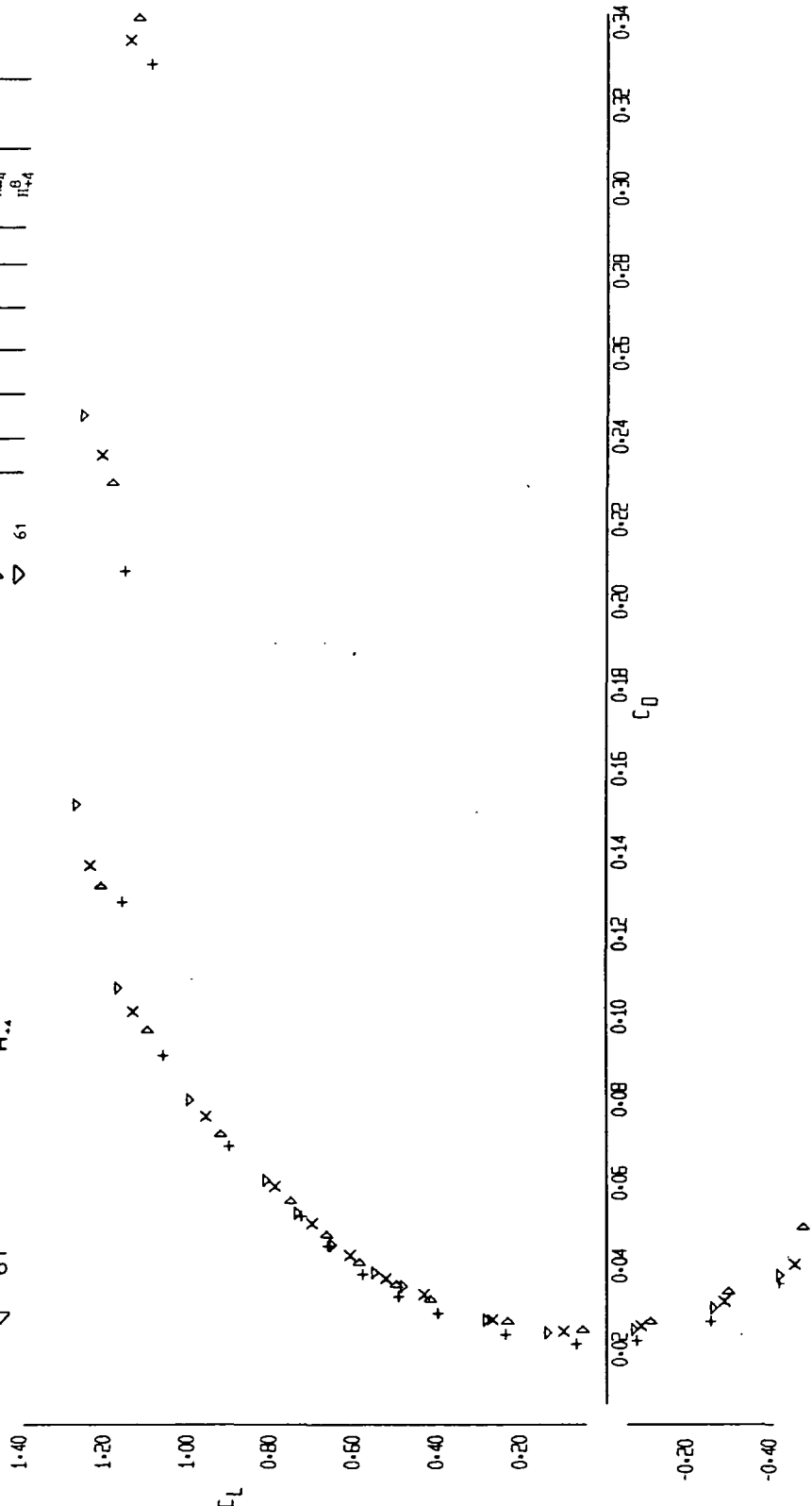


FIGURE 1 (SHEET 1)

UF-20

19-10-73

ES 58 19
+ X ▽ ▽

STABILIZER EFFECTIVENESS

ORBITER OFF

LR LFL-353 PAGE FIG.

SYM	RUN	CONFIGURATION
+	63	S ₁ a ₁₀ Q ₁₃ r ₃₇
X	57	b ₁₆ v ₉ B ₈ 12,13 r _{7,8}
▷	60	H _{2A} B ₈
▽	61	H _{2A} B ₈

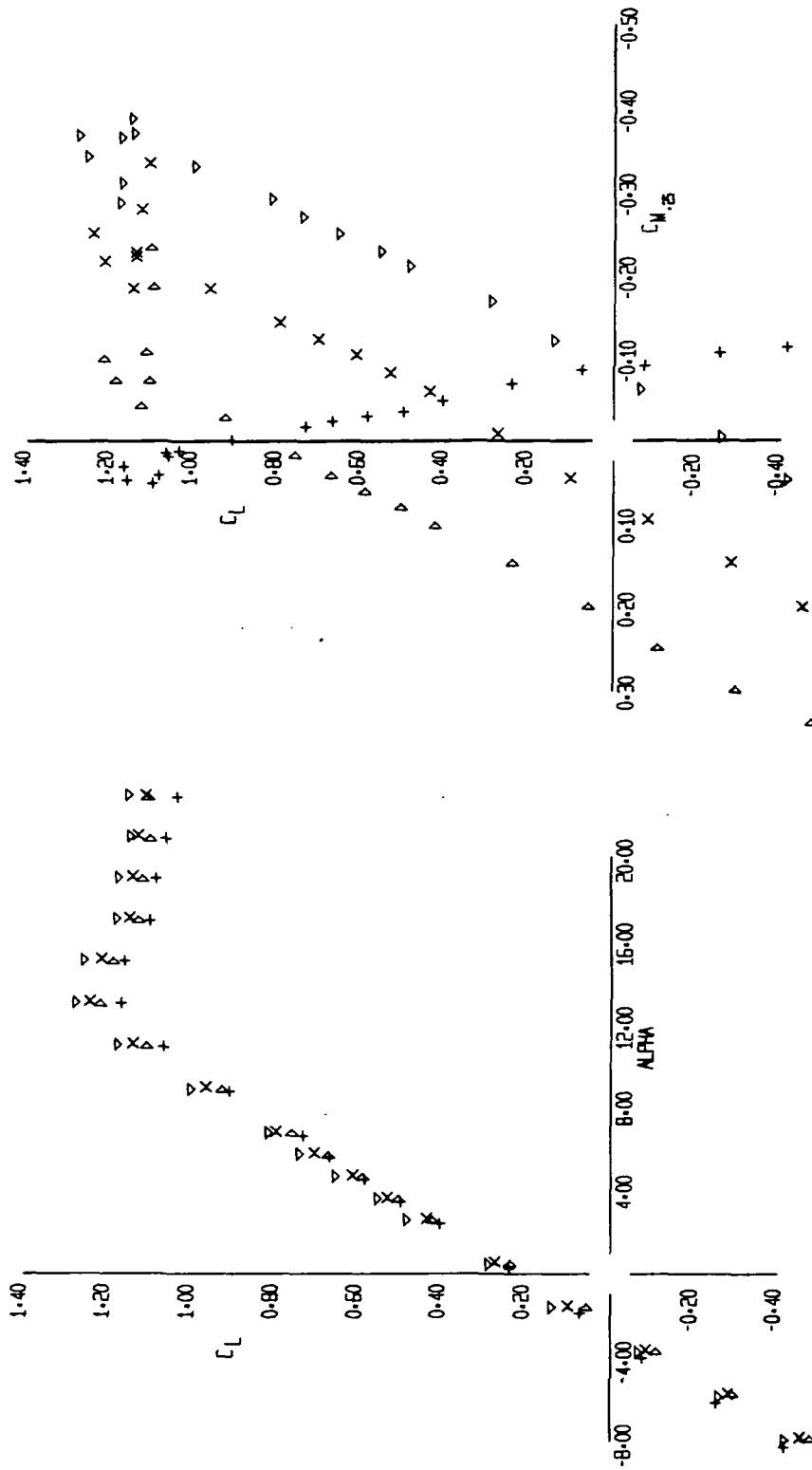


FIGURE 1 (SHEET 2)

EB 63 60
+ X ▷ ▽

10-10-73

LP-III

STABILIZER EFFECTIVENESS

ORBITER OFF

LR- LFL L- PAGE FIG.

SYM	RUN	CONFIGURATION
+	65	S ₁ 8 10 13 17
X	57	b ₁₆ b ₈ v ₉ H ₈
△	60	H ₈ H ₄ H ₉
▽	61	z _{7,8}

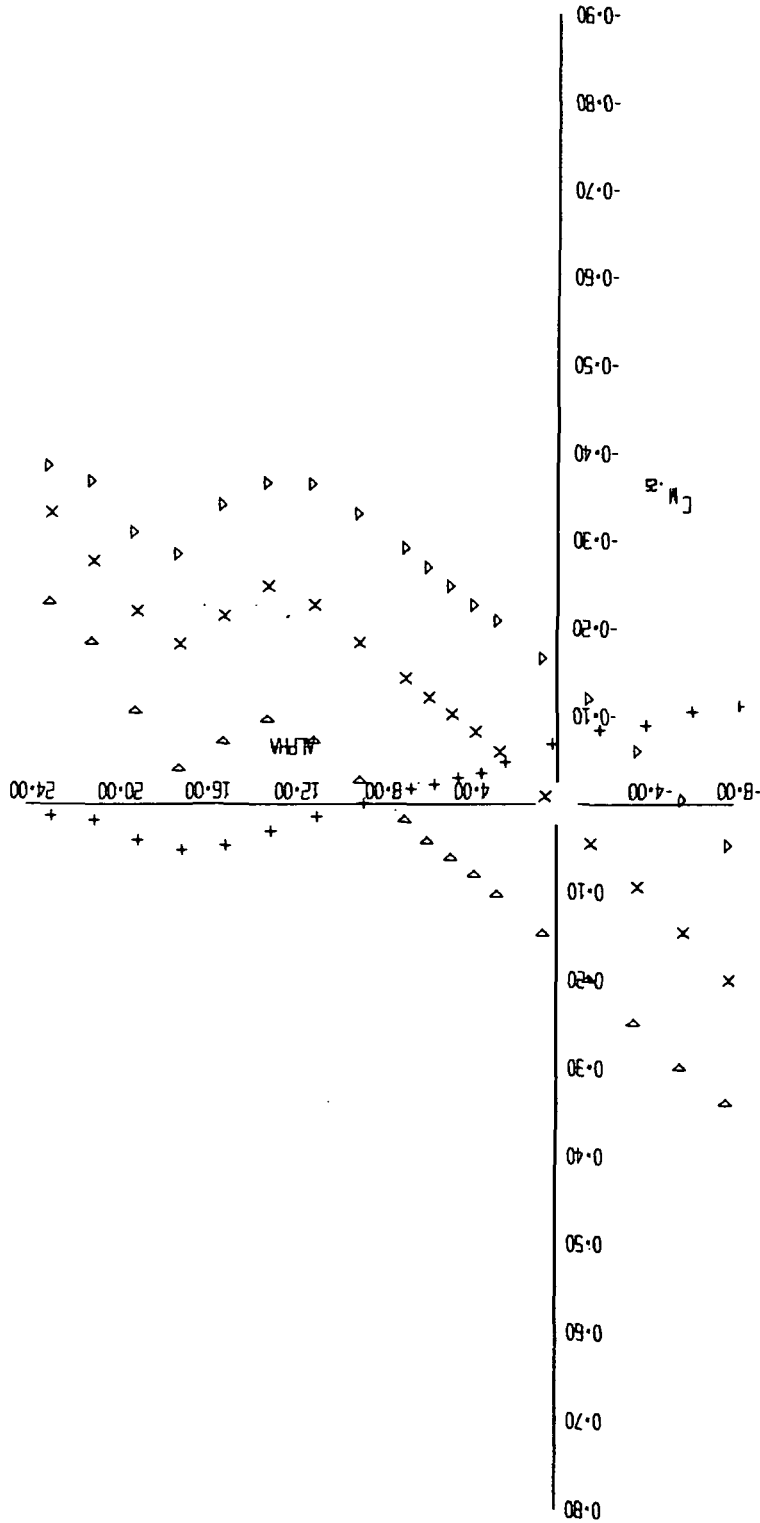


FIGURE 1 (SHEET 3)

▽ △ X +
61 60 57 65

10-10-73

LP-10H

STABILIZER EFFECTIVENESS
ORBITER OFF

LR- C/L L-353 PAGE FIG.

SYN RUN CONFIGURATION

SYN	RUN	CONFIGURATION
+	63	s ¹ a ¹⁰ q ¹³ r ³⁷
x	57	b ¹⁶ d ⁸ v ⁹
▷	61	h ⁸ h ⁸⁴ h ⁸⁴ z ^{7,8}

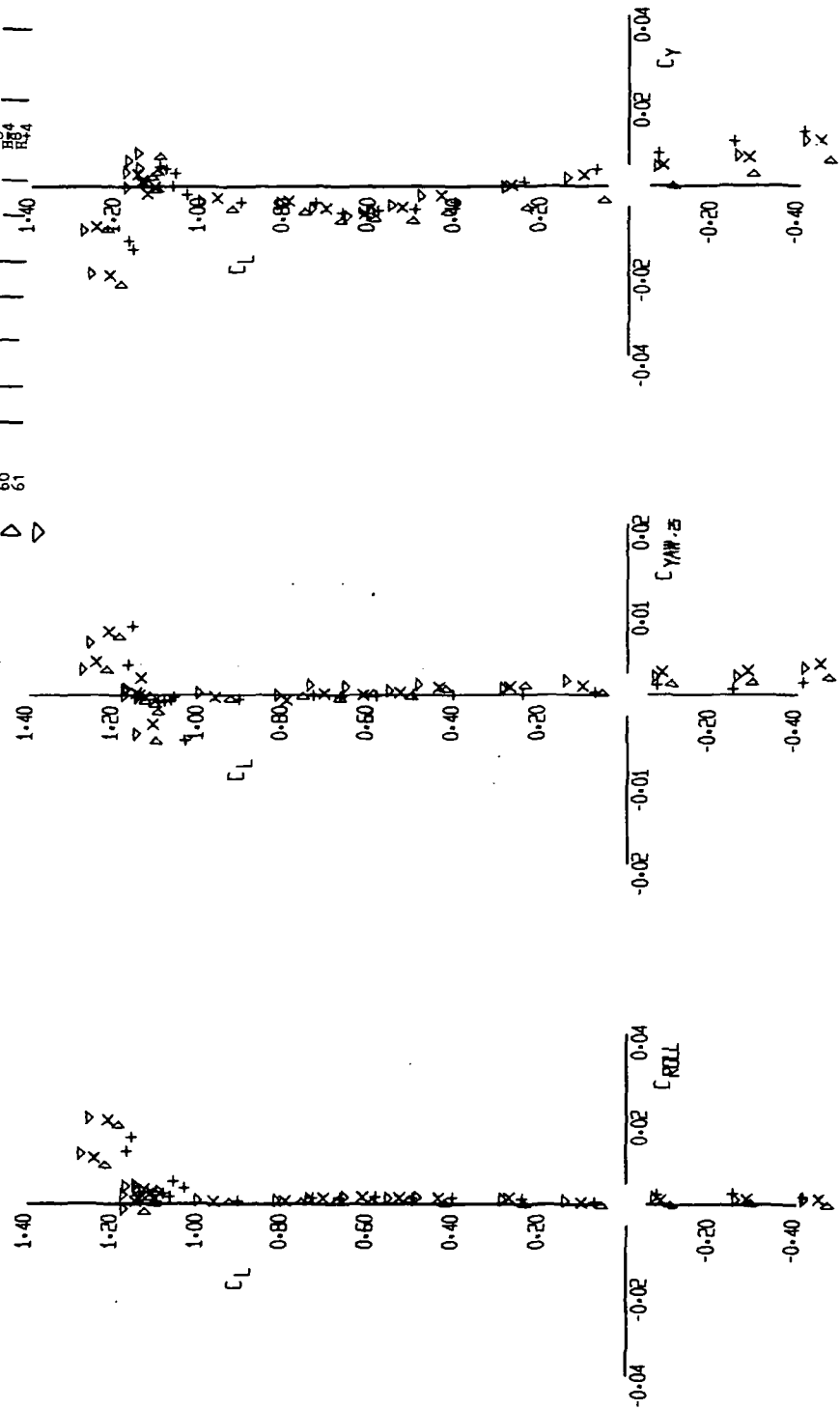


FIGURE 1 (SHEET 4)

8 6 8 9
+ x ▷ ▽

12-10-71

LF-III

EFFECT OF ORBITER POSITION
TAIL ON AND TAIL OFF

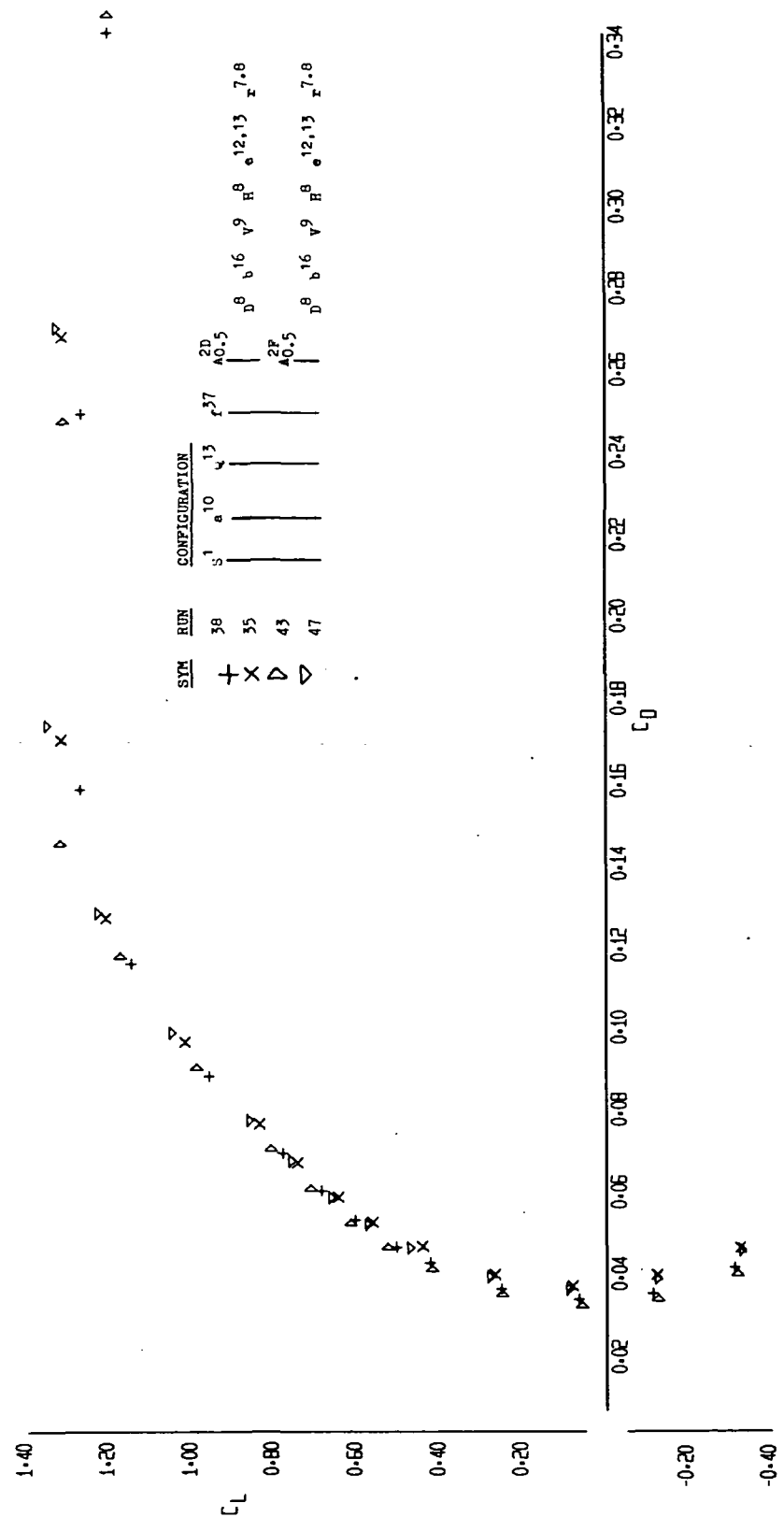


FIGURE 2 (SHEET 1)

EFFECT OF ORBITER POSITION
TAIL ON AND TAIL OFF

LR- LFL L-363 PAGE FIG.

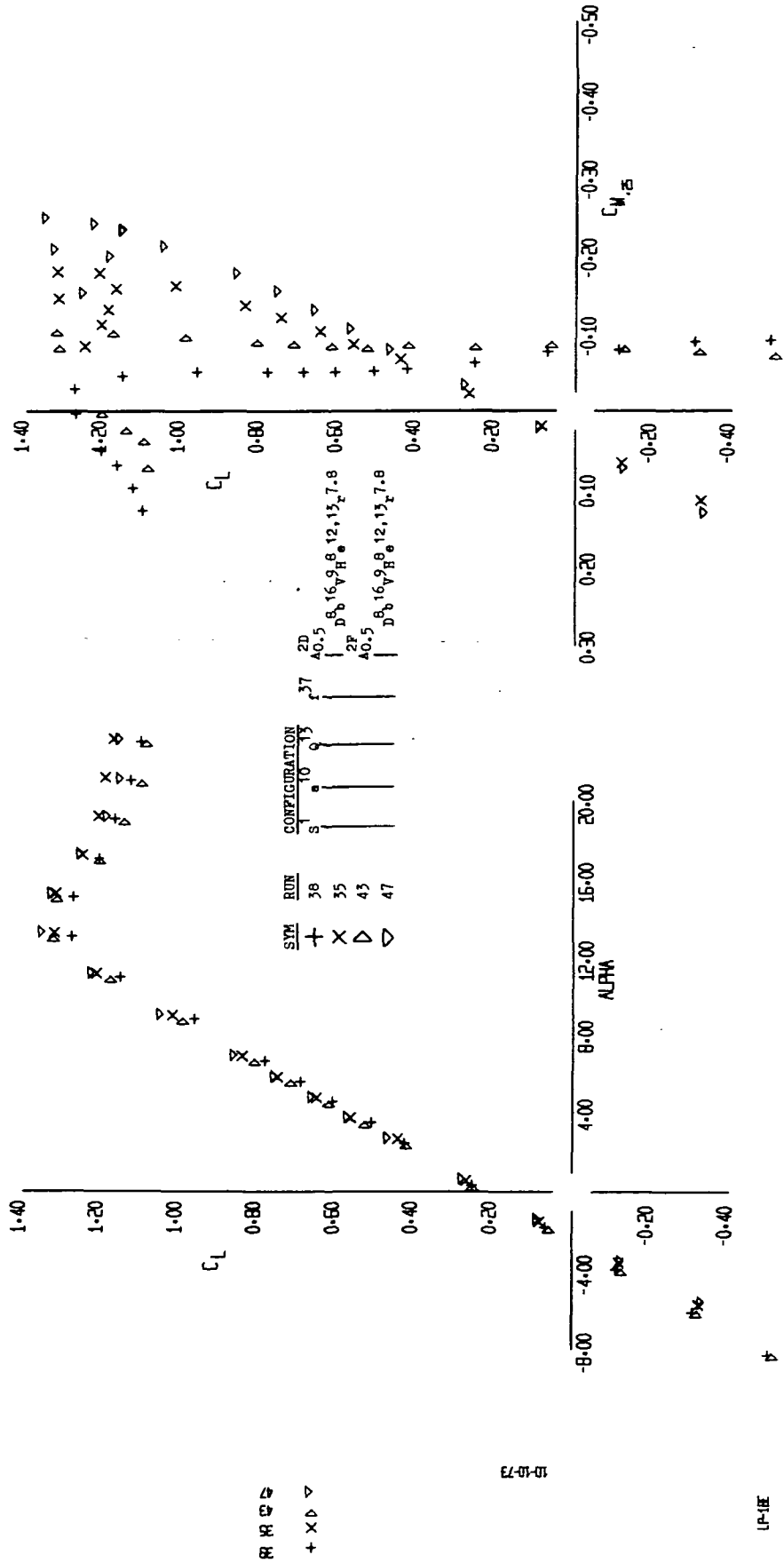


FIGURE 2 (SHEET 2)

EFFECT OF ORBITER POSITION
TAIL ON AND TAIL OFF

LR- PAGE
LFL- FIG.

SYM	RUN	CONFIGURATION
+	38	S ¹ 0 10 Q 13 r ³⁷ A _{0,5} ^{2D}
X	35	D ⁸ b ¹⁶ v ⁹ H ⁸ 12,13 7,8
△	43	A _{0,5} ^{2F}
▽	47	D ⁸ b ¹⁶ v ⁹ H ⁸ 12,13 7,8

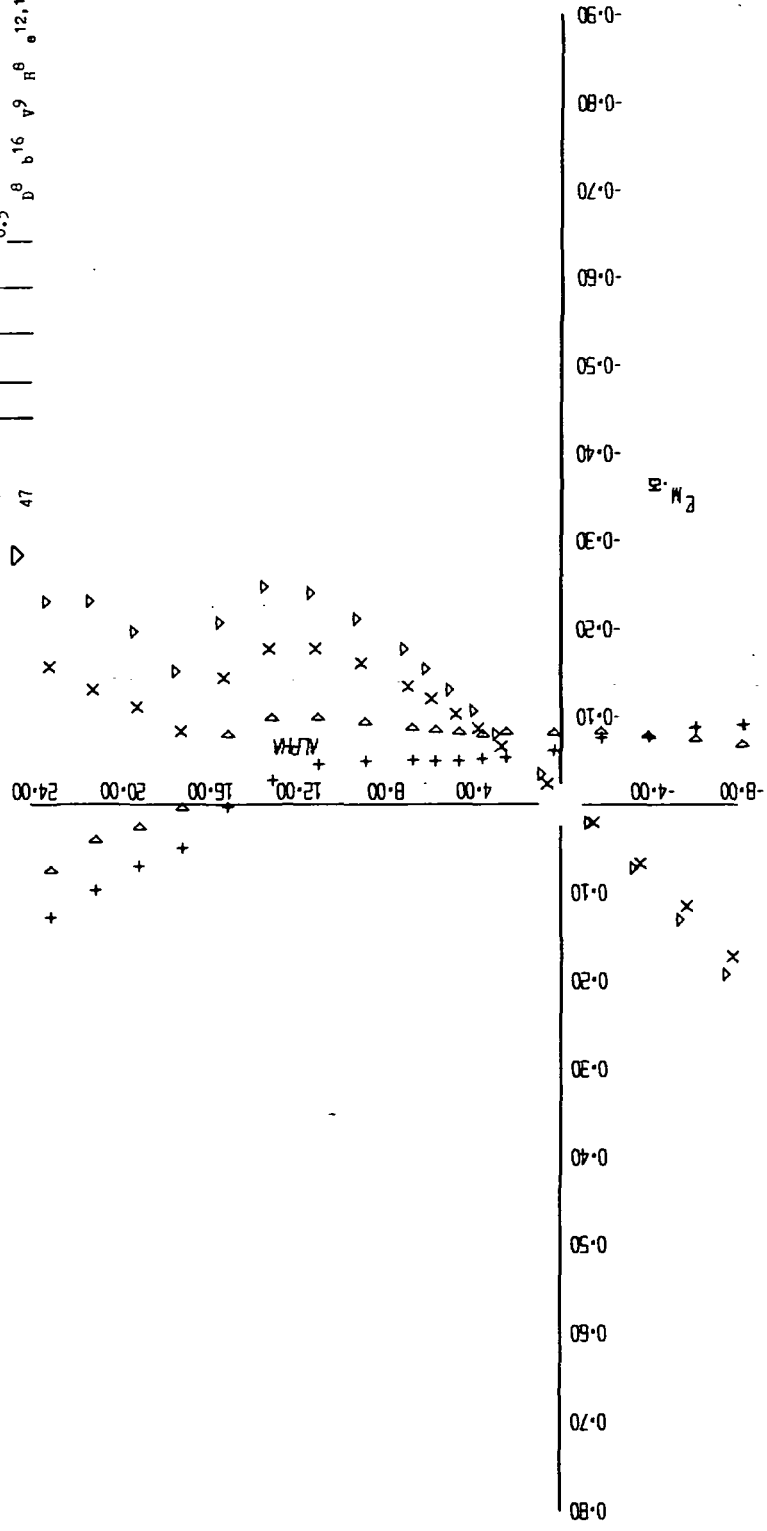


FIGURE 2 (SHEET 3)

△ X +
X X X
43 35 38

10-10-73

(110)

EFFECT OF ORBITER POSITION

TAIL ON AND TAIL OFF

SYM	RUN	CONFIGURATION	TAIL ON	TAIL OFF
+	38	S ¹ R ¹⁰ Q ¹³ T ³⁷ A ²⁰	D ⁸ b ¹⁶ V ⁹ R ⁸ 12,13 7.8	D ⁸ b ¹⁶ V ⁹ R ⁸ 12,13 7.8
x	35	A ²⁰ S ¹ R ¹⁰ Q ¹³ T ³⁷	D ⁸ b ¹⁶ V ⁹ R ⁸ 12,13 7.8	D ⁸ b ¹⁶ V ⁹ R ⁸ 12,13 7.8
△	45	A ²⁰ S ¹ R ¹⁰ Q ¹³ T ³⁷	D ⁸ b ¹⁶ V ⁹ R ⁸ 12,13 7.8	D ⁸ b ¹⁶ V ⁹ R ⁸ 12,13 7.8
▽	47	A ²⁰ S ¹ R ¹⁰ Q ¹³ T ³⁷	D ⁸ b ¹⁶ V ⁹ R ⁸ 12,13 7.8	D ⁸ b ¹⁶ V ⁹ R ⁸ 12,13 7.8

LR- LFL 1-353 PAGE FIG.

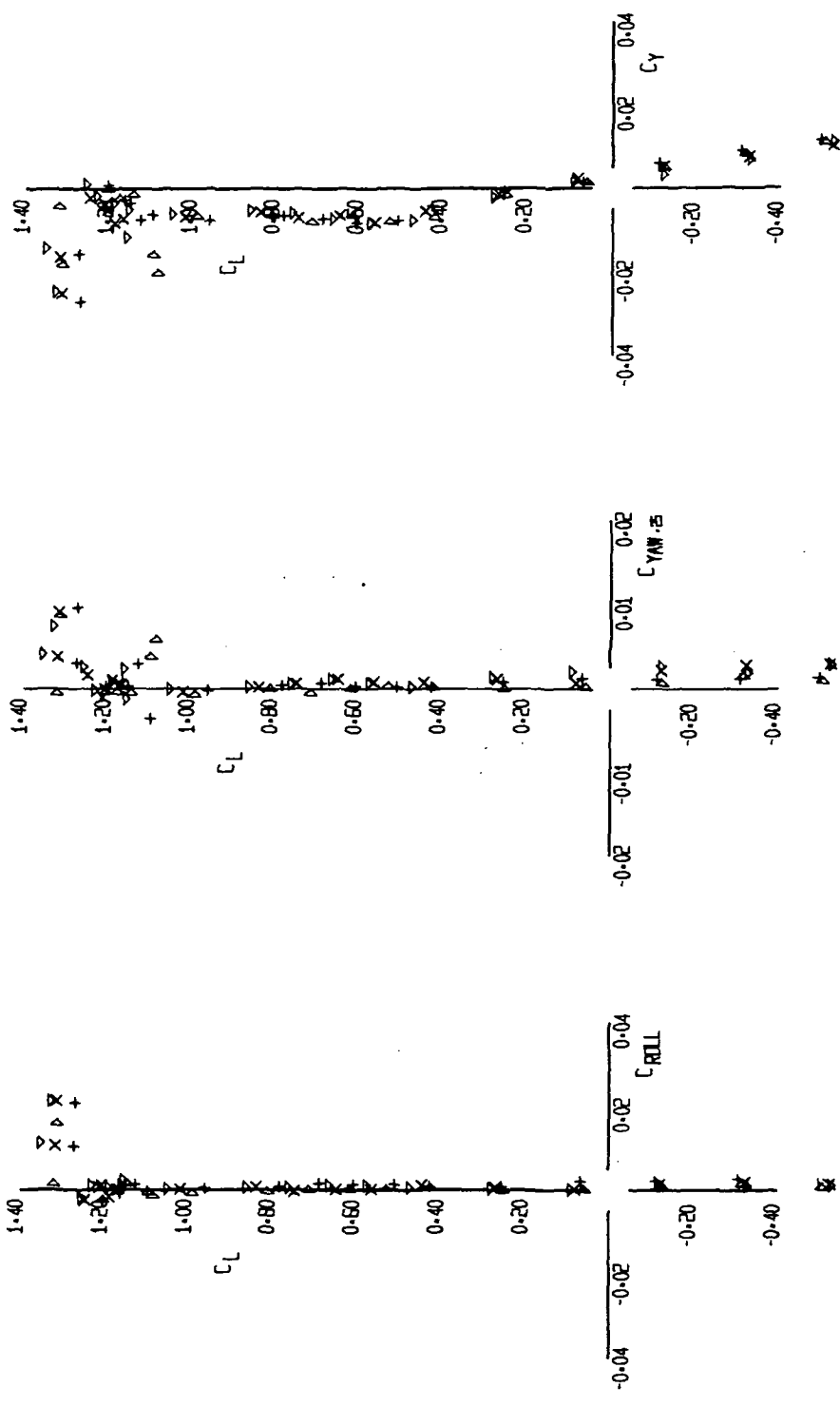


FIGURE 2 (SHEET 4)

RR RR
+ x △ ▽

15-15-73

LR-35

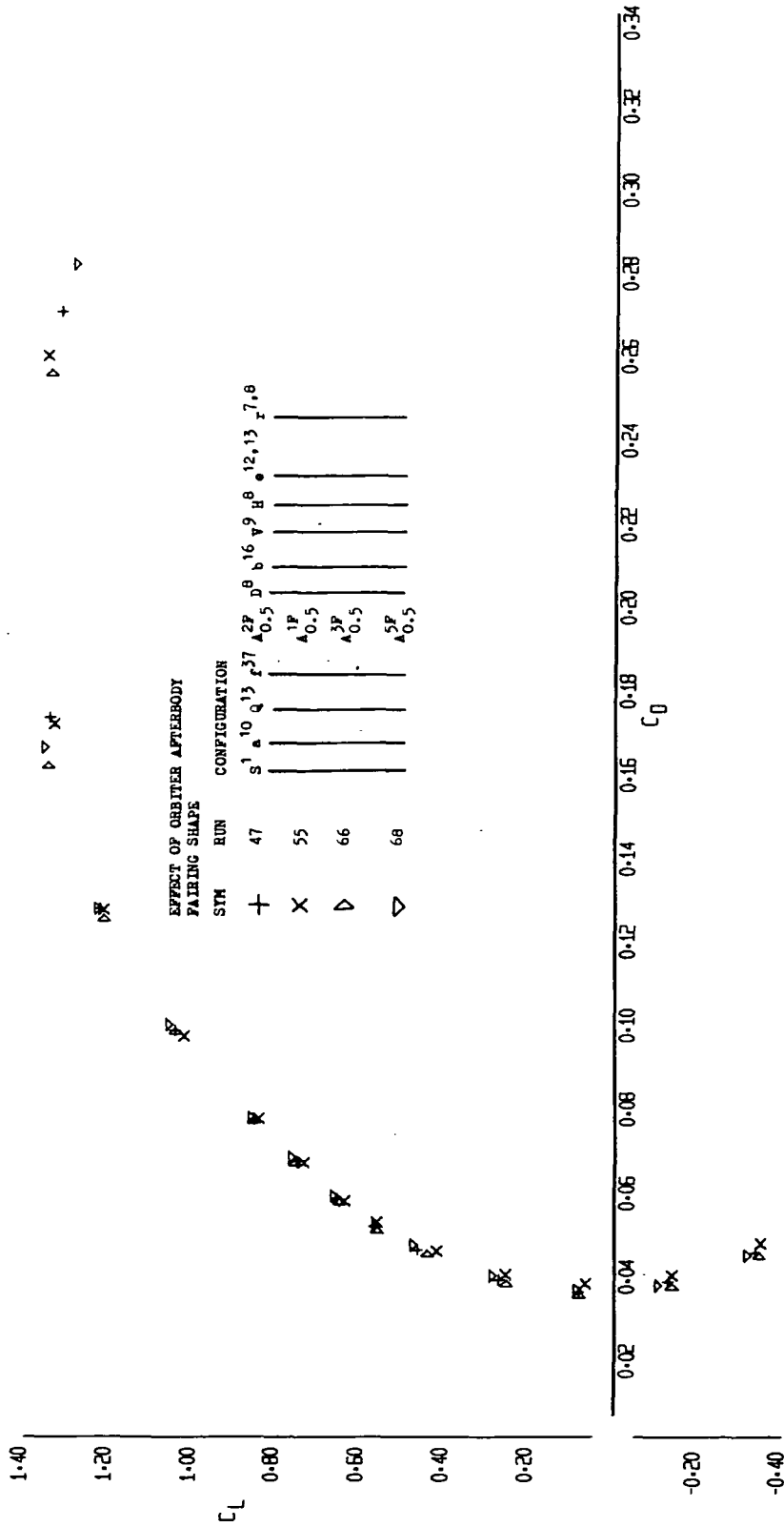


FIGURE 3 (SHEET 1)

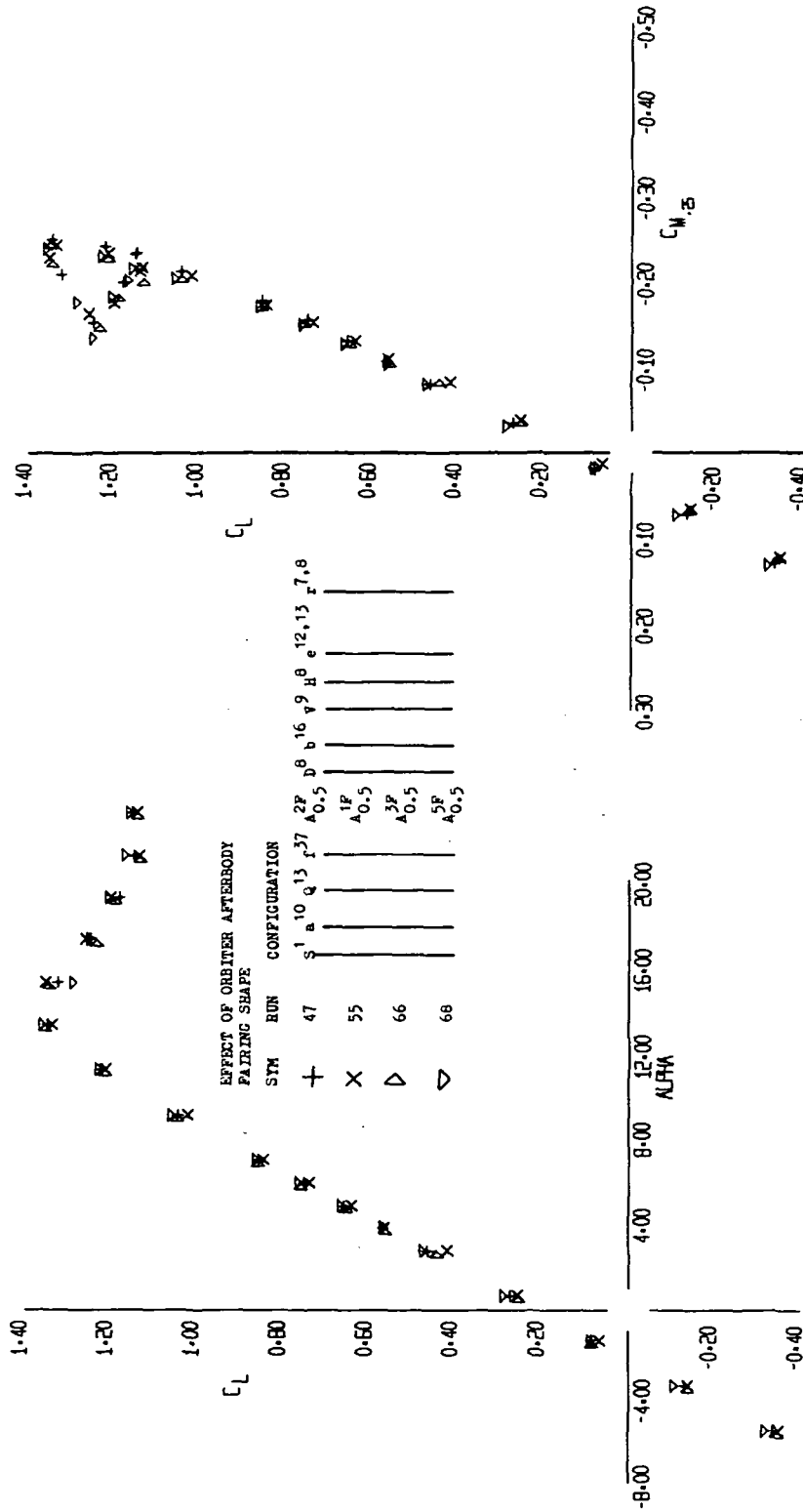


FIGURE 3 (SHEET 2)

→ 出 出 出
+ x ▷ ▽

10-10-73

UP-1E

PAGE

FIG.

LR- LFL L-

EFFECT OF ORBITER AFTERBODY PAIRING SHAPE
 SYM RUN CONFIGURATION

47	+	47	S	1	10	2	13	3	37	A	2P	D	8	R	16	Y	9	H	8	12	13	X	7.8
55	X	55	A	1P	0.5																		
66	▷	66	A	3P	0.5																		
68	△	68	A	5P	0.5																		

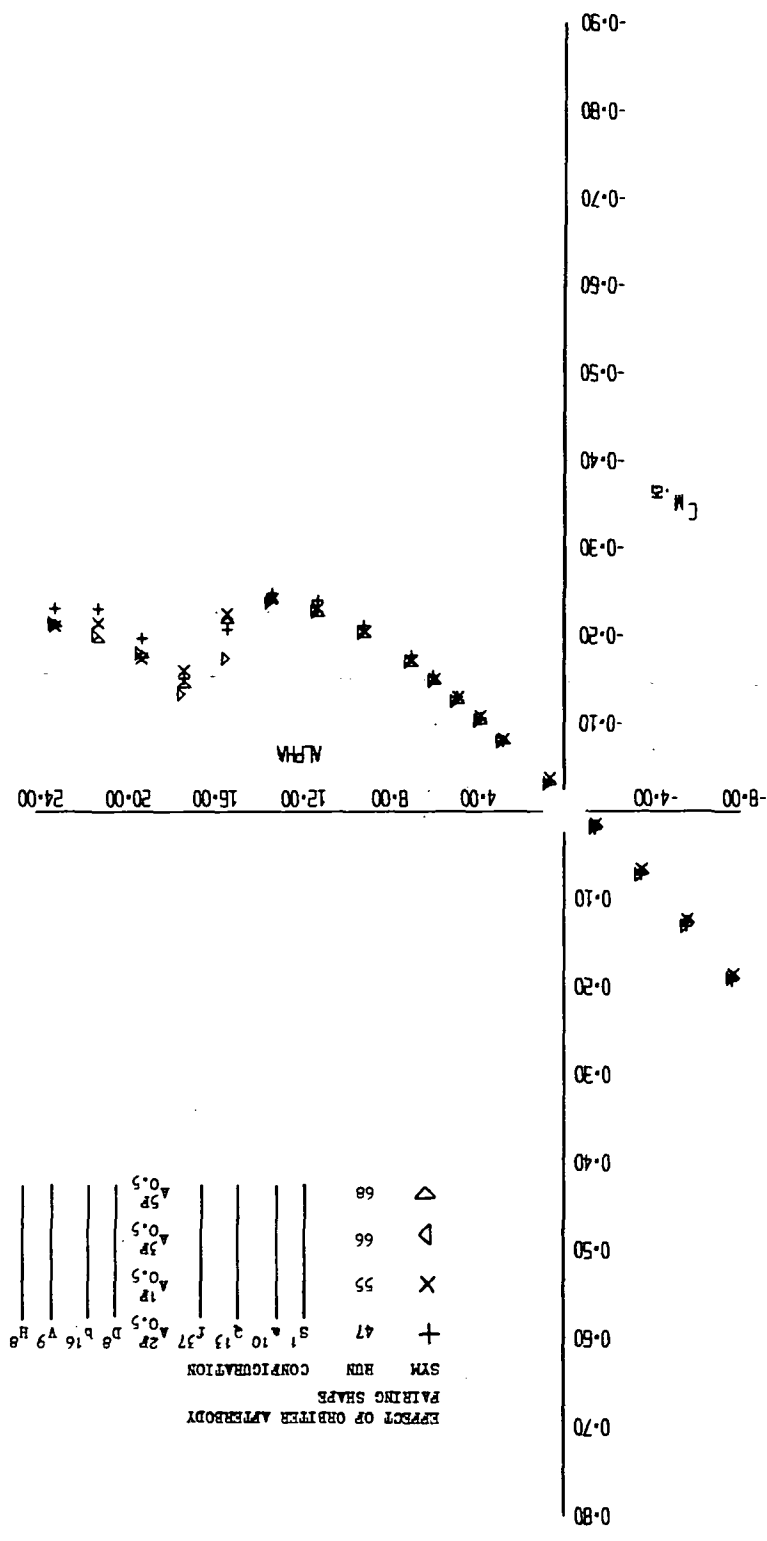


FIGURE 3 (SHEET 3)

10-10-73

LR-101

△ X +
 BB BB BB

EFFECT OF ORBITER AFTERBODY

LP-
LFL 1-33

PAI
FIG.

PAIRING SHAPE

SYM	RUN	CONFIGURATION	2P	D	B	16	9	H	12,13	r	7,8
+	47	S ₁ a	1.57								
x	55	A ₁ P ₅	40.5								
△	66	A ₁ P ₅	40.5								
▽	68	A ₁ P ₅	40.5								

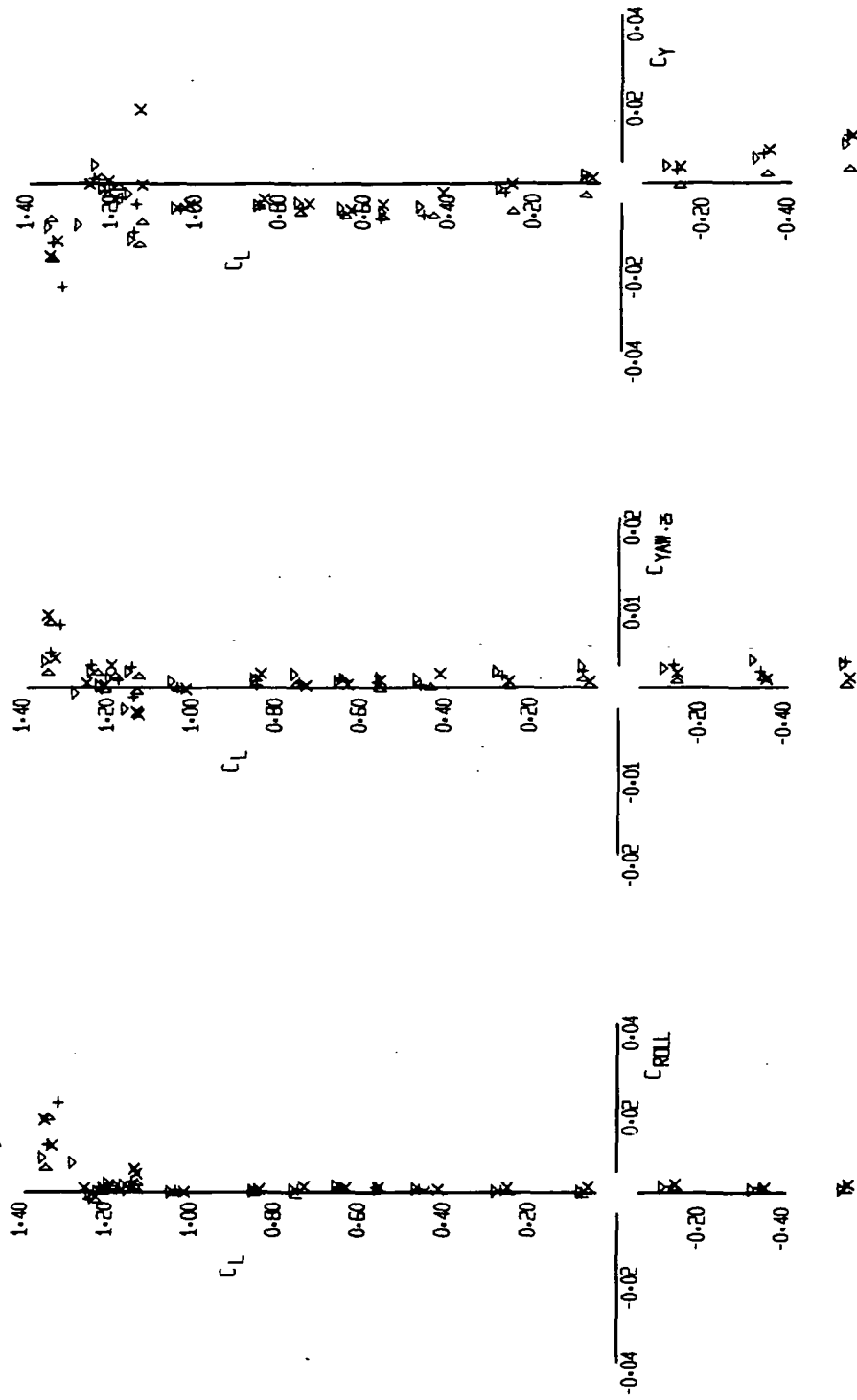


FIGURE 3 (SHEET 4)

△ x △ +

LP-33

LP-33

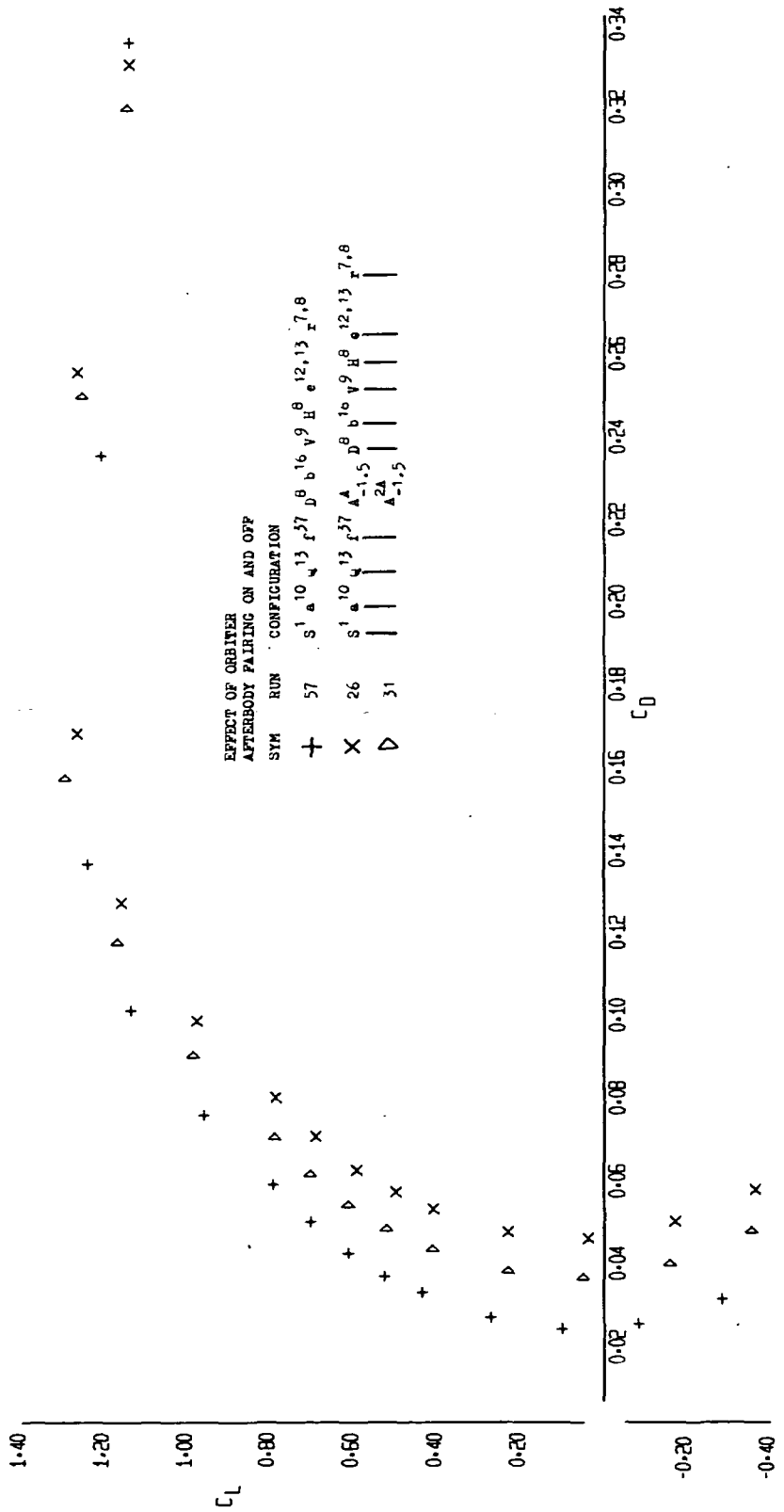


FIGURE 4 (SHEET 1)

10-11-73

LR-363
+ x D

LR-363

LP- U1 L-353
PAGE FIG.

EFFECT OF ORBITER

AFTEROODY PAIRING ON AND OFF

RUN	CONFIGURATION	37	16	9	12,13	7,8
57	S1 10 Q13	f37	D ^B b ¹⁶	y ⁹	B ^B 12,13	r ^{7,8}
26	S1 10 Q13	f37	A ^A 1.5	D ^B b ¹⁶	y ⁹ B ^B 12,13	r ^{7,8}
31	S1 10 Q13	f37	A ^A 2.5	D ^B b ¹⁶	y ⁹ B ^B 12,13	r ^{7,8}

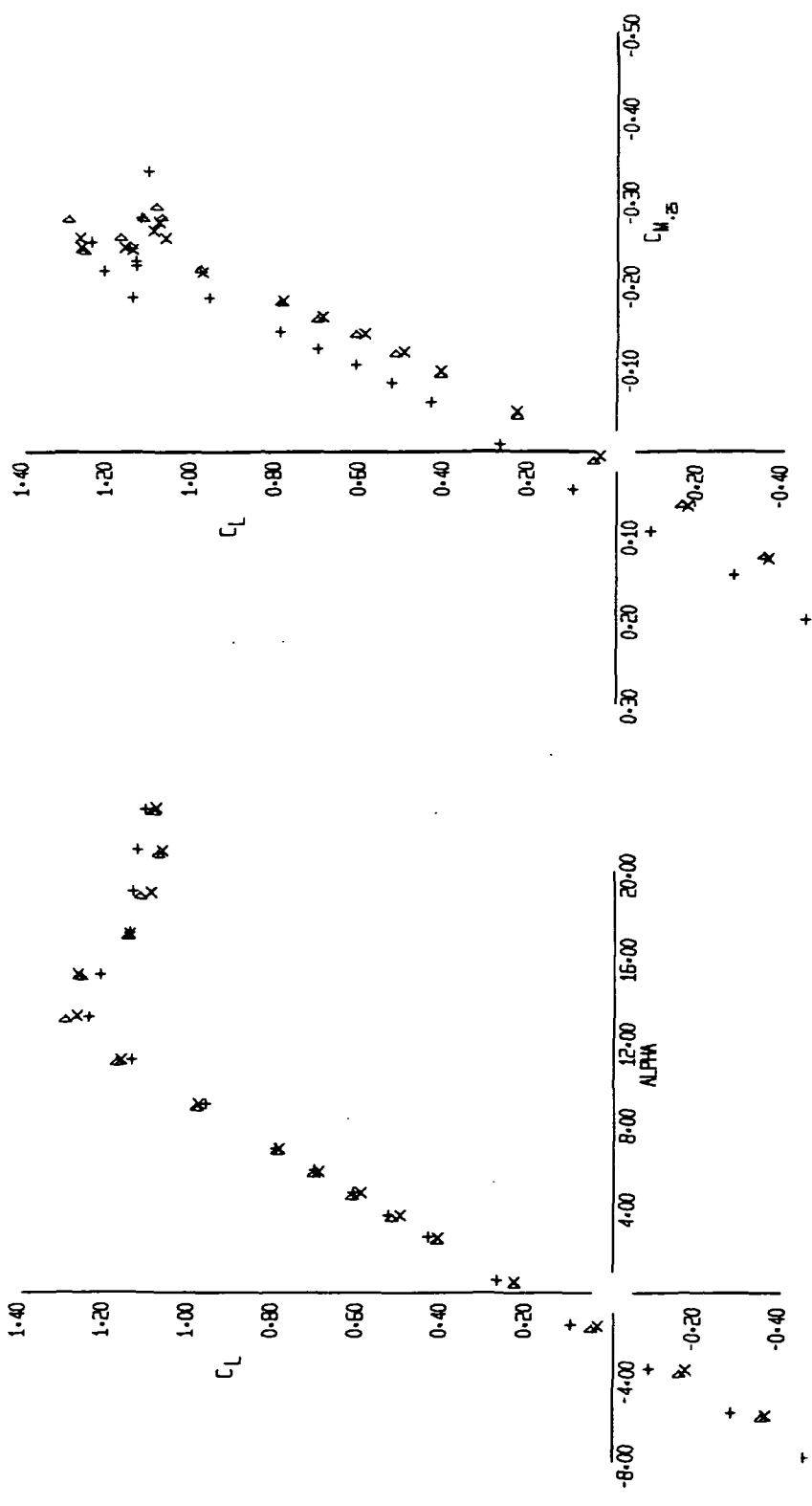


FIGURE 4 (SHEET 2)

10-11-73

DRB
+ x Δ

LP-18E

EFFECT OF ORBITER
AFTERBODY FAIRING ON AND OFF

SYM	RUN	CONFIGURATION	
		ON	OFF
+	57	S ¹ Q ¹³ r ³⁷ D ⁸ V ⁹ R ⁸ 12,13	r ^{7,8}
X	26	S ¹ Q ¹³ r ³⁷ A ^{1,5} D ⁸ V ⁹ R ⁸ 12,13	r ^{7,8}
Δ	31	A ^{1,5} D ⁸ V ⁹ R ⁸ 12,13	

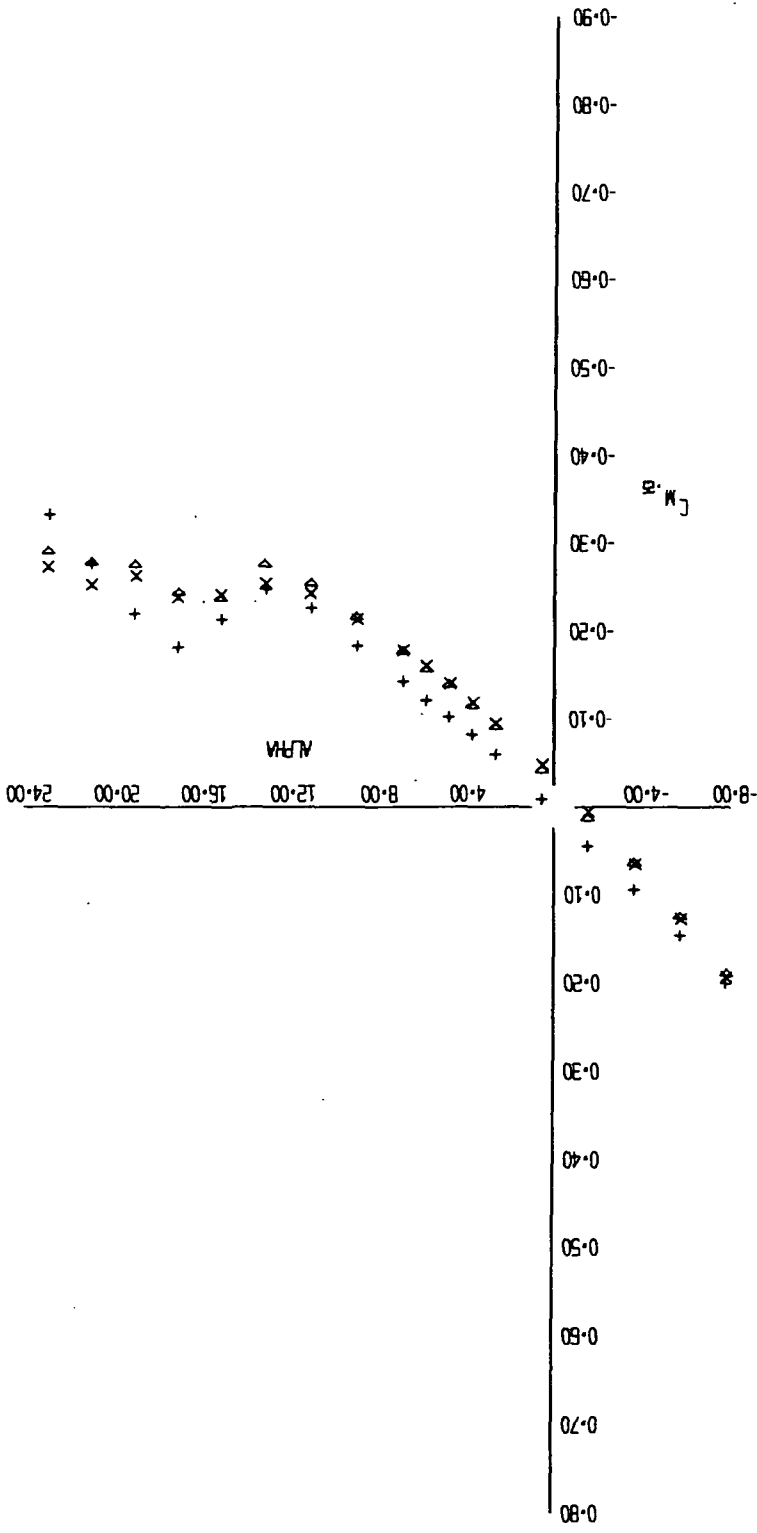


FIGURE 4 (SHEET 3)

10-11-73

Δ X +
M B Q

LP-108

EFFECT OF ORBITER

AFTERBODY FAIRING ON AND OFF

SYM	RUN	CONFIGURATION
+	57	S ¹ a ¹⁰ Q ¹³ f ³⁷ D ⁸ b ¹⁶ v ⁹ R ⁸ 12,13 7,8
X	26	S ¹ a ¹⁰ Q ¹³ f ³⁷ A ^{1,5} D ⁸ b ¹⁶ v ⁹ R ⁸ 12,13 7,8
▷	31	A ^{1,5}

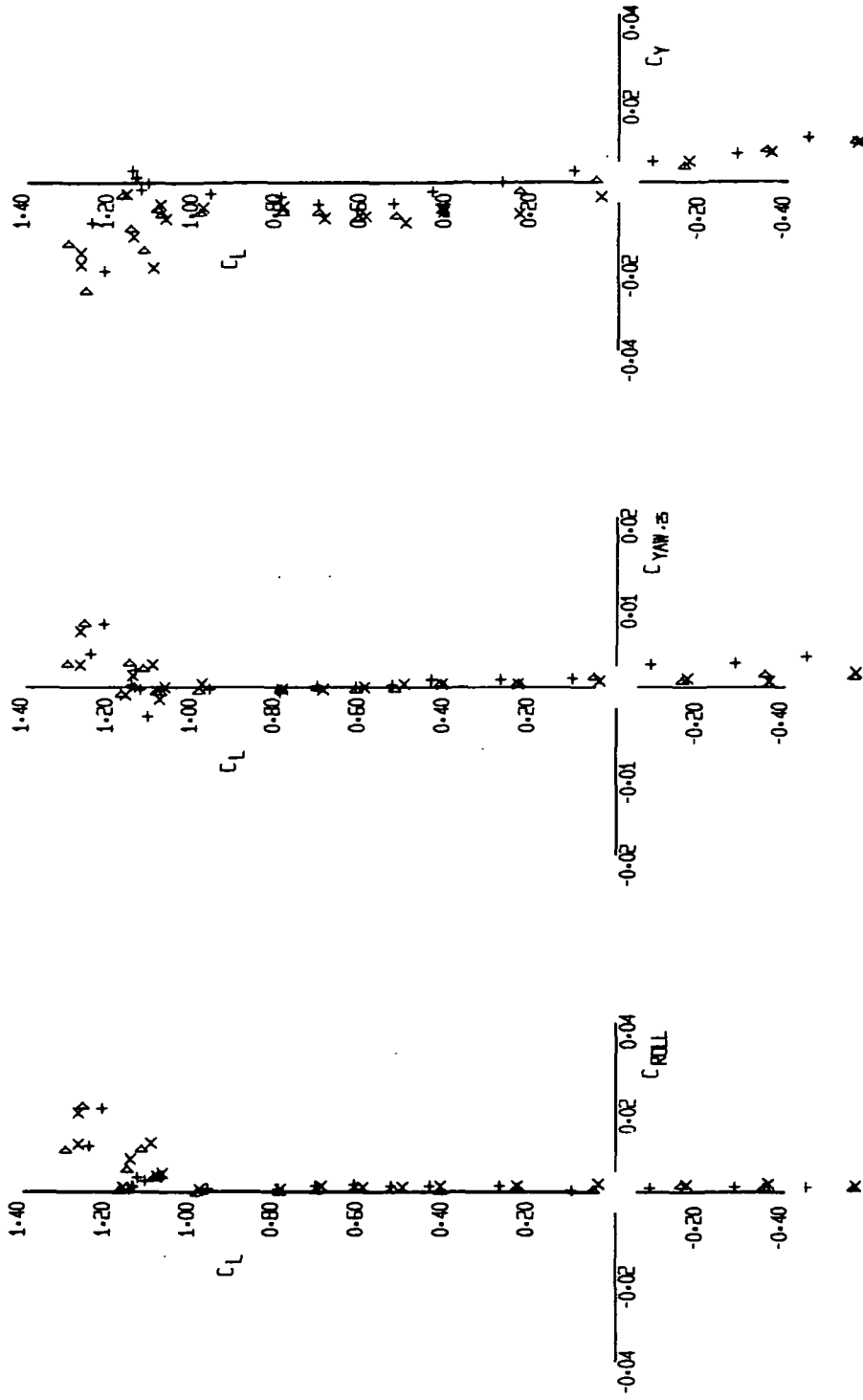


FIGURE 4 (SHEET 4)

LR-363

LR-363

EFFECT OF ORBITER INCIDENCE ANGLE

LR
LFL-353

PAVE
FIG.

RUN	SYM	CONFIGURATION	2A	D ⁸	b ¹⁶	v ⁹	H ⁸	e ^{12,13}	r ^{7,8}
33	+	S ¹ a ¹⁰ Q ¹⁵ r ²⁷	A ₂						
31	X	A ₂							
68	△	A ₂							
70	▽	A ₂							

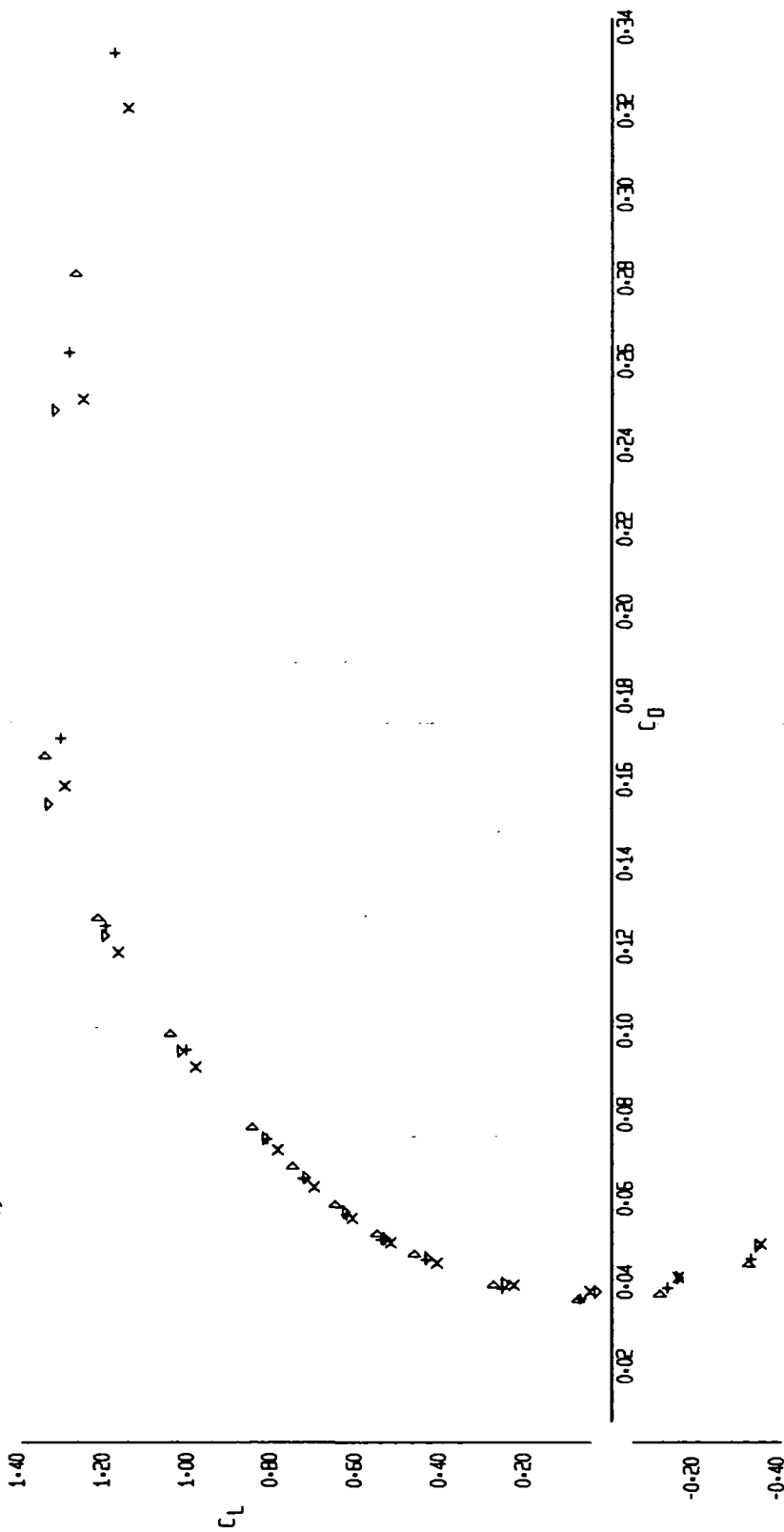


FIGURE 5 (SHEET 1)

EFFECT OF ORBITER INCIDENCE ANGLE

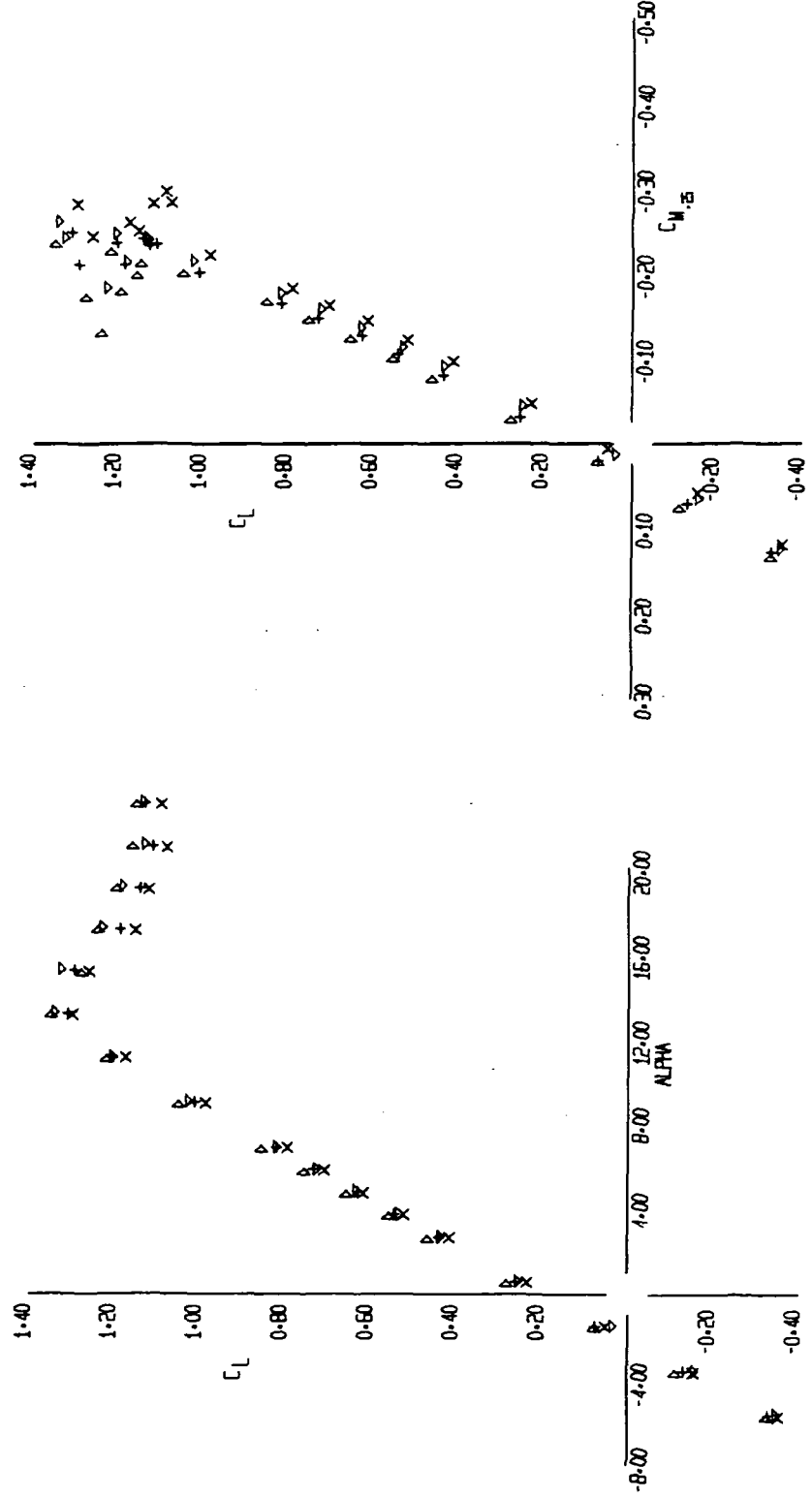
LR
LFL L-363

PAGE
FIG.

RUN	SYM
33	+
31	x
68	▷
70	◁

CONFIGURATION	
S ₁	10
Q	13
f ₁	37
A ₁	5
A ₂	1.5
A ₃	1.5
A ₄	1.5

2A	8
D	16
b	9
V	8
H	12, 13
r	7, 8



RRRR
+ x ▷ ◁

10-11-73

LP-105

FIGURE 5 (SHEET 2)

EFFECT OF ORBITER INCIDENCE ANGLE

SYM	RUN	CONFIGURATION		A _{2A}	D ₈	b ₁₆	V ₉	H ₈	e _{12,13}	r _{7,8}
		S ₁	Q ₁₃							
+	33			0.5						
X	31			1.5						
△	68			0.5						
▽	70			1.5						

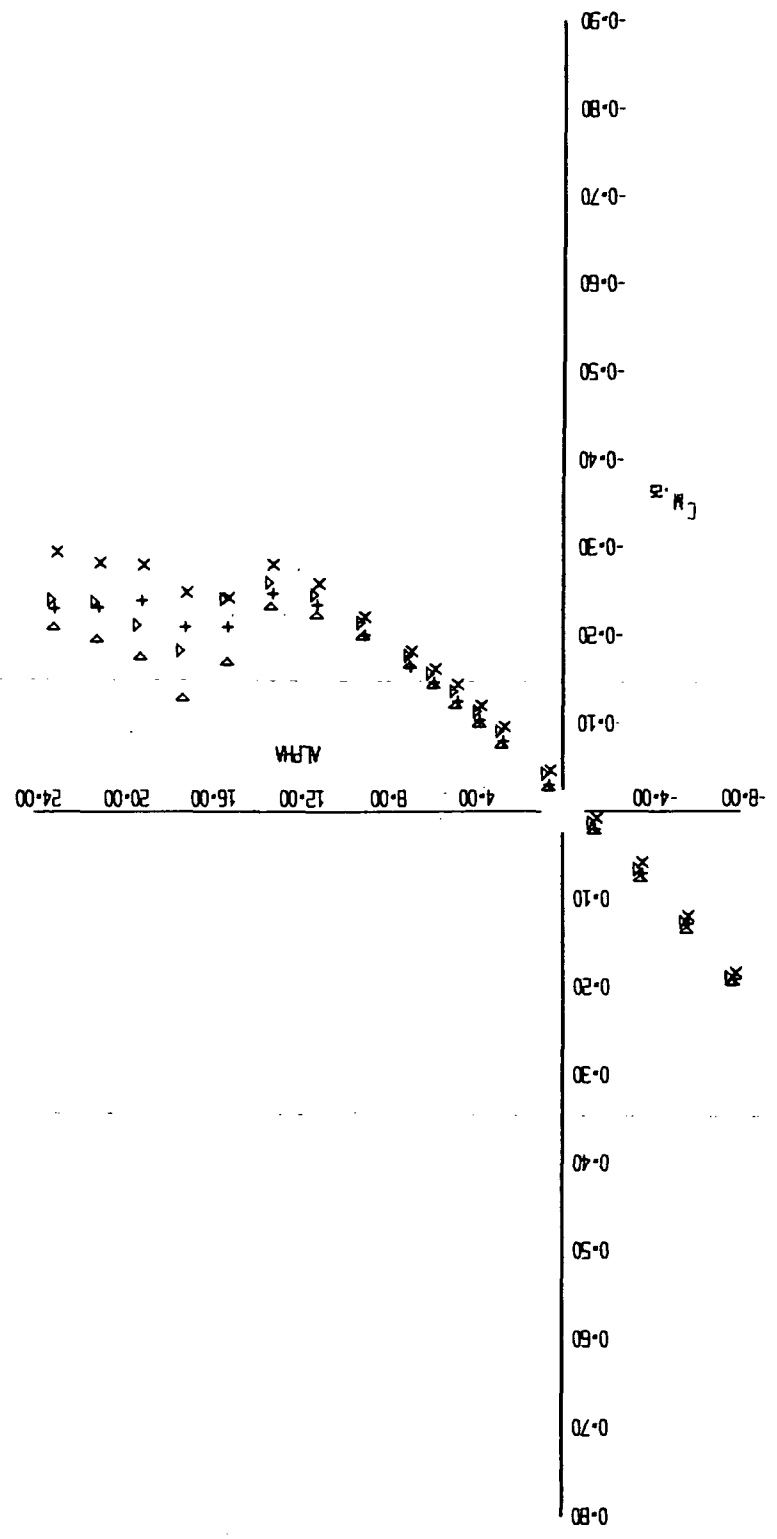


FIGURE 5 (SHEET 3)

RR RR R
+ X X △

LP-14-73

LP-10H

EFFECT OF ORBITER INCIDENCE ANGLE

PAGE
FIG.

LR
L/L-363

RUN	CONFIGURATION	1	2	3	4	5	6	7	8	9	10	11	12	13	14
35	A ₁ -1.5	1.00	1.00	1.00	1.00	1.00	1.00	1.00	1.00	1.00	1.00	1.00	1.00	1.00	1.00
51	A ₂ -1.5	1.00	1.00	1.00	1.00	1.00	1.00	1.00	1.00	1.00	1.00	1.00	1.00	1.00	1.00
68	A ₃ -1.5	1.00	1.00	1.00	1.00	1.00	1.00	1.00	1.00	1.00	1.00	1.00	1.00	1.00	1.00
70	A ₄ -1.5	1.00	1.00	1.00	1.00	1.00	1.00	1.00	1.00	1.00	1.00	1.00	1.00	1.00	1.00

SIZE
+ X Δ ▽

RR RR R
+ X Δ ▽

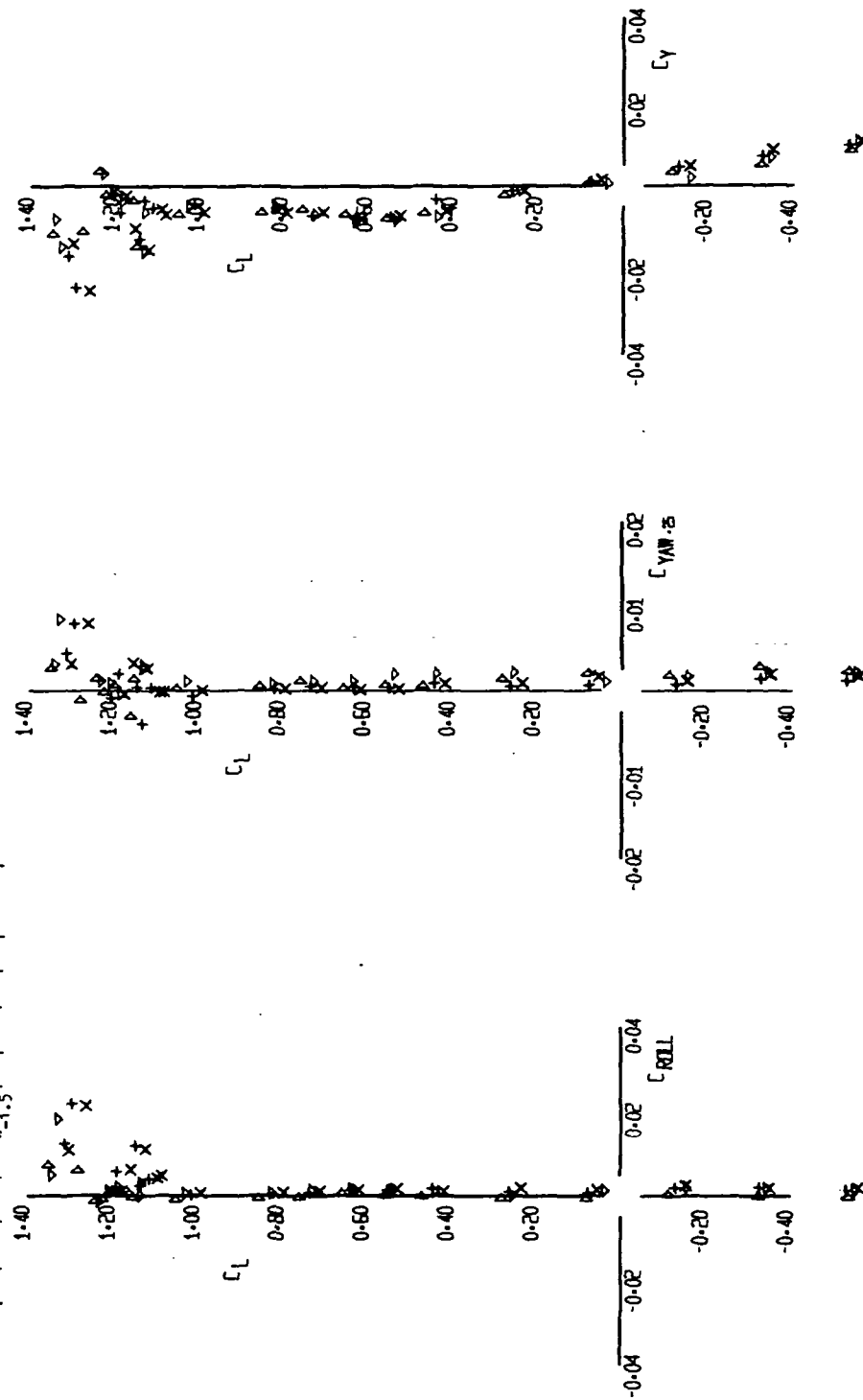


FIGURE 5 (SHEET 4)

LR-11-73

LR-35

EFFECT OF ORBITER POSITION AND AFTERBODY FINISH SHAPE

LR LFL-363 PAGE FIG.

SYM	RUN	CONFIGURATION
+	49	S ¹ a ¹⁰ Q ¹³ r ³⁷ 2C A0.5
X	53	A1C A0.5 1P A0.5
D	55	D ⁸ b ¹⁶ v ⁹ H ⁸ 12,13 7,8

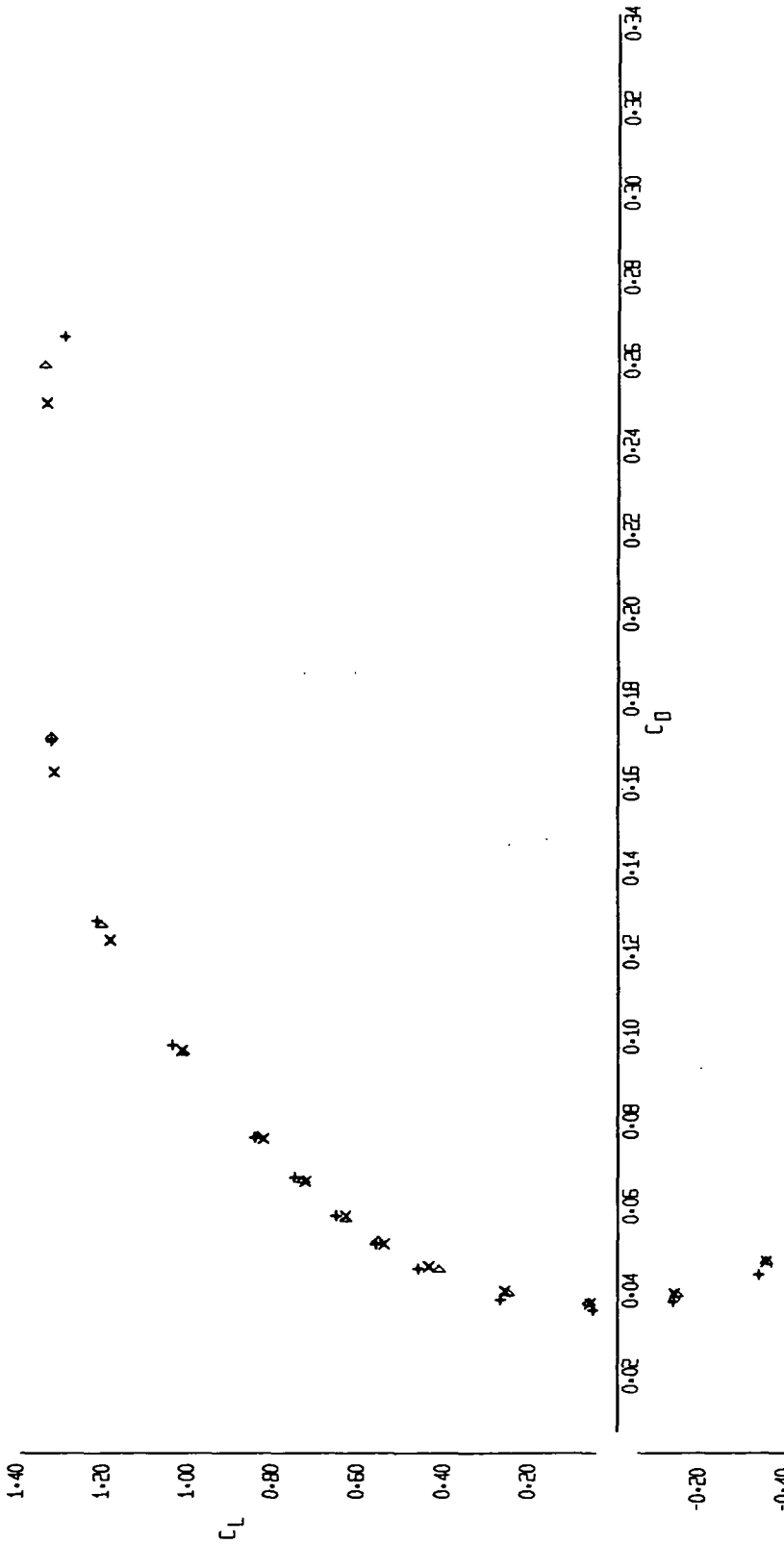


FIGURE 6 (SHEET 1)

LP-20

EFFECT OF ORBITER POSITION AND AFTERBODY FAIRING SHAPE

LR- [FL 1-363] PAGE FIG.

SYN	RUN	CONFIGURATION
+	49	S1, 10, Q13, f37, A2C, 0.5, D, b, 16, v9, R8, 12, 13, r, 7, 8
X	53	A1C, 0.5, 1P, A0.5
D	55	

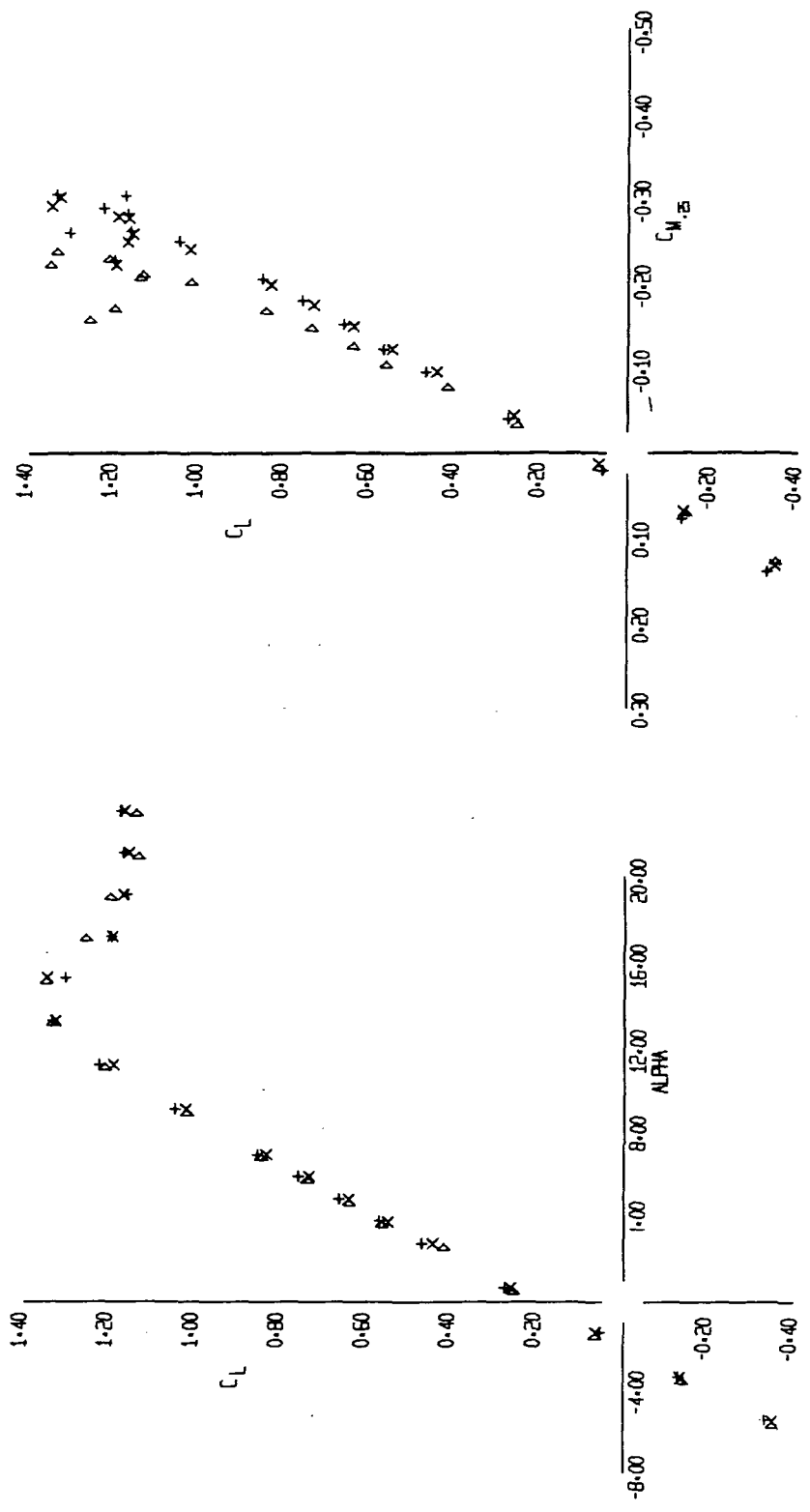


FIGURE 6 (SHEET 2)

55 55
+ X D

15-11-73

1P-1E

EFFECT OF ORBITER POSITION AND AFTERBODY PAIRING SHAPES

LR- UFL L- PAGE FIG.

SYM	RUN	CONFIGURATION
+	49	S1, 10, 13, 37
X	53	A2C, 0.5, 10, 13, 37
Δ	55	A1C, 0.5, 10, 13, 37; A1F, 0.5

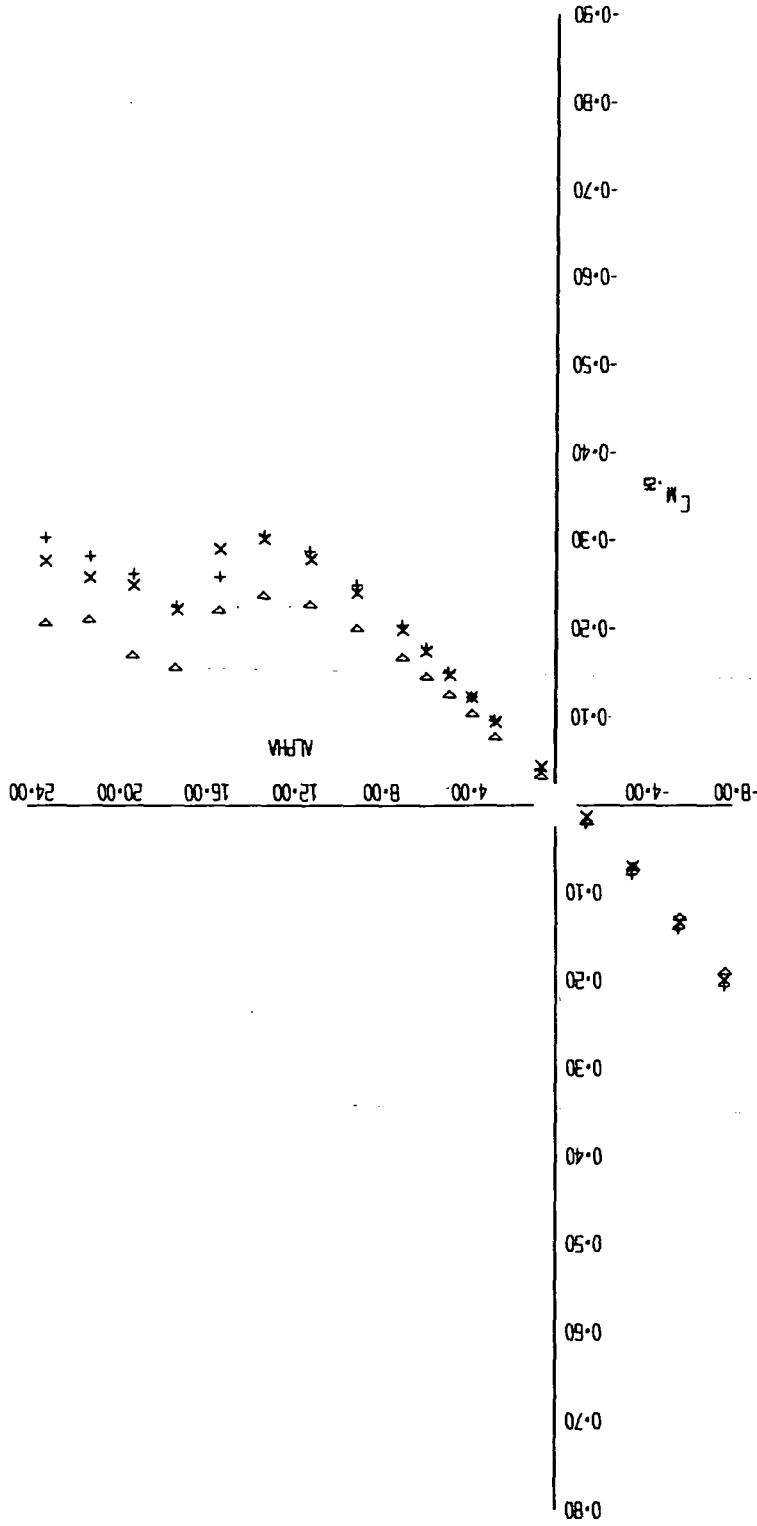


FIGURE 6 (SHEET 3)

10-11-73

UFL-OR

EFFECT OF ORBITER POSITION AND AFTERBODY PAIRING SHAPE

LR
UFL 1-353

PAGE
FIG.

RUN	SYM
49	+
53	x
55	D

CONFIGURATION

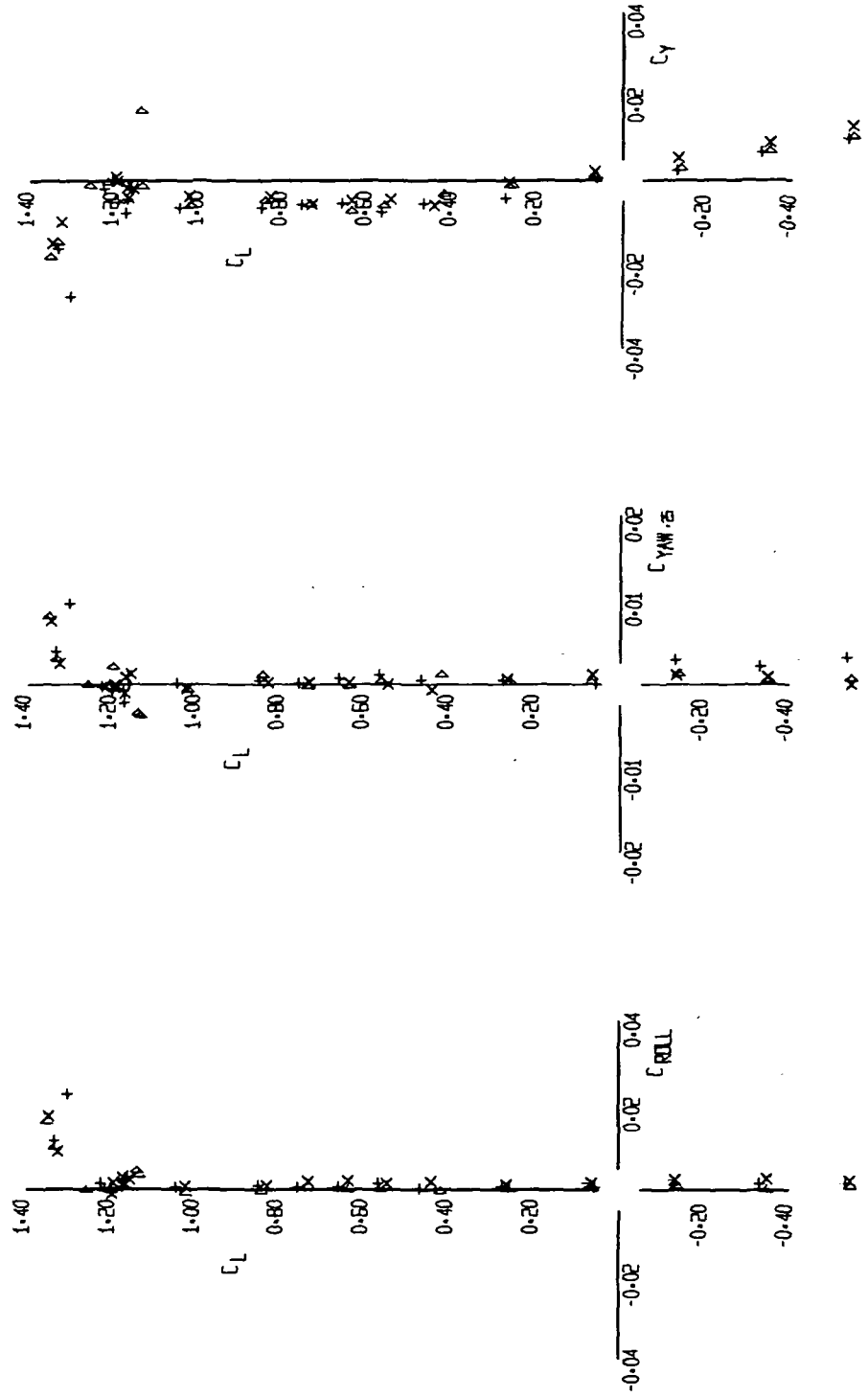
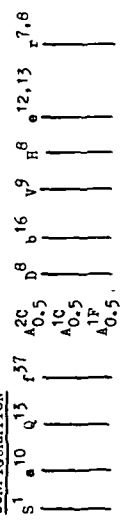


FIGURE 6 (SHEET 4)

LR 11-73
+ x D

LR 300

CONFIGURATION

RUN

SYM

s^1_{10} q^{13} r^{37} b^8 b^{16} v^9 h^8 $e^{12,13}$ $r^{7,8}$
 s^1_{10} q^{13} r^{37} b^8 b^{16} v^9 h^8 $e^{12,13}$ $r^{7,8}$ s^{22}
 s^1_{10} q^{13} r^{37} b^8 b^{16} v^9 h^8 $e^{12,13}$ $r^{7,8}$ s^{22} $x^{1,8}$ v^1
 s^1_{10} q^{13} r^{37} b^8 b^{16} v^9 h^8 $e^{12,13}$ $r^{7,8}$ s^{22} $x^{1,8}$ v^1 s^{60}

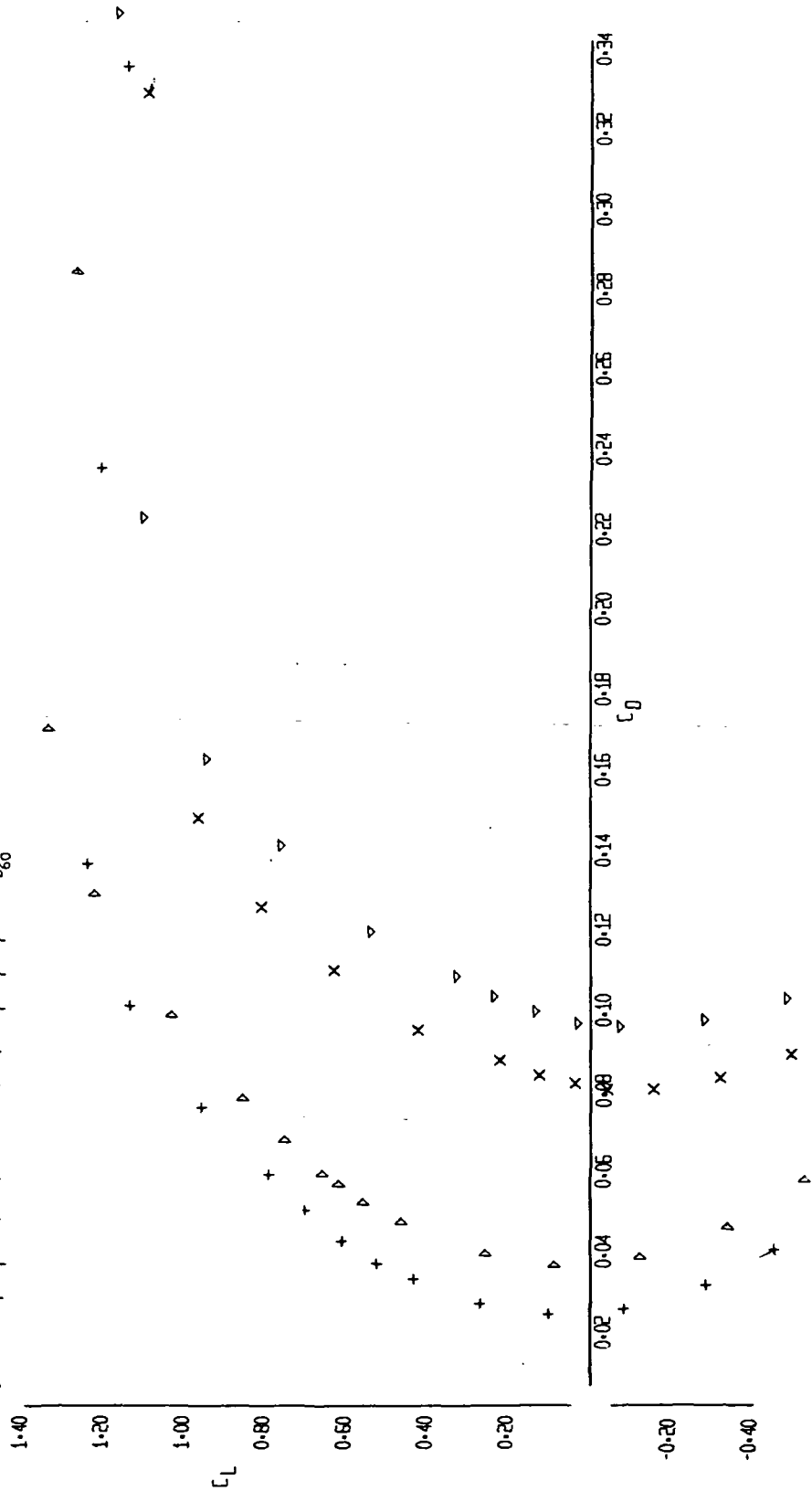


FIGURE 7 (SHEET 1)

58 ZB
+ < > △

10-11-72

LR-20

SPOILER EFFECTIVENESS, ORBITER ON AND OFF

SYM	RUN	CONFIGURATION
+	57	S ¹ 9 10 Q ¹³ P ³⁷ B ¹⁶ V ⁹ H ⁸ 12,13 7,8
x	65	S ¹ 9 10 Q ¹³ P ³⁷ A ^{0.5} B ¹⁶ V ⁹ H ⁸ 12,13 7,8 1
△	74	S ¹ 9 10 Q ¹³ P ³⁷ A ^{0.5} B ¹⁶ V ⁹ H ⁸ 12,13 7,8 1
▽	83	S ¹ 9 10 Q ¹³ P ³⁷ A ^{0.5} B ¹⁶ V ⁹ H ⁸ 12,13 7,8 1

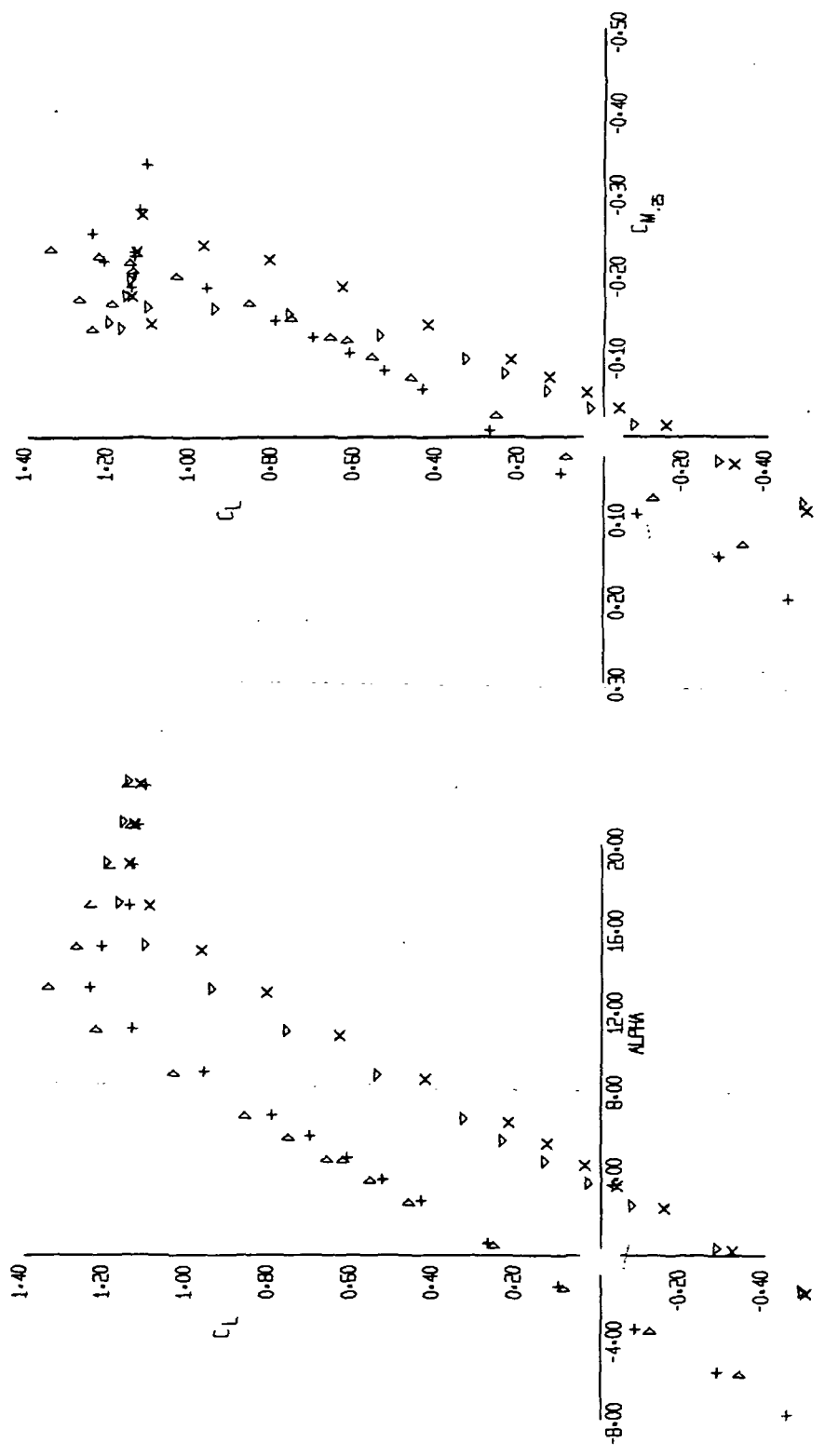


FIGURE 7 (SHEET 2)

57 65 74 83
+ x x △ ▽

10-11-73

LP-EE

SPOILER EFFECTIVENESS, ORBITER ON AND OFF

SYM	RUN	CONFIGURATION
△	57	S ¹ a ¹⁰ q ¹³ f ³⁷ b ¹⁶ v ⁹ h ⁸ e ^{12,13} r ^{7,8}
X	65	
+	74	S ¹ a ¹⁰ q ¹³ f ³⁷ a ^{5P} b ¹⁶ v ⁹ h ⁸ e ^{12,13} r ^{7,8} v ¹
△	83	

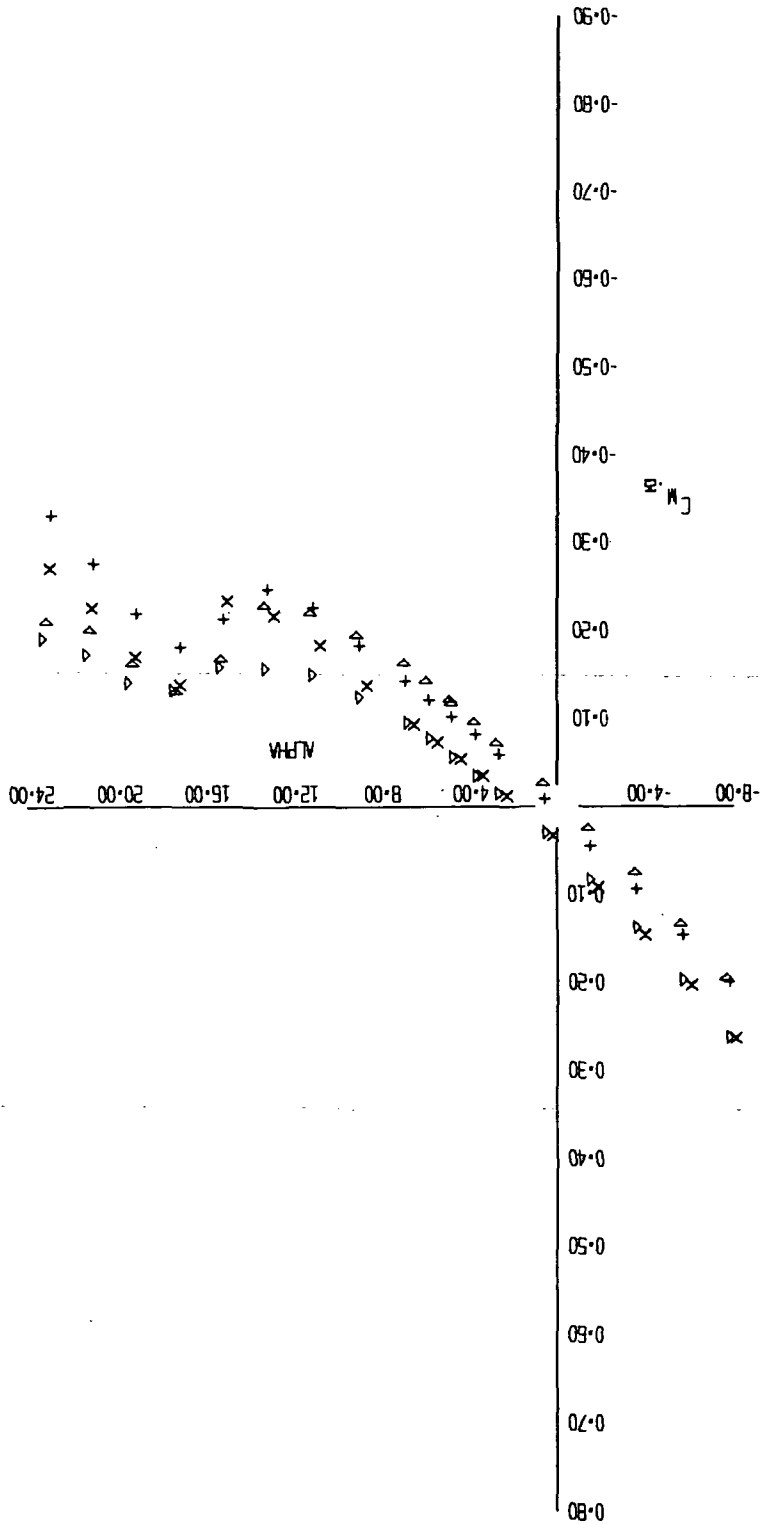


FIGURE 7 (SHEET 3)

△ X +
74 85 97

1D-11-73

LR-104

SPOILER EFFECTIVENESS, ORBITER ON AND OFF

SYM	RUN	CONFIGURATION
+	57	S ¹ a ¹⁰ q ¹³ r ³⁷ b ⁸ b ¹⁶ v ⁹ H ^B e ^{12,13} r ^{7,8}
x	65	S ²⁶
▷	74	S ¹ a ¹⁰ q ¹³ r ³⁷ s ^{5F} d ⁸ b ¹⁶ v ⁹ H ^B e ^{12,13} r ^{7,8} v ¹
▽	83	S ²⁶

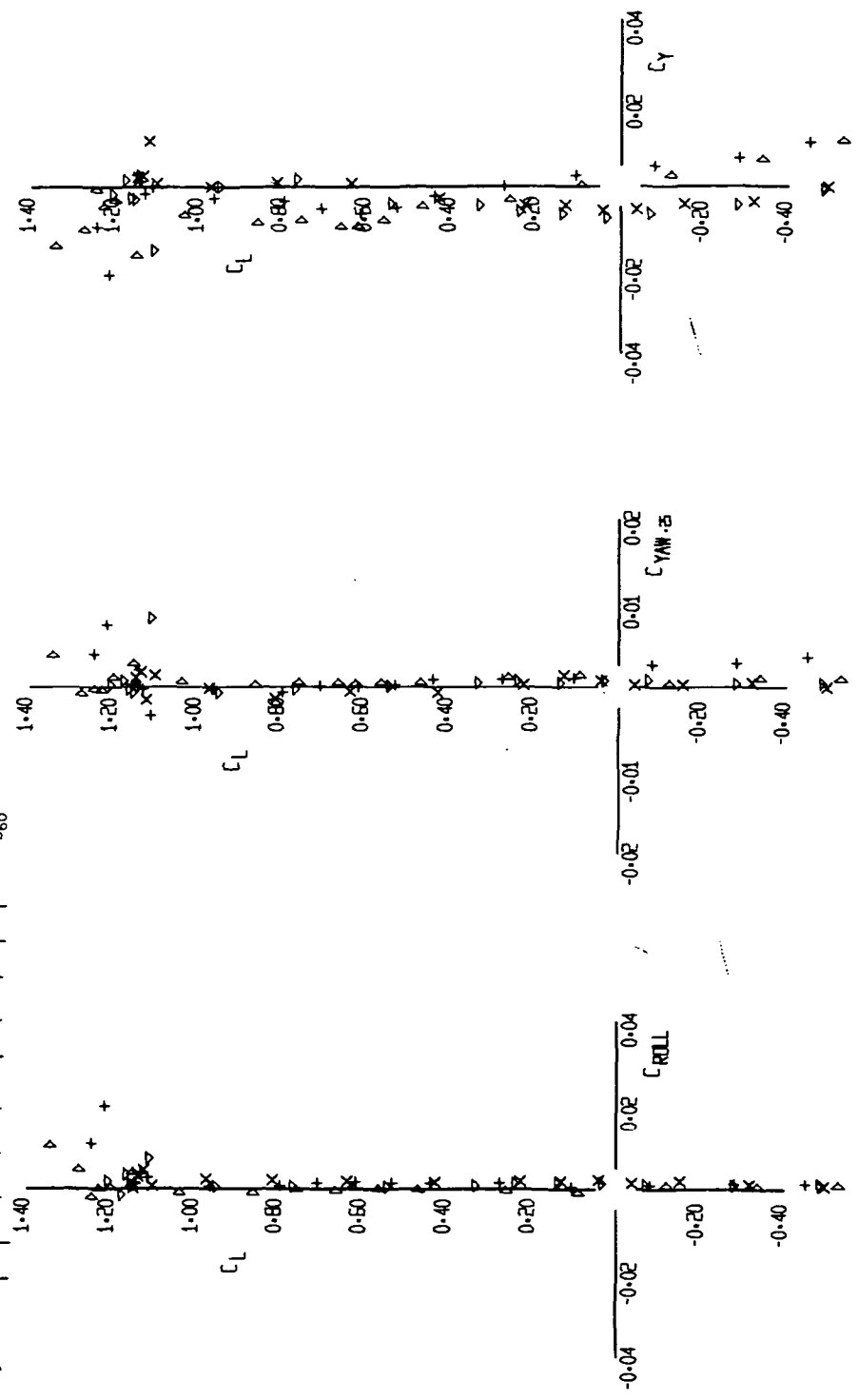


FIGURE 7 (SHEET 4)

58 74 ▽
+ x ▷ ▽

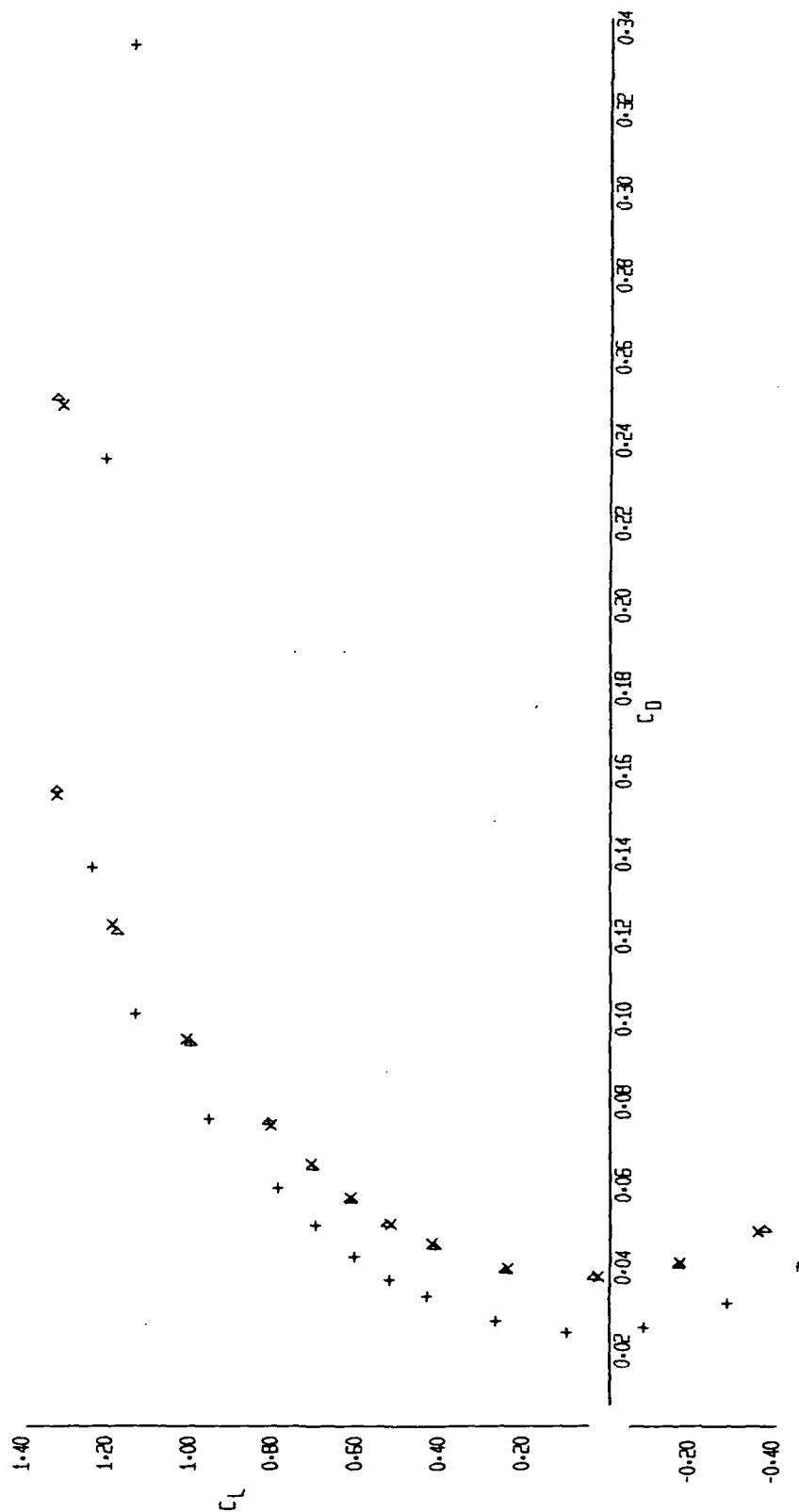
10-11-73

LR-353

EFFECT OF CENTER VERTICAL STABILIZER EXTENSION

LR- LFL 1-353
PAE FIG.

S/N	RUN	CONFIGURATION
+	57	S ¹ a ₁₀ Q ₁₃ f ₃₇ D ⁸ b ₁₆ v ⁹ H ⁸ e _{12,13} r _{7,8}
X	70	S ¹ a ₁₀ Q ₁₃ f ₃₇ D ⁸ b ₁₆ v ⁹ H ⁸ e _{12,13} r _{7,8}
D	72	S ¹ a ₁₀ Q ₁₃ f ₃₇ D ⁸ b ₁₆ v ⁹ H ⁸ e _{12,13} r _{7,8}



12-12-73

11-20

FIGURE 8 (SHEET 1)

EFFECT OF CENTER VERTICAL STABILIZER EXTENSION

LR PAGE
LFL 1-353 FIG.

SYM	RUN	CONFIGURATION													
		s ¹	a ¹⁰	q ¹³	r ³⁷	d ⁸	b ¹⁶	v ⁹	h ⁸	e ^{12,13}	x ^{7,8}	v ¹			
+	57														
x	70														
Δ	72														

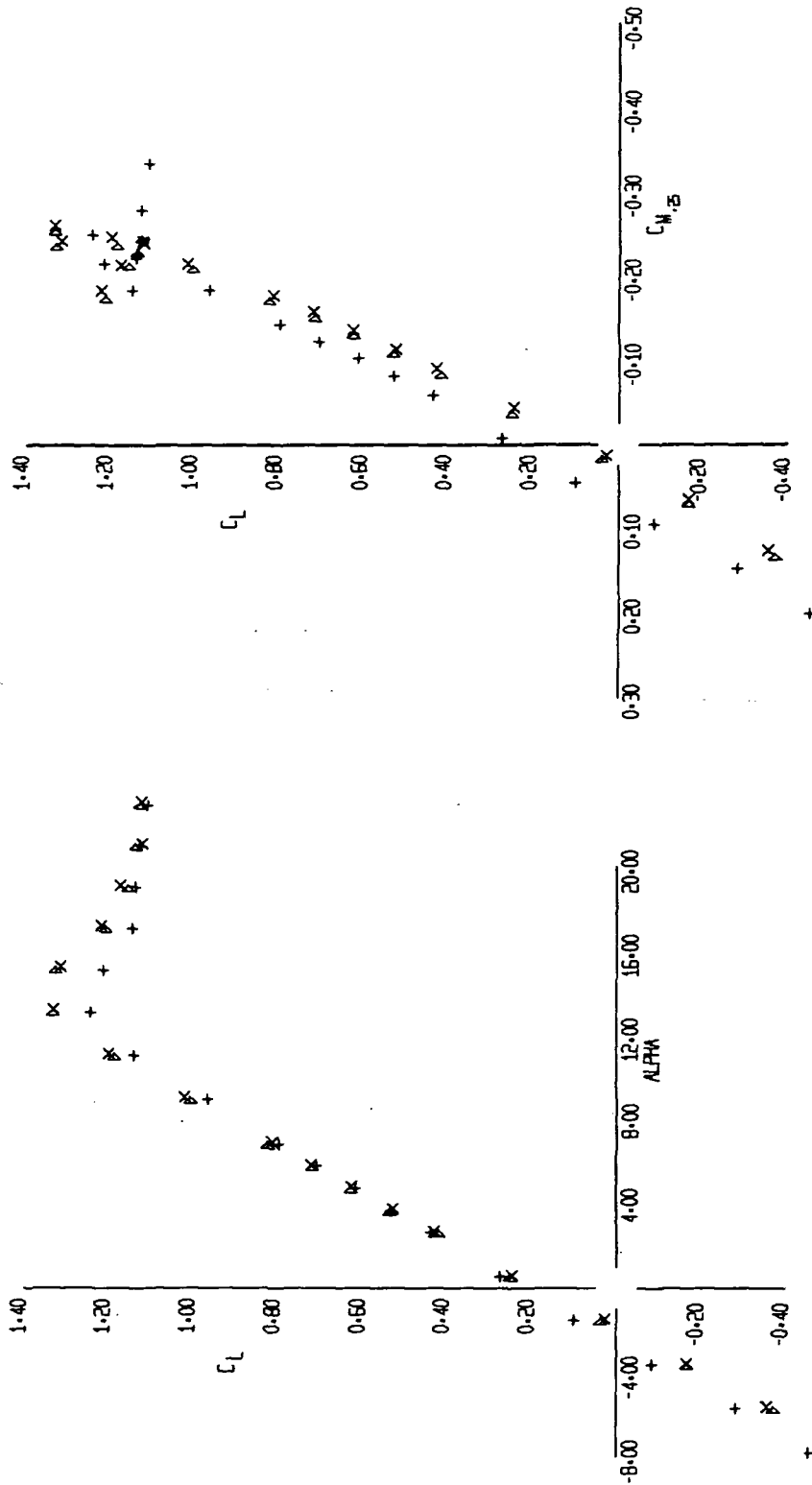


FIGURE 8 (SHEET 2)

57
70
72
+ x Δ

12-73

UP-11E

12-73

12-73

EFFECT OF CENTER VERTICAL STABILIZER EXTENSION

PAGE
FIG.

LR
LFL L-

SYM	RUN	CONFIGURATION	LR	LFL L-
+	57	S ₁ a ₁₀ Q ₁₃ P ₃₇ D ₈ b ₁₆ V ₉ B ₈ 12,13 7,8		
X	70	S ₁ a ₁₀ Q ₁₃ P ₃₇ D ₈ b ₁₆ V ₉ B ₈ 12,13 7,8		
Δ	72	S ₁ a ₁₀ Q ₁₃ P ₃₇ D ₈ b ₁₆ V ₉ B ₈ 12,13 7,8		

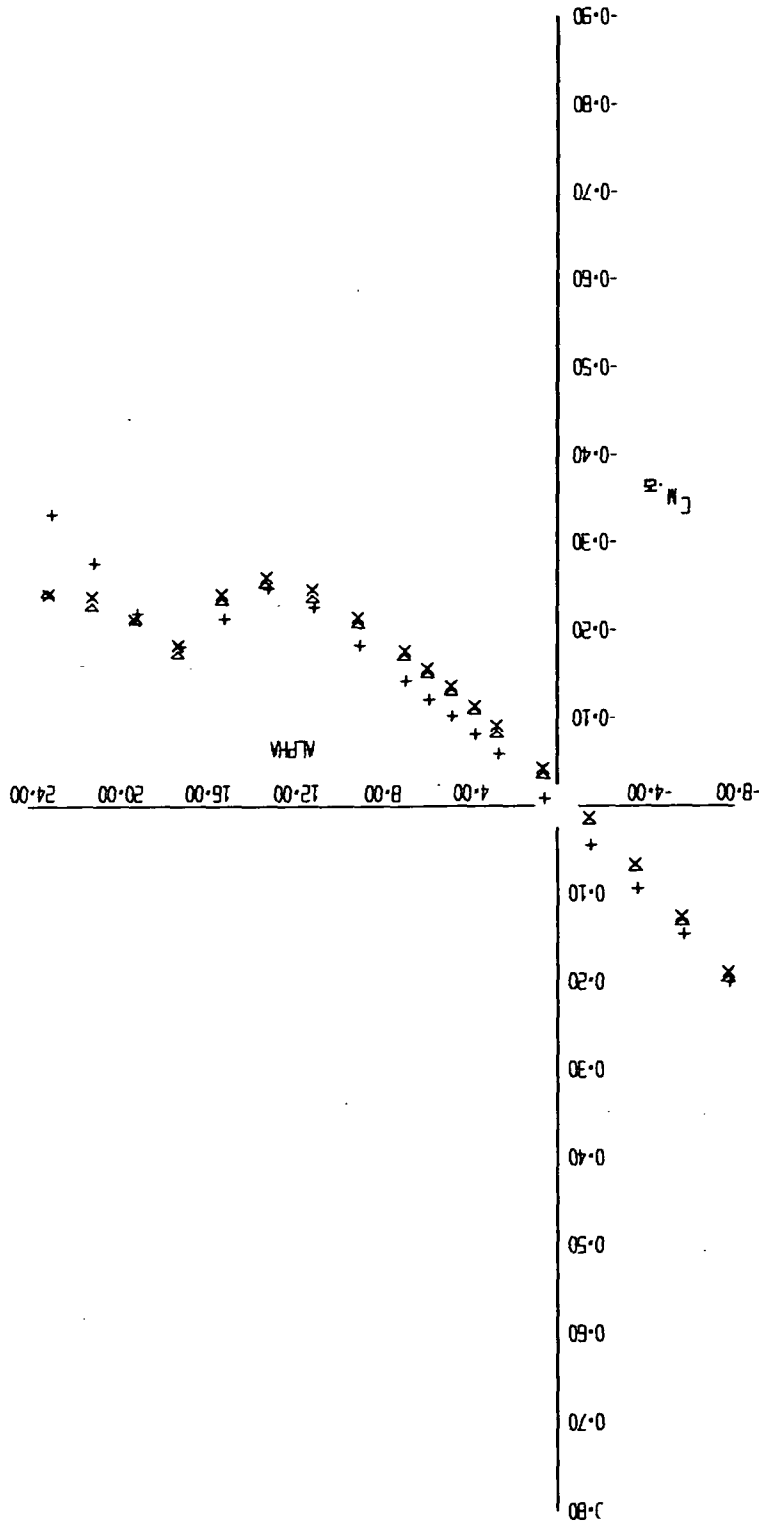


FIGURE 8 (SHEET 3)

Δ X +
72 70 57

10-12-73

LP-108

EFFECT OF ORBITER INCIDENCE

LR-
FIG.

LR-
LFL L-333

CONFIGURATION
 S¹ a¹⁰ q¹³ r³⁷ s⁵ t⁸ u¹⁶ v⁹ w¹² x¹³ y⁷ z⁸
 40.5 431.5

RUN
 74
 72

SYM
 +
 X

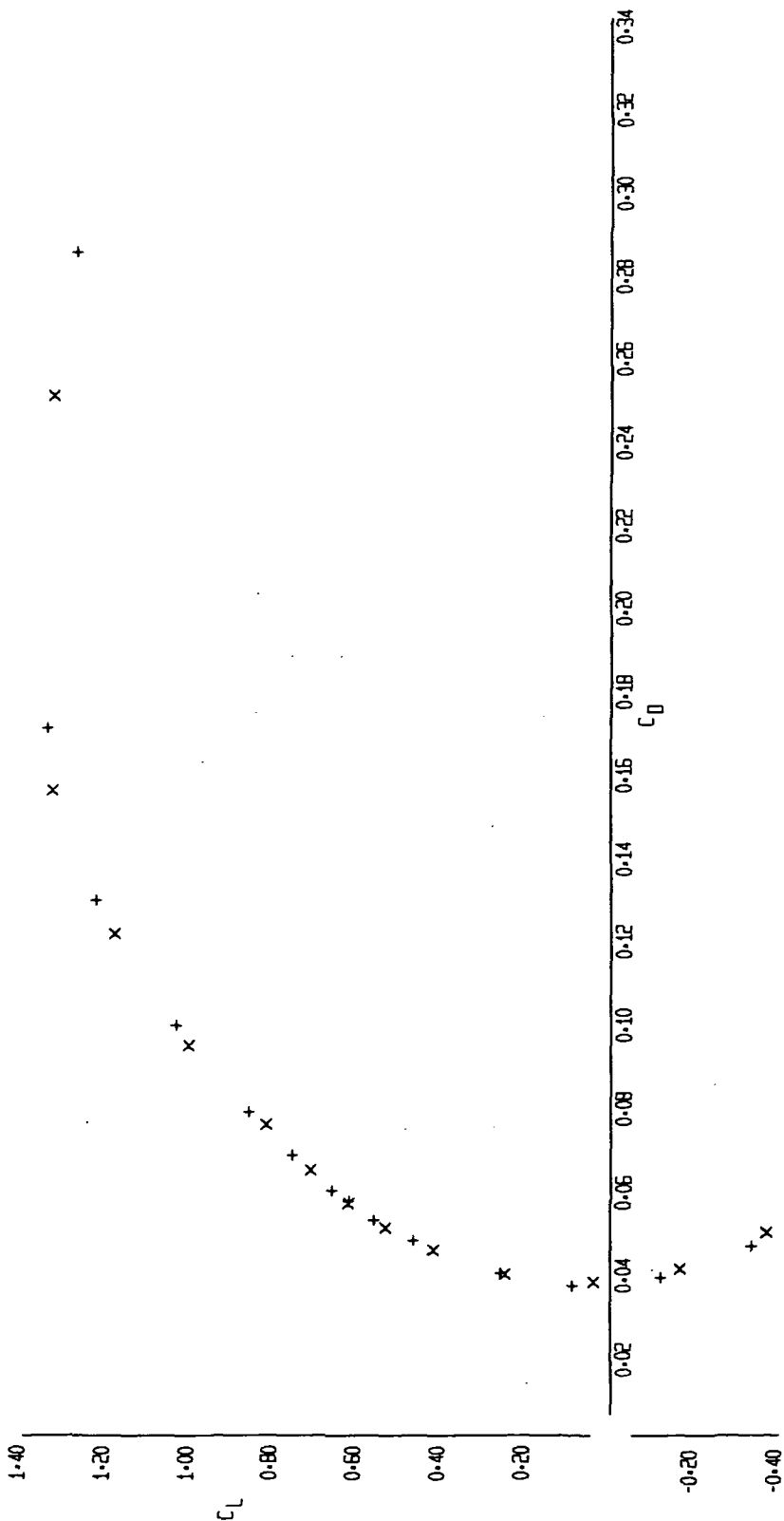


FIGURE 9 (SHEET 1)

72
 +
 X

10-12-73

LR-207

EFFECT OF ORBITER INCIDENCE

PAGE
FIG.

LR-
UFL-353

CONFIGURATION
 S^1 a^{10} q^{13} r^{37} $A5F$ b^8 b^{16} v^9 H^8 $e^{12,13}$ $r^{7,8}$
 $A5F$ $A-1.5$ | | | | | | | | | | v^1

RUN
74
72

SYM
+
X

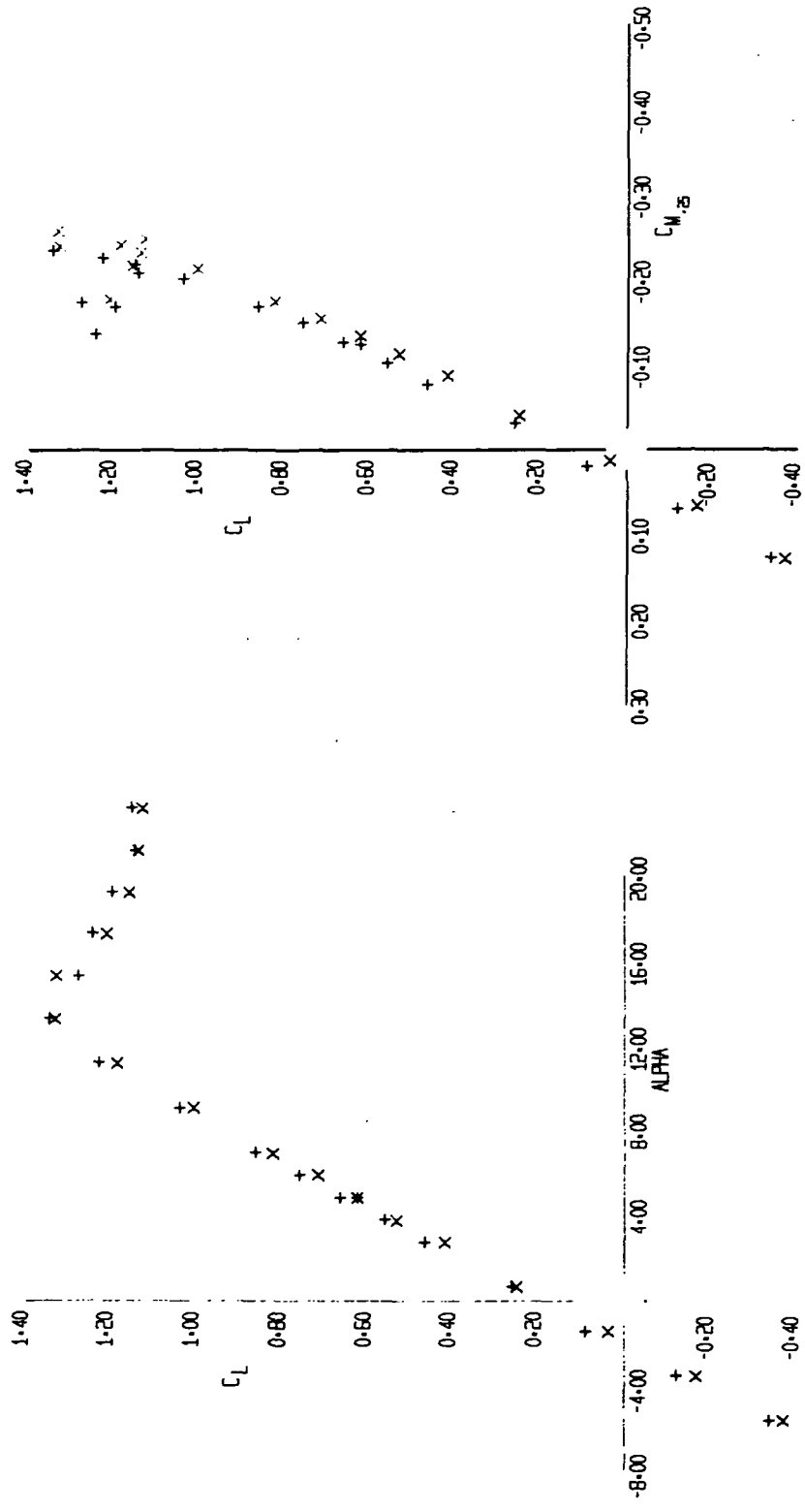


FIGURE 9 (SHEET 2)

10-12-73

74
+

LP-11E

EFFECT OF ORBITER INCIDENCE

PAGE
FIG.

LR
LRL-

SIN	RUN	CONFIGURATION	A_{SP}^{37}	a^{10}	q^{13}	$A_{SP}^{0.5}$	b^8	b^{16}	v^9	H^8	$e^{12,13}$	$r^{7,8}$	v^1
+	74												
X	72												

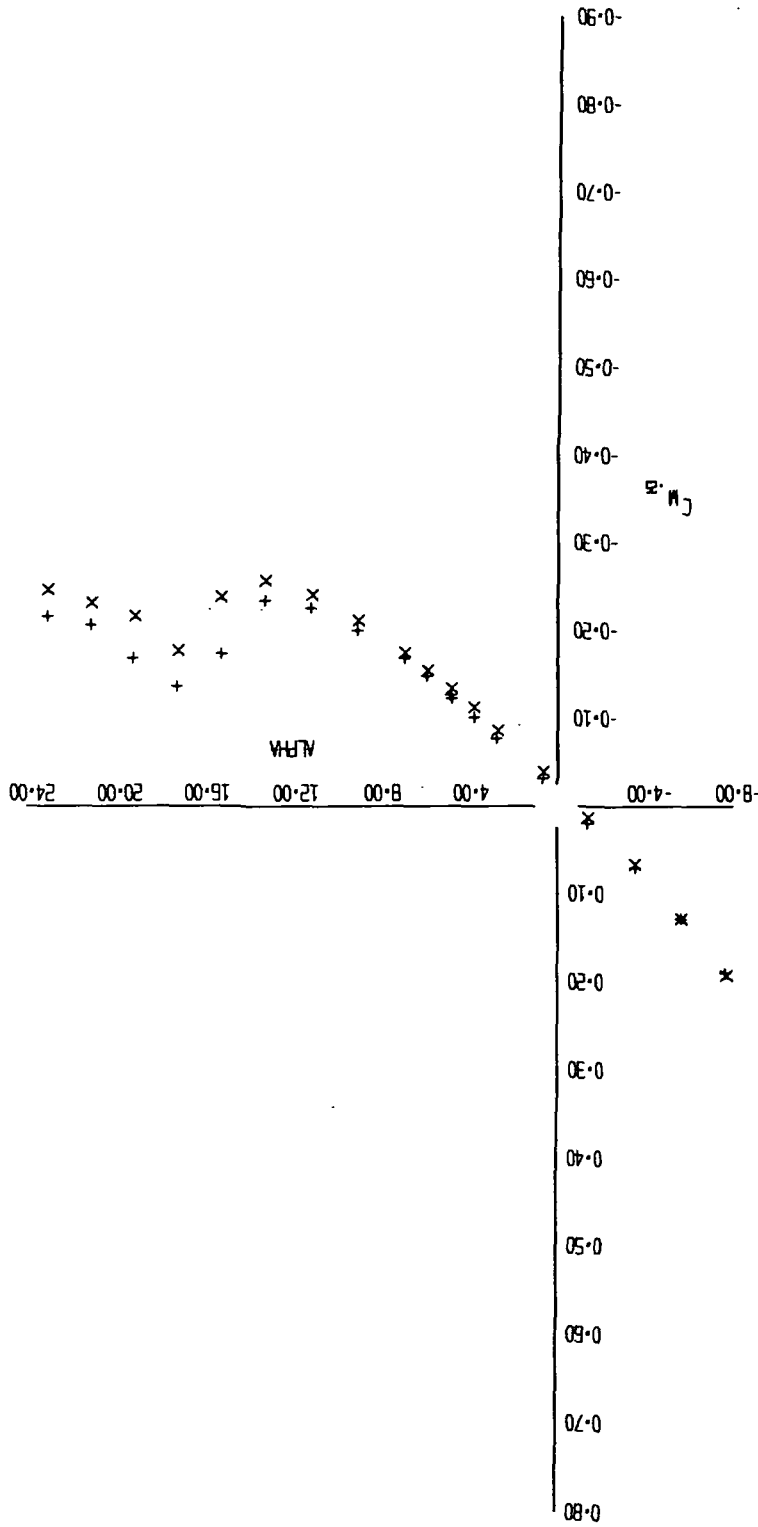


FIGURE 9 (SHEET 3)

10-12-73

X +
72 74

LP-108

EFFECT OF ORBITER INCIDENCE

PAGE
FIG.

LR
LFL (353)

SYM		RUN	CONFIGURATION											
+	X	74	S ¹	a ¹⁰	q ¹³	f ³⁷	A _{0,5}	D ^B	b ¹⁶	v ⁹	r ^B	θ ^{12,13}	r ^{7,8}	v ¹
		74												
		72												

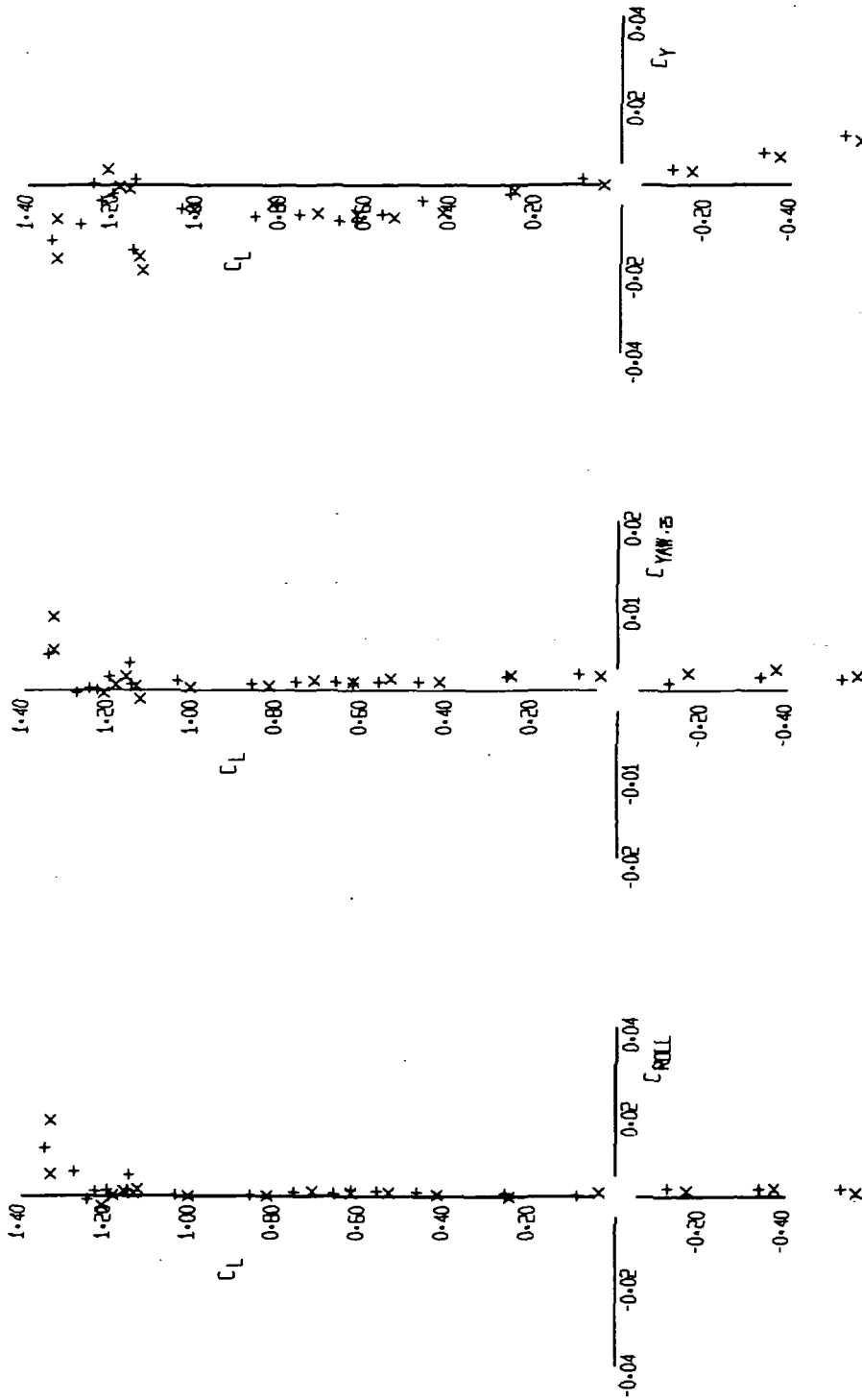


FIGURE 9 (SHEET 4)

74
+

18-12-73

LP-3E

STABILIZER EFFECTIVENESS ORBITER ON

PAGE
FIG.

LR
LFL L-3B

CONFIGURATION	SYM	RUN
S ¹ a ¹⁰ q ¹³ r ²⁷ a ^{5P}	+	78
b ⁸ v ⁹ H ⁸ e ^{12,13} z ^{7,8} v ¹	X	74
H ⁸ H ⁸ H ⁸	▷	80
H ⁸ H ⁸ H ⁸	▽	81

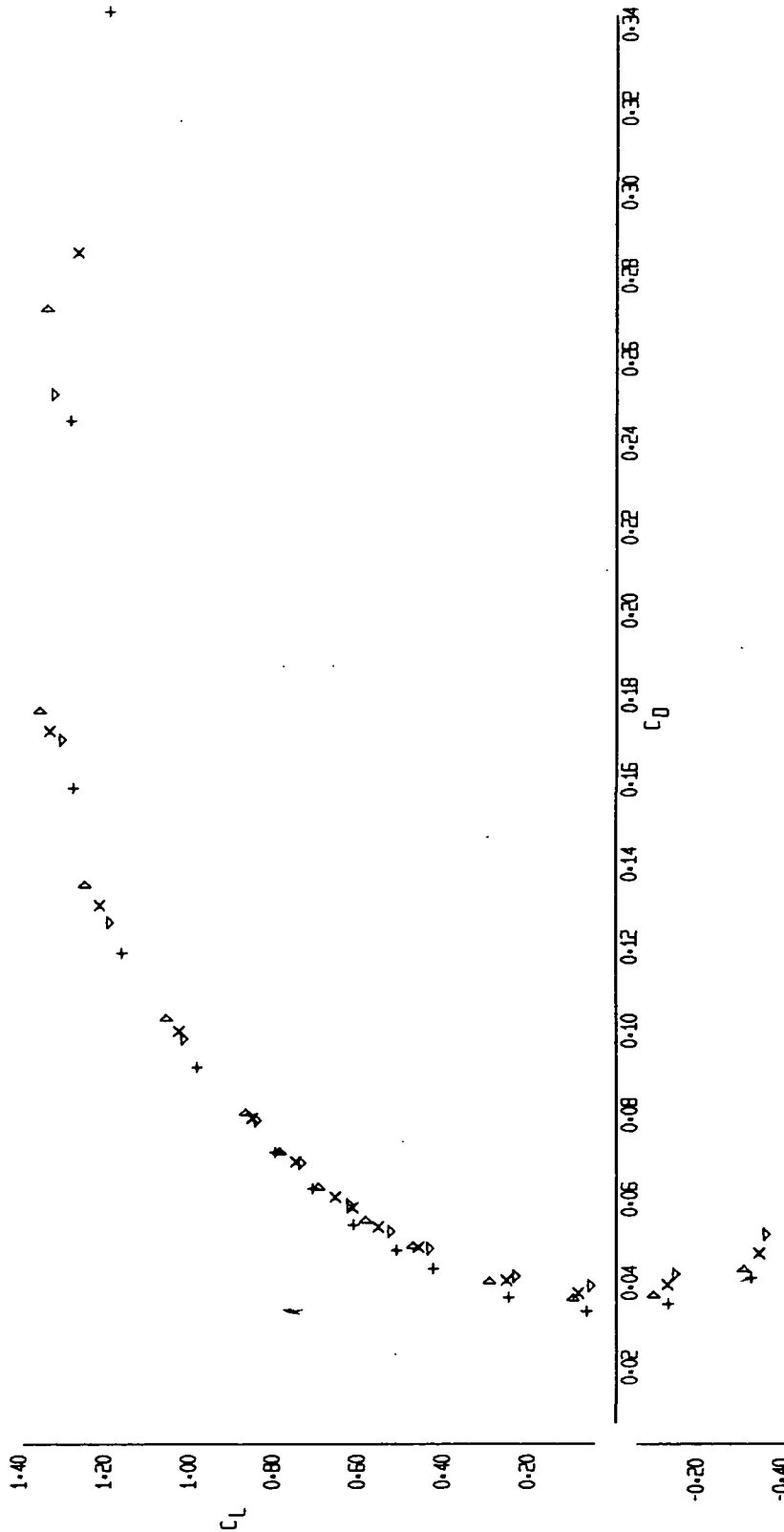


FIGURE 10 (SHEET 1)

R Z B B
+ X ▷ ▽

15-12-73

LP-20

STABILIZER EFFECTIVENESS ORBITER ON

PAGE
FIG.

LR-
LFL I-353

SYM	RUN	CONFIGURATION
+	78	S ¹ a ¹⁰ q ¹³ r ³⁷ A ^{5P} 0.5
x	74	H ⁶ v ⁹ b ¹⁶ v ⁸ e ^{12,13} x ^{7,8} v ¹
△	80	H ⁸ H ⁴
▽	81	H ⁴

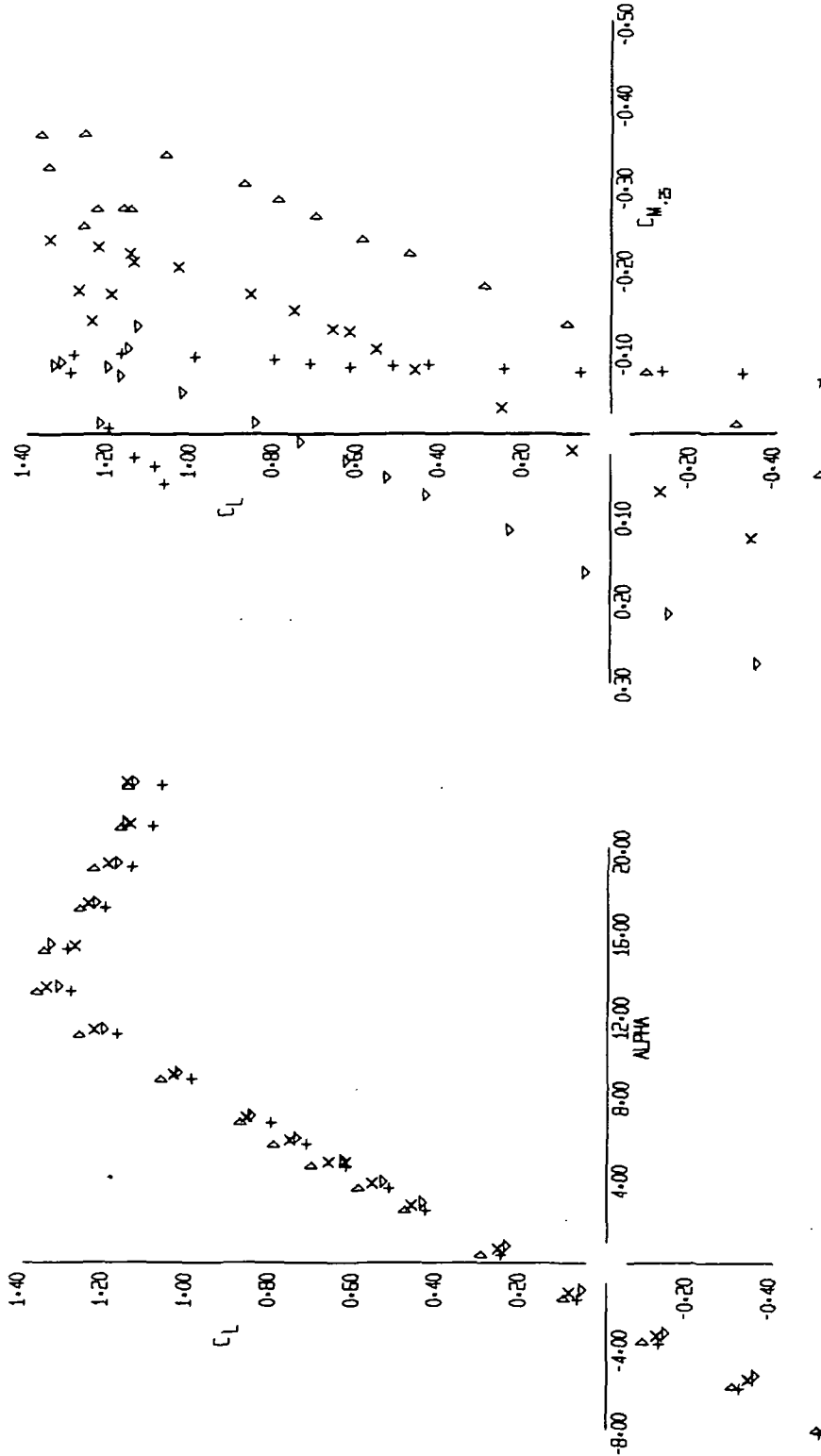


FIGURE 10 (SHEET 2)

△ x x +
74 78

10-12-73

LR-18E

LR-
LFL L-

RUN	CONFIGURATION	5P
78	S ¹ a ¹⁰ v ¹³ r ³⁷	40,5
74		
80		
81		

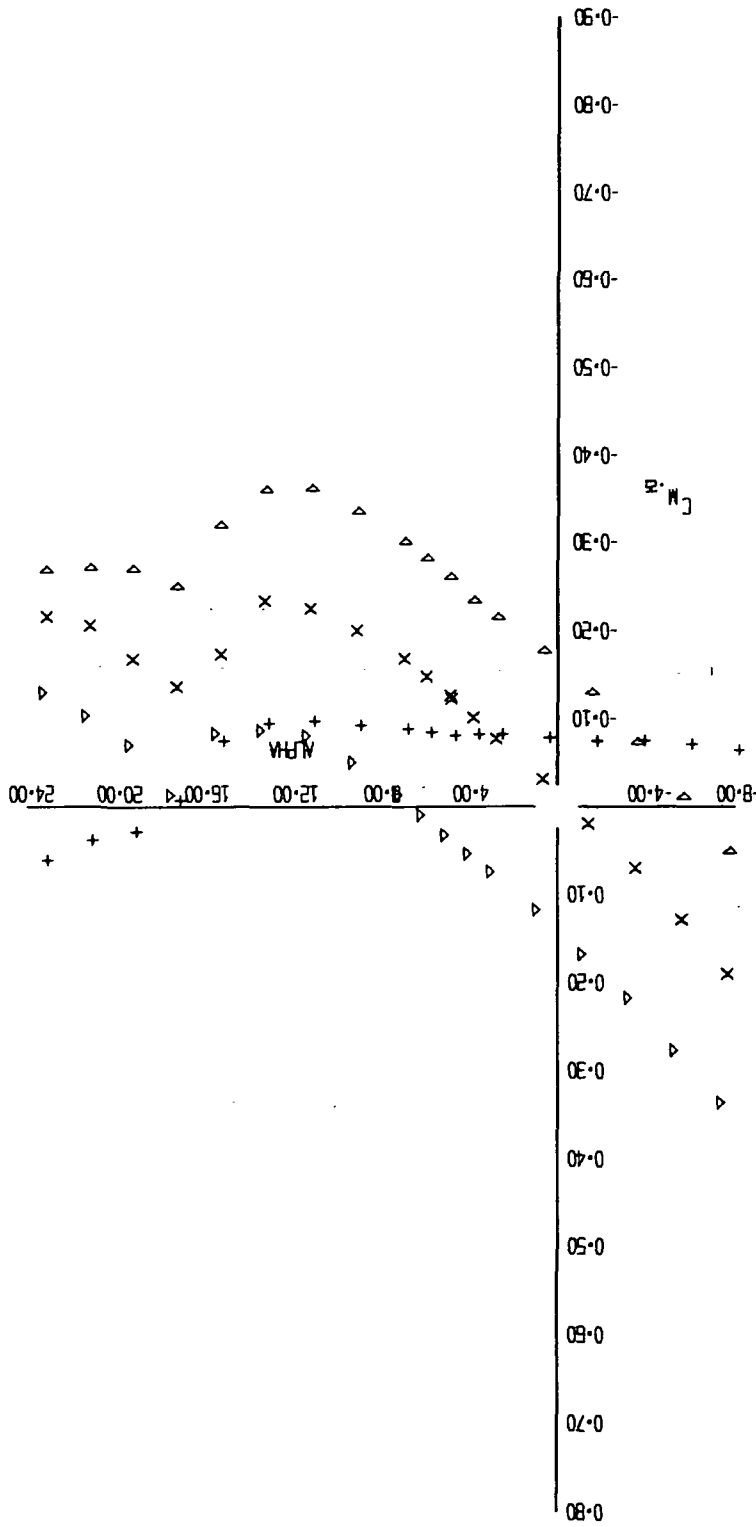


FIGURE 10 (SHEET 3)

STABILIZER EFFECTIVENESS ORBITER ON

▲ X +
80 74
78

10-12-73

(10)

LR-
LFL 1-353

STABILIZER EFFECTIVENESS ORBITER ON

CONFIGURATION	
S ¹	a ¹⁰
Q ¹³	r ³⁷
A ^{5F}	0.5
D ⁸	b ¹⁶
H ⁸	v ⁹
H ⁸	e ^{12,13}
H ⁸	r ^{7,8}
H ⁸	v ¹

RUN	SYM
78	+
74	x
80	△
81	▽

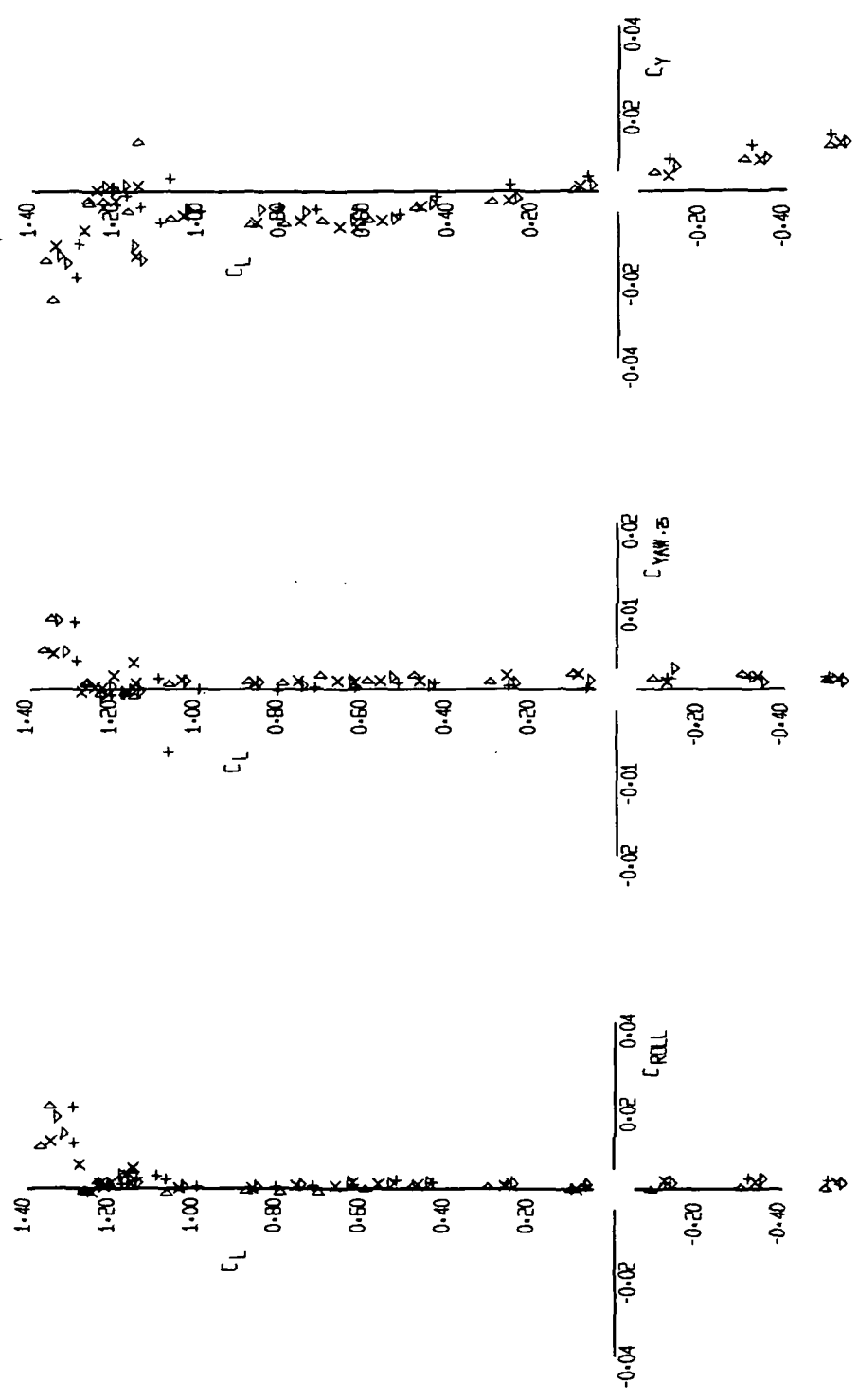


FIGURE 10 (SHEET 4)

RZ 88 8
+ x △ ▽

15-12-73

LR-III

EFFECT OF ORBITER INCIDENCE AND POSITION

PNCE
FIG.

LR-

LFL L-363

5A 8 b16 v9 e12,13 r7,0 y1
A0,5 D | | | | | |
A-1,5 | | | | | |

CONFIGURATION

1 10 13 37

76 72

SYN
+ X

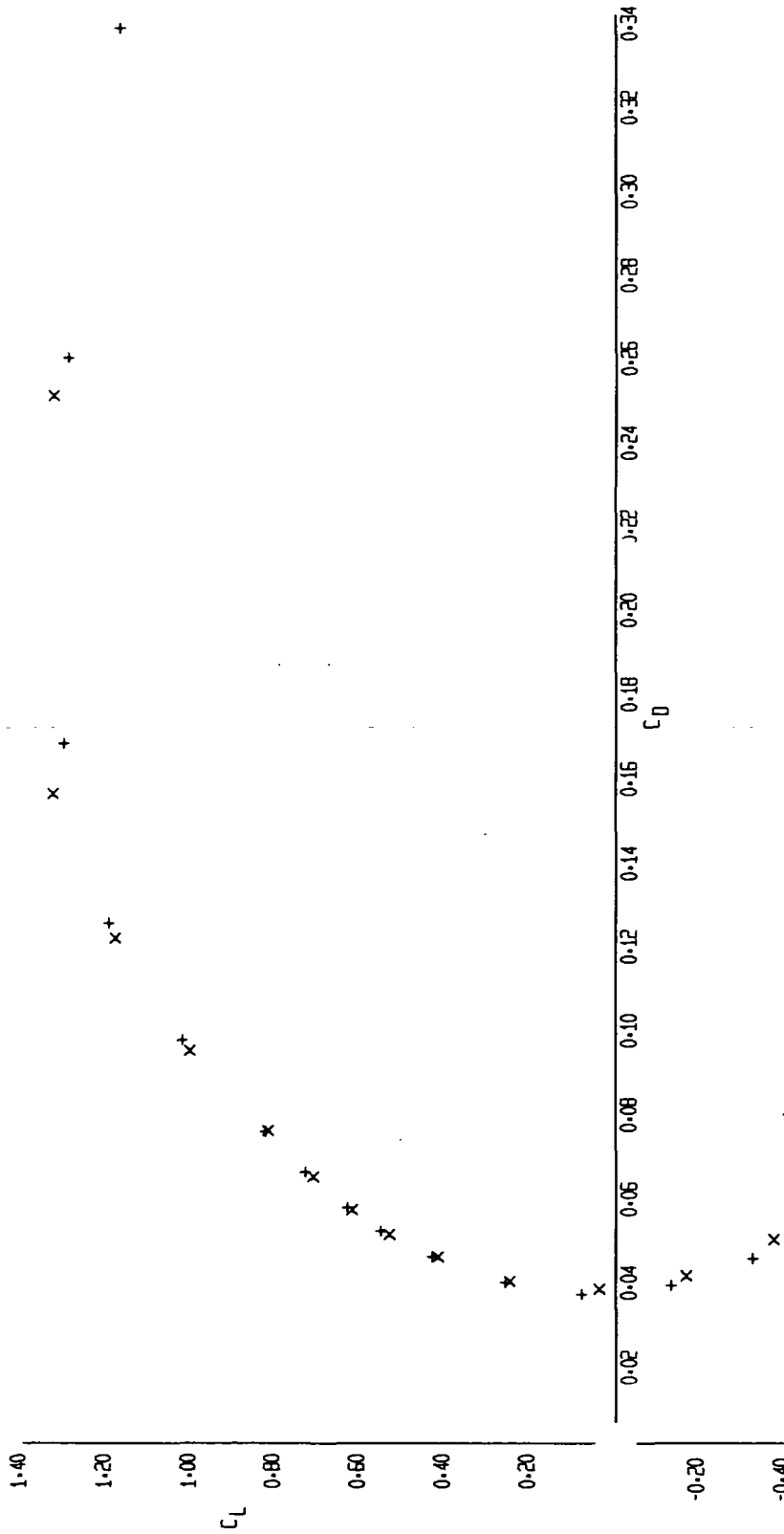


FIGURE 11 (SHEET 1)

LP-20

EFFECT OF ORBITER INCIDENCE AND POSITION

PAGE
FIG.

LR
UL-353

SYM	RUN	CONFIGURATION											
		S ¹	a ¹⁰	q ¹³	r ³⁷	A _{0.5} ^{5A}	b ^B	b ¹⁶	p ²	B ^B	g ^{12,13}	r ^{7,8}	v ¹
+	76												
X	72												

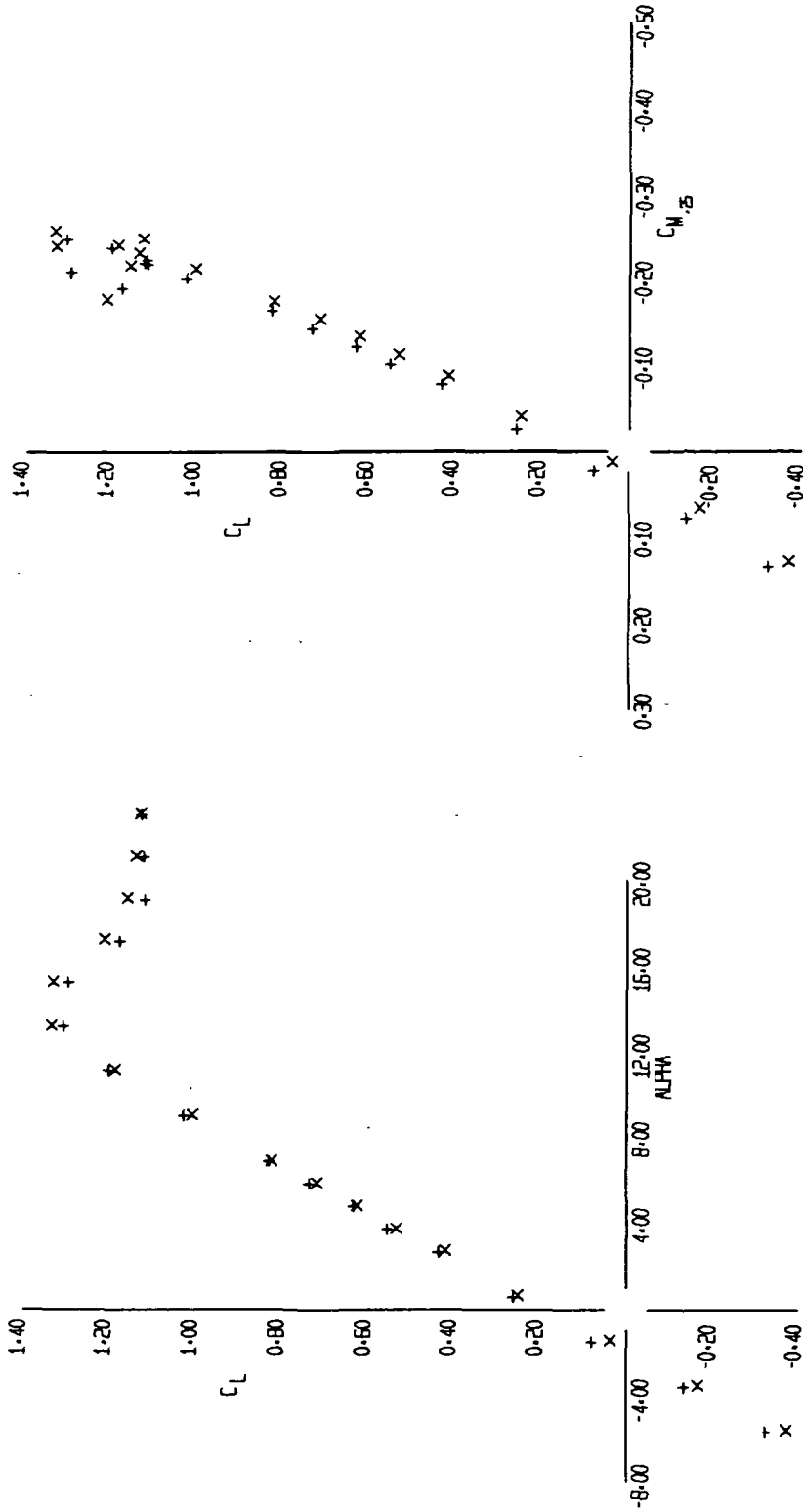


FIGURE 11 (SHEET 2)

22
72
+ X

10-12-73

UP-11E

EFFECT OF ORBITER INCIDENCE AND POSITION

PAGE
FIG.

SYM	RUN	CONFIGURATION		LR	
		S ¹	e ¹⁵	LFL	L
X	76	A ^{2A}	r ²⁷	7,8	v ¹
X	72	0.5	B ^B	12,13	v ¹
		5P	v ⁹		
		1,5	b ¹⁶		

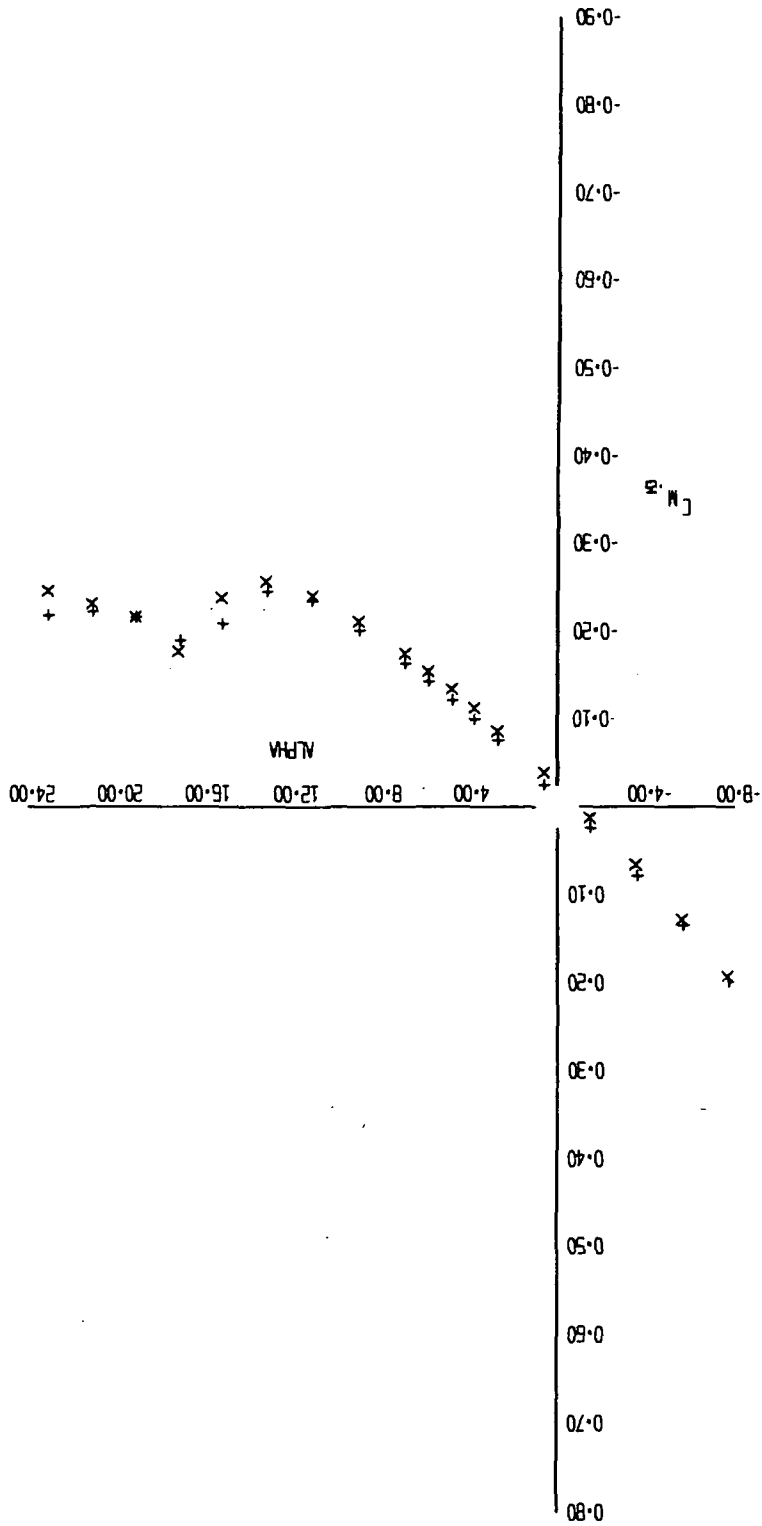


FIGURE 11 (SHEET 3)

X 76
+ 72

10-12-73

LP-101

EFFECT OF ORBITER INCIDENCE AND POSITION:

SYN	RUN	CONFIGURATION															
		s ¹	a ¹⁰	q ¹³	r ¹⁷	A _{0.5}	b ⁸	b ¹⁶	v ⁹	H ⁶	e ^{12,13}	v ¹					
+	76																
X	72																

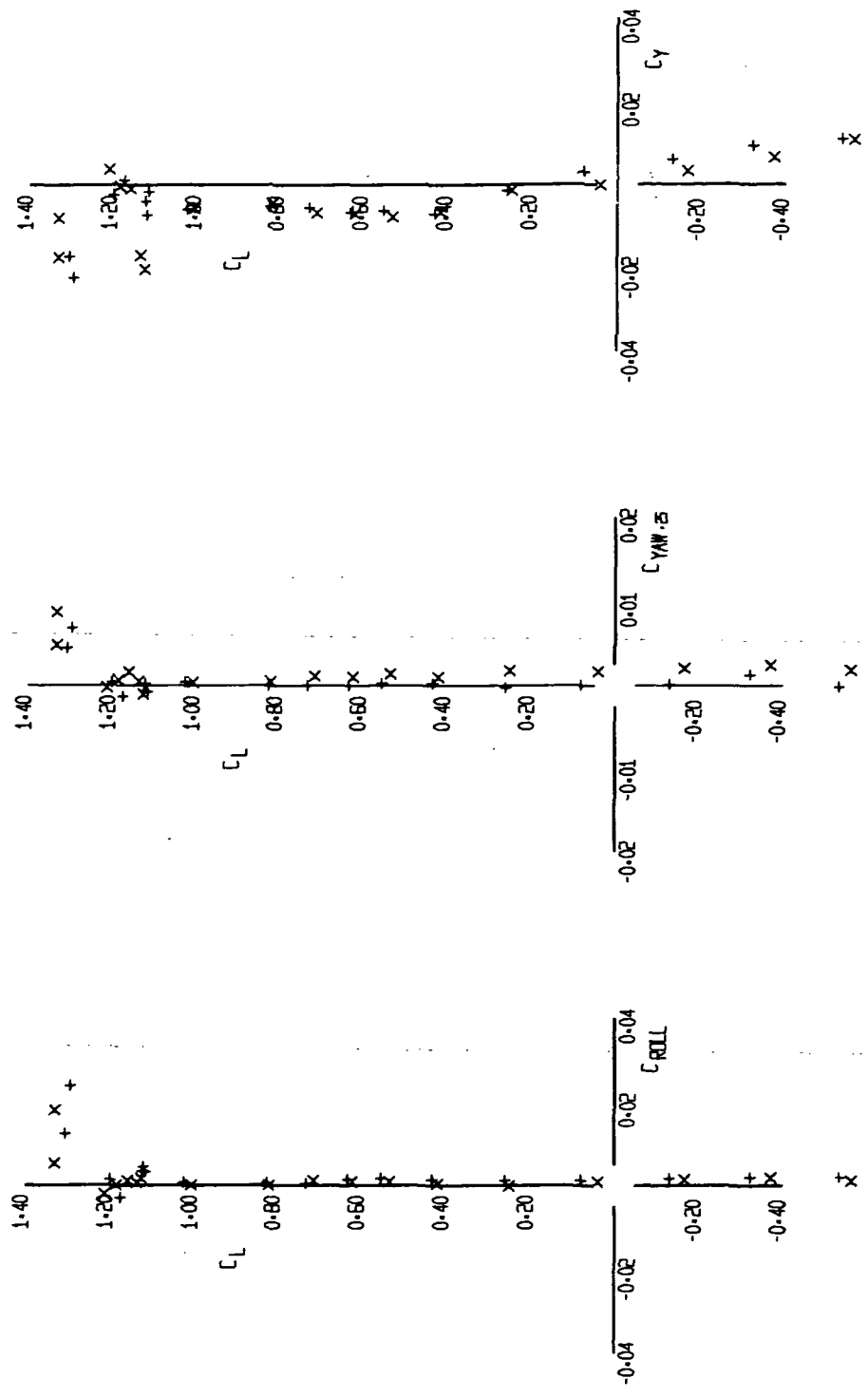


FIGURE 11 (SHEET 4)

RZ
+ X

12-12-73

LR-353

RUDDER EFFECTIVENESS ORBITER OFF

LR- LFL 1-353
PNC FIG.

SYM	RUN	CONFIGURATION
+	64	S ¹ a ¹⁰ q ¹³ r ³⁷
X	58	D ⁸ b ¹⁶ v ⁹ H ^{12,13} r ^{7,8}
▷	59	r ^{7,8} r ^{7,8}

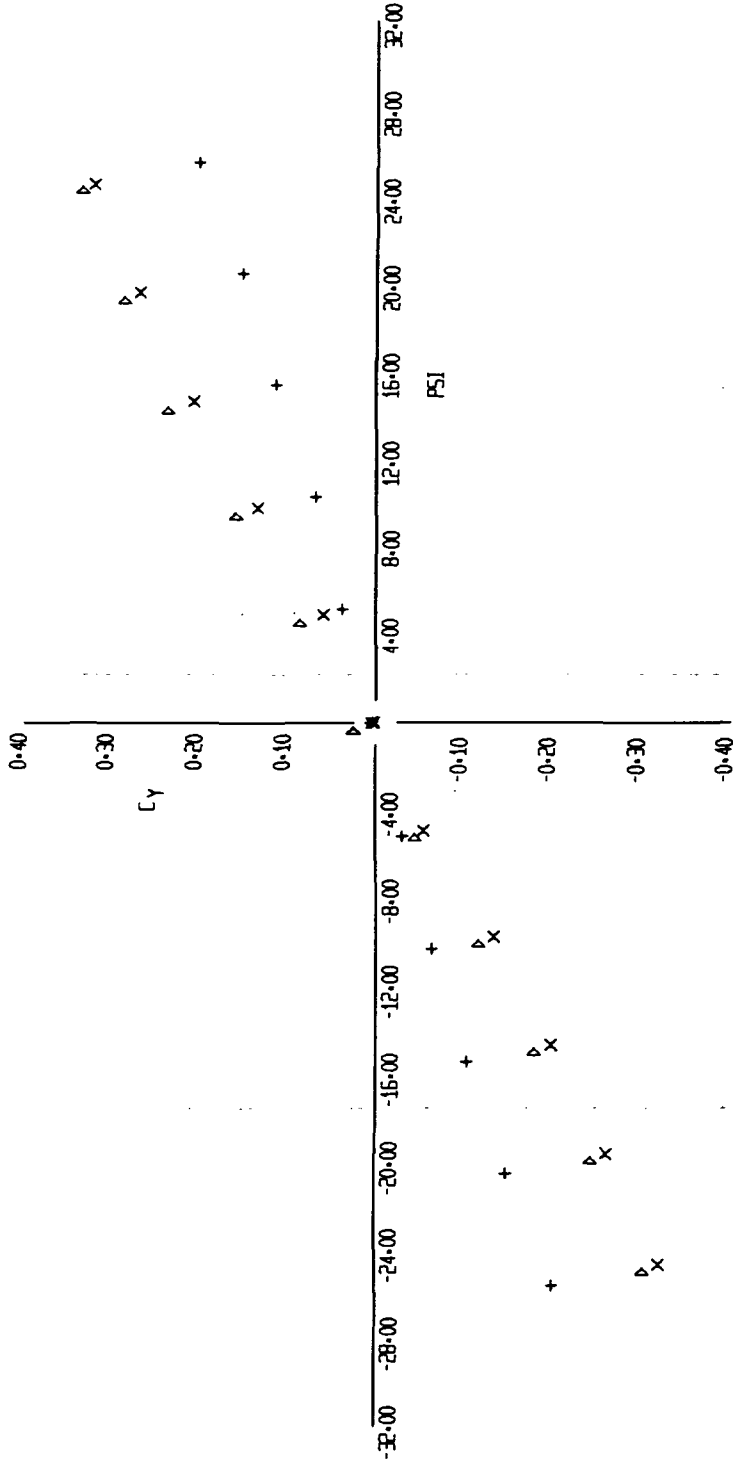


FIGURE 12 (SHEET 1)

▷ X +

10-12-73

11-6E

RUDDER EFFECTIVENESS ORBITER OFF

PAGE
FIG.

LR
LFL L-353

RUN	CONFIGURATION
64	S ¹ a ¹⁰ Q ¹³ r ³⁷
58	b ⁸ b ¹⁶ v ⁹ H ⁸ e ^{12,13} r ^{7,8}
59	r ^{7,8} r ^{7,8} r ^{7,8}

SIG	RUN
+	64
X	58
▷	59

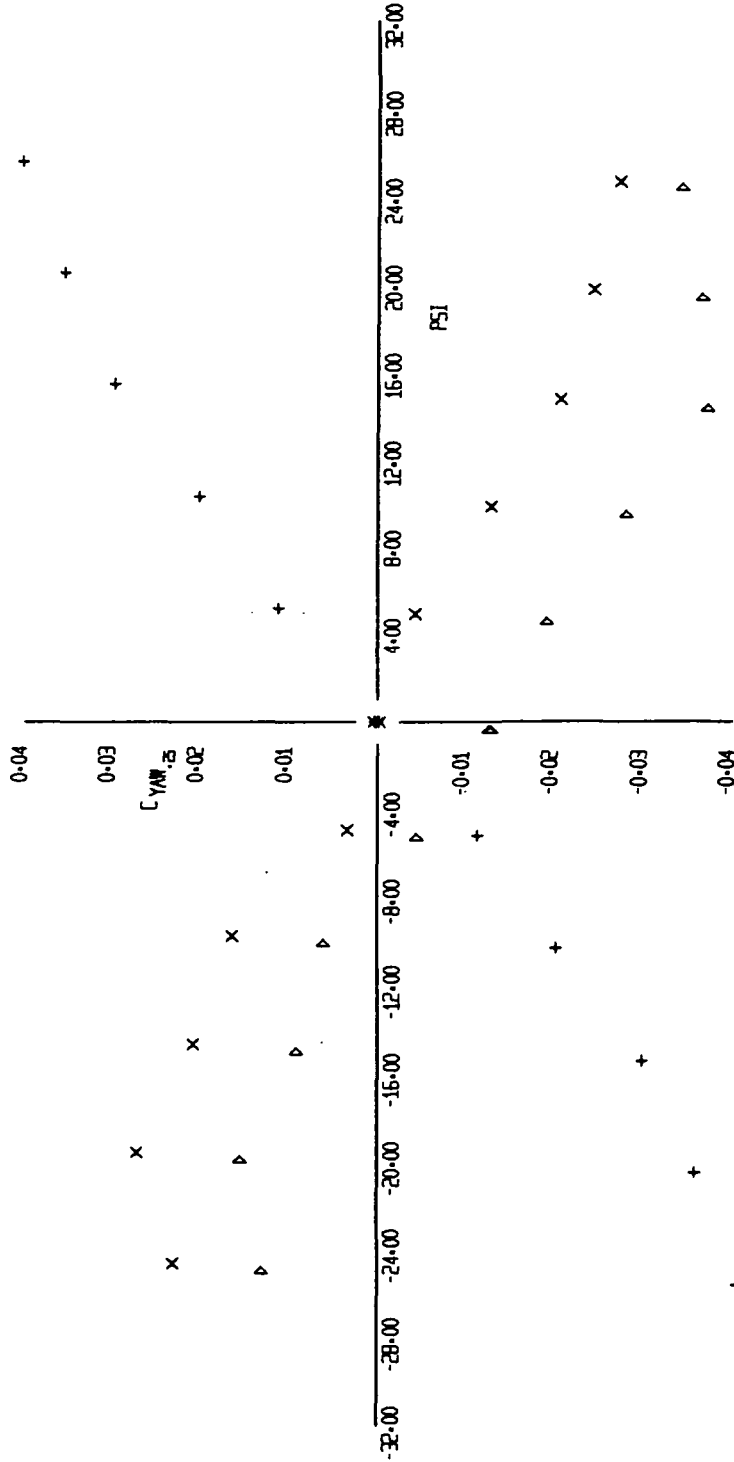


FIGURE 12 (SHEET 2)

LR-40
←→

LR-40

LR-40

RUDDER EFFECTIVENESS ORBITER OFF

PACE
FIG.

LR
LFL

SYM	RUI	CONFIGURATION									
		S ¹	a ¹⁰	q ¹³	r ³⁷	b ⁸	b ¹⁶	v ⁹	H ⁸	e ^{12,13}	r ^{7,8}
+	64										
X	58										
D	59										

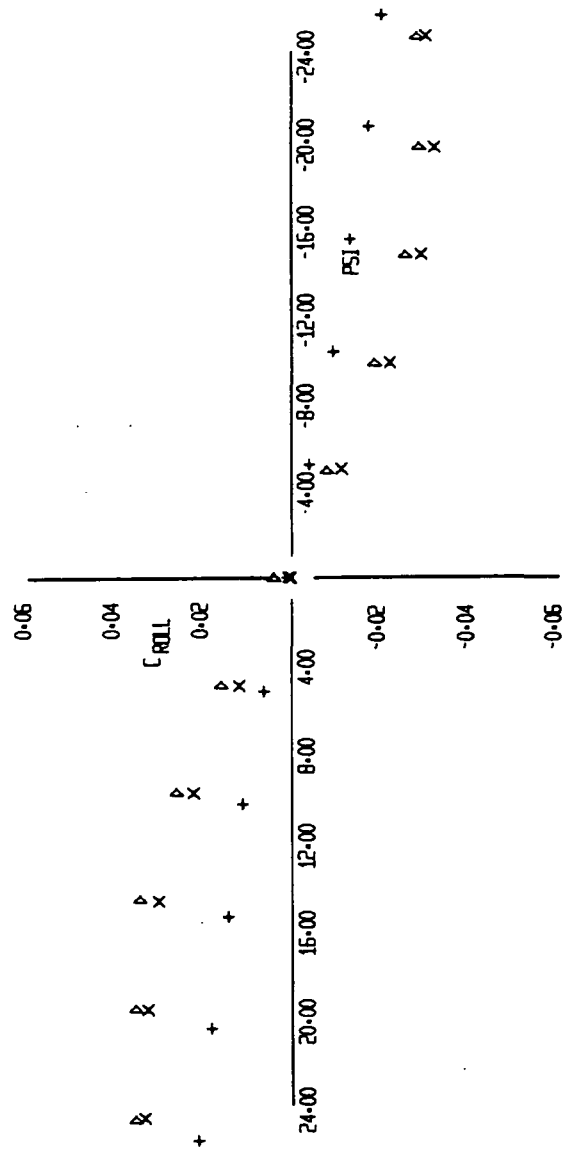


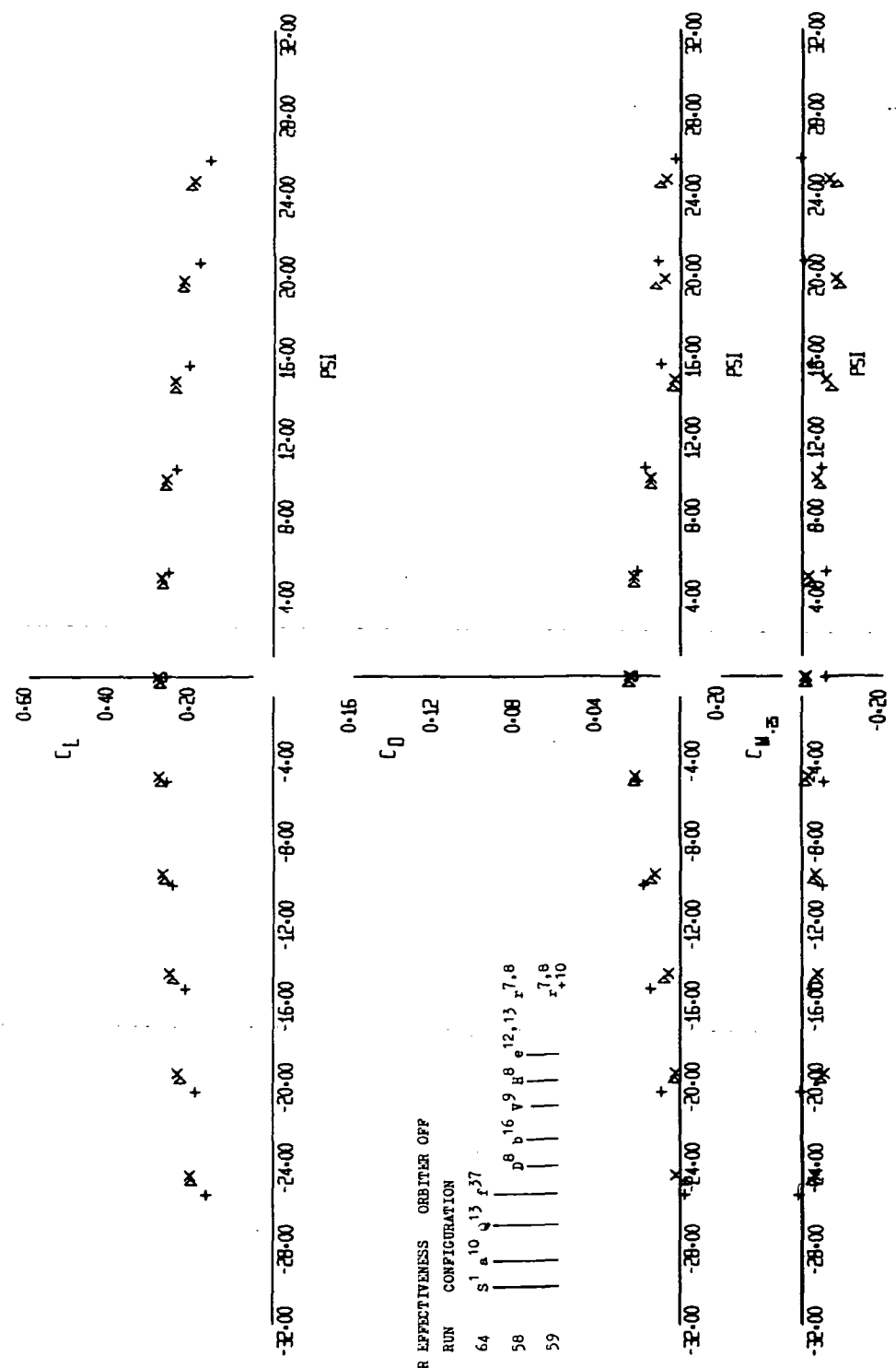
FIGURE 12 (SHEET 3)

3 8 8
+ X >

12-12-73

11-48

RUDDER EFFECTIVENESS ORBITER OFF



3 88 88
+ x D

RUDDER EFFECTIVENESS ORBITER OFF

SYM	RUN	CONFIGURATION
+	64	S ¹ a ¹⁰ u ¹³ r ²⁷
x	58	b ⁸ v ¹⁶ y ⁹ B ⁸ e ^{12,13} r ^{7,8}
D	59	r ^{7,8} x ⁺¹⁰

1011-33

FIGURE 12 (SHEET 4)

1011-33

EFFECT OF ORBITER AFTERBODY PAIRING

SYM	RUN	CONFIGURATION
+	58	S ¹ a ¹⁰ q ¹³ r ³⁷ p ⁸ b ¹⁶ v ⁹ H ⁸ e ^{12,13} r ^{7,8}
X	27	S ¹ a ¹⁰ q ¹³ r ³⁷ A ⁶ p ⁸ b ¹⁶ v ⁹ H ⁸ e ^{12,13} r ^{7,8}
D	32	A ^{2A} _{-1.5} A ^{2A} _{-1.5}

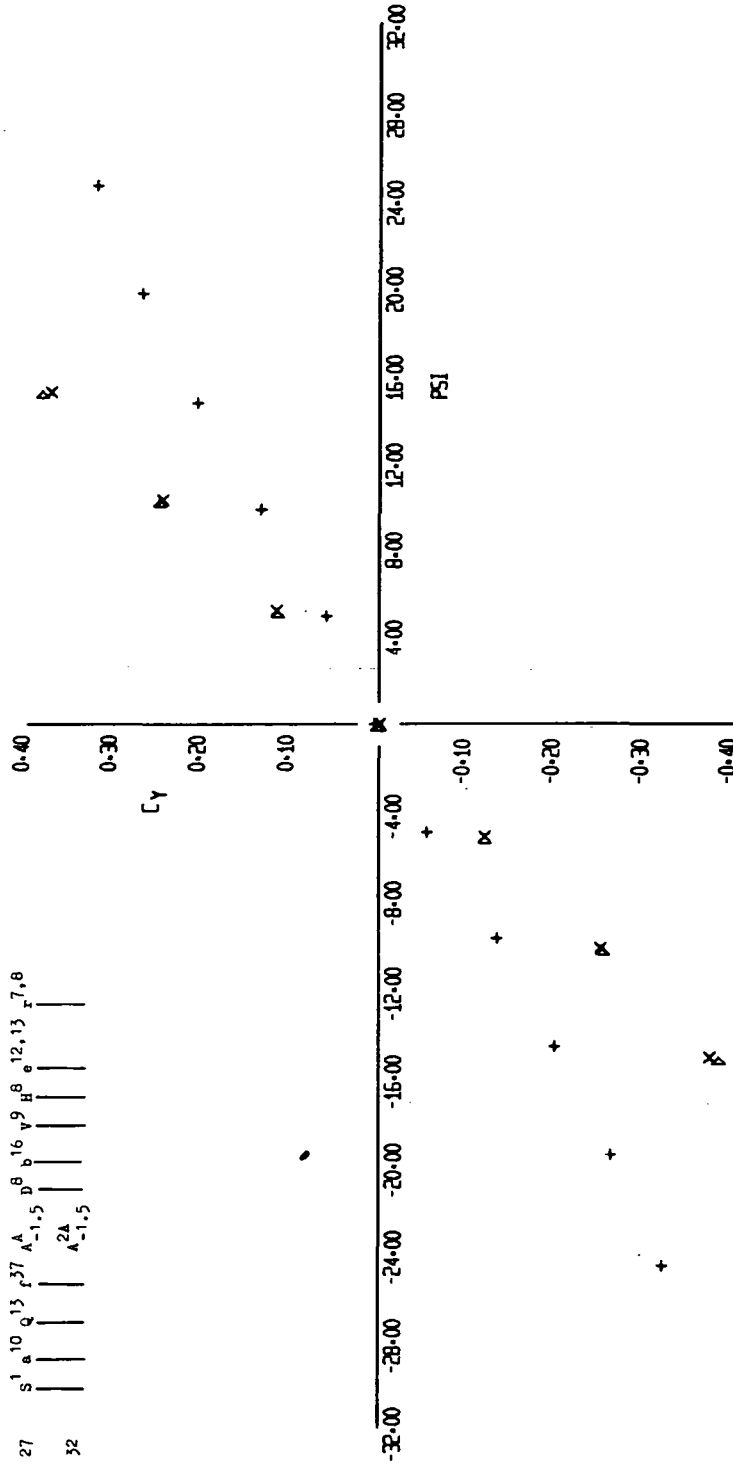


FIGURE 13 (SHEET 1)

88 24
+ X +

10-12-73

25-41

EFFECT OF ORBITER AFTERBODY FAIRING

SYM RUN CONFIGURATION

+	58	S ¹	a ¹⁰	r ¹³	p ⁸	b ¹⁶	v ⁹	H ⁸	e ^{12,13}	r ^{7,8}	
X	27	S ¹	a ¹⁰	r ¹³	A ^{1,5}	p ⁸	b ¹⁶	v ⁹	H ⁸	e ^{12,13}	r ^{7,8}
▷	32				A ^{2A}						

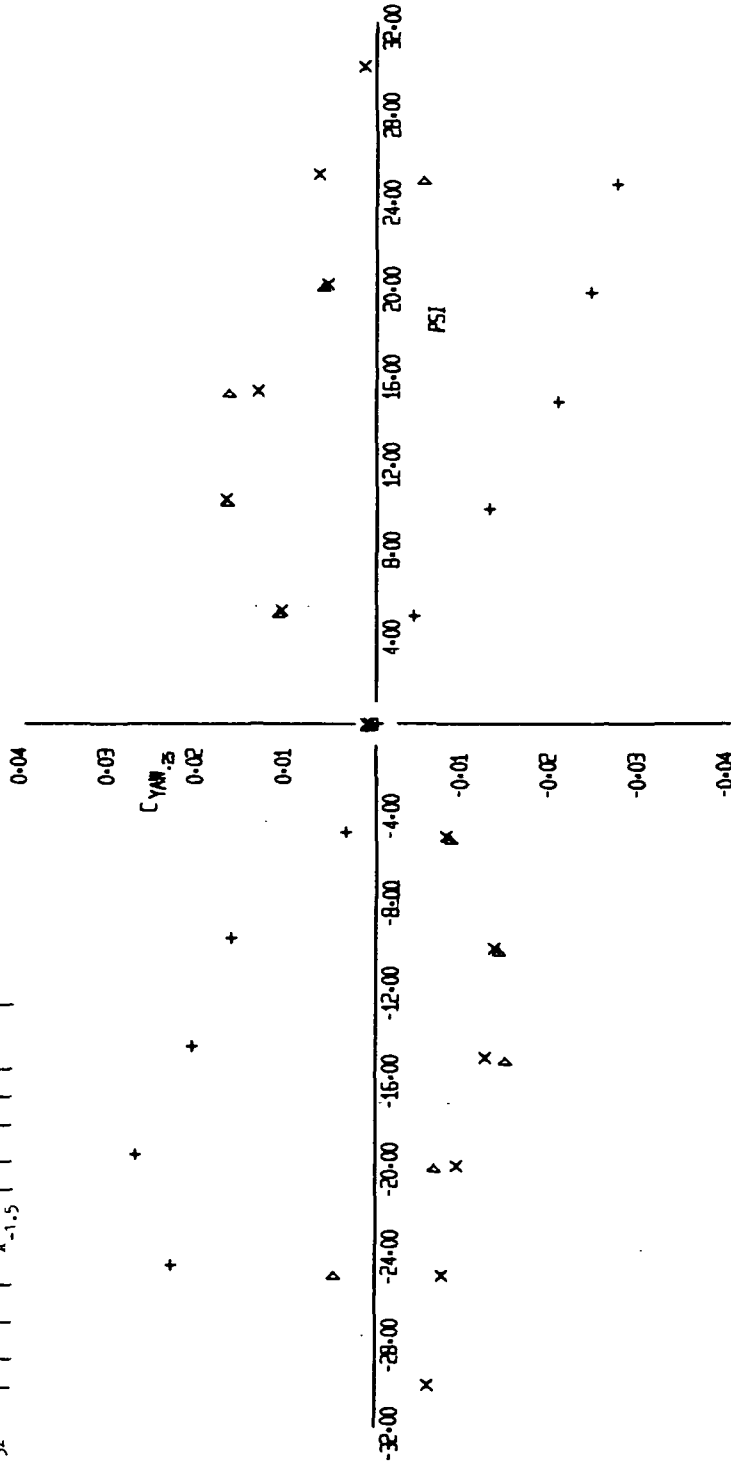


FIGURE 13 (SHEET 2)

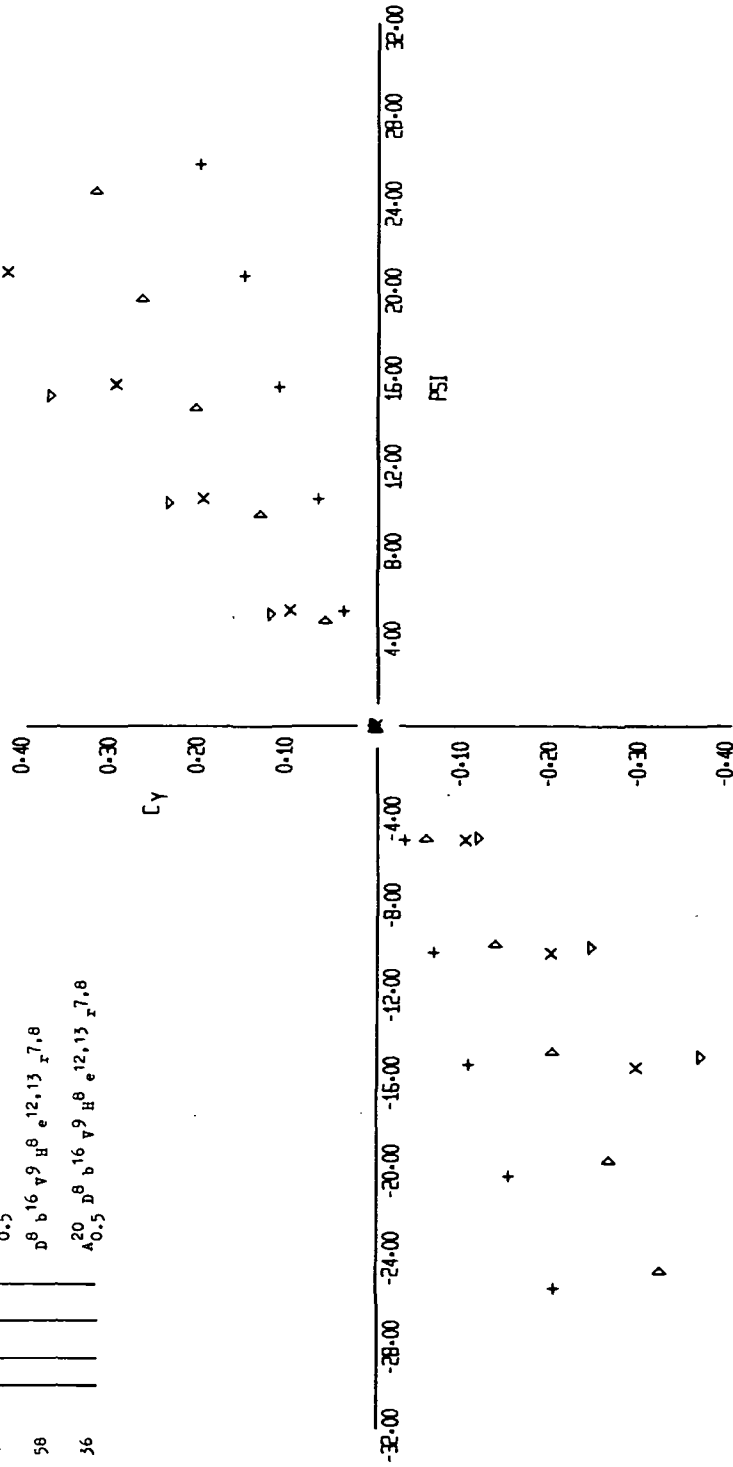
BR BK
 + X ▷

10-12-73

10-41

EFFECT OF ORBITER
TAIL ON AND TAIL OFF

SYM	RUN	CONFIGURATION
+	64	S ¹ A ¹⁰ Q ¹³ P ³⁷
X	40	A ²⁰ _{0.5}
▷	58	B ⁸ b ¹⁶ v ⁹ e ¹² , 13 x ^{7,8}
▽	56	A ²⁰ _{0.5} B ⁸ b ¹⁶ v ⁹ e ¹² , 13 x ^{7,8}



3 5 8 4 4
+ X X ▽

10-11-73

LFL-41

FIGURE 14 (SHEET 1)

EFFECT OF ORBITER
TAIL ON AND TAIL OFF

SYM	RUN	CONFIGURATION
+	64	S ¹ a ¹⁰ j ¹³ p ³⁷
x	40	A ²⁰ _{0.5}
▷	58	D ⁸ b ¹⁶ v ⁹ H ⁸ e ^{12,13} r ^{7,8}
▽	56	A ²⁰ _{0.5} D ⁸ b ¹⁶ v ⁹ H ⁸ e ^{12,13} r ^{7,8}

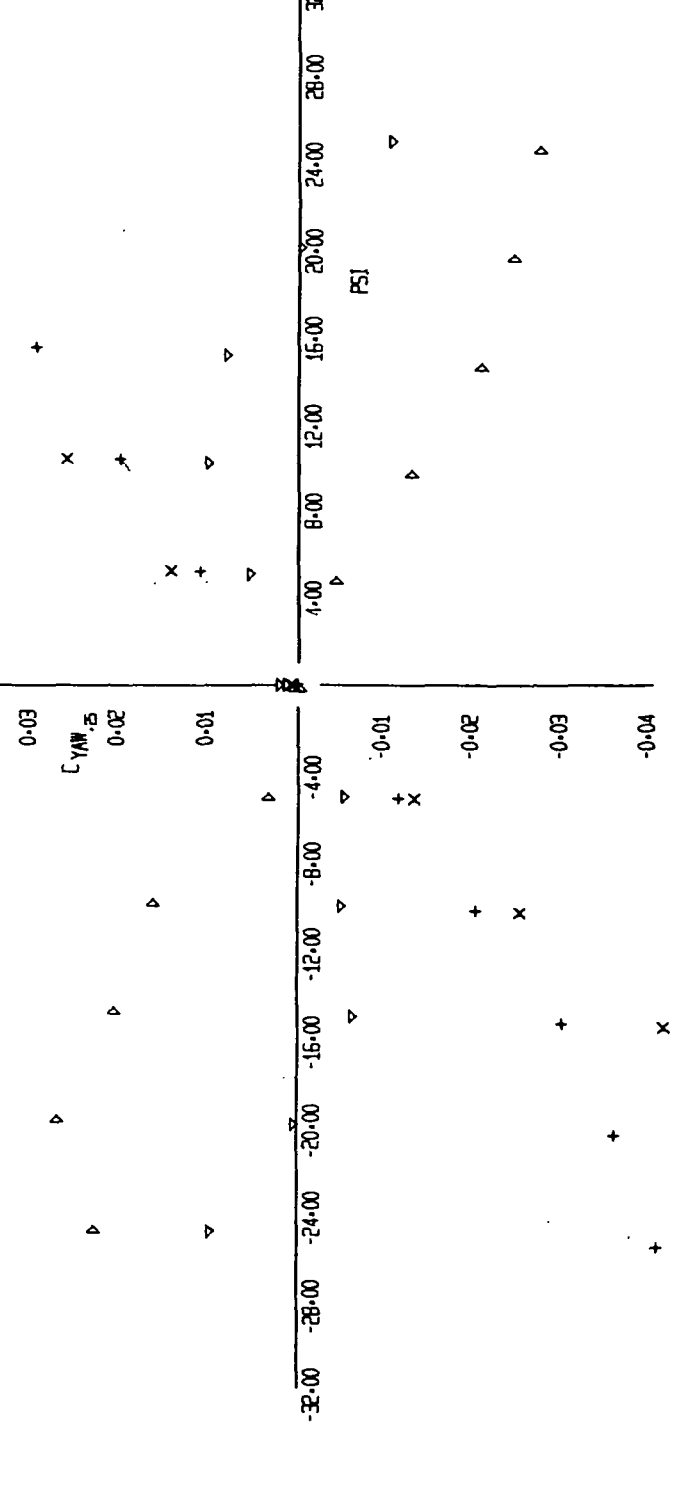


FIGURE 14 (SHEET 2)

3 号 明 示
+ x ▷ ▽

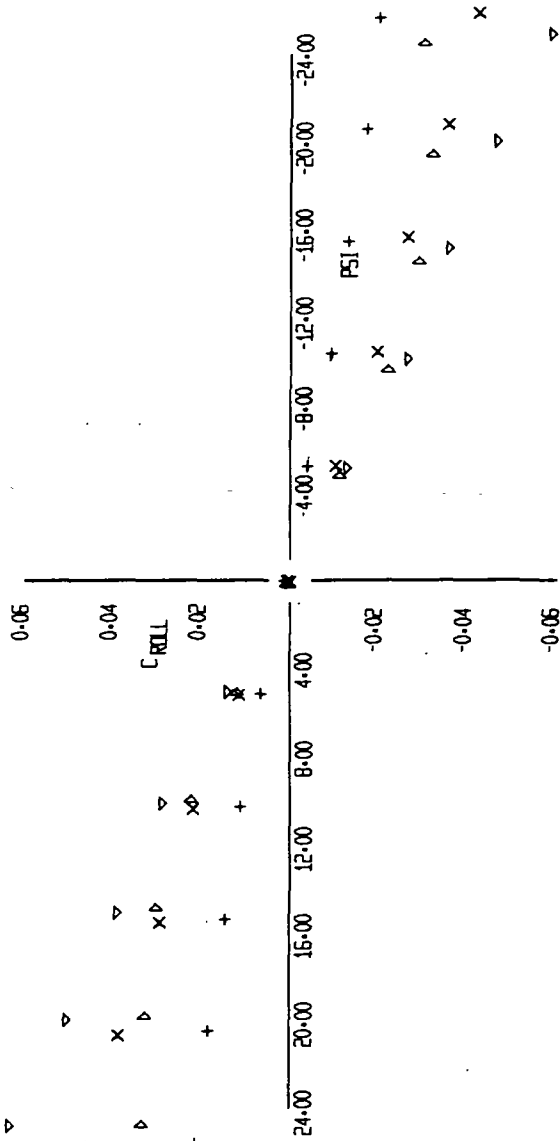
12-14-73

12-40

EFFECT OF ORBITER
TAIL ON AND TAIL OFF

SYM RUN CONFIGURATION

+	64	S ¹ a ¹⁰ r ¹³ c ²⁷
X	40	A ²⁰ _{0.5}
▷	58	D ⁸ b ¹⁶ v ⁹ H ⁸ e ^{12,13} r ^{7,8}
▽	36	A ²⁰ D ⁸ b ¹⁶ v ⁹ H ⁸ e ^{12,13} r ^{7,8} _{0.5}



5 5 5 5 5
+ X ▷ ▽

5-12-73

LR-08

FIGURE 14 (SHEET 3)

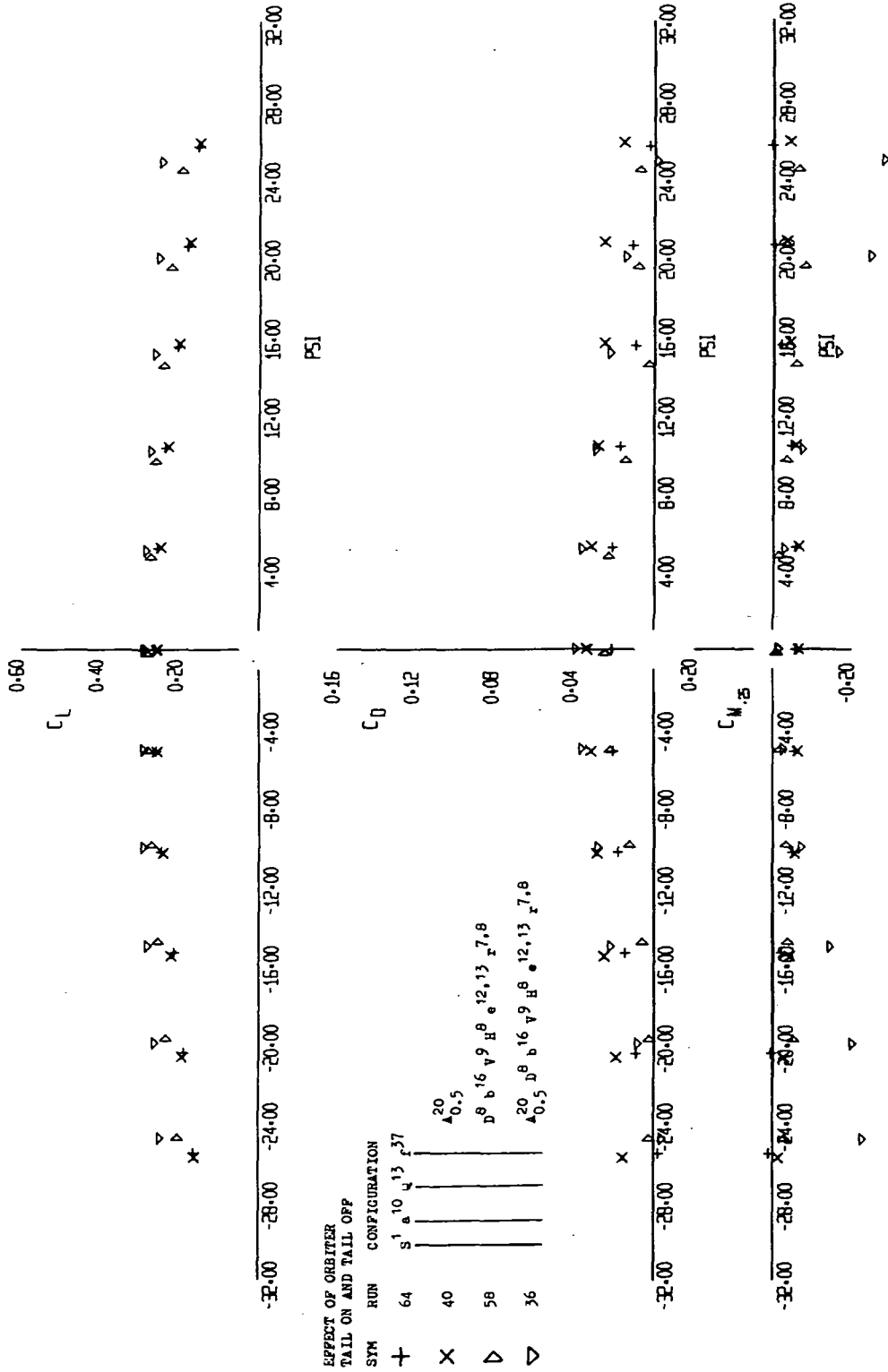
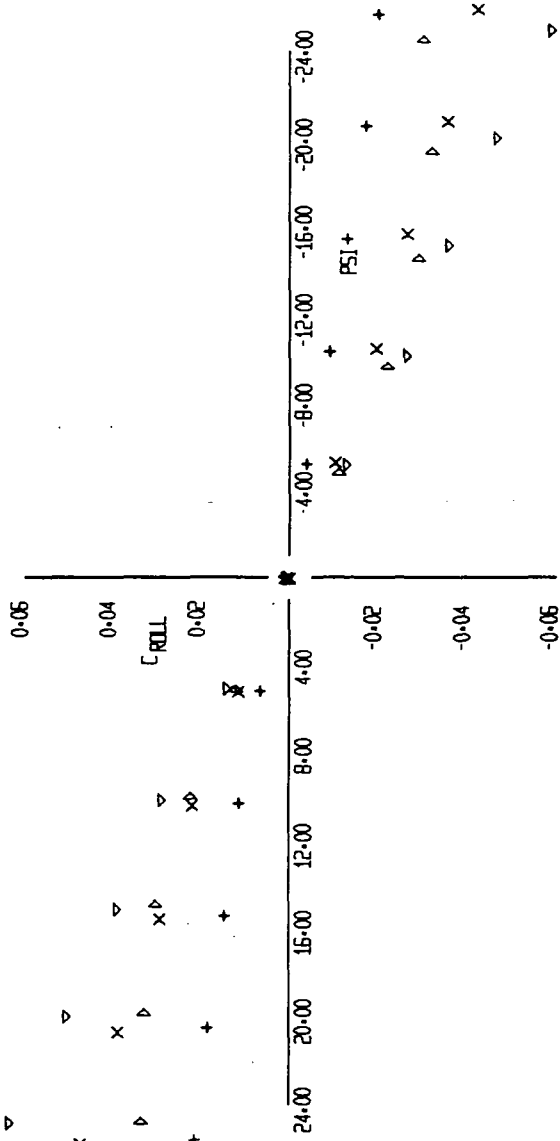


FIGURE 14 (SHEET 4)

EFFECT OF ORBITER
TAIL ON AND TAIL OFF

SYM RUN CONFIGURATION

+	64	S ¹ a ¹⁰ q ¹³ r ²⁷
X	40	A _{0,5} ²⁰
▷	58	D ⁸ b ¹⁶ v ⁹ H ⁸ e ^{12,13} x ^{7,8}
▽	36	A _{0,5} ²⁰ D ⁸ b ¹⁶ v ⁹ H ⁸ e ^{12,13} x ^{7,8}



▽ X ▷ +

11-11-73

LFL-08

FIGURE 14 (SHEET 5)

VERTICAL TAIL EFFECTIVENESS WITH
CENTER VERTICAL EXTENSION

SYM	HUN	CONFIGURATION
+	79	S ¹ a ¹⁰ q ¹³ f ³⁷ A ^{5P}
x	84	D ⁸ b ¹⁶ v ⁹ B ⁸ e ^{12,13} r ^{7,8} v ¹

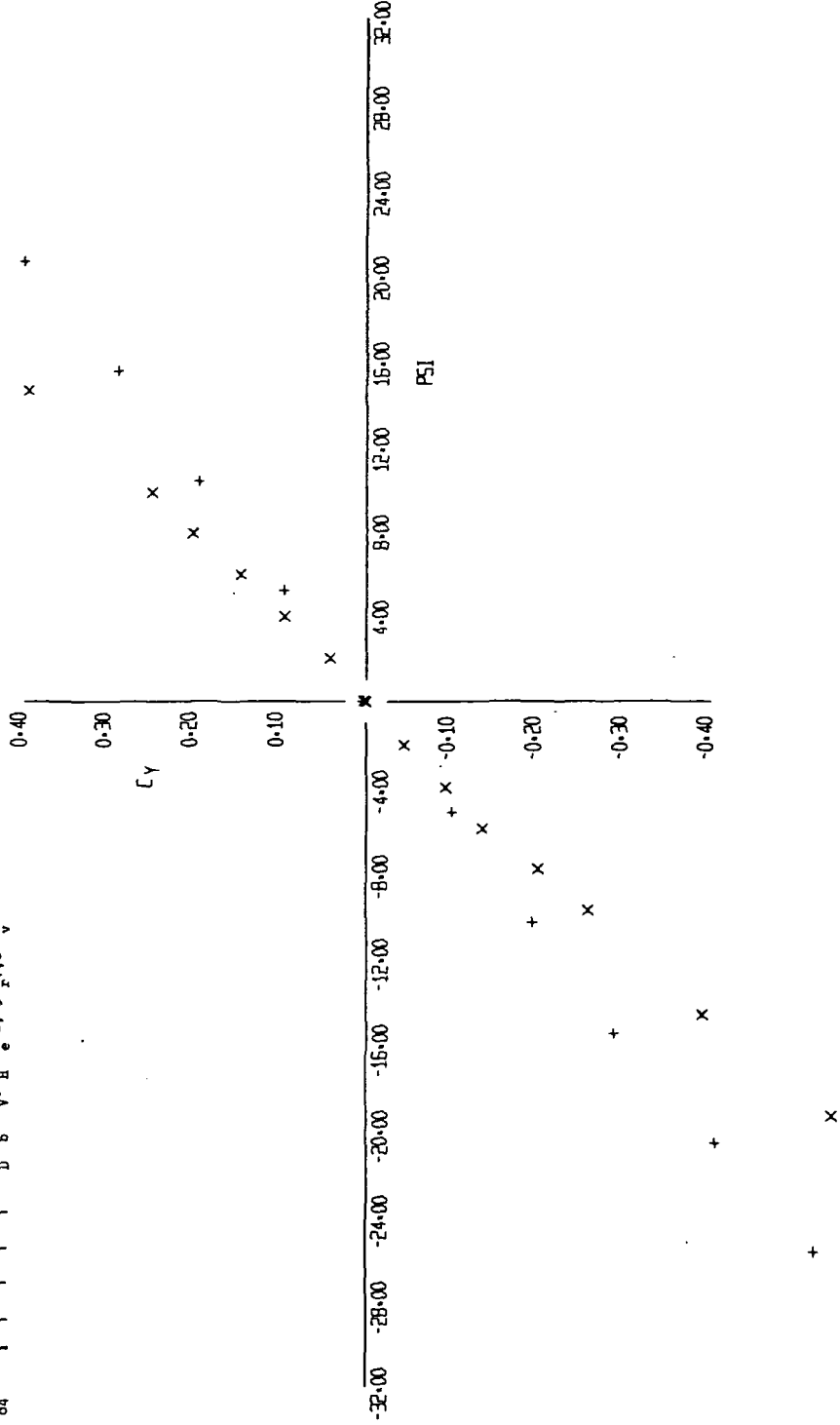


FIGURE 15 (SHEET 1)

79 +
84 x

10-11-73

11-21

VERTICAL TAIL EFFECTIVENESS
WITH CENTER VERTICAL EXTENSION

SYM RUN CONFIGURATION
79 S¹ a¹⁰ Q¹³ r²⁷ a^{5F}
84 D^B b¹⁶ v⁹ B^B a^{12,13} z^{7,8} v¹

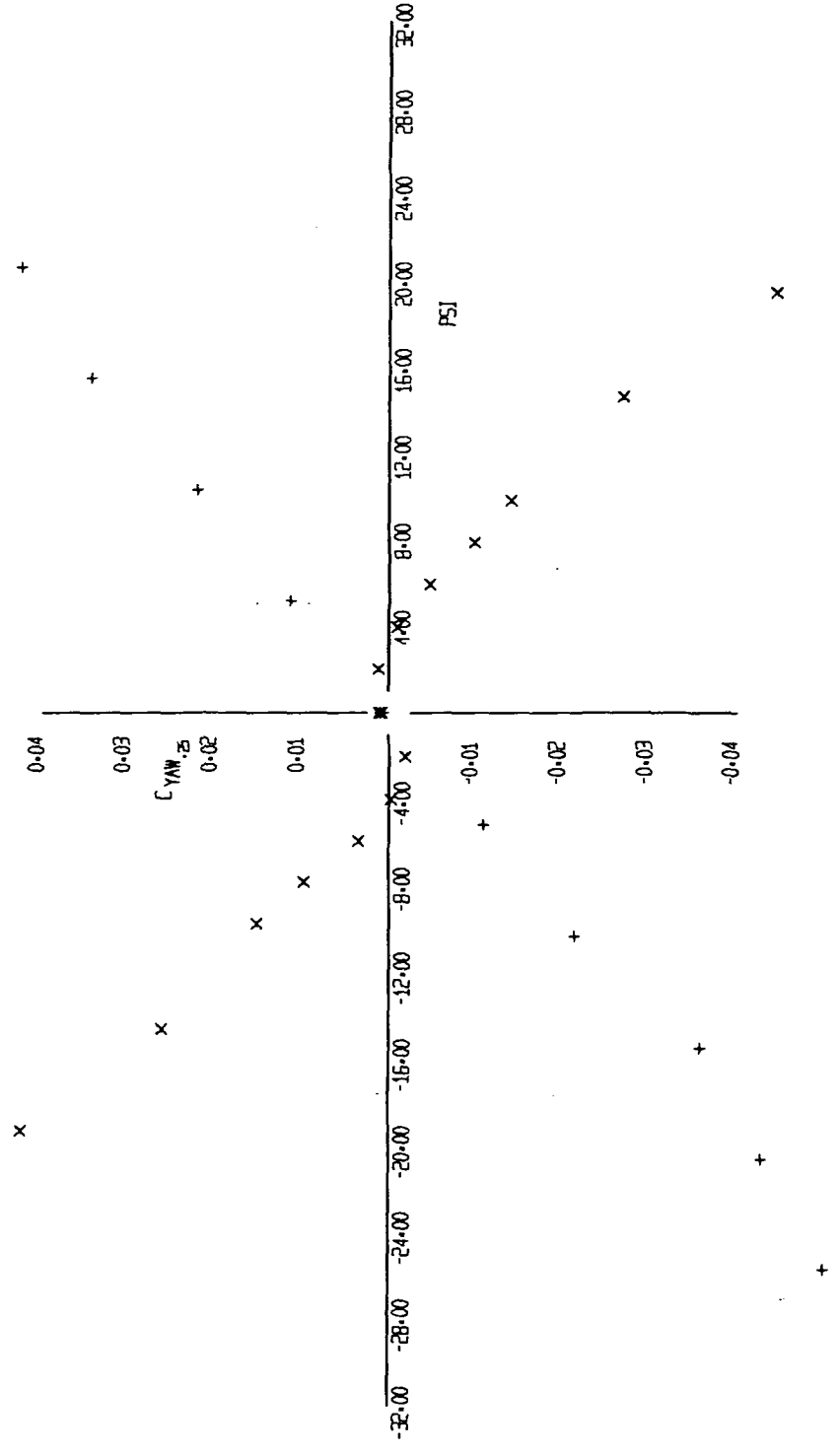


FIGURE 15 (SHEET 2)

R 8
+

10-11-73

11-4-71

11-4-71

VERTICAL TAIL EFFECTIVENESS WITH
CENTER VERTICAL EXTENSION

SYM	RUN	CONFIGURATION
+	79	S ¹ a ¹⁰ q ¹³ r ²⁷ A ^{5P}
X	84	D ⁸ b ¹⁶ v ⁹ H ⁸ e ^{12,13} I ^{7,8} v ¹

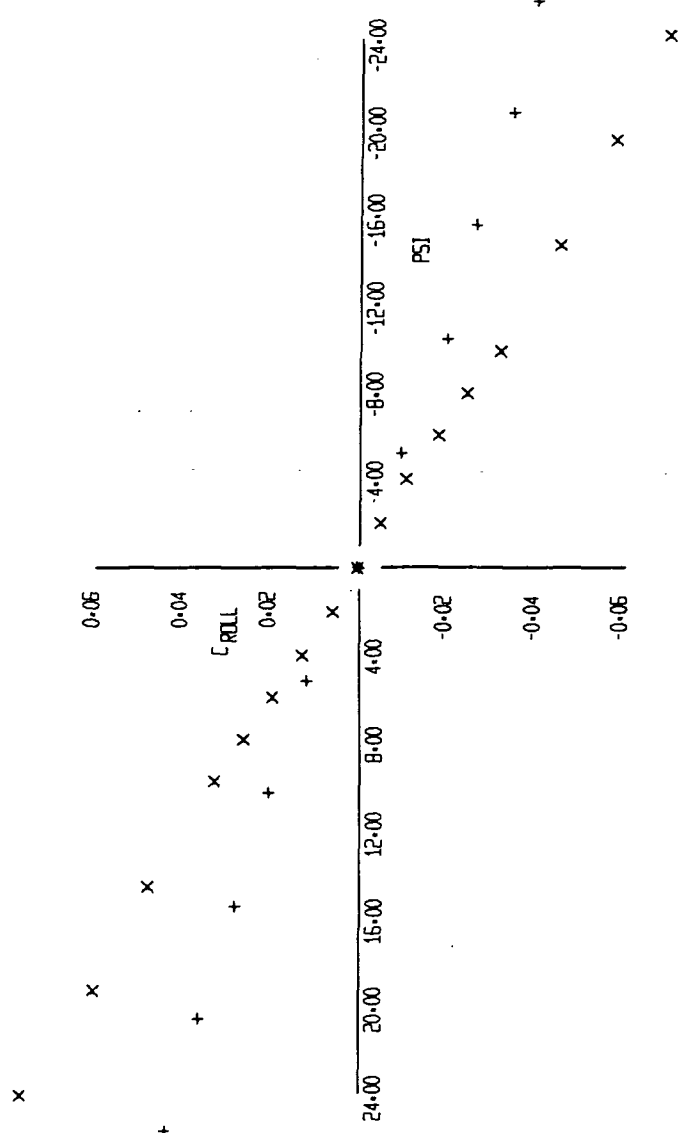


FIGURE 15 (SHEET 3)

79 +
84 X

10-11-73

L1-48

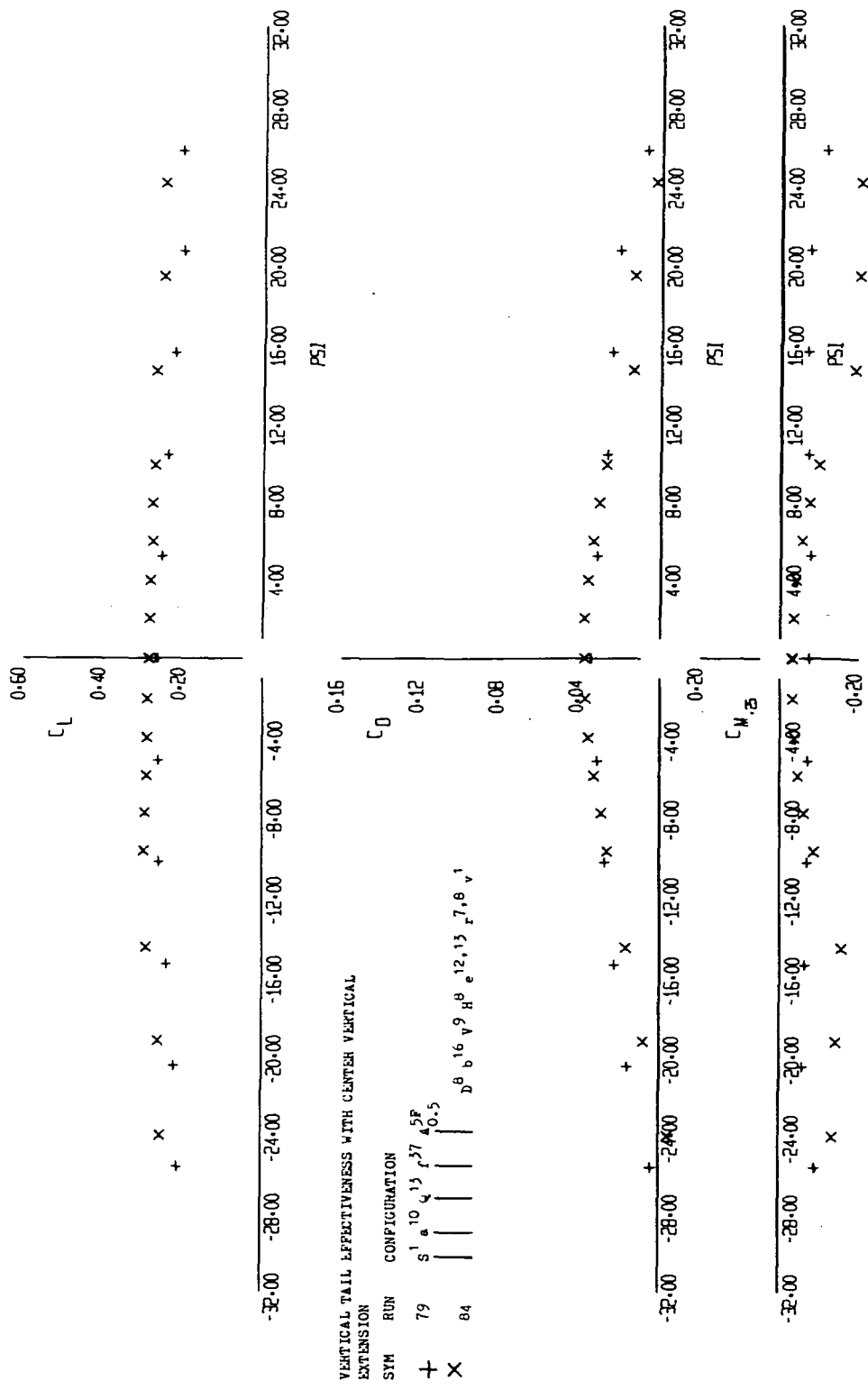


FIGURE 15 (SHEET 4)

RZ
+ X

10-11-73

11-60

EFFECT OF VERTICAL TAIL MODIFICATIONS
 ORBITER OFF FLAPS EXTENDED

SYM	RUN	CONFIGURATION
+	92	S ¹ A ¹⁰ Q ¹³ P ¹⁷ R ¹⁶ V ⁹ B ¹² C ¹¹ X ⁷ F ⁸
X	96	
△	93	
▽	94	

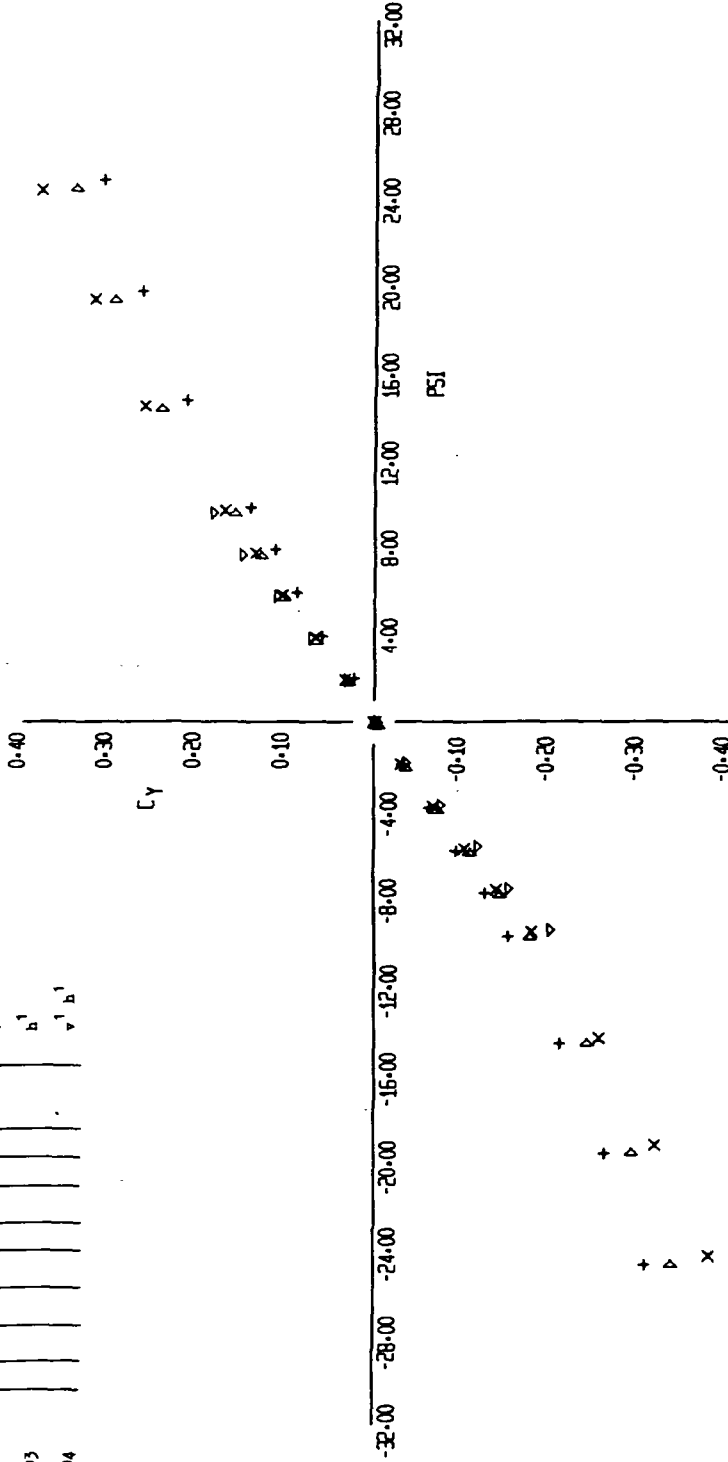


FIGURE 16 (SHEET 1)

88 88 88
 △ △ △
 +

15-15-73

15-15

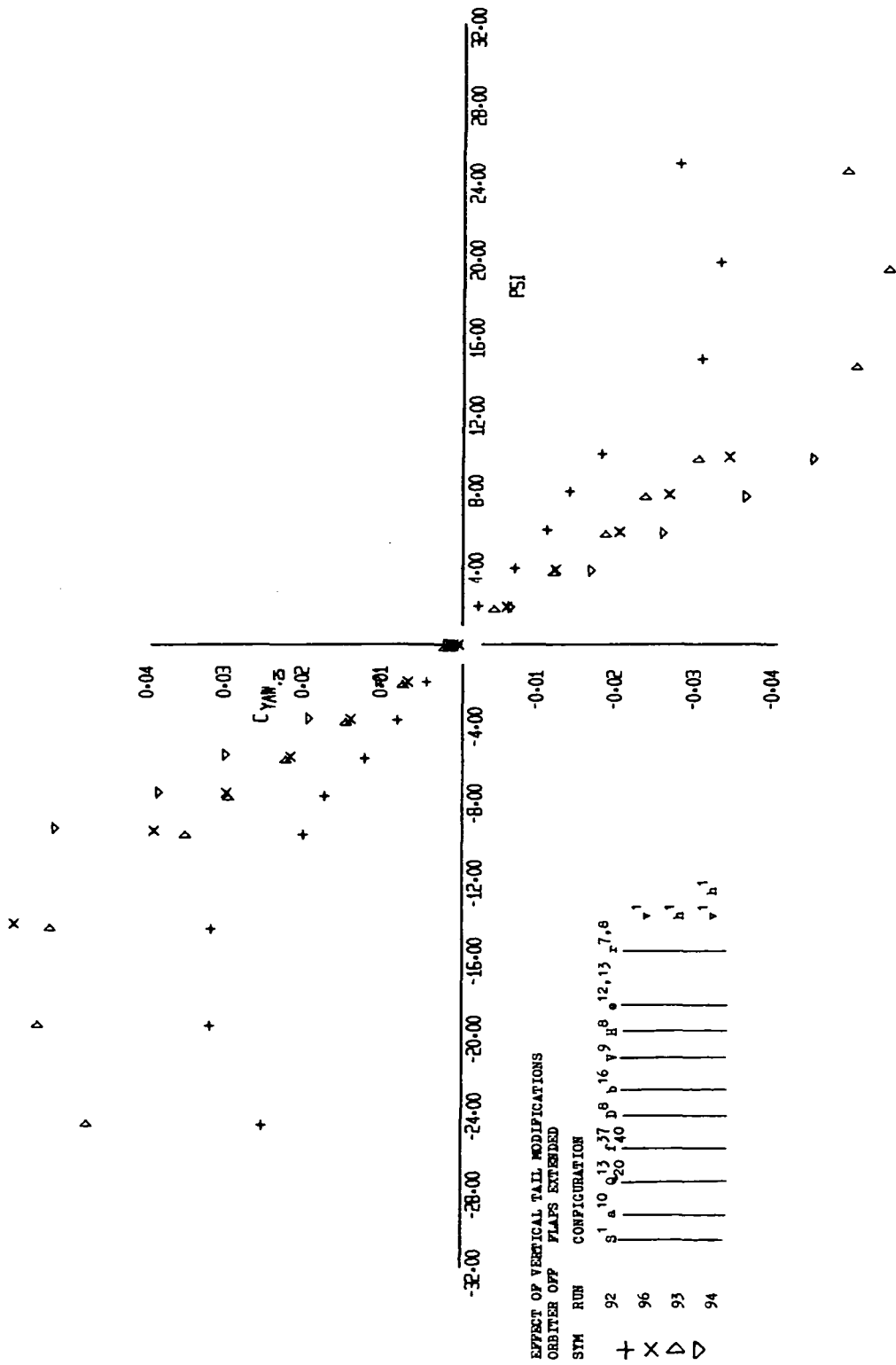


FIGURE 16 (SHEET 2)

LR- PAGE
 UFL- FIG.

EFFECT OF VERTICAL TAIL MODIFICATIONS
 ORBITER OFF FLAPS EXTENDED

SYM	RUN	CONFIGURATION
+	92	S ¹ a ¹⁰ Q ¹³ r ¹⁷ D ⁸ b ¹⁶ v ⁹ B ⁶ e ^{12,13} z ^{7,8}
x	96	v ¹
△	93	b ¹
▽	94	v ¹ b ¹

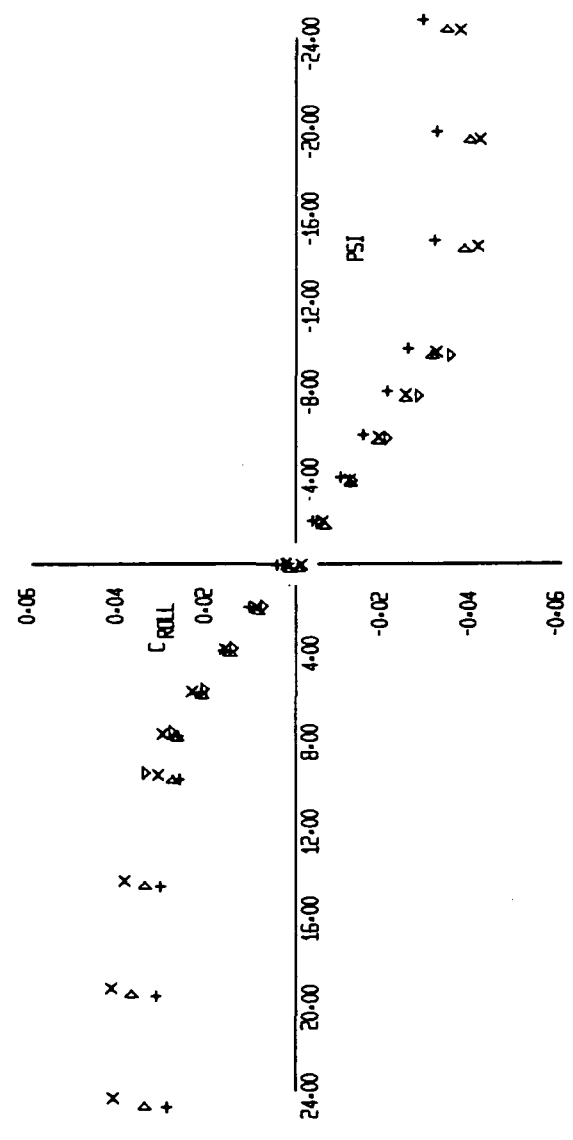


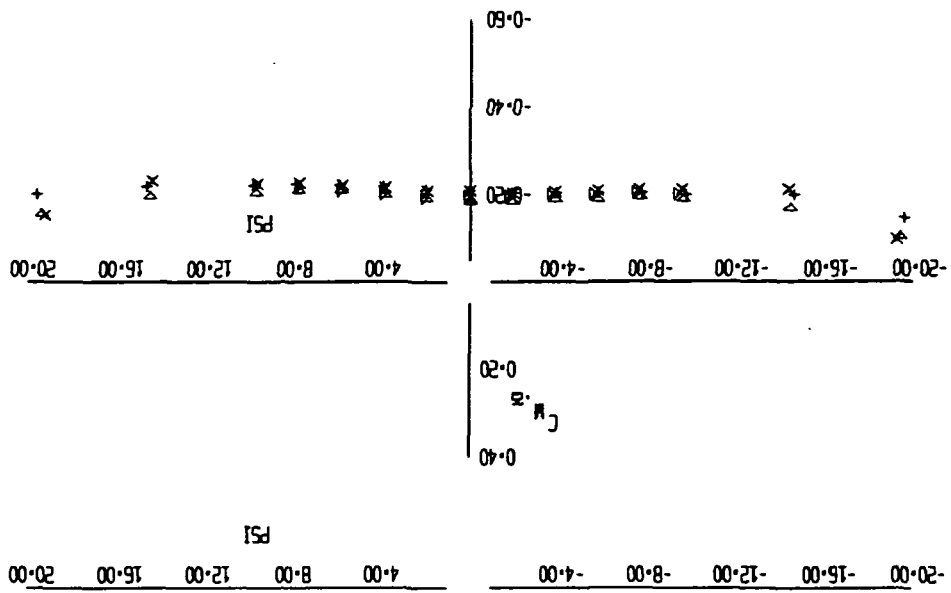
FIGURE 16 (SHEET 3)

88 88 88
 + x △ ▽

10-15-73

11-48

△ X +
▽ X +



EFFECT OF VERTICAL TAIL MODIFICATIONS
ORDER OFF FLAPS EXTENDED

SYM	RUN	CONFIGURATION
△	92	S 1
X	93	A 10
X	96	Q 13
+	94	F 20
		F 31
		D 40
		B 8
		A 9
		H 16
		A 9
		H 8
		12, 13
		7, 8

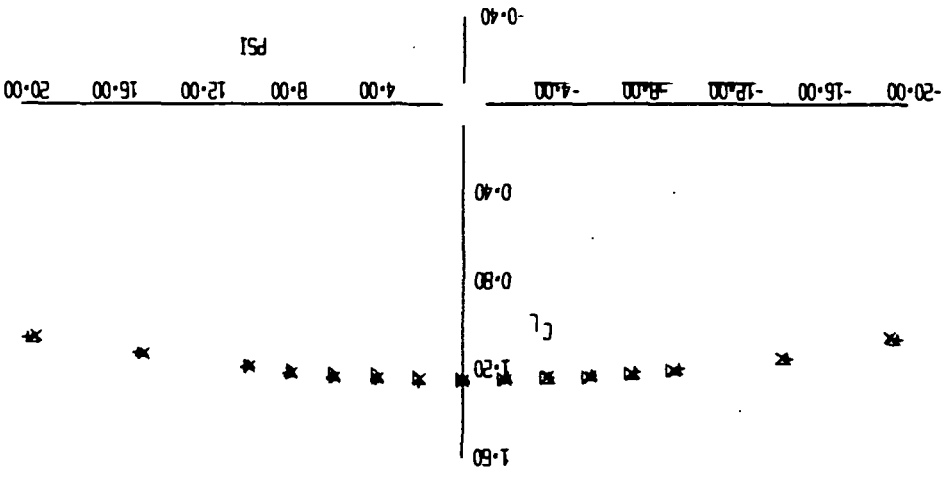
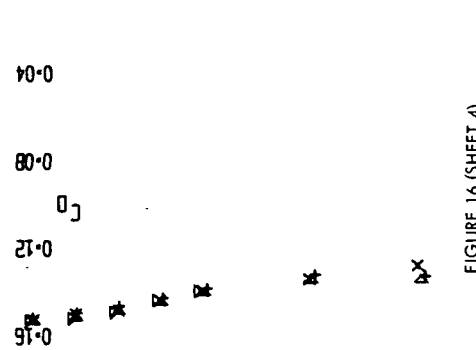


FIGURE 16 (SHEET 4)

△ X +
▽ X +

10-15-73

11-11

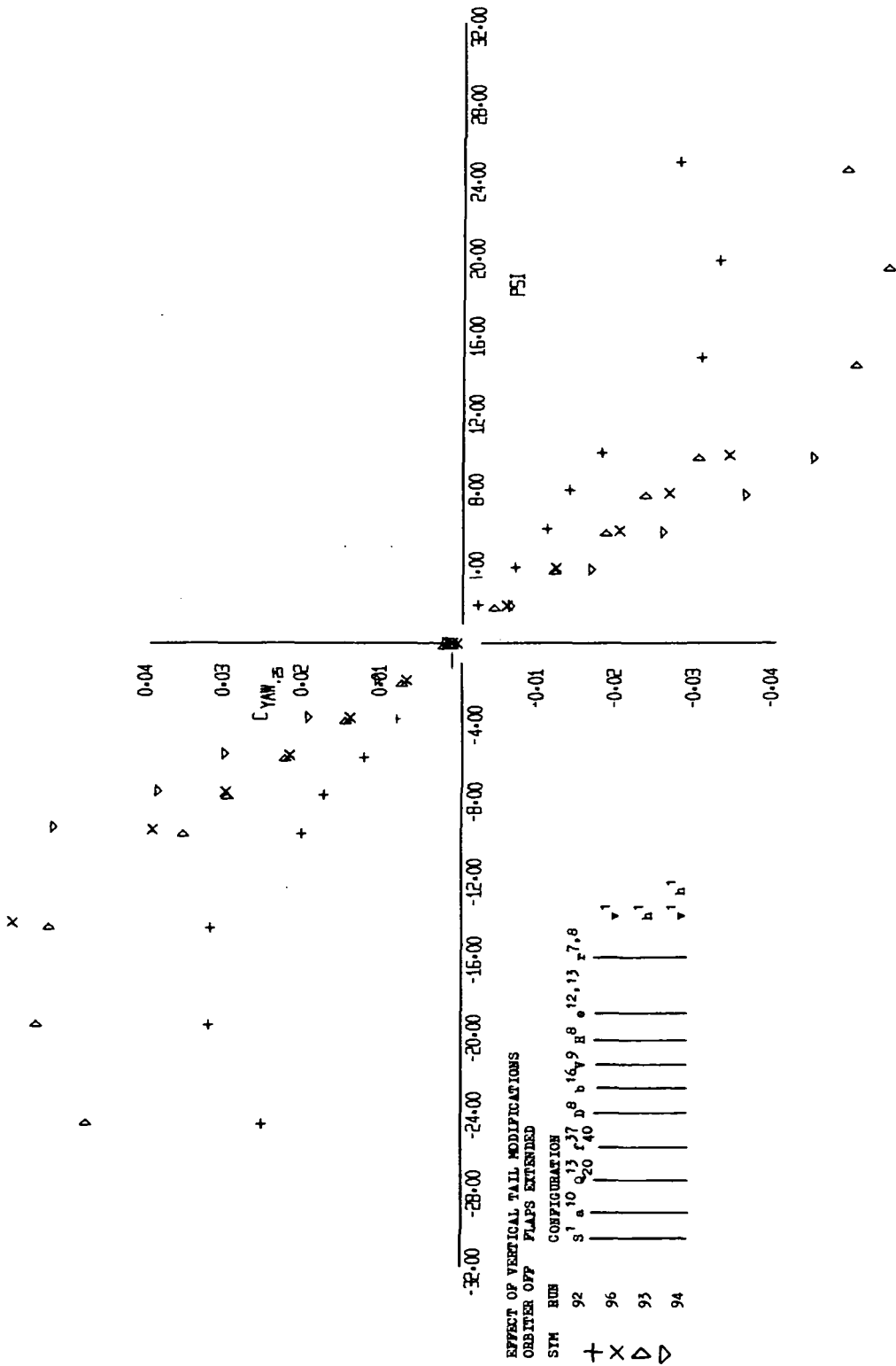


FIGURE 16 (SHEET 5)

BR BR
 + X Δ ▽

15-15-73

15-40

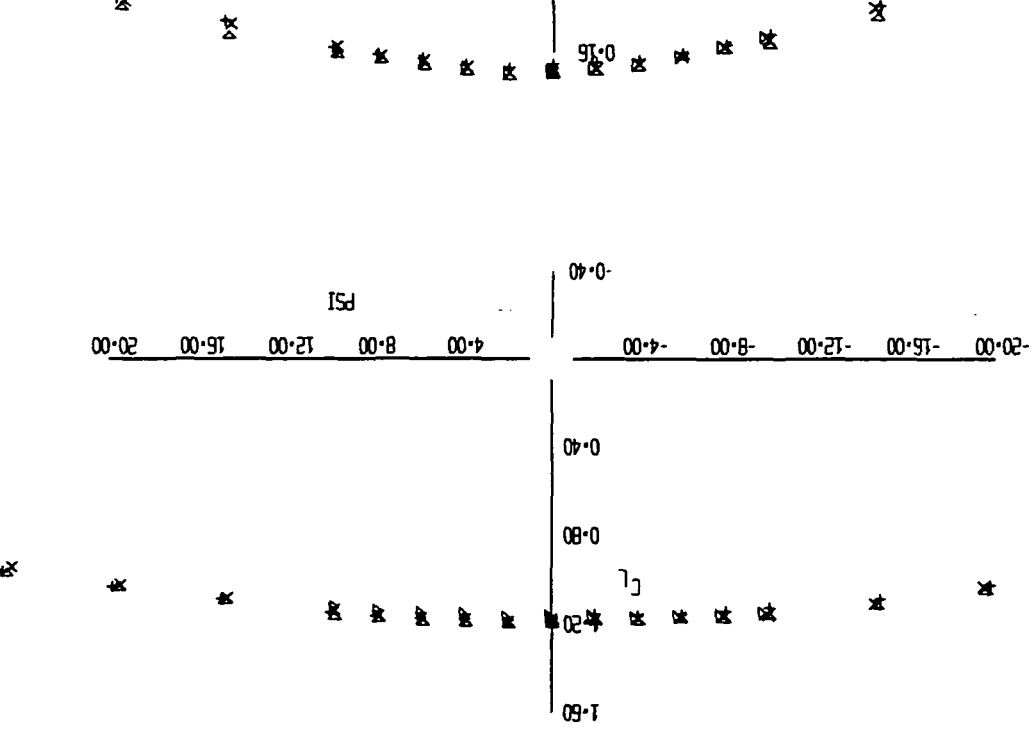
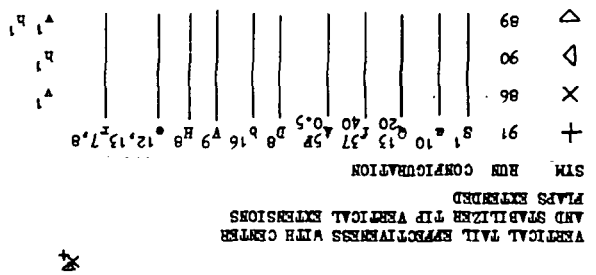
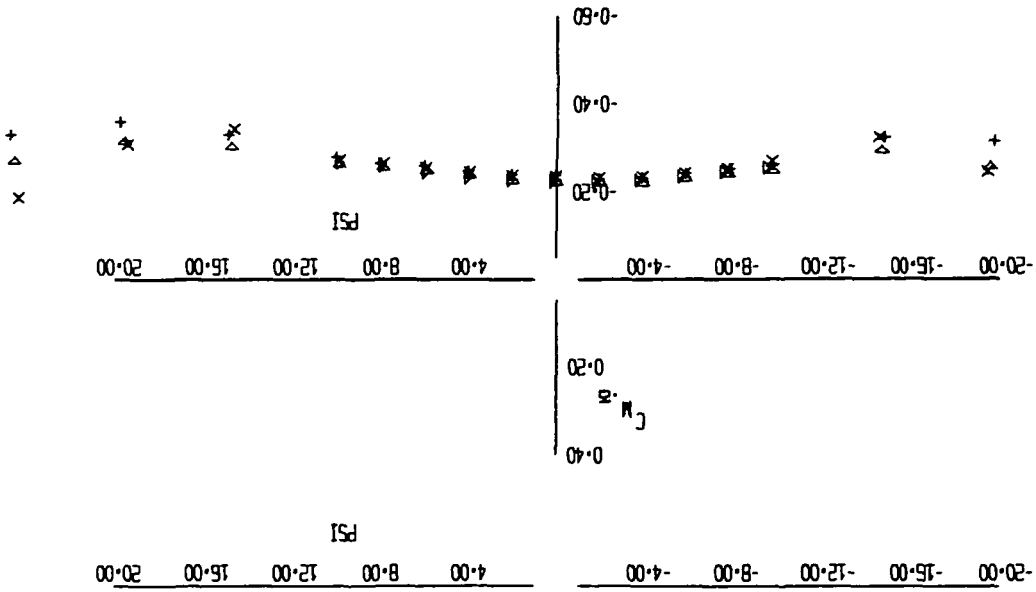


FIGURE 17 (SHEET 1)

△ x x +
88 89 90

10-15-73

(17-41)

VERTICAL TAIL EFFECTIVENESS WITH CENTER
 AND STABILIZER TIP VERTICAL EXTENSIONS
 FLAPS EXTENDED

STN	RUN CONFIGURATION
91	S ¹ 10 13 17 20 24 28 32 36 40 45 50 55 60 65 70 75 80 85 90 95 100
86	S ¹ 10 13 17 20 24 28 32 36 40 45 50 55 60 65 70 75 80 85 90 95 100
90	S ¹ 10 13 17 20 24 28 32 36 40 45 50 55 60 65 70 75 80 85 90 95 100
89	S ¹ 10 13 17 20 24 28 32 36 40 45 50 55 60 65 70 75 80 85 90 95 100

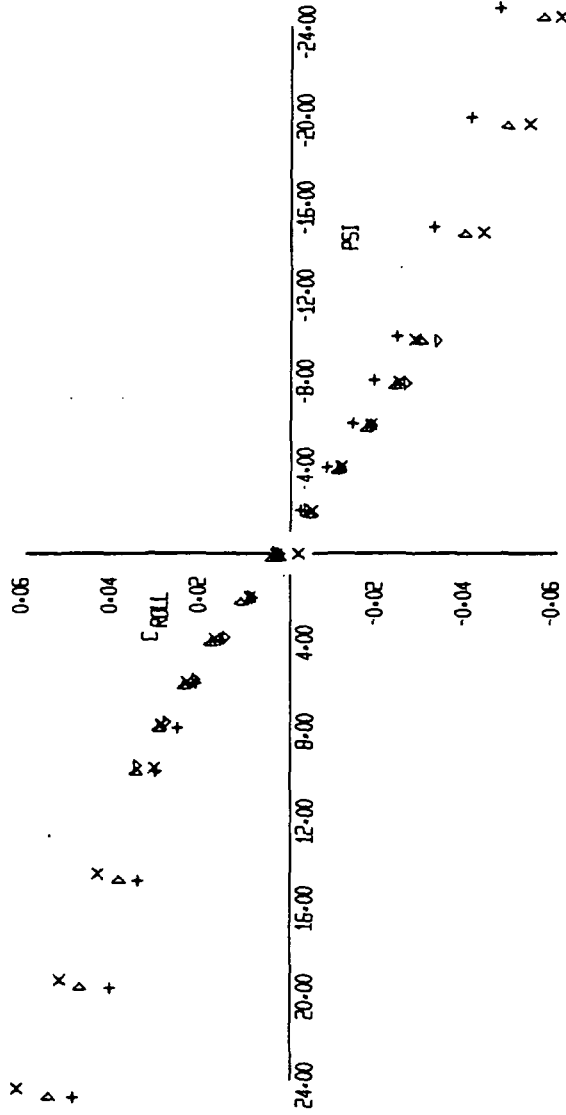


FIGURE 17 (SHEET 2)

88 88 88
 + x Δ

15-15-73

14-48

VERTICAL TAIL EFFECTIVENESS WITH CENTER
 AND STABILIZER TIP VERTICAL EXTENSIONS
 FLAPS EXTENDED

SYM	RUN	CONFIGURATION
+	91	s ¹ a ¹⁰ 13 ¹⁷ 5P ⁸ b ¹⁶ v ⁹ h ^{12,13} r ^{7,8}
X	86	
▷	90	
▽	89	

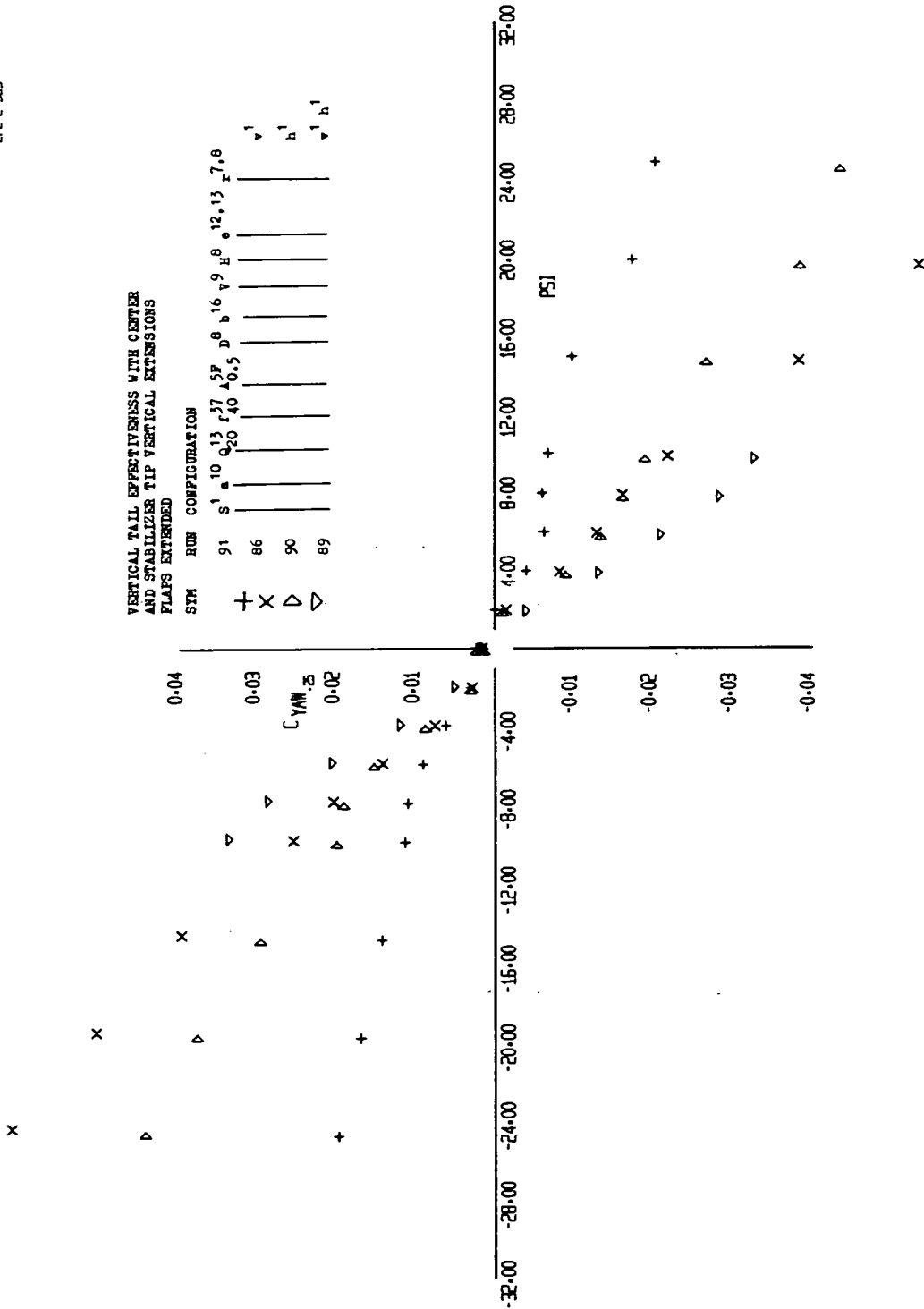


FIGURE 17 (SHEET 3)

88888
 + X ▷ ▽

10-15-73

UFL-400

x
▷
+

VERTICAL TAIL EFFECTIVENESS WITH CENTER AND STABILIZER TIP VERTICAL EXTENSIONS FLAPS EXTENDED

SYM	RUN	CONFIGURATION
+	91	s ¹ a ¹⁰ r ¹³ 27 ^{5P} Δ 0.5 ¹⁶ v ⁹ B ^{12,13} F ^{7,8}
x	86	
▷	90	
▷	89	

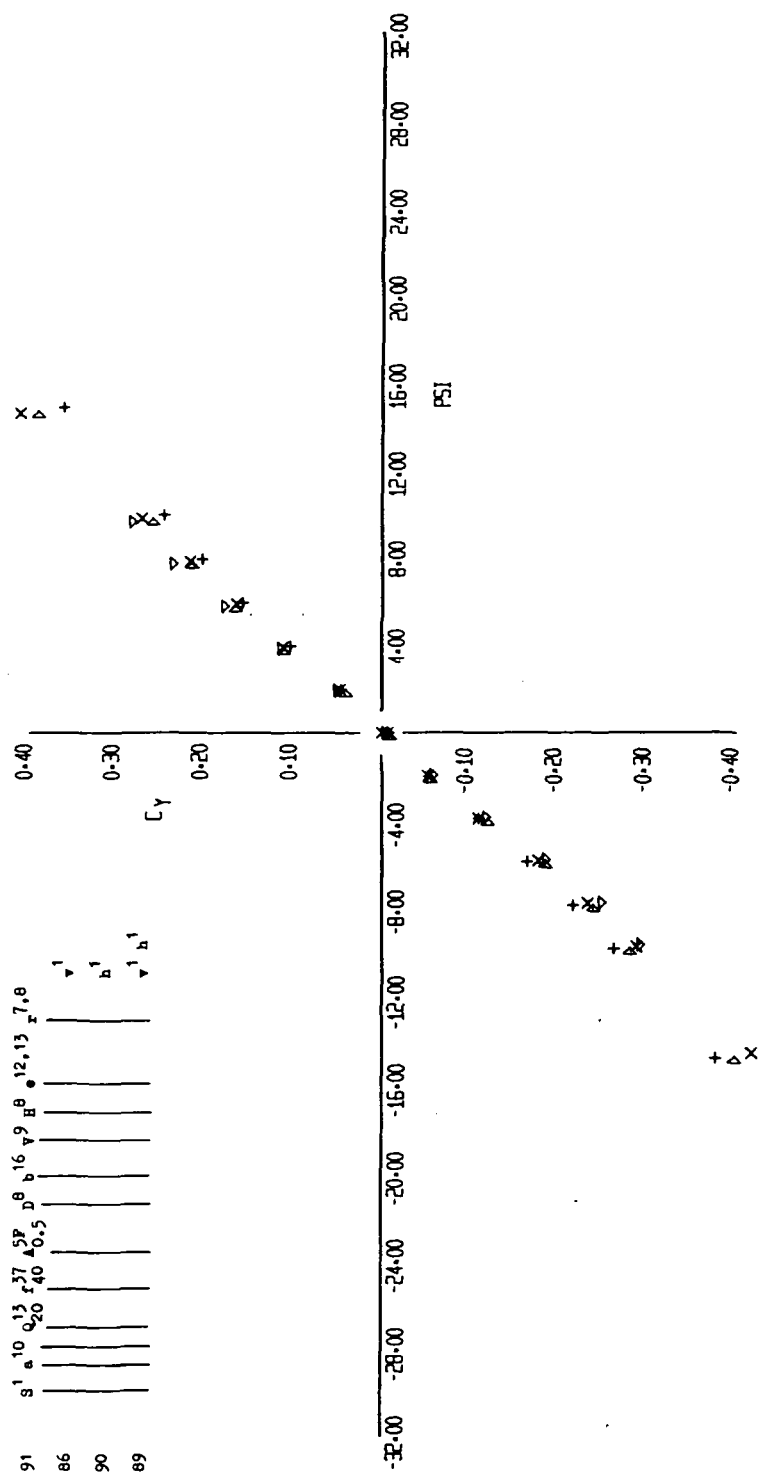


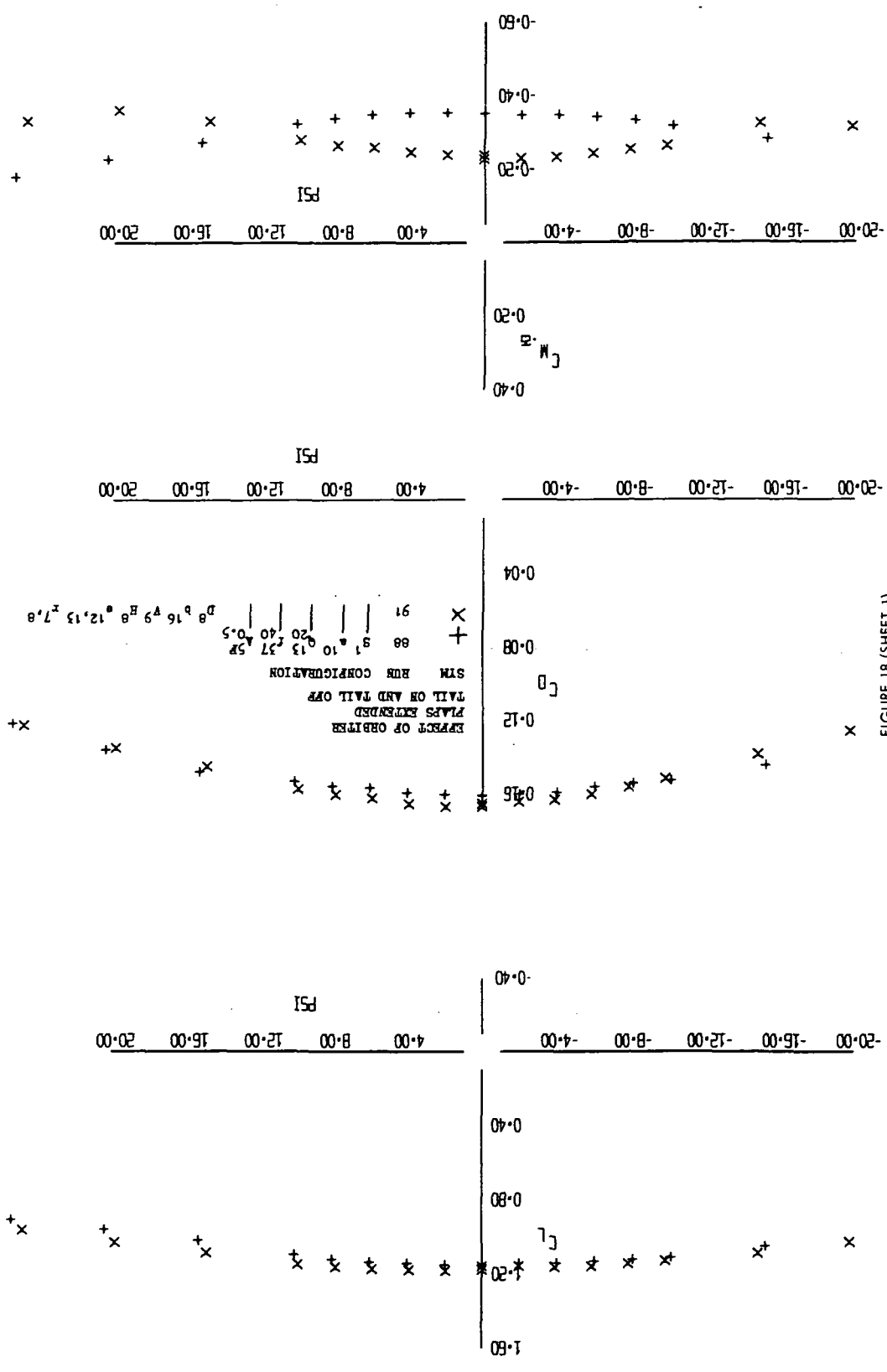
FIGURE 17 (SHEET 4)

88 88 88
+ x x
+

15-15-73

LR-6E

LR- UFL-363 PAGE FIG-



EFFECT OF ORBITER
PLACES EXTENDED
TAIL ON AND TAIL OFF
STM RUN CONFIGURATION

91	X
88	+
85	*
82	*
79	*
76	*
73	*
70	*
67	*
64	*
61	*
58	*
55	*
52	*
49	*
46	*
43	*
40	*
37	*
34	*
31	*
28	*
25	*
22	*
19	*
16	*
13	*
10	*
7	*
4	*

FIGURE 18 (SHEET 1)

10-15-73

(P-4)

X +
BB

EFFECT OF ORBITER
FLAPS EXTENDED
TAIL ON AND TAIL OFF

SYM RUN CONFIGURATION

+ 88 S¹ 10 13 37 5P
X 91 | 20 40 0.5 | D⁸ b¹⁶ V⁹ H⁸ e^{12,13} r^{7,8}

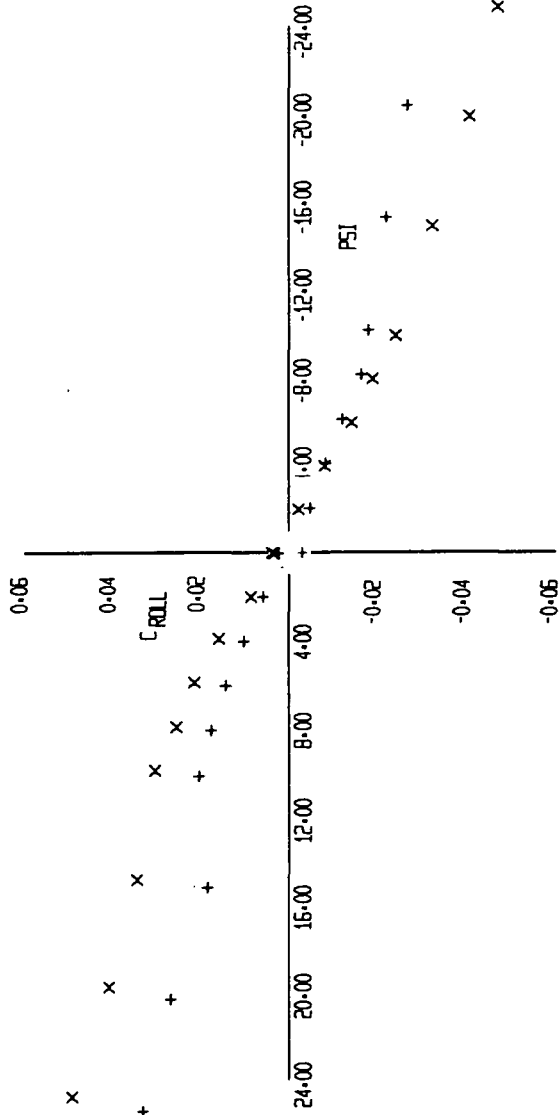


FIGURE 18 (SHEET 2)

88 S1
+ X

10-15-73

LFL-08

EFFECT OF ORBITER
 FLAPS EXTENDED
 TAIL ON AND TAIL OFF
 SYN RUN CONFIGURATION

+	88	S ¹	a ¹⁰	q ¹³	f ³⁷	f ^{5P}
X	91					

D^B b¹⁶ v⁹ H^B a^{12,13} r^{7,8}

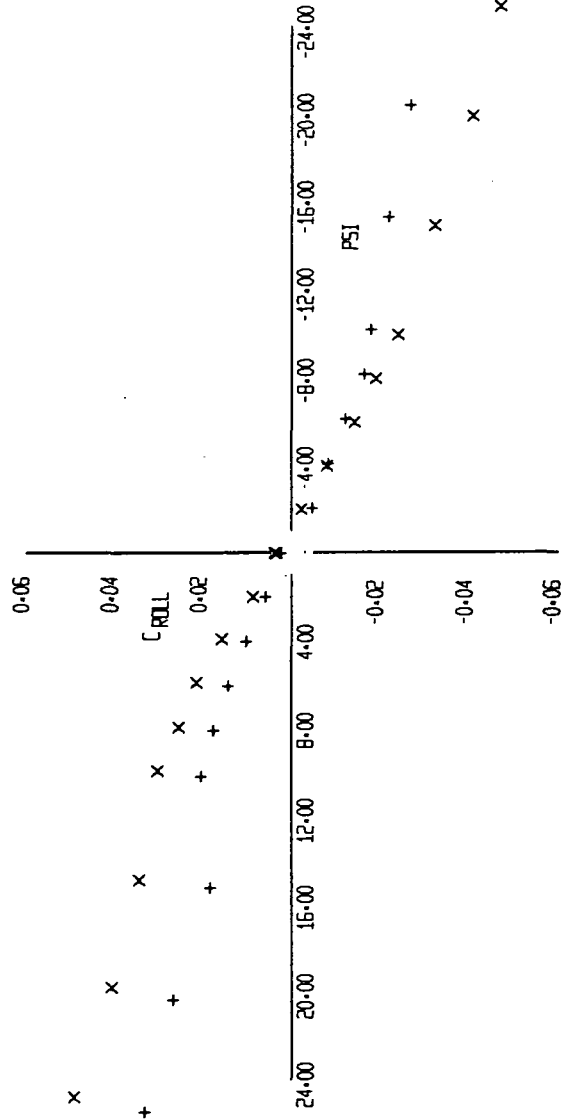


FIGURE 18 (SHEET 3)

88
 + X

10-15-73

10-48

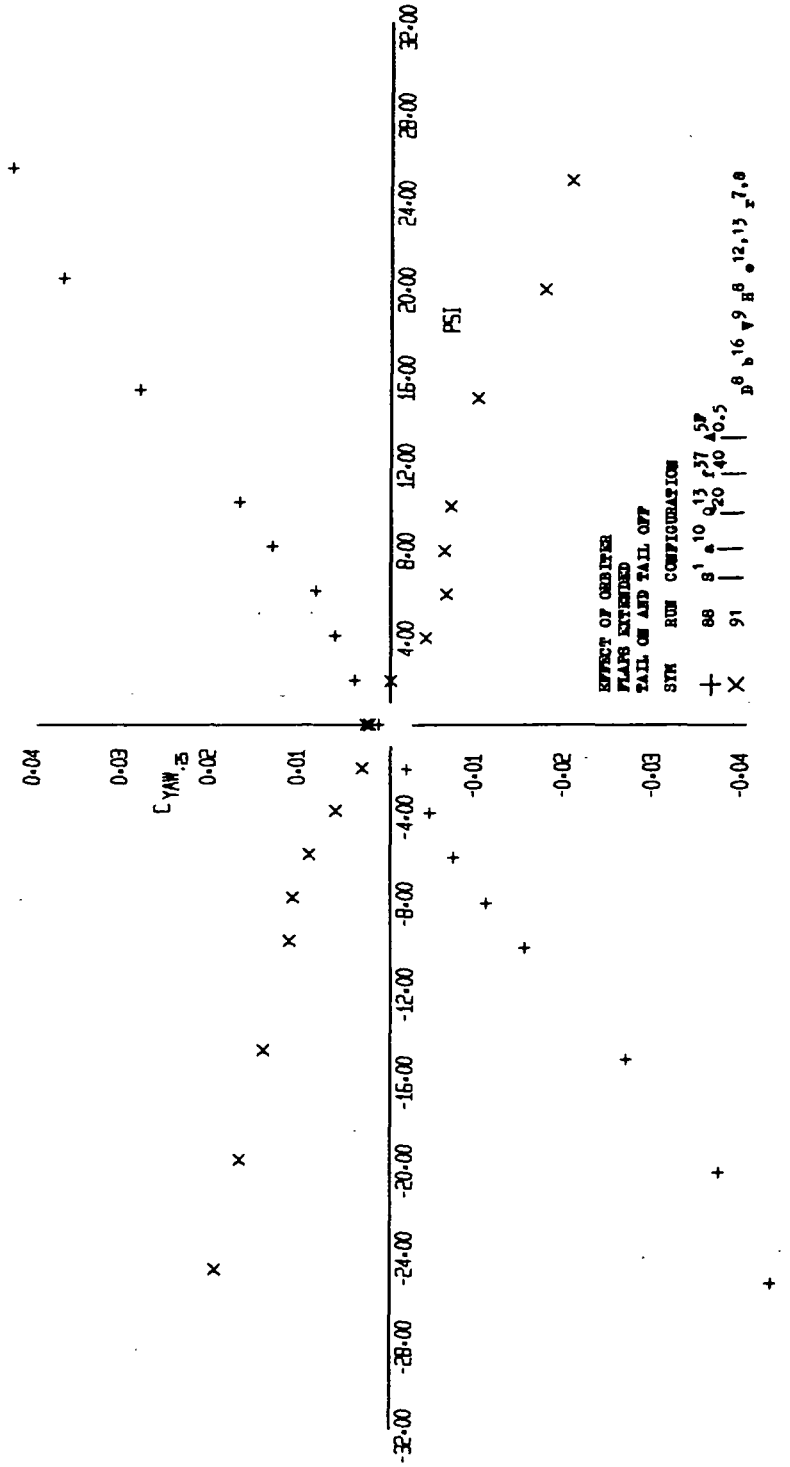


FIGURE 18 (SHEET 4)

88 81
 + X

10-15-73

18-40

EFFECT OF ORBITER
FLAPS EXTENDED
TAIL ON AND TAIL OFF

SYM	RUN	CONFIGURATION
+	88	S ¹ 10 0 ¹³ 27 5P 20 40 0.5
X	91	D ⁸ 16 9 ⁸ 12, 13, 7, 8

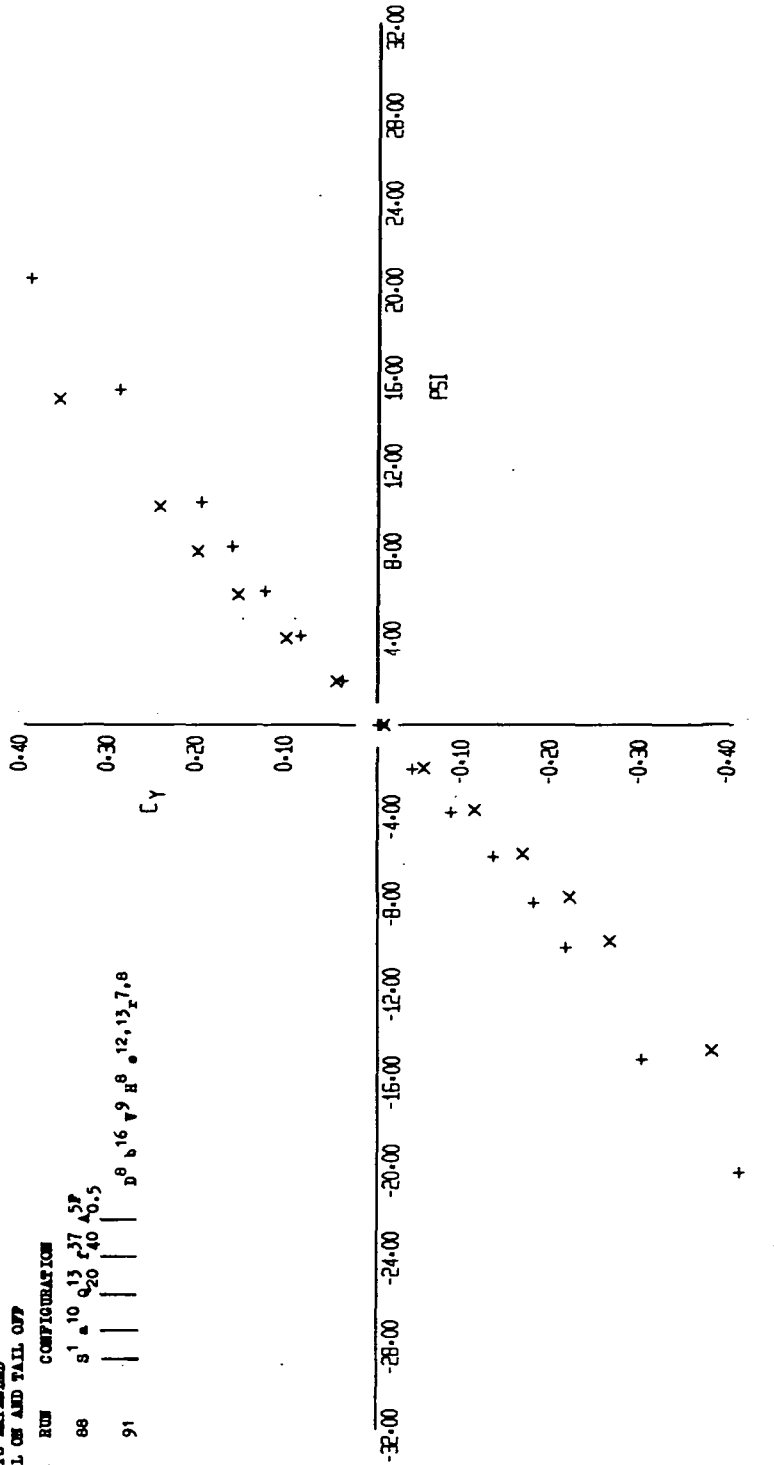


FIGURE 18 (SHEET 5)

88 +
91 X

10-15-73

10-15-73

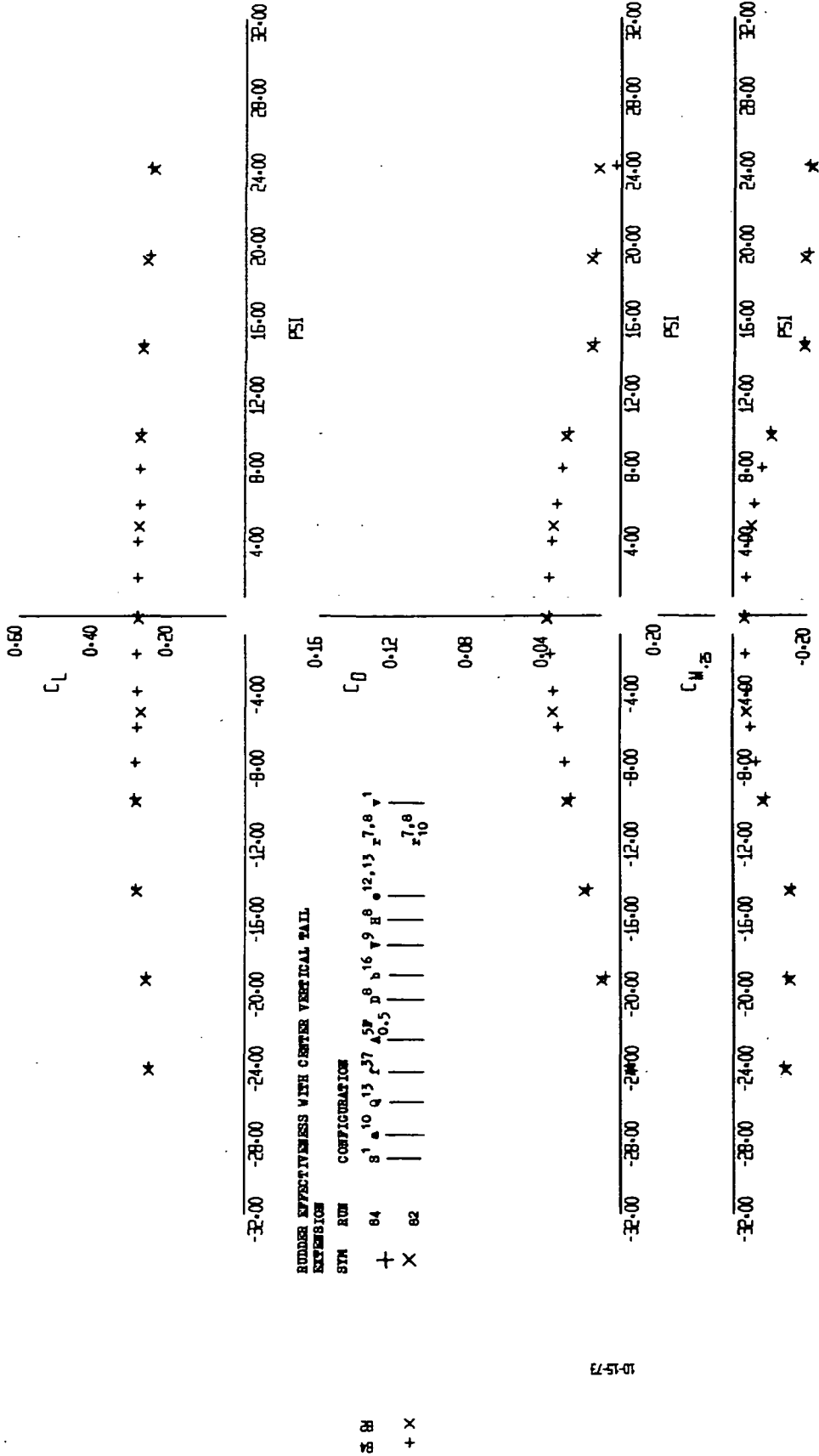


FIGURE 19 (SHEET 1)

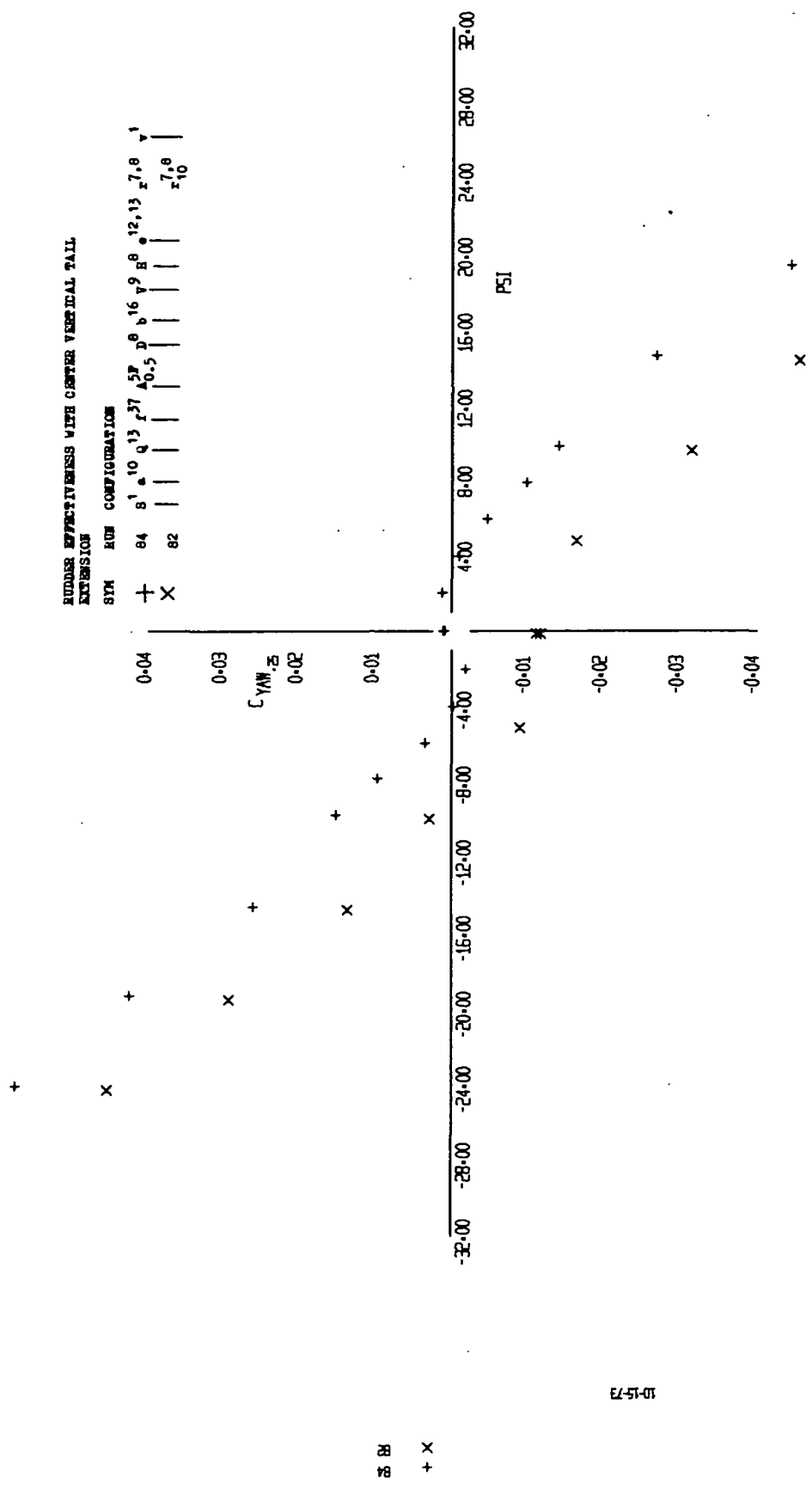


FIGURE 19 (SHEET 3)

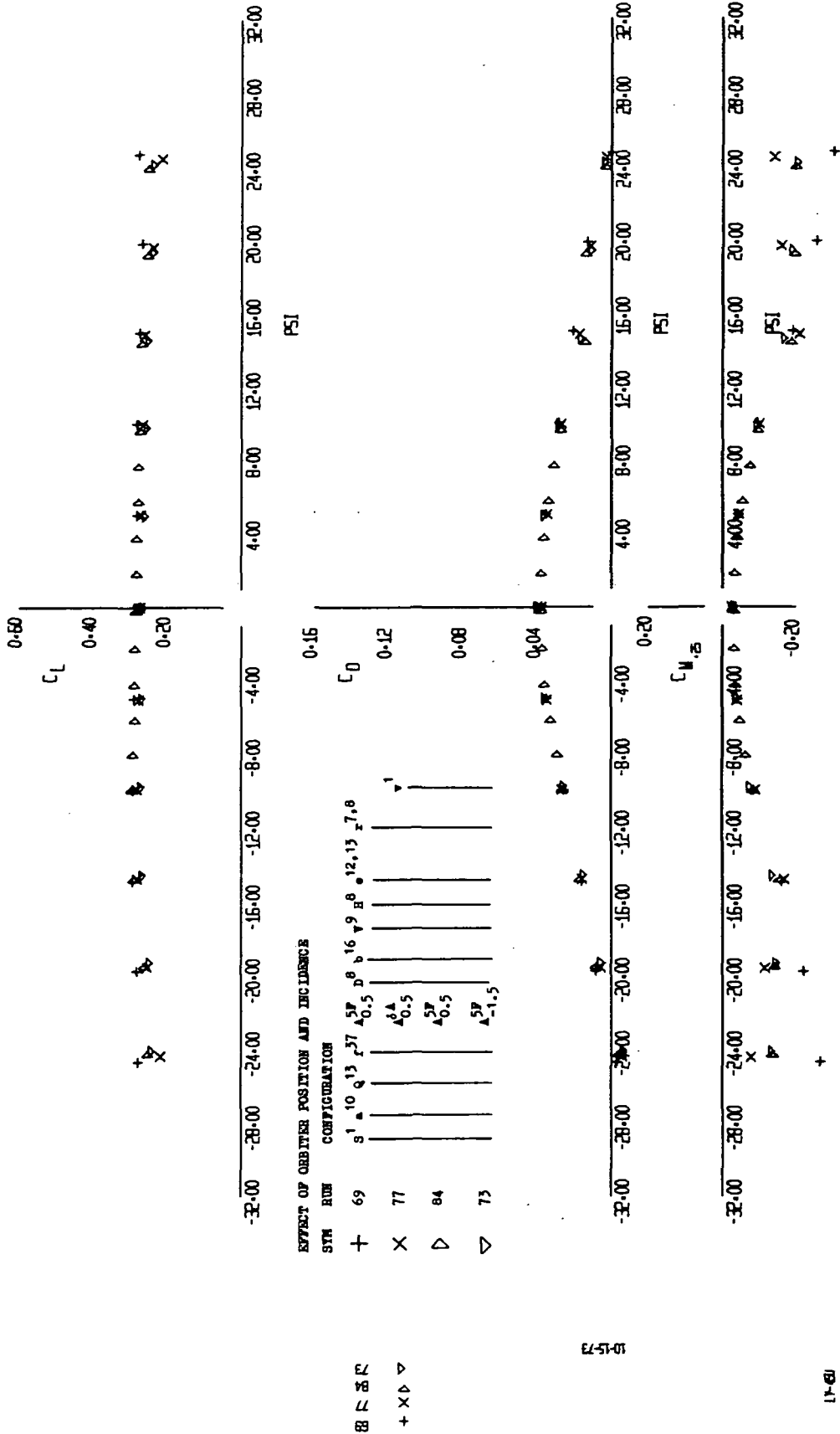


FIGURE 20 (SHEET 1)

EFFECT OF ORBITER POSITION AND INCIDENCE

STA RUN CONFIGURATION

+	69	S ¹	10	Q ¹³	P ³⁷	A ^{5P}	D ⁸	B ¹⁶	T ⁹	H ⁶	12,13	Z ^{7,8}
X	77					0.5						
△	84					0.5						
▽	73					0.5						

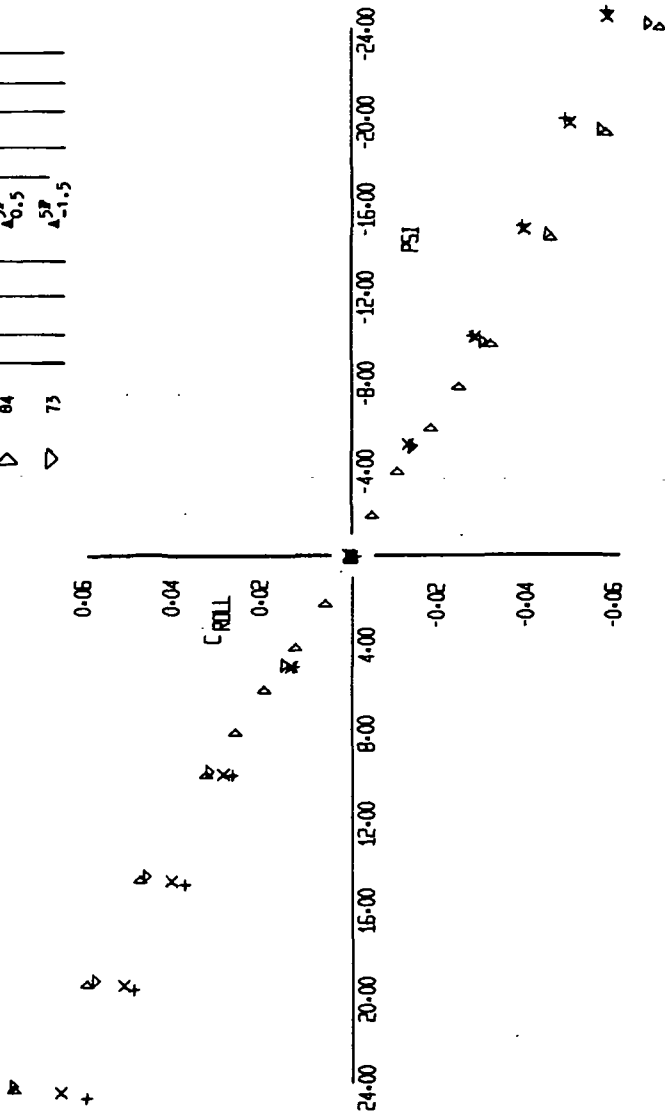


FIGURE 20 (SHEET 2)

BZSE
+ X +

10-15-73

14-08

EFFECT OF OBSERVER POSITION AND INCIDENCE

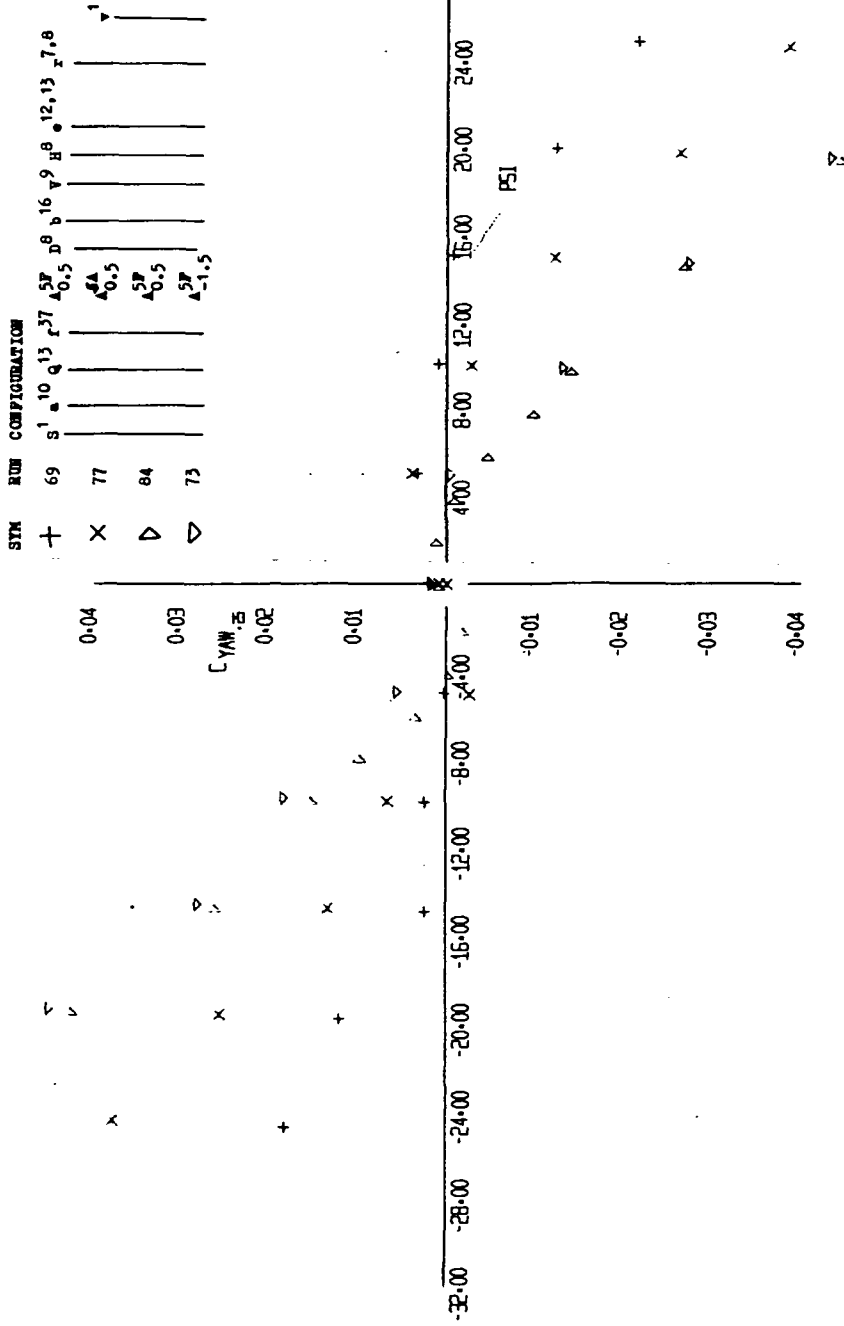


FIGURE 20 (SHEET 3)

73
77
84
+

10-15-73

1A-40

EFFECT OF ORBITER POSITION AND INCIDENCE

SYM	RUE	CONFIGURATION
+	69	S ¹ A ¹⁰ Q ¹³ P ³⁷ A ^{0.5} B ¹⁶ V ⁹ H ⁶ 12,13 z7.8
x	77	A ^{0.5}
▷	84	S ⁷ A ^{0.5}
▽	73	S ⁷ A ^{-1.5}

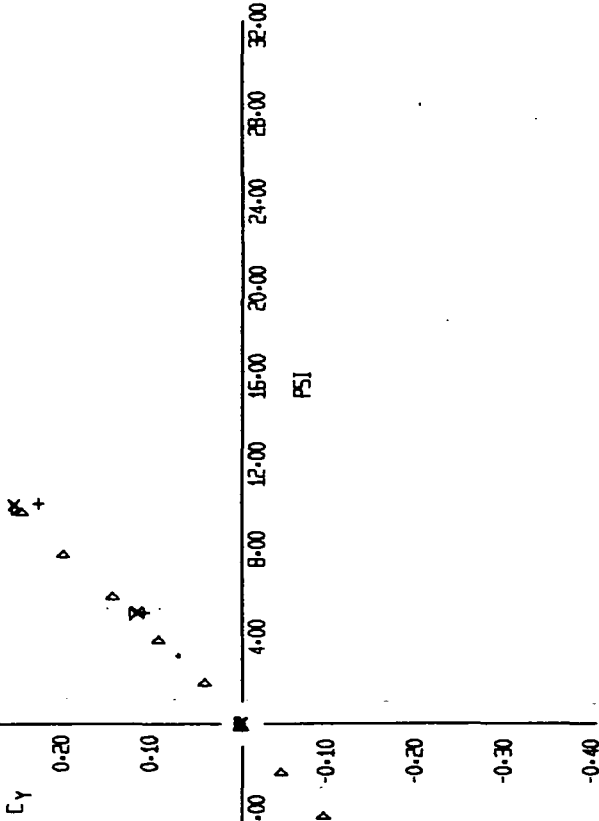
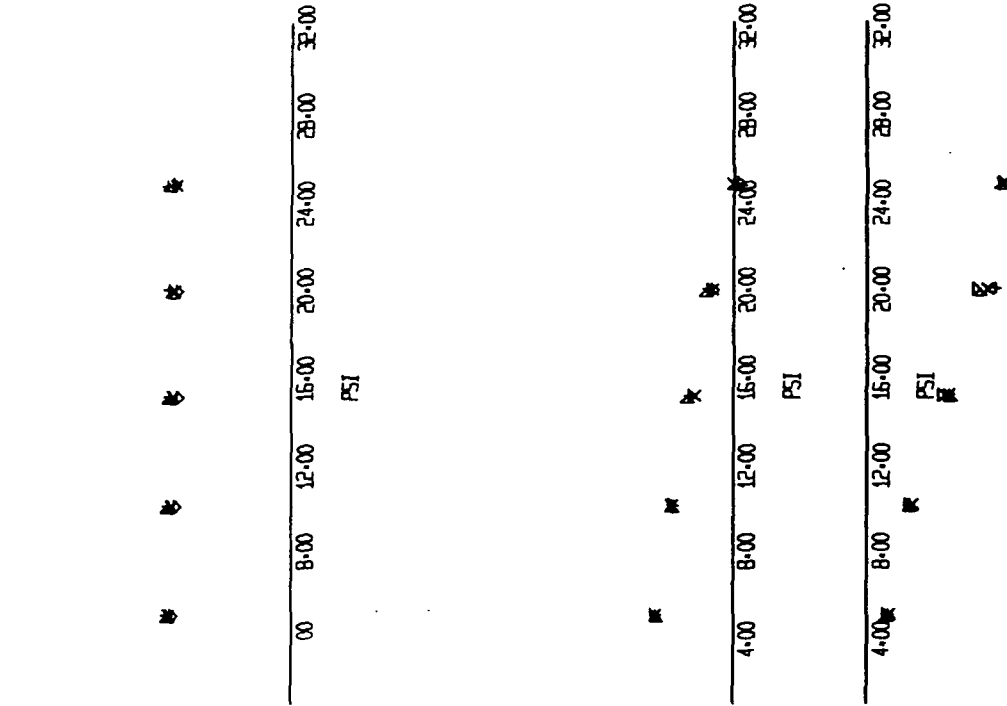


FIGURE 20 (SHEET 4)

8 7 3 7
+ x ▷ ▽

10-15-73

11-6E

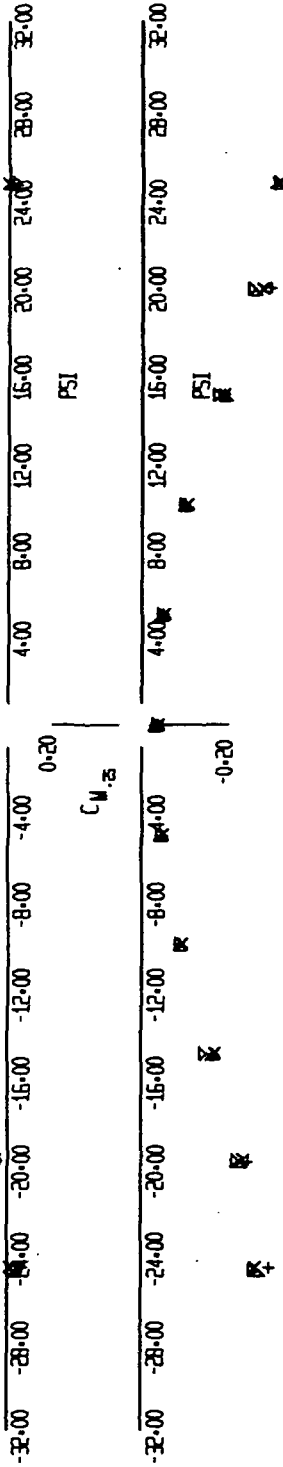


EFFECT OF ORBITER INCIDENCE AND PAIRING SHAPE

SYM	RUN	CONFIGURATION	C_D
+	48	S ¹ A ¹⁰ Q ¹³ r ²⁷ A ²⁷ D ⁸ b ¹⁶ v ⁹ B ⁸ 12,13 z ^{7,8}	0.15
X	67	A ²⁷ 0.5	0.12
▷	69	A ²⁷ 0.5	0.08
▷	71	A ²⁷ -1.5	0.04

⊕ ⊠ ⊞ ⊚
 + X ▷ ▷

12-15-73



12-15-73

FIGURE 21 (SHEET 1)

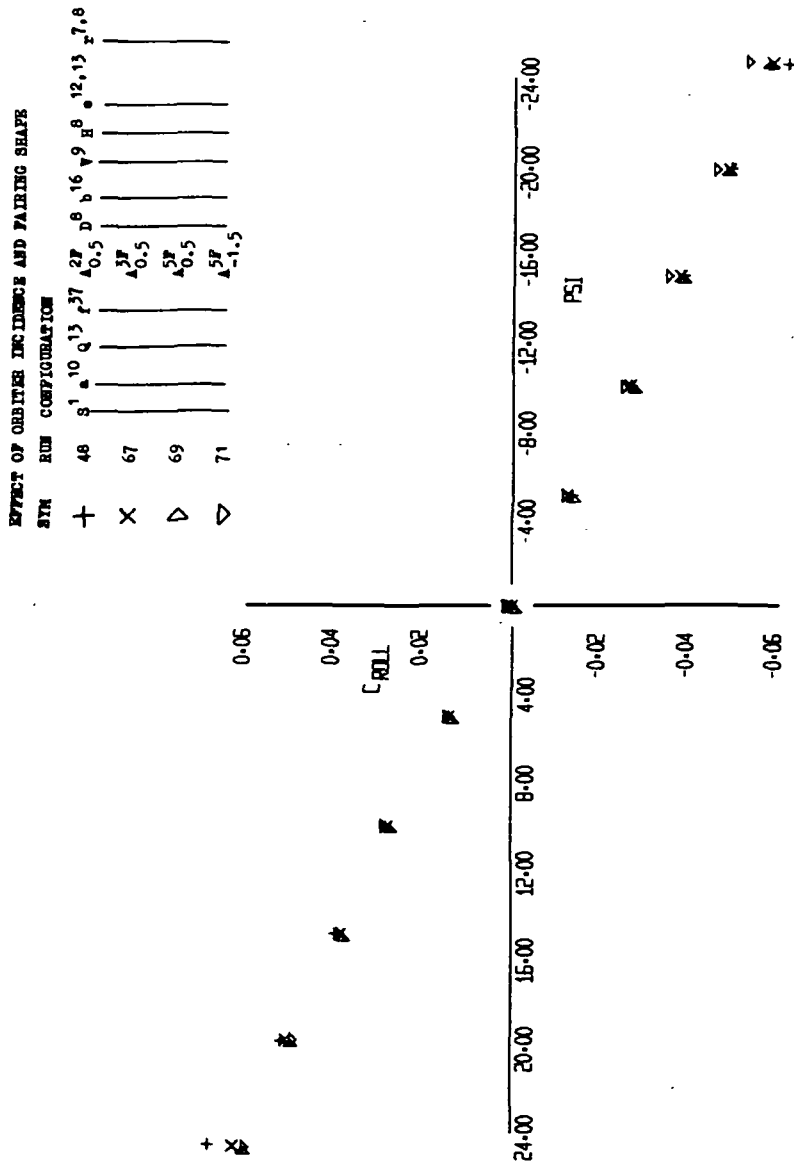


FIGURE 21 (SHEET 2)

⊕ ⊙ ⊗ ⊚
 + x D v

10-15-73

11-48

EFFECT OF ORBITER INCIDENCE AND PAIRING SHAPS

SYM RUN CONFIGURATION

+	48	S ¹	a ¹⁰	q ¹³	r ¹⁷	2P	a ^{0.5}	b ^{0.5}	8	16	v ⁹	8	12	13	7.8
x	67														
▷	69														
▽	71														

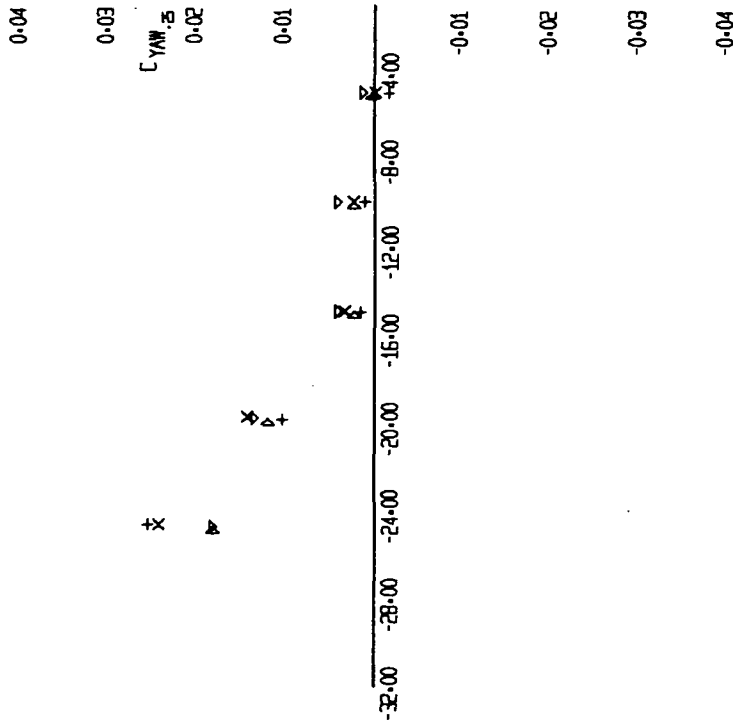


FIGURE 21 (SHEET 3)

21
 48
 67
 +

15-15-73

14-40

EFFECT OF ORDER INCIDENCE AND PAIRING SHAPE

SYM	RUN	CONFIGURATION
+	48	S ¹ a ¹⁰ q ¹³ p ³⁷ 2P ^{0.5} D ⁸ b ¹⁶ v ⁹ R ⁸ 12,13 z ^{7,8}
x	67	3P ^{0.5}
▷	69	5P ^{0.5}
▽	71	5P ^{0.5}

⊗ ⊙ ⊗ ⊗
+ x x +

10-15-73

17-6

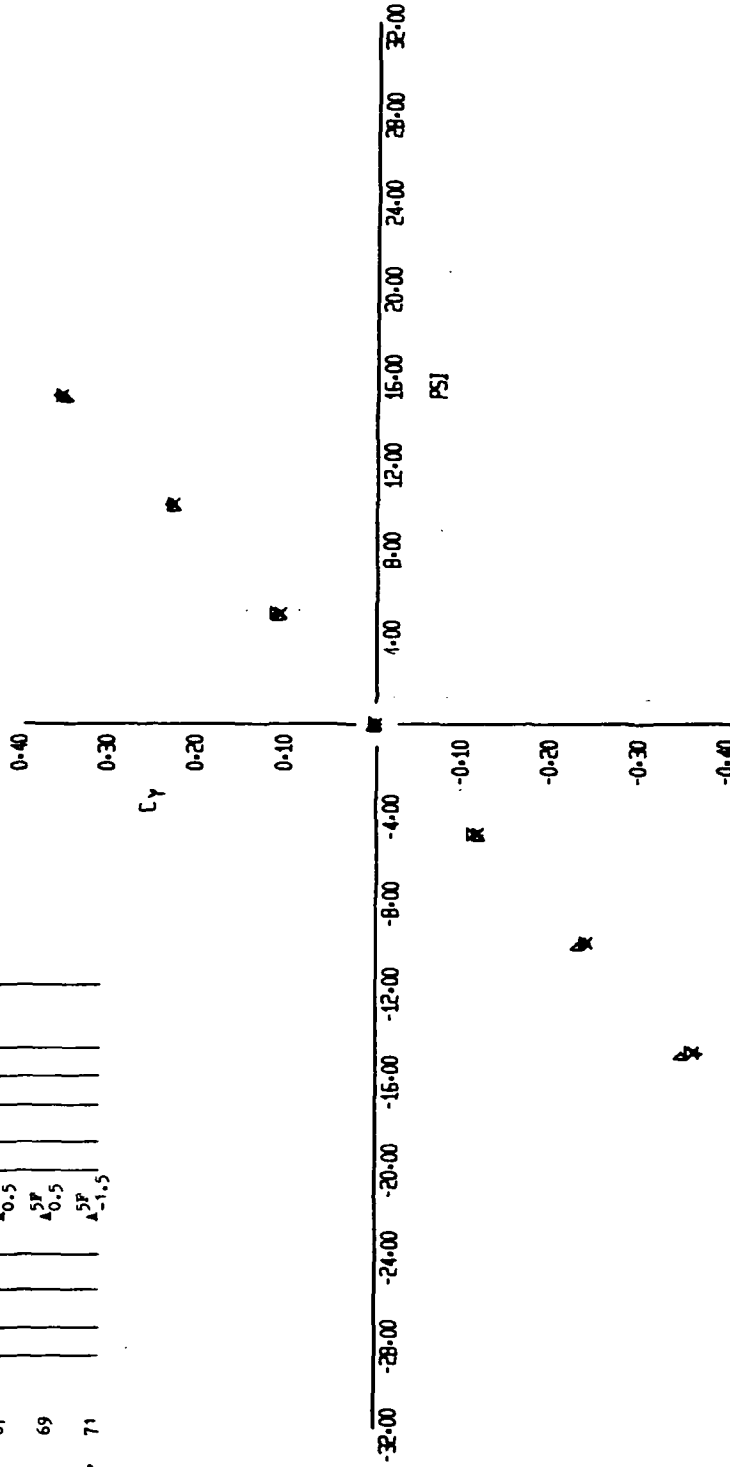


FIGURE 21 (SHEET 4)

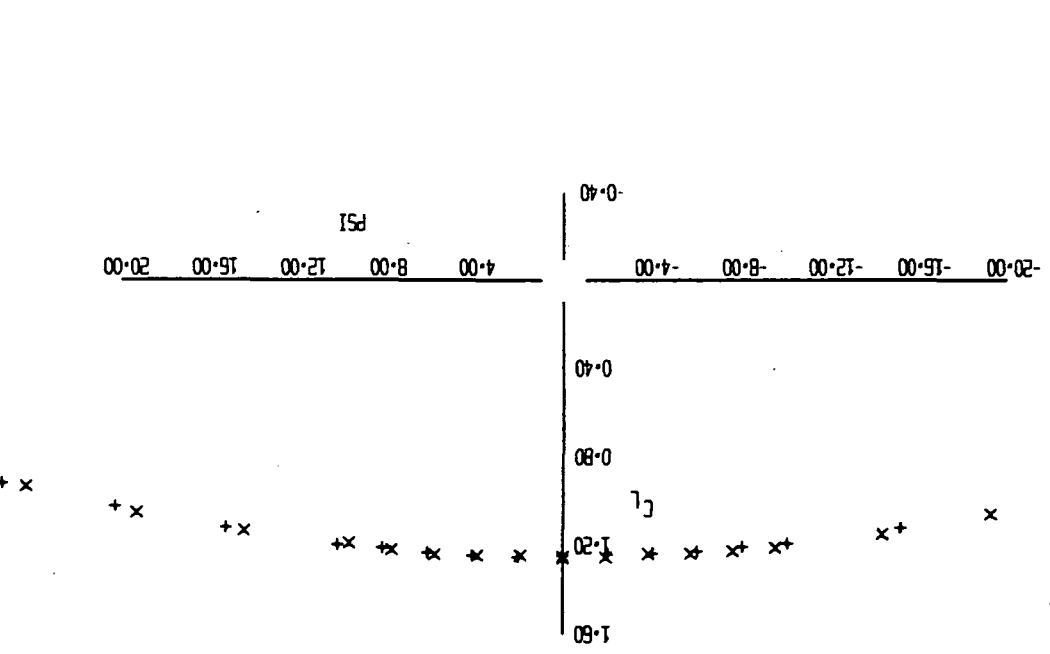
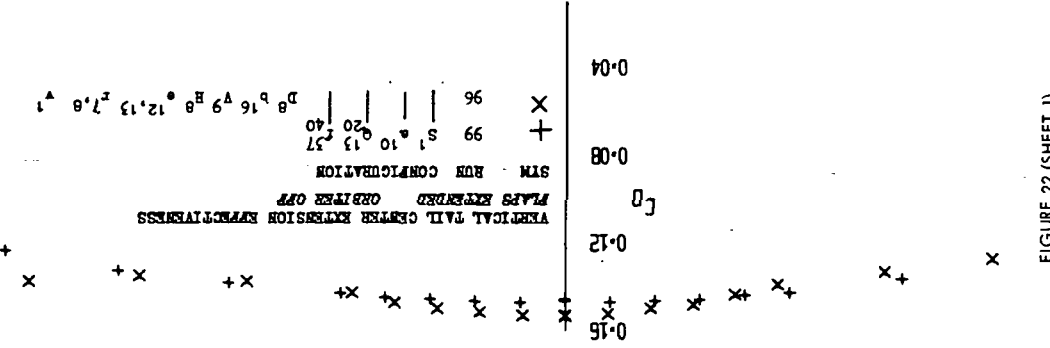
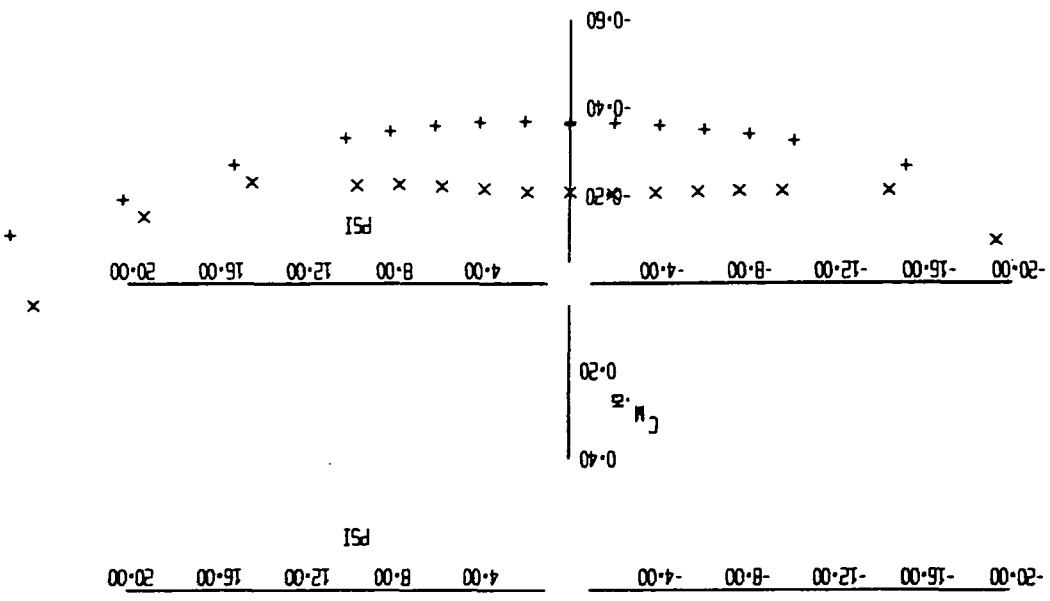


FIGURE 22 (SHEET 1)

10-15-73

(9-41)

X +
96 99

VERTICAL TAIL CENTER EXTENSION EFFECTIVENESS

FLAPS EXTENDED ORBITER OFF

SYM RUN CONFIGURATION

+ 99 S¹ A¹⁰ Q¹³ F²⁷

X 96 | | | D⁶ V¹⁶ P⁹ E^{12,13} T^{7,8} V¹

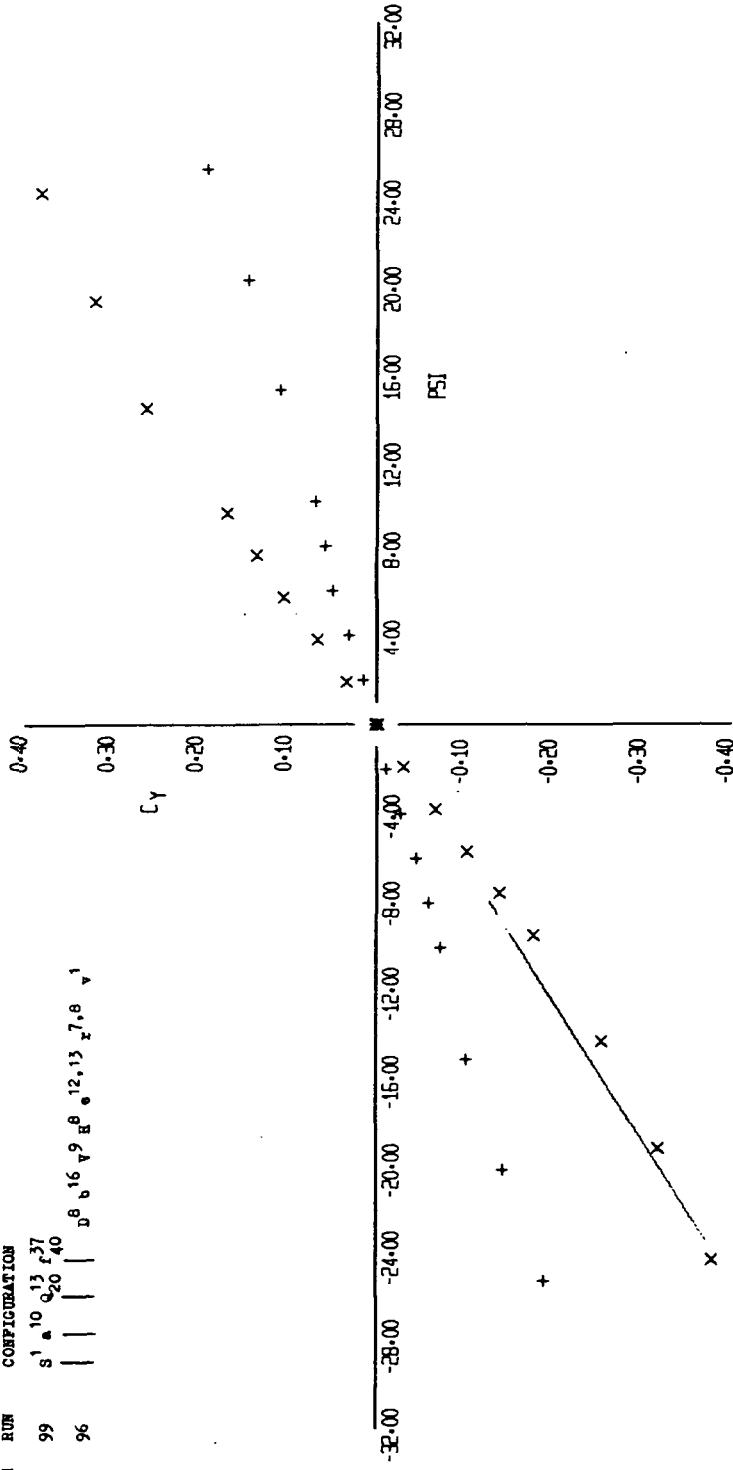


FIGURE 22 (SHEET 4)

81 98

+ X

10-15-73

17-6E

VERTICAL TAIL CENTER EXTENSION EFFECTIVENESS
FLAPS EXTENDED ORBITER OF

STN	RUN	CONFIGURATION
+	87	S ¹ 10 13 27 5P
X	85	20 40 0.5

D⁸ 16 9 H⁸ 12, 13 7, 8 1

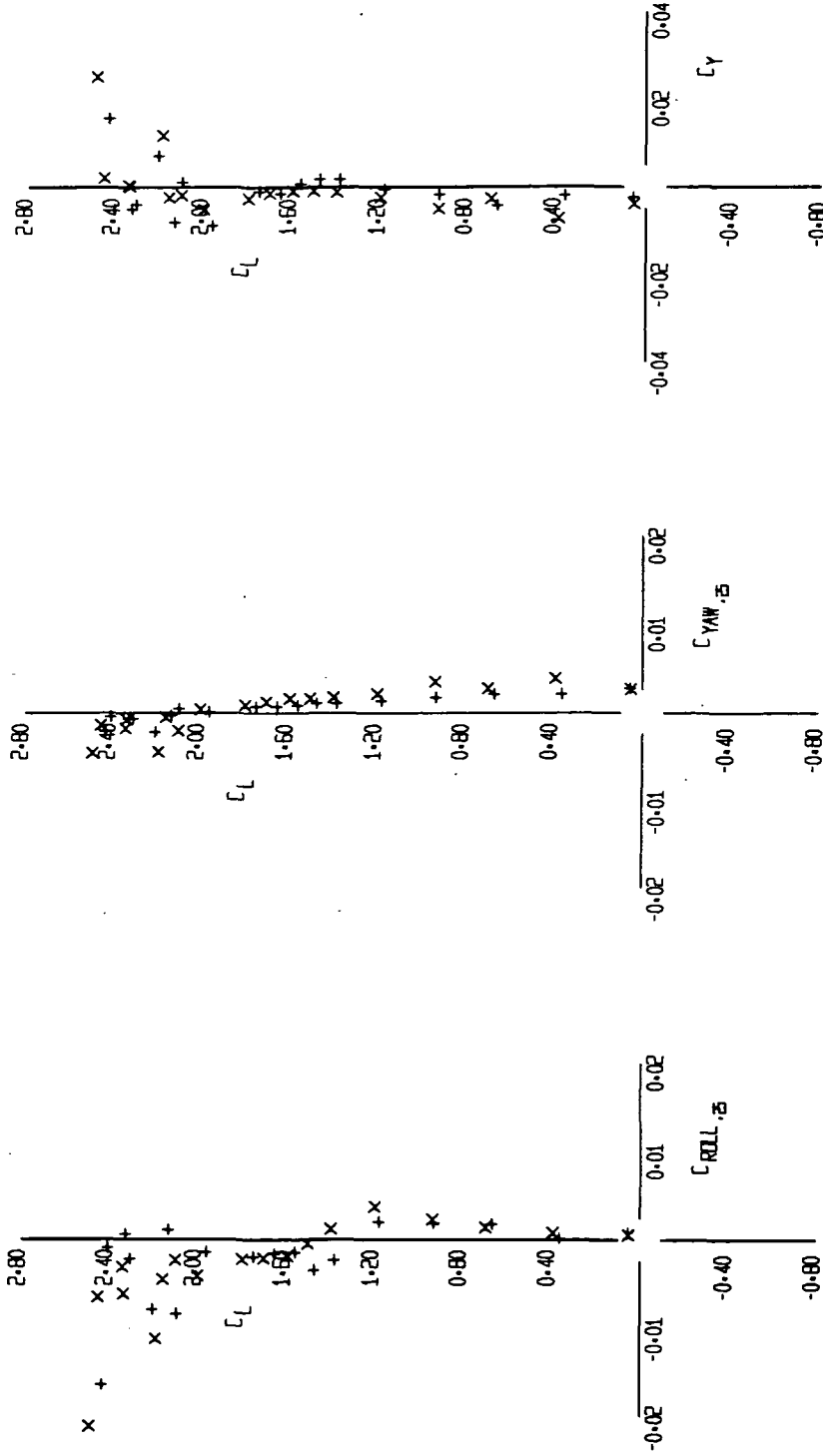


FIGURE 23 (SHEET 1)

SB
+ X

15-72

UP-33

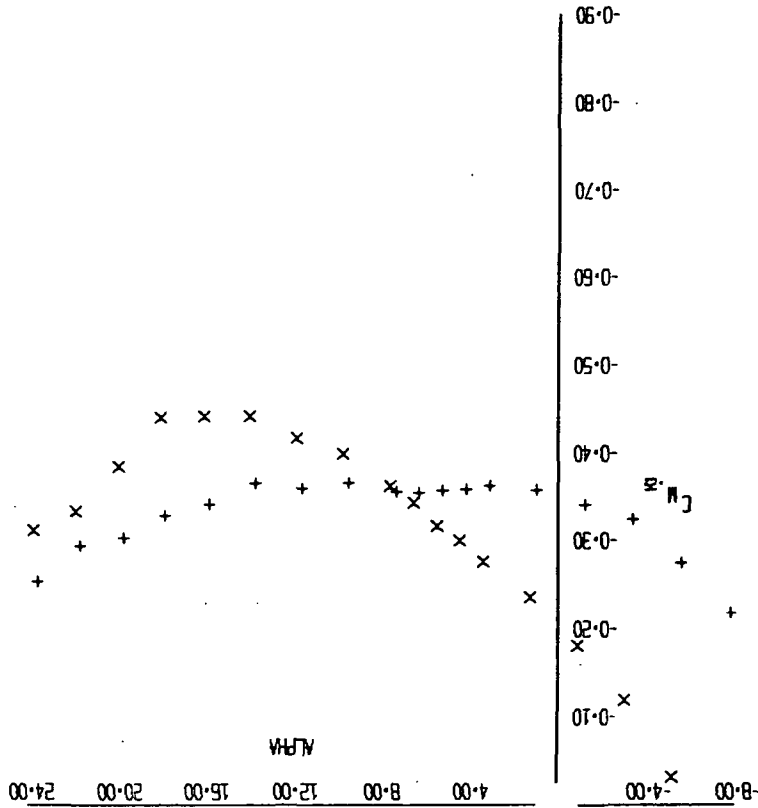


FIGURE 23 (SHEET 2)

VERTICAL TAIL CENTER EXTENSION EFFICIENCIES
 FLAPS EXTENDED ORBITER ON
 STM RUB CONFIGURATION

Symbol	Value
x	85
+	87
	10
	13
	17
	20
	27
	40
	52
	0.5
	16
	19
	28
	12, 13
	7, 8
	1

10-15-73

x +
85 87

LR-101

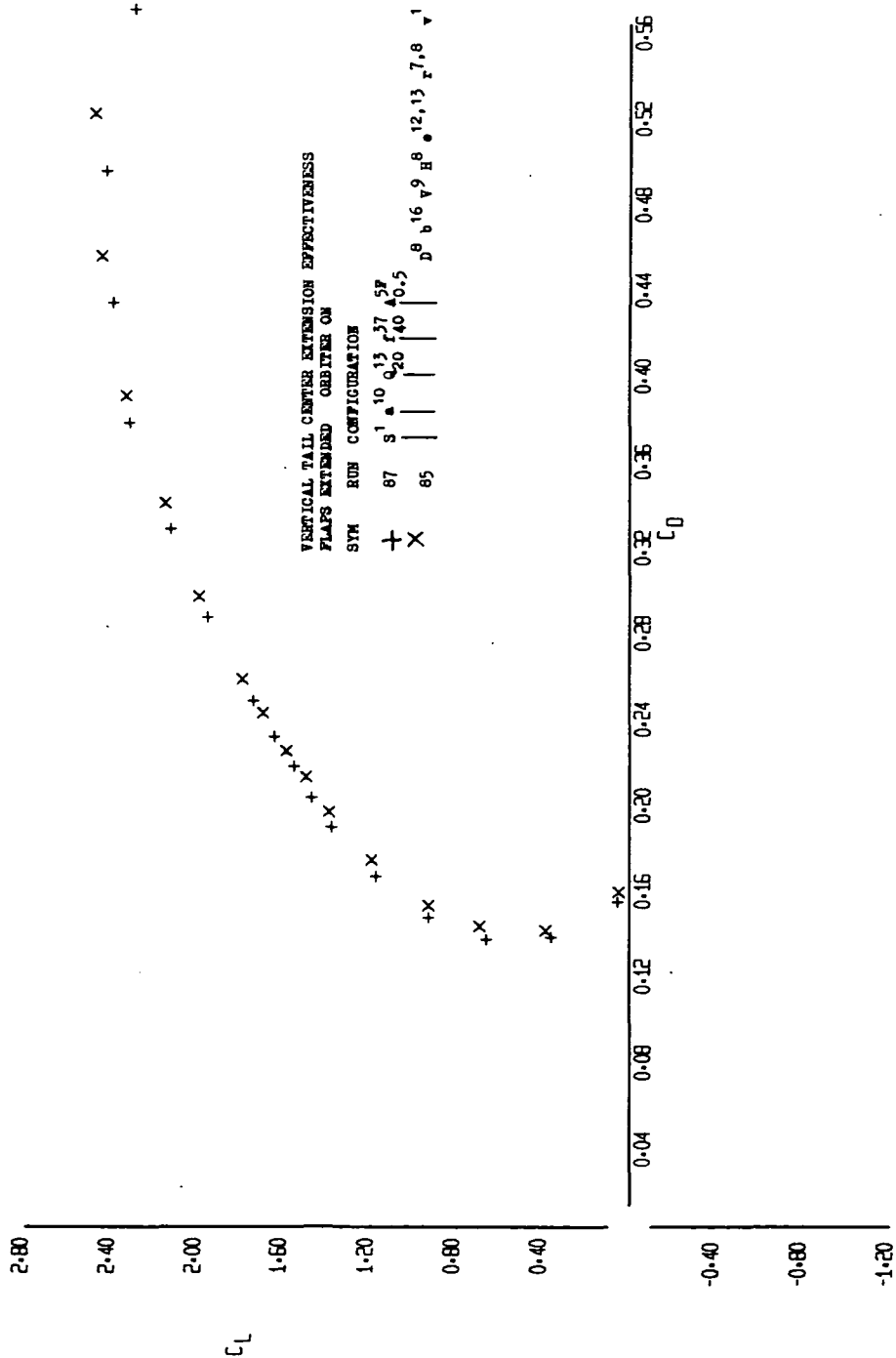


FIGURE 23 (SHEET 3)

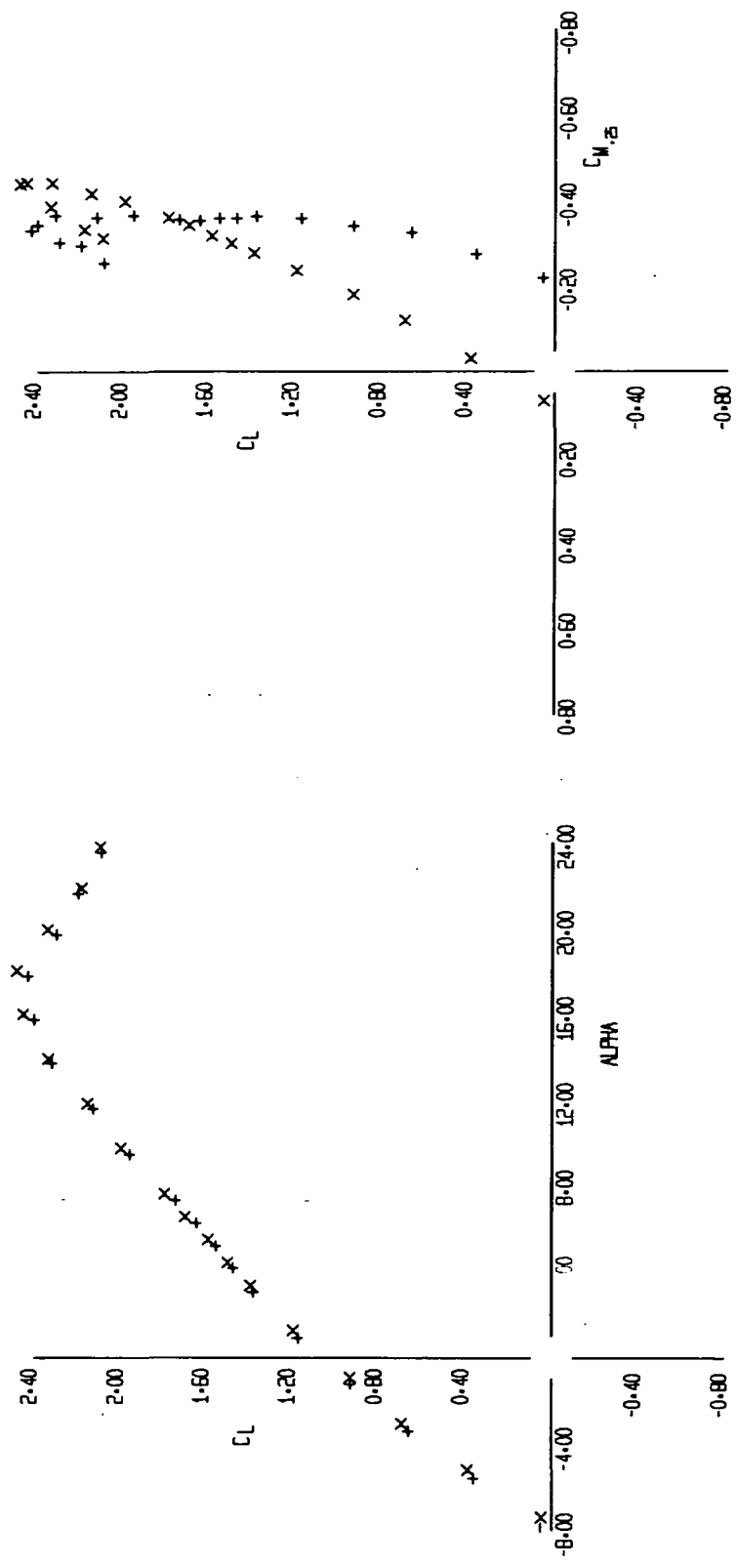
VERTICAL TAIL CENTER EXTENSION EFFECTIVENESS

FLAPS EXTENDED ORBITER CM

SYM RUN CONFIGURATION

+	87	S ¹	a ¹⁰	r ¹³	f ³⁷	SP
X	85		a ²⁰	r ⁴⁰	f ^{40.5}	

D⁸ b¹⁶ v⁹ B⁶ 12,13 z^{7.8} v¹



B B
 + X

10-15-73

LR-18

FIGURE 23 (SHEET 4)

EFFECT OF PAIRING SHAPS AND ORBITER LOCATION

SYM	RUB	CONFIGURATION												
		S ¹	A ¹⁰	Q ¹³	r ³⁷	2C _{0.5}	D ⁸	b ¹⁶	p ⁹	B ⁸	12,13	r ^{7,8}		
+	50													
X	54													
▷	48													
▽	56													

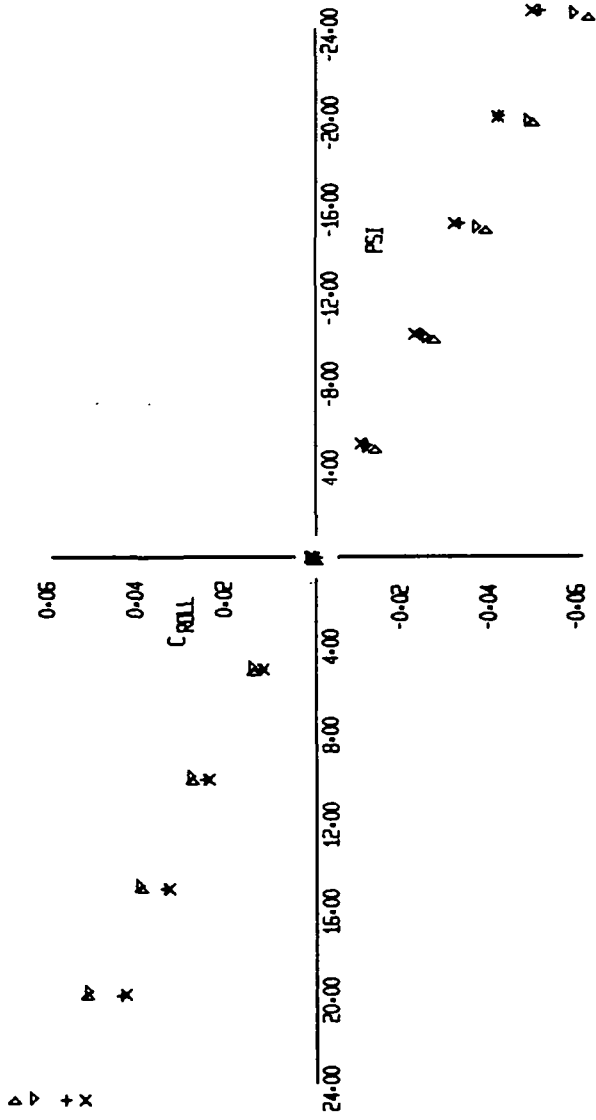


FIGURE 24 (SHEET 2)

OR X X X
+ X X X

10-15-73

LR-11-1

EFFECT OF PAIRING SHAPE AND ORBITER LOCATION

SIM	RUN	CONFIGURATION
+	50	S ¹ a ¹⁰ q ¹³ r ²⁷ A ²⁰ b ¹⁶ v ⁹ H ^{12,13} z ^{7,8}
X	54	A ¹⁰ 0.5
▷	48	A ^{2P} 0.5
▽	56	A ^{1P} 0.5

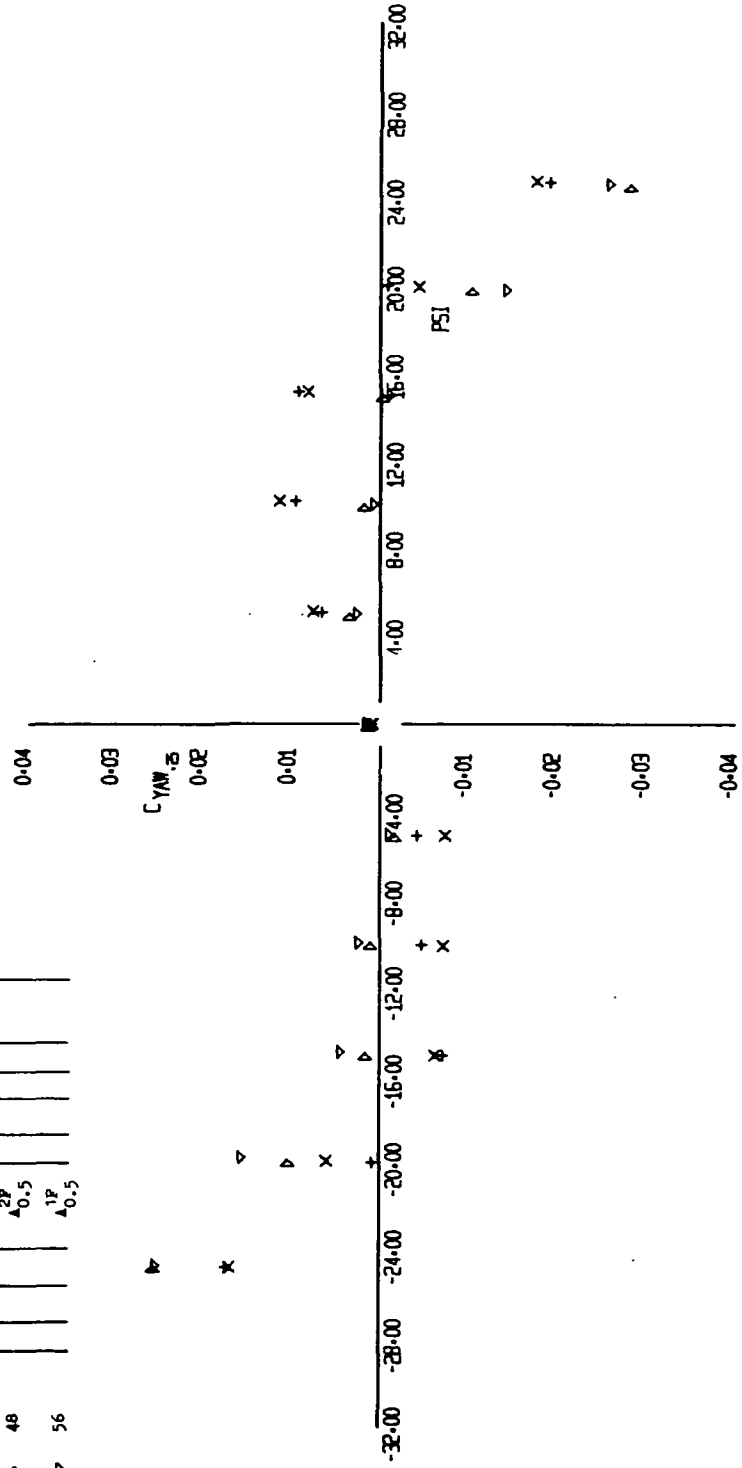


FIGURE 24 (SHEET 3)

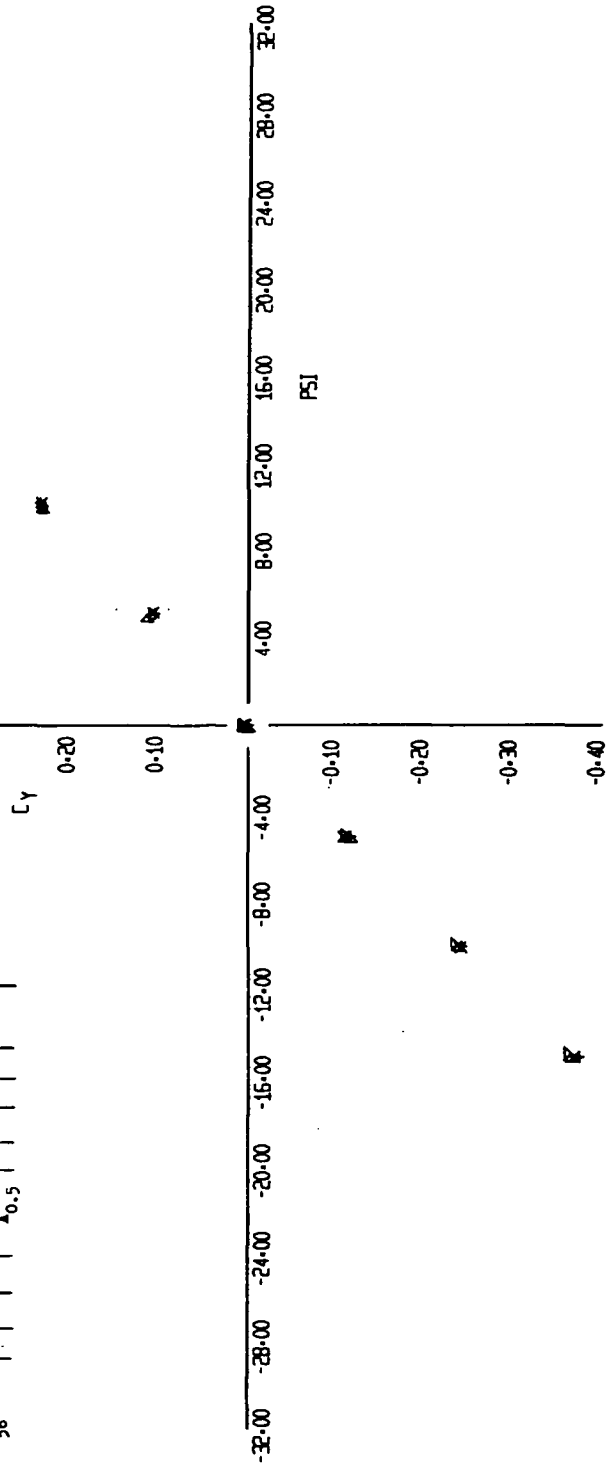
SI 50 54
+ X ▷ ▽

10-15-73

10-4-40

EFFECT OF PAIRING SHAPE AND ORBITER LOCATION

SYM	RUN	CONFIGURATION
+	50	S ¹ a ¹⁰ q ¹³ r ²⁷ A ²⁰ D ⁸ b ¹⁶ v ⁹ B ⁸ 12,13 7,8
X	54	A ¹⁰ 0.5
D	48	A ^{2P} 0.5
▽	56	A ^{1P} 0.5

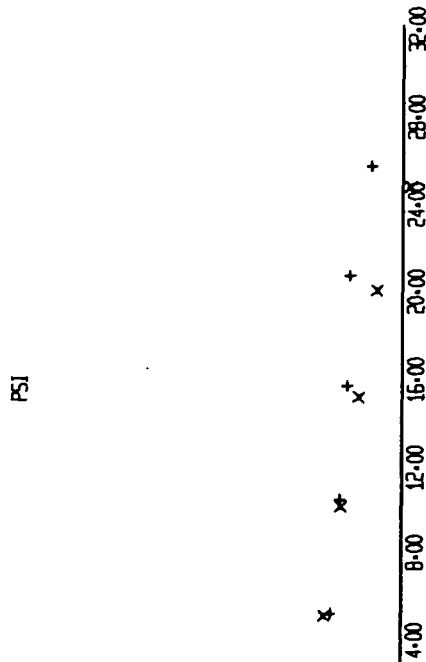
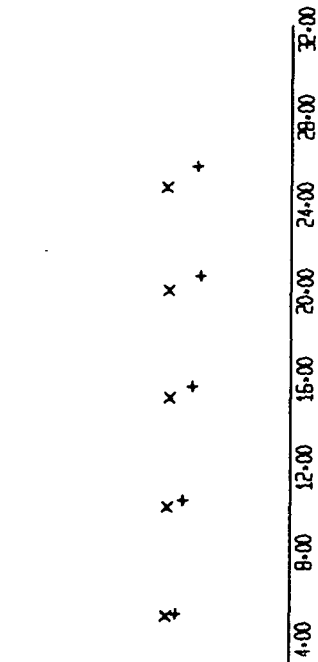


8 8 8 8
+ X 1 ▽

12-15-73

11-6E

FIGURE 24 (SHEET 4)



EFFECT OF ORBITER
 TAIL ON AND TAIL OFF

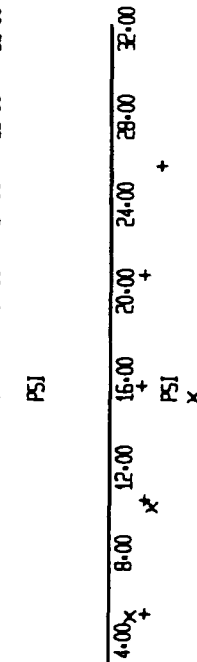
SYM RUN CONFIGURATION

+ 44 S¹ 10¹³ P³⁷ 2P²
 A_{0.5}

x 48 D⁸ b¹⁶ v⁹ H⁸ e^{12,13} r^{7,8}

LR-51

3 9
 + x



LR-61

FIGURE 25 (SHEET 1)

Effect of Orbiter
Tail On and Tail Off

SYM	RUN	CONFIGURATION
+	44	S ¹ A ¹⁰ Q ¹³ r ²⁷ Δ ^{2F}
X	46	D ⁸ b ¹⁶ v ⁹ H ⁸ • 12,13 r ^{7,8}

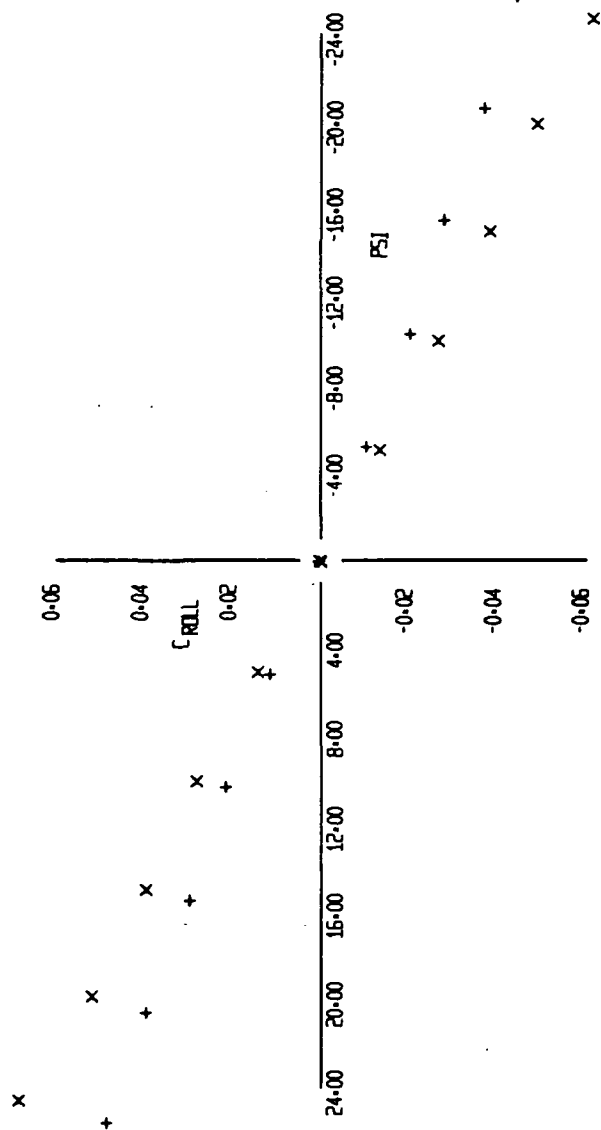


FIGURE 25 (SHEET 2)

12-15-73

LY-48

EFFECT OF ORBITER
TAIL ON AED TAIL OFF

SYM RUN CONFIGURATION

+ 44 S¹ a¹⁰ q¹³ r³⁷ z^{2P}
X 48 D⁸ b¹⁶ v⁹ H⁸ e^{12,13} z^{7,8}

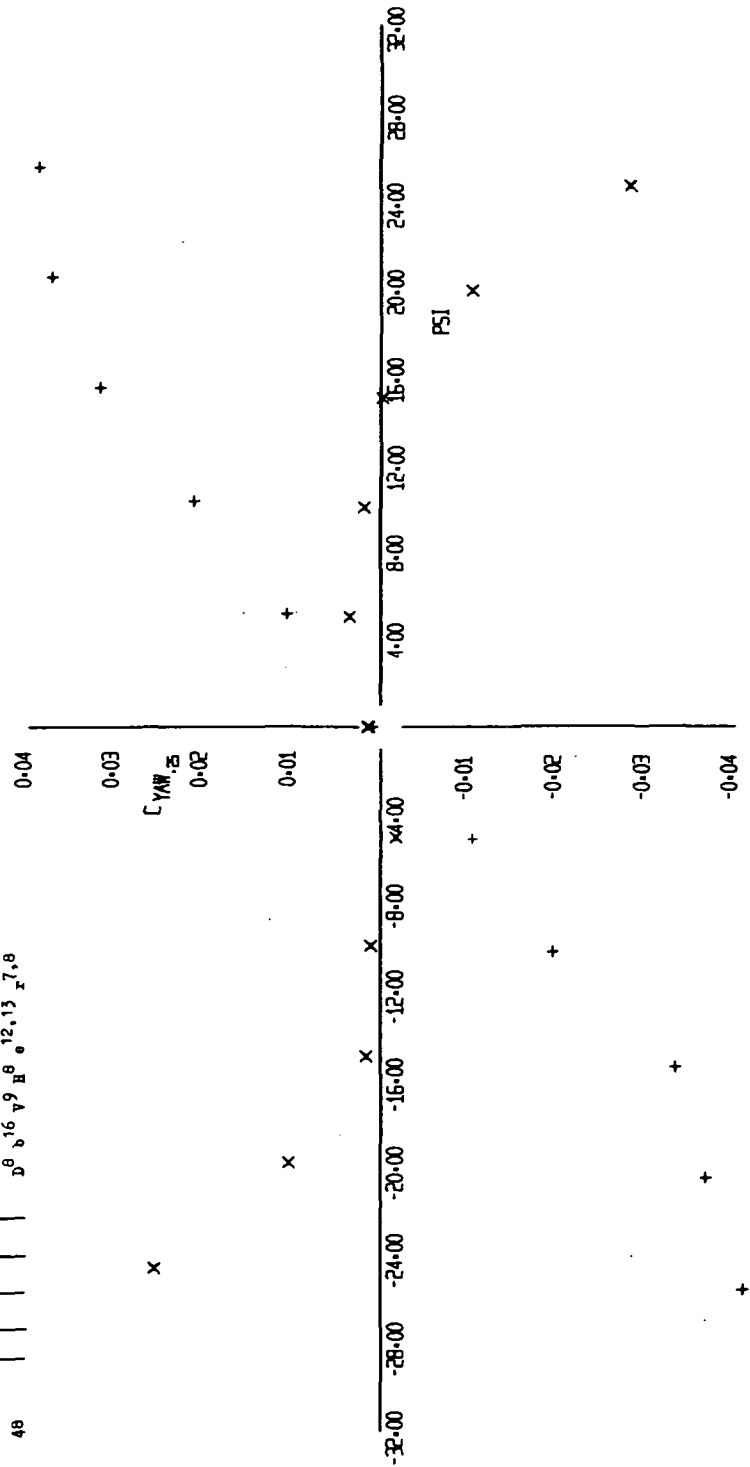


FIGURE 25 (SHEET 3)

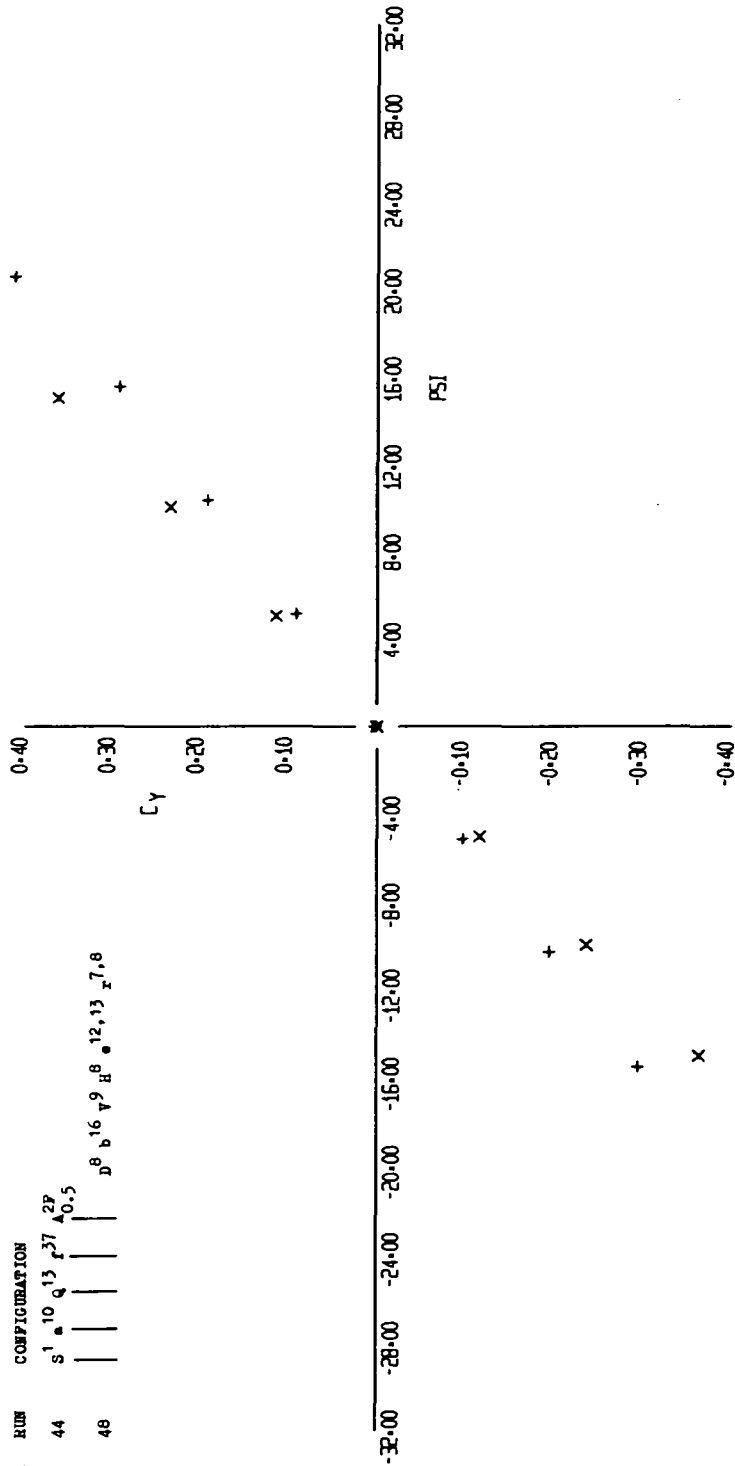
3 8
+ X

EZ-51-01

(14-40)

+

X



EFFECT OF ORBITER
TAIL ON AND TAIL OFF

SYM RUN CONFIGURATION

44 s¹ 10 13 37 2P
X 46 b⁸ v⁹ 8 12,13 7,8

CY

PSI

3 8
+ X

12-15-73

17-11

FIGURE 25 (SHEET 4)

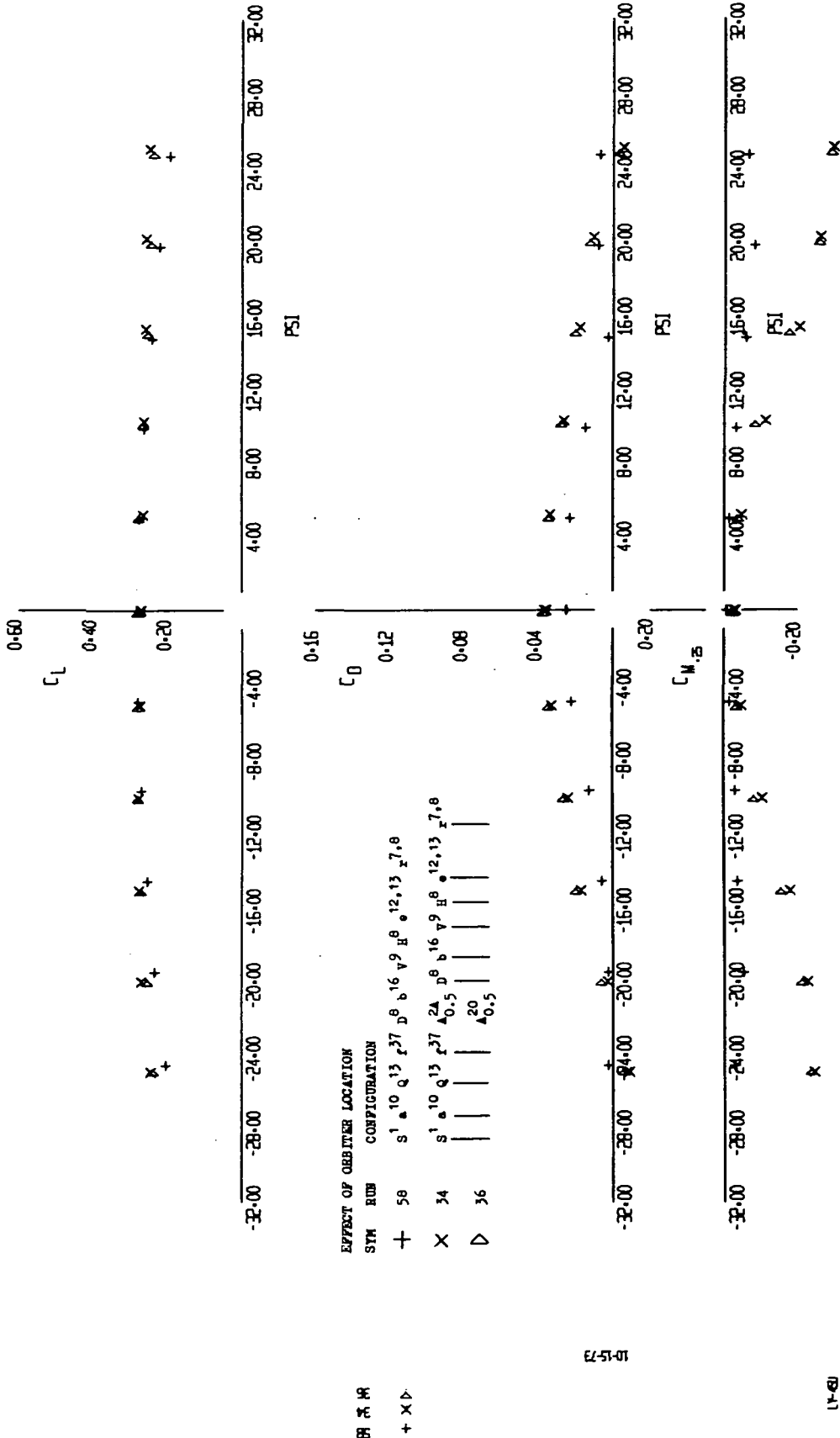


FIGURE 26 (SHEET 1)

EFFECT OF ORBITER LOCATION

SYM	RUN	CONFIGURATION
+	58	S ¹ a ¹⁰ Q ¹³ r ²⁷ D ⁸ b ¹⁶ v ⁹ B ⁸ a ^{12,13} r ^{7,8}
X	34	S ¹ a ¹⁰ Q ¹³ r ²⁷ A ^{0,5} D ⁸ b ¹⁶ v ⁹ B ⁸ a ^{12,13} r ^{7,8}
D	36	A ^{0,5} D ⁸ b ¹⁶ v ⁹ B ⁸ a ^{12,13} r ^{7,8}

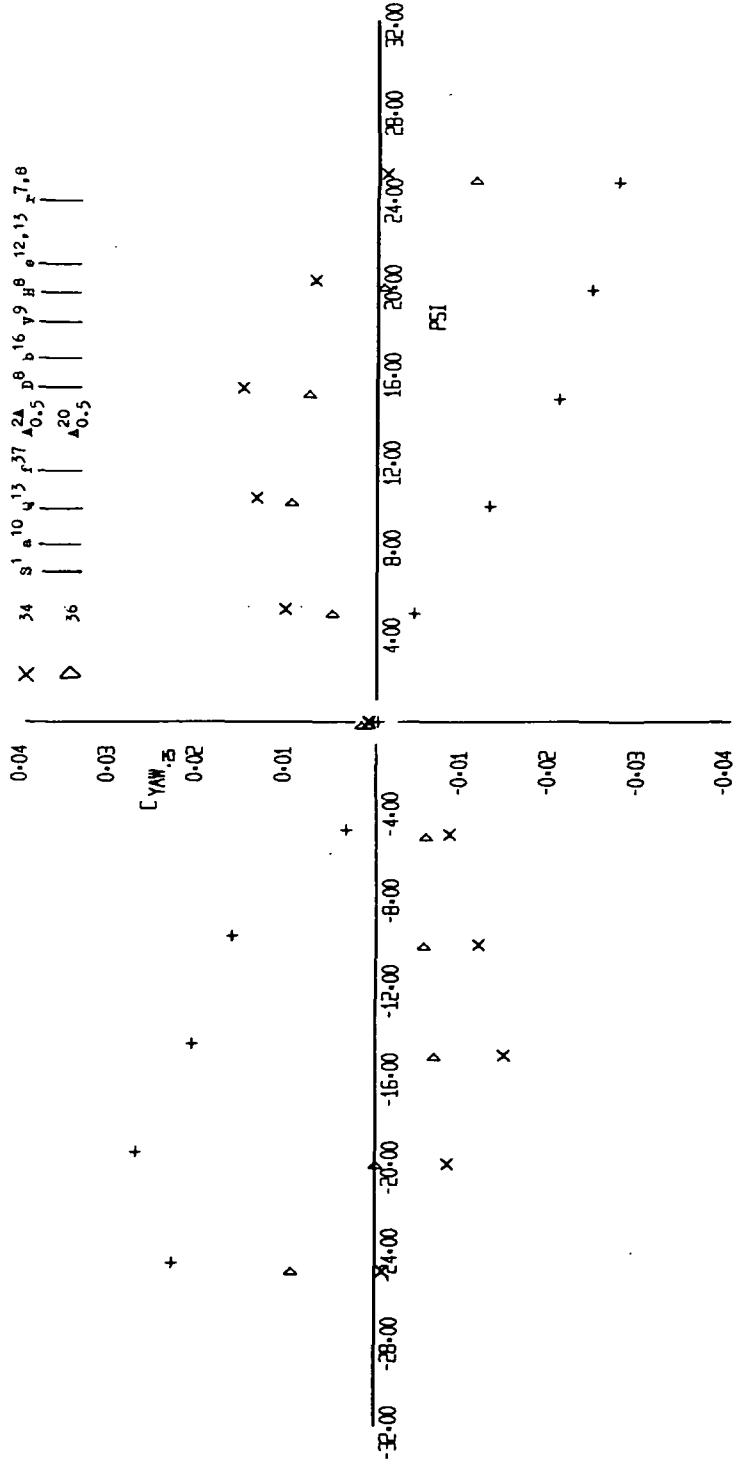


FIGURE 26 (SHEET 3)

PSI
 + X D

10-15-73

11-40

EFFECT OF ORBITER LOCATION

SYM	RUN	CONFIGURATION
+	58	$s^1 a^{10} q^{13} r^{37} d^8 b^{16} v^9 H^8 e^{12,13} z^{7,8}$
X	34	$s^1 a^{10} q^{13} r^{37} A_{0.5}^{24} d^8 b^{16} v^9 H^8 e^{12,13} z^{7,8}$
D	36	$A_{0.5}^{20}$

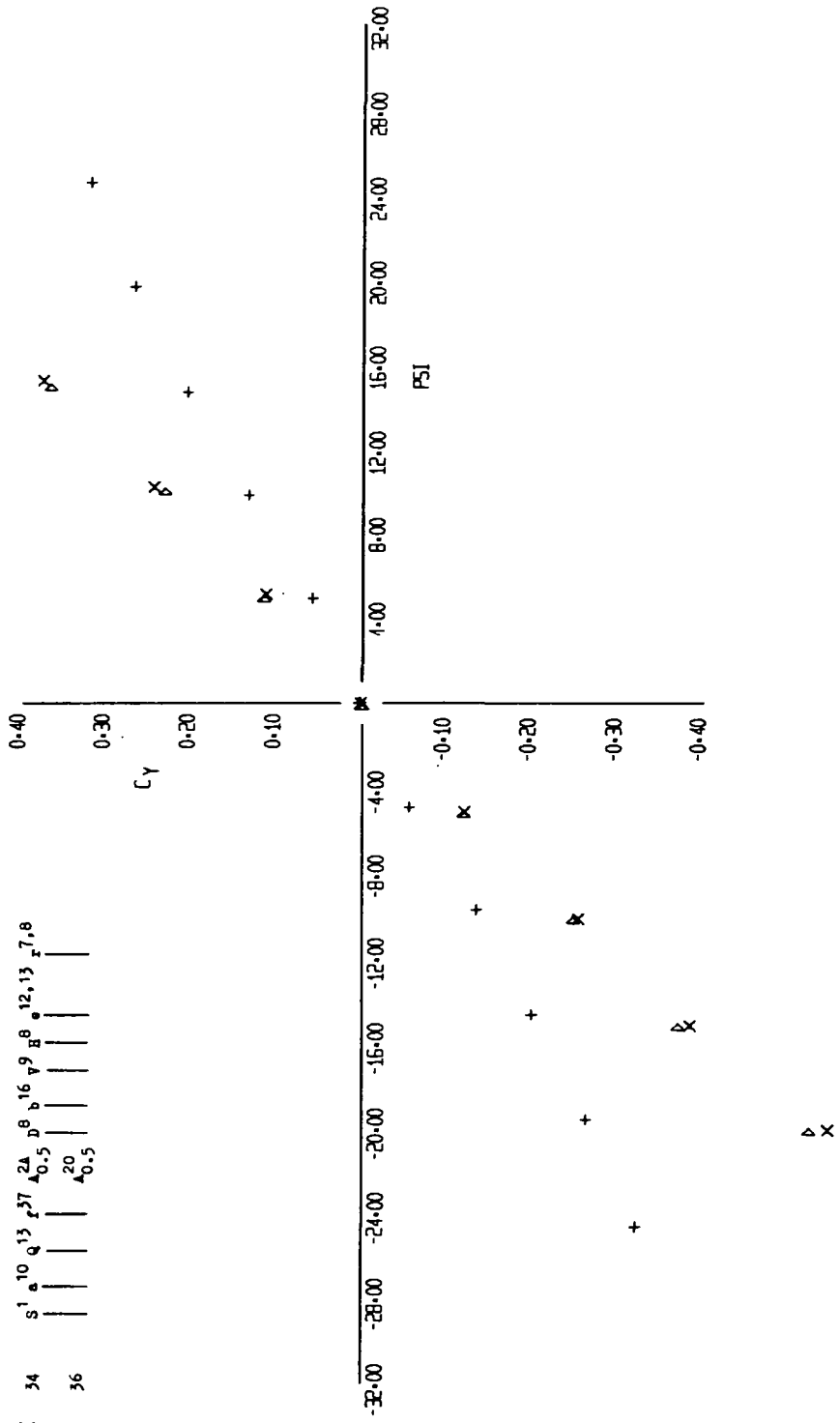


FIGURE 26 (SHEET 4)

LR-363
+ X D

10-15-73

LR-363

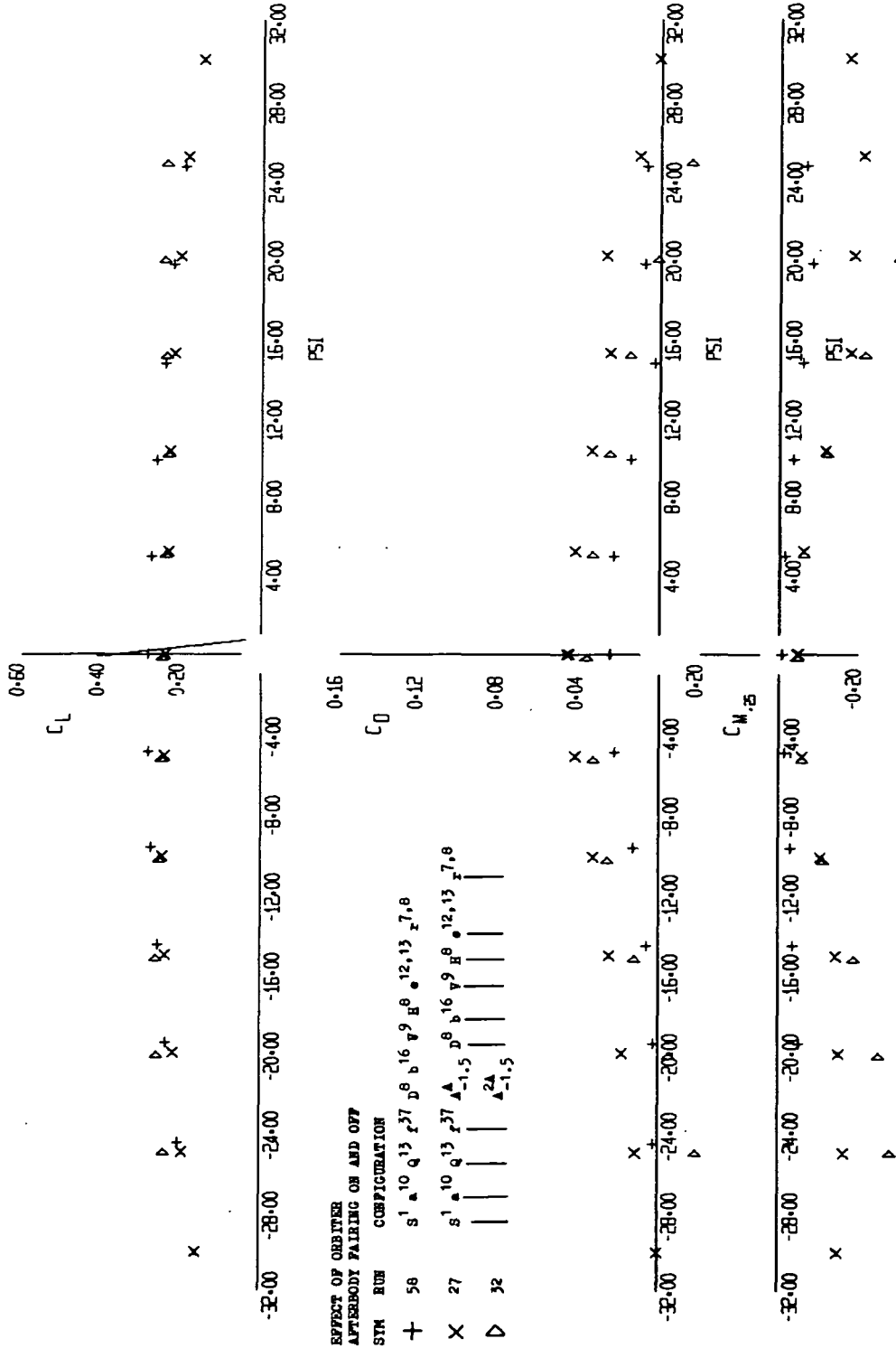


FIGURE 27 (SHEET 1)

EFFECT OF ORBITER
AFTERBODY PAIRING ON AND OFF
SYN RUN CONFIGURATION

+	58	S ¹ a ¹⁰ q ¹³ r ²⁷ D ⁸ b ¹⁶ v ⁹ H ⁸ 12,13 7,8
X	27	S ¹ a ¹⁰ q ¹³ r ²⁷ A ^{1,5} D ⁸ b ¹⁶ v ⁹ H ⁸ 12,13 7,8
▷	32	A ^{2A} A ^{-1,5}

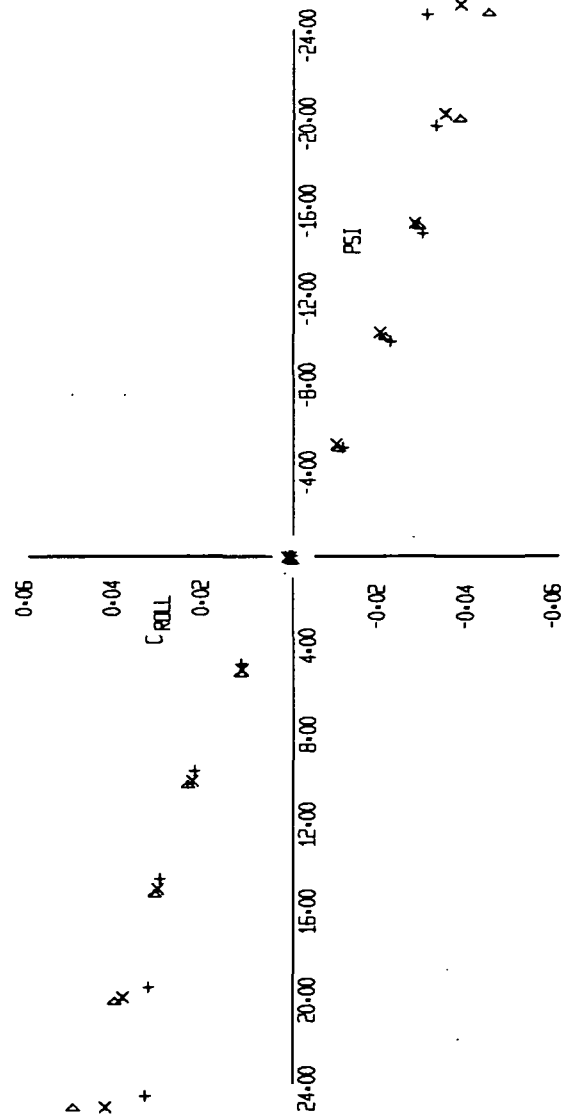


FIGURE 27 (SHEET 2)

B+ B+
+ X ▷

10-15-73

L1-08

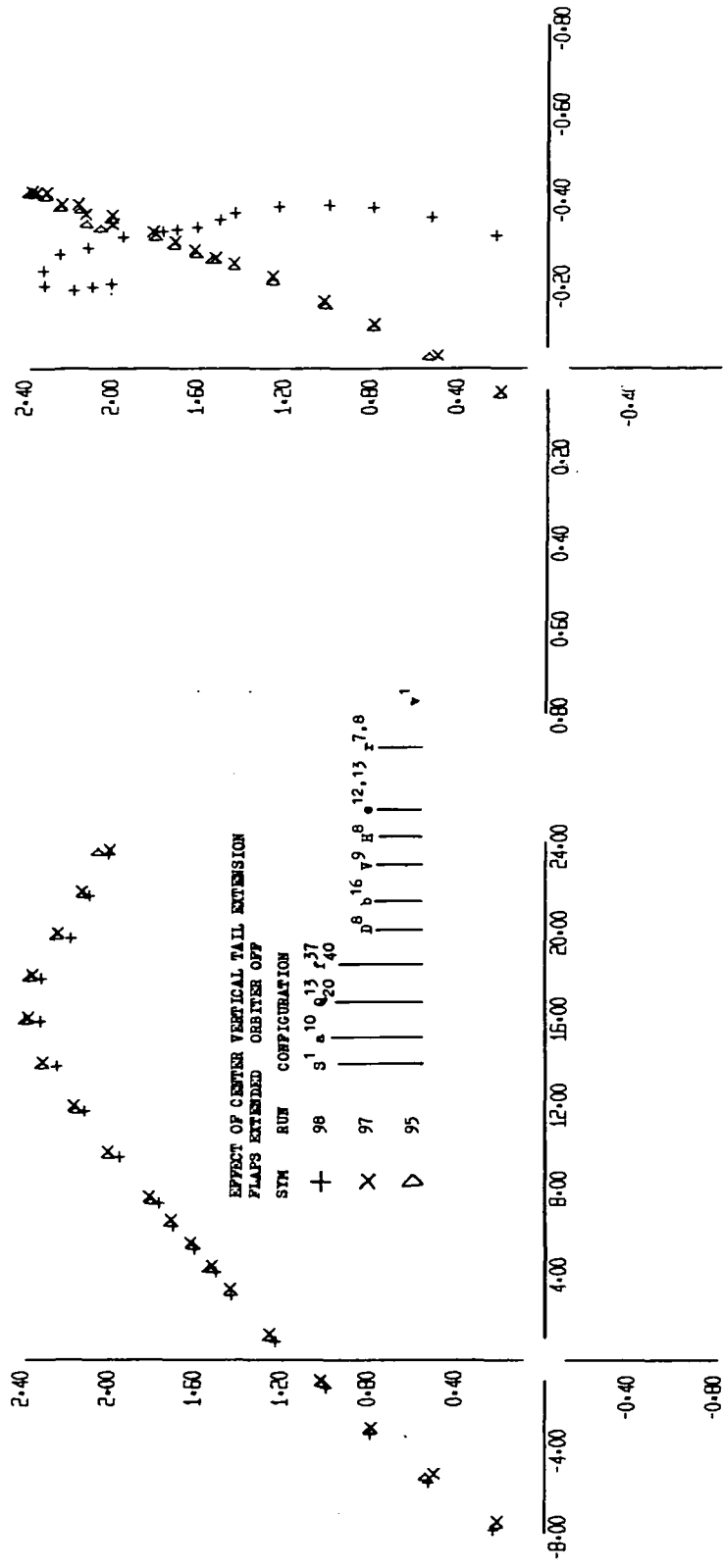


FIGURE 28 (SHEET 1)

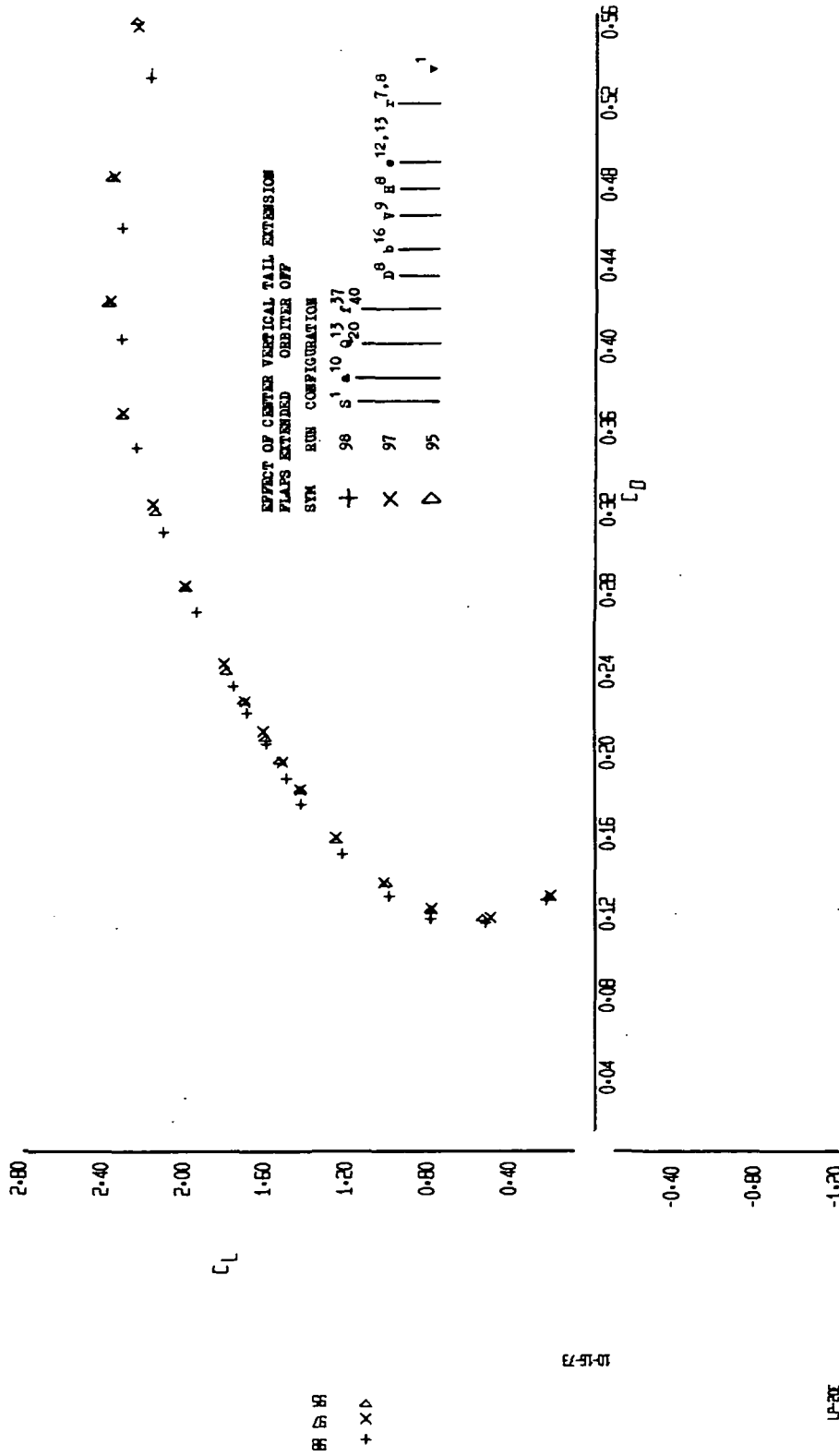


FIGURE 28 (SHEET 2)

EFFECT OF CENTER VERTICAL TAIL EXTENSION
 FLAPS EXTENDED ORBITER OFF

SYM RUN CONFIGURATION

+	96	S	1	a	10	13	r	37
X	97				20	40		
Δ	95				b	8	a	9
								12,13
								r, 7, 8

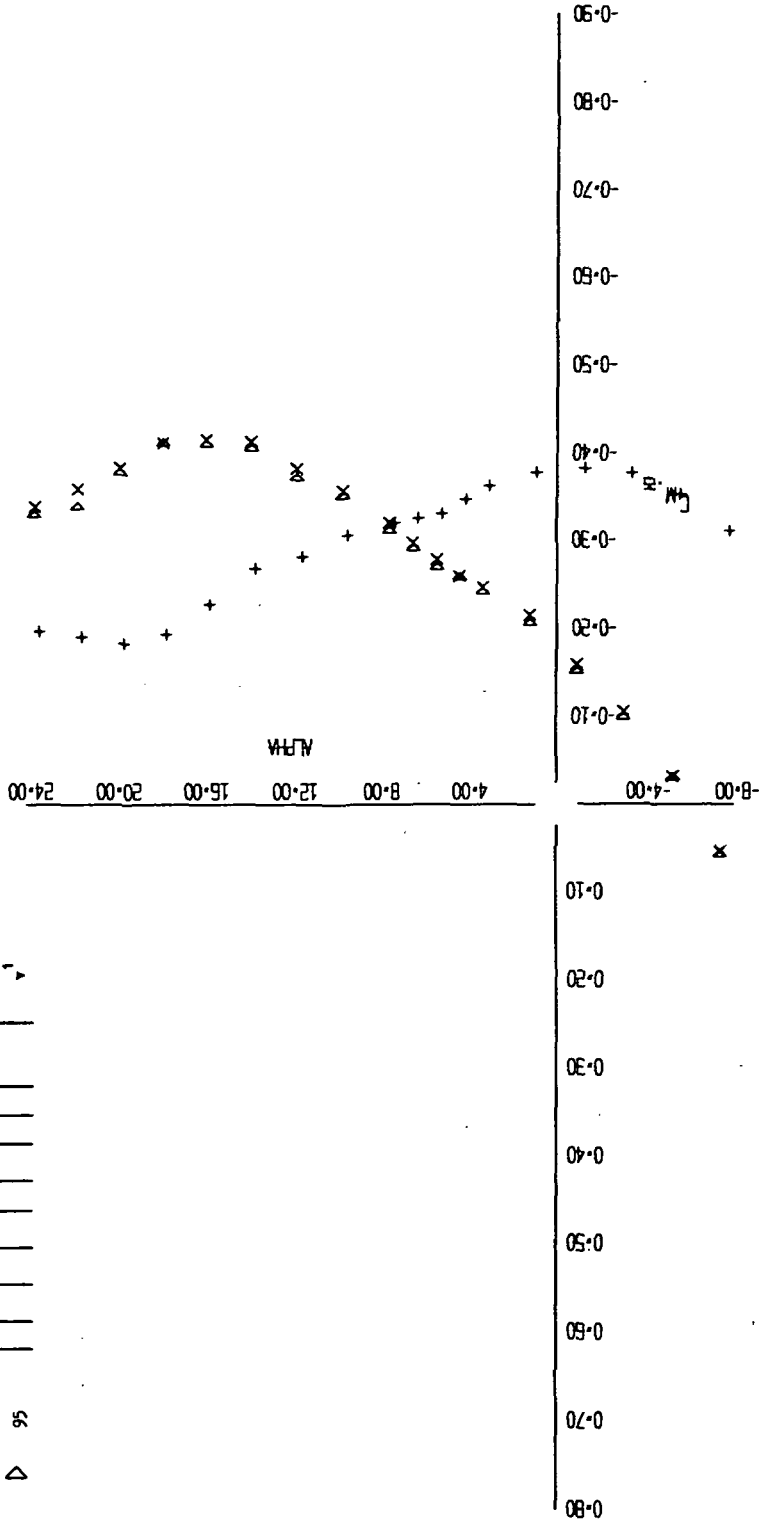


FIGURE 28 (SHEET 3)

96
 97
 +

10-15-73

LP-101

EFFECT OF CENTER VERTICAL TAIL EXTENSION
 FLAPS EXTENDED GEOMETRIC OFF
 SYN RUN CONFIGURATION

SYN	RUN	CONFIGURATION
+	98	S ¹ a ¹⁰ Q ¹³ f ³⁷
X	97	1.20 1.40
Δ	95	1.6 1.6 9 1.6 12.13 7.8

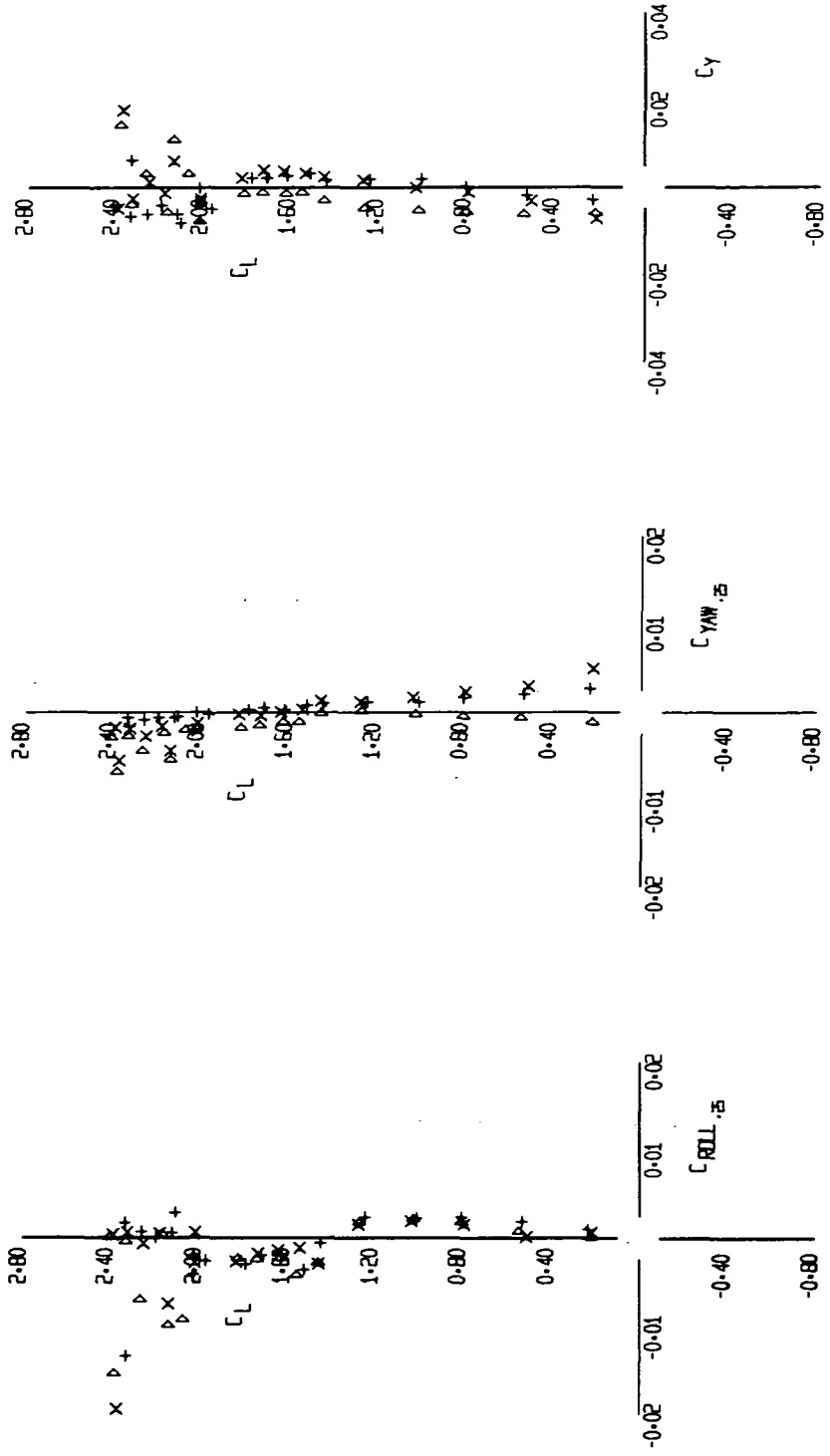


FIGURE 28 (SHEET 4)

BR BR BR
 + X Δ

10-15-73

LF-38

EFFECT OF CENTER VERTICAL TAIL EXTENSION
FLAPS RETRACTED ORBITER OFF

SYM	RUN	CONFIGURATION
+	58	s ¹ a ¹⁰ q ¹³ r ¹⁷ b ¹⁶ v ⁹ h ⁸ 12,13 z ^{7,8}
x	101	v ¹

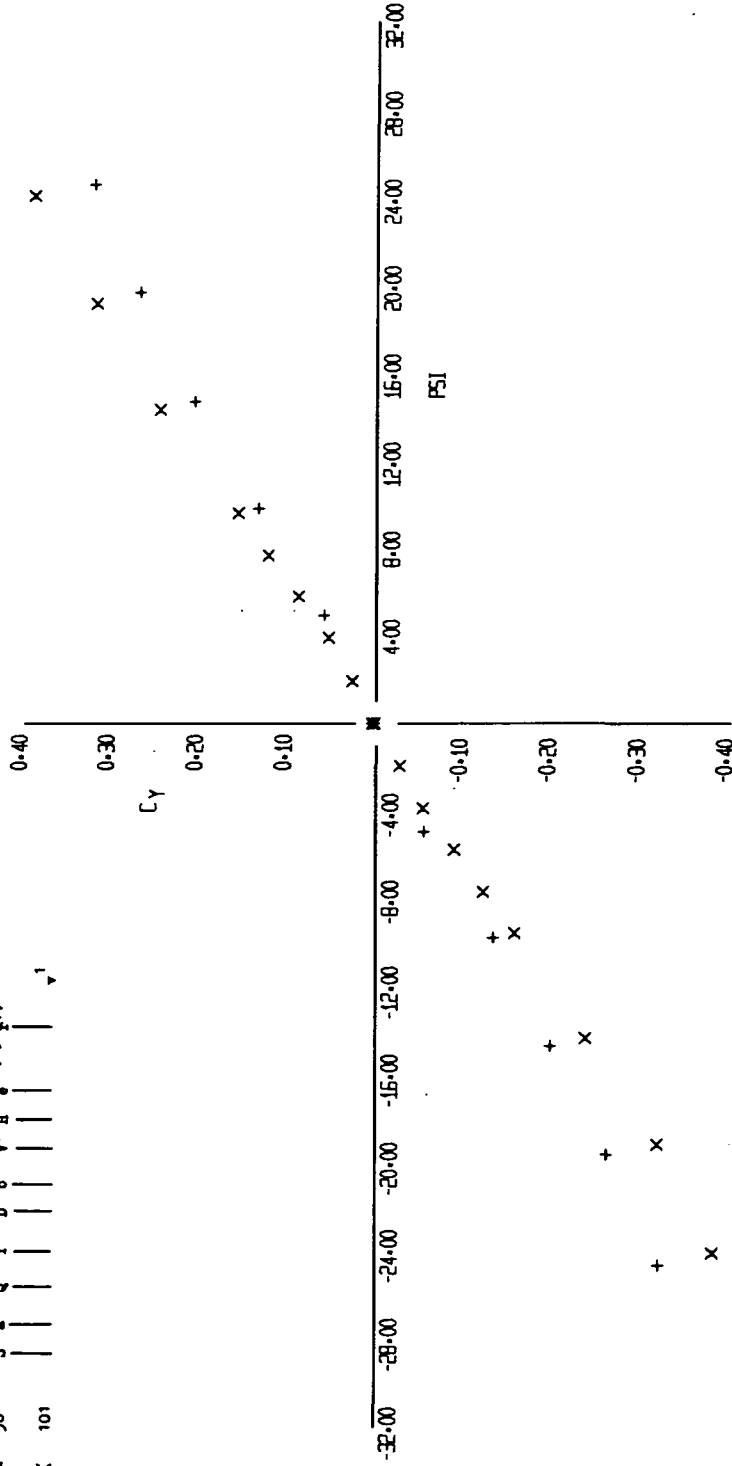


FIGURE 29 (SHEET 1)

88 5
+ x

10-15-73

10-11

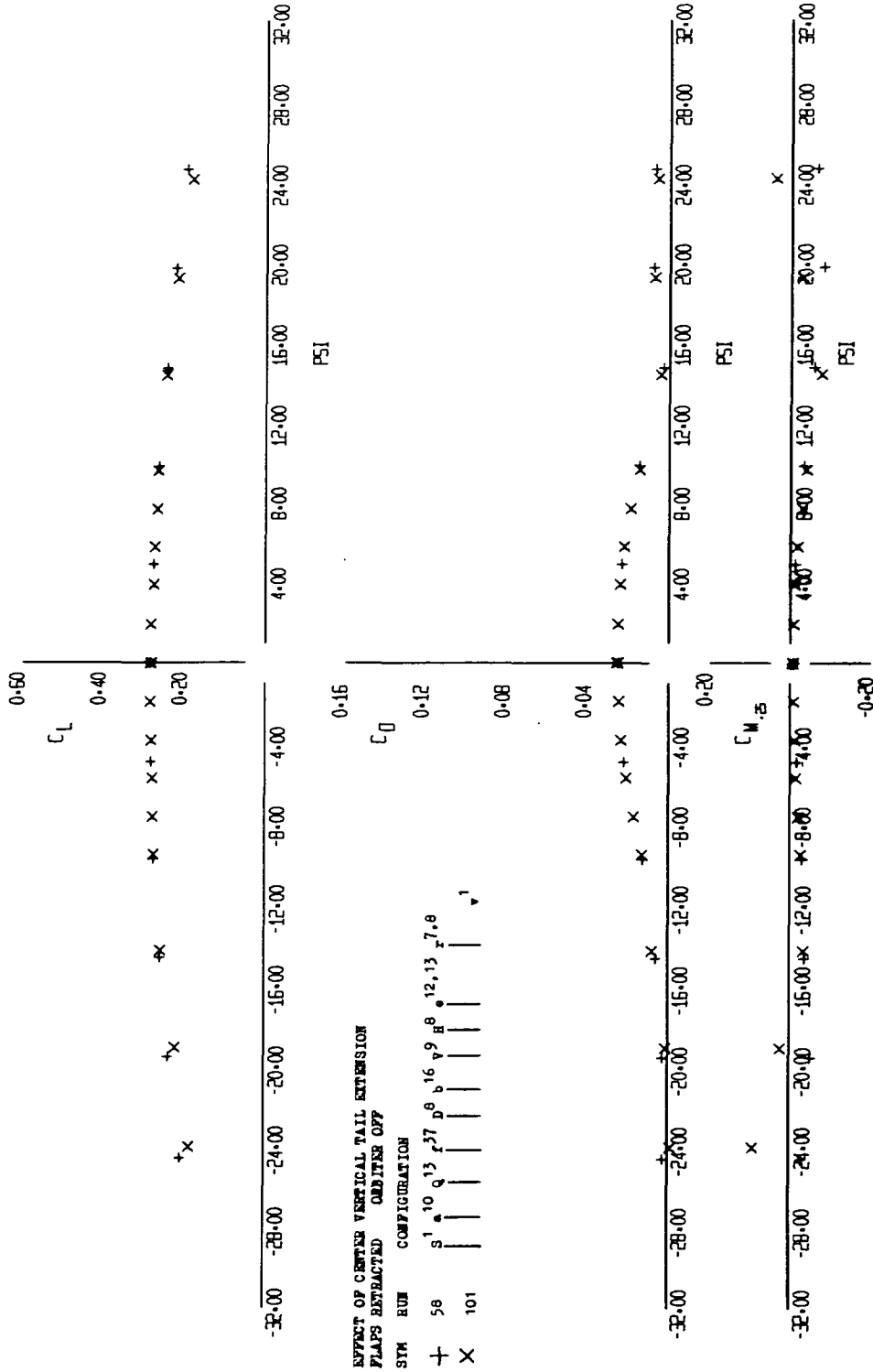
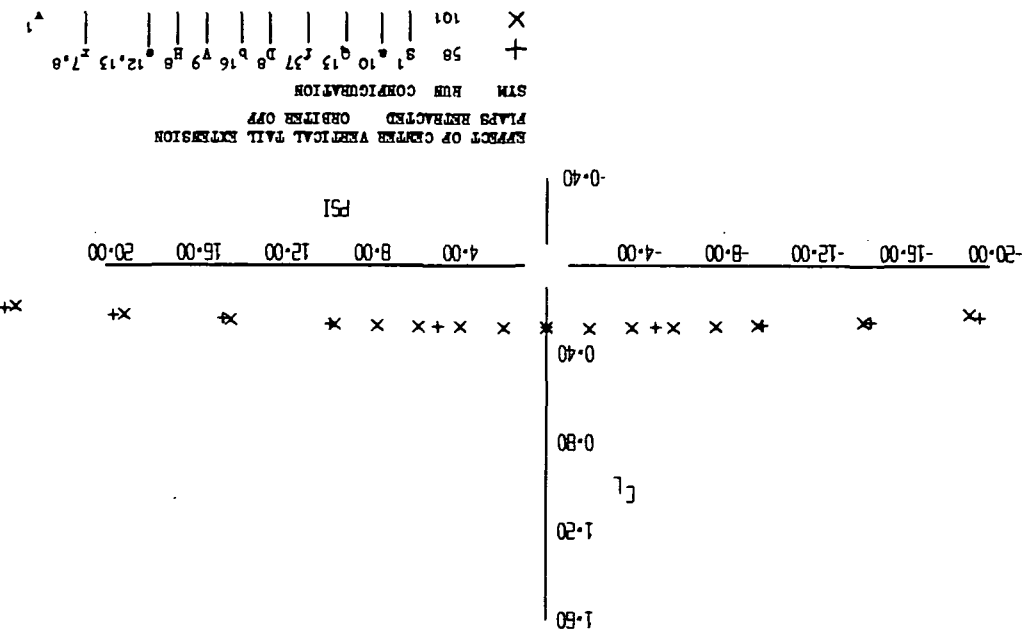
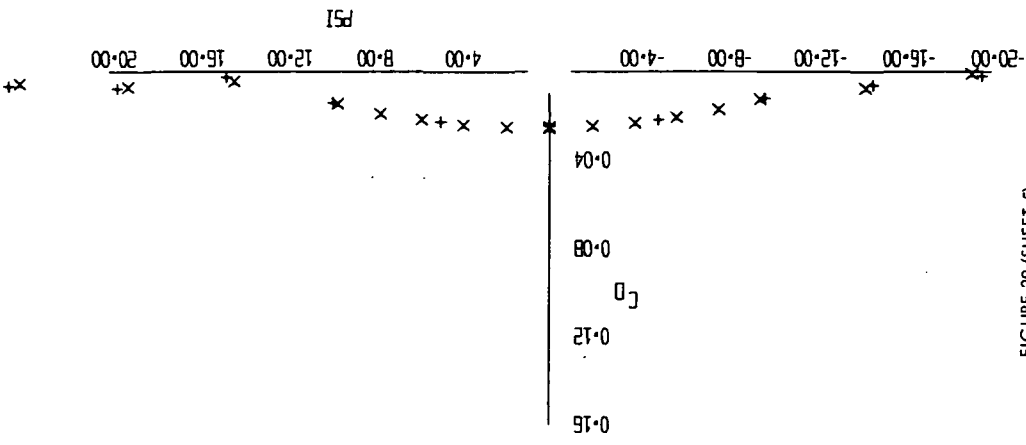
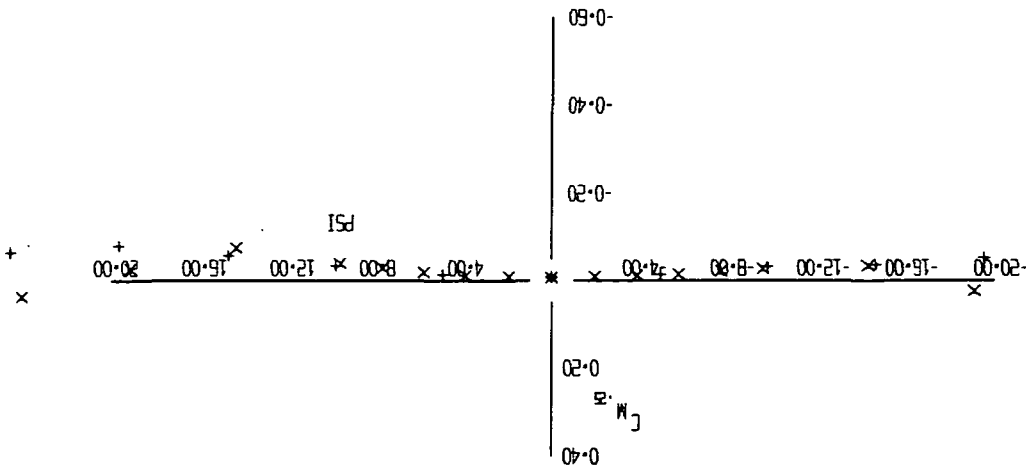


FIGURE 29 (SHEET 4)



X +
 101 58
 STM RUN CONFIGURATION
 FLAPS RETRACTED ORBITER OFF
 EFFECT OF CENTER VERTICAL TAIL EXTENSION

FIGURE 29 (SHEET 5)

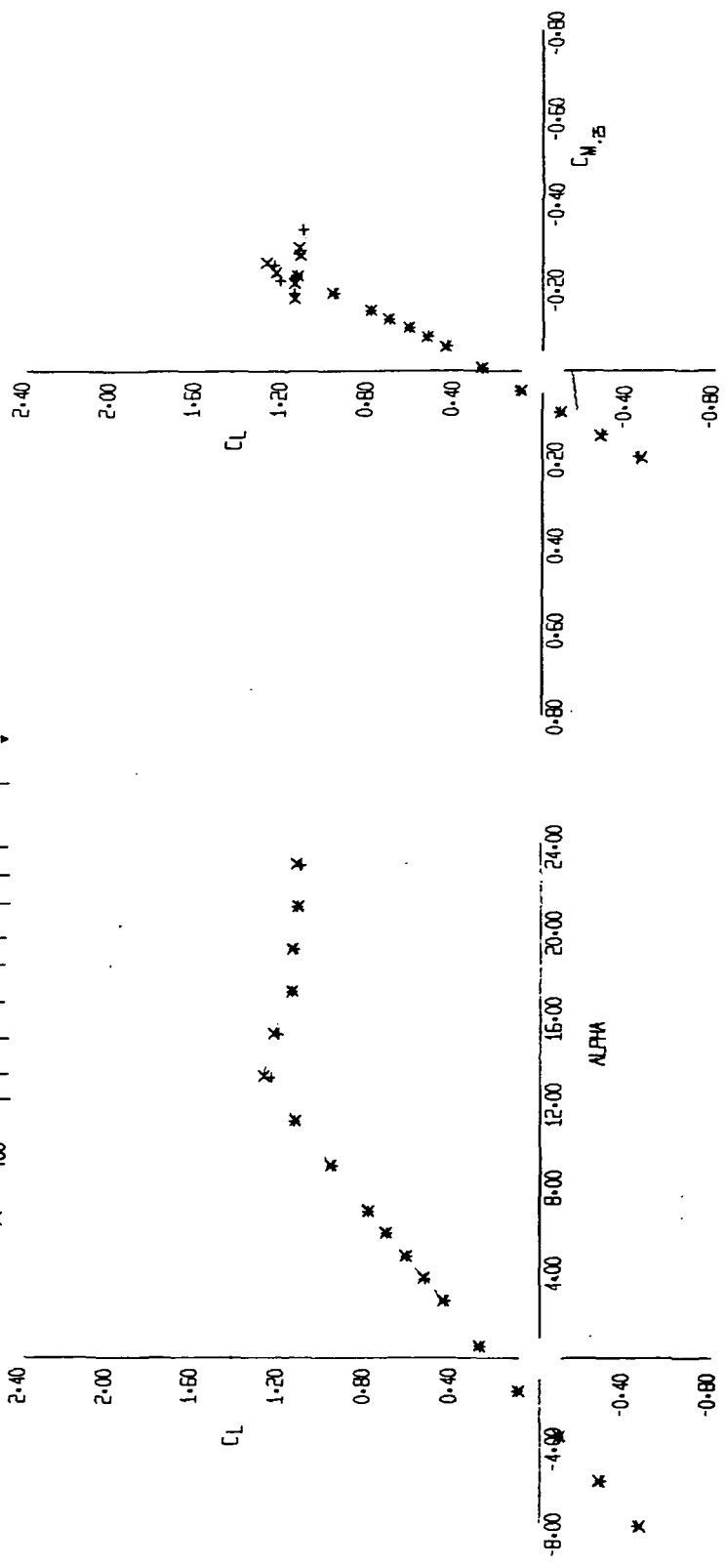
10-15-73

(9-1)

X +
101 58

EFFECT OF CENTER VERTICAL TAIL EXTENSION
FLAPS RETRACTED ORBITER OFF

STN	ROW	CONFIGURATION
+	57	s ¹ u ¹⁰ q ¹³ r ¹⁶ b ¹⁶ v ⁹ h ⁸ 12,13 z ⁷ ,8
x	100	



5 5
+ x

53-15-73

UP-18A

FIGURE 30 (SHEET 1)

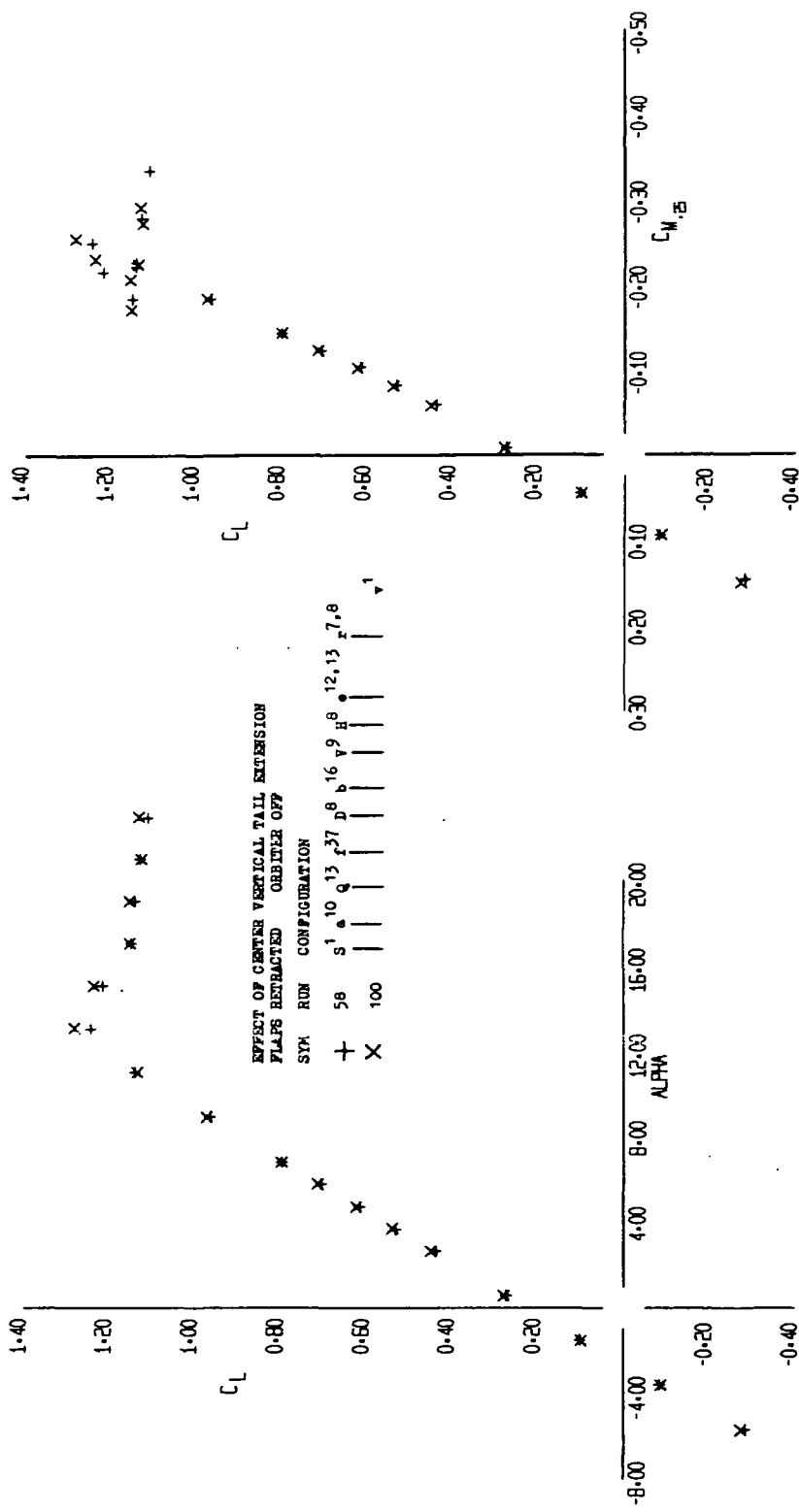


FIGURE 30 (SHEET 2)

59
x
+

10-15-73

UP-11E

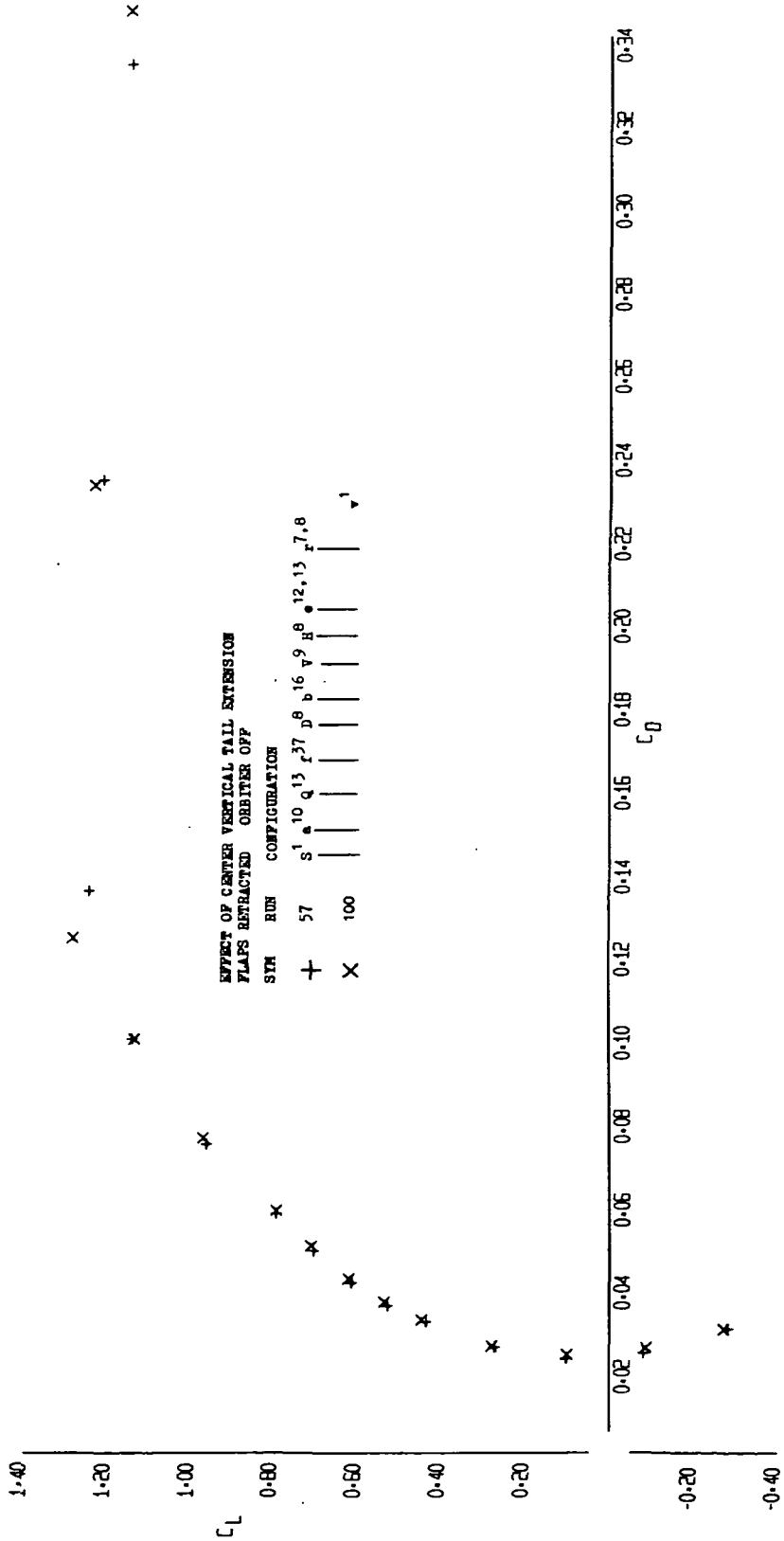


FIGURE 30 (SHEET 3)

EFFECT OF CENTER VERTICAL TAIL EXTENSION
FLAPS RETRACTED ORBITER OFF

SYM	RUN	CONFIGURATION
+	57	s ¹ a ¹⁰ q ¹³ r ²⁷ d ⁸ b ¹⁶ v ⁹ B ⁸ 12,13 r ^{7,8}
X	100	v ¹

+ 57
X 100

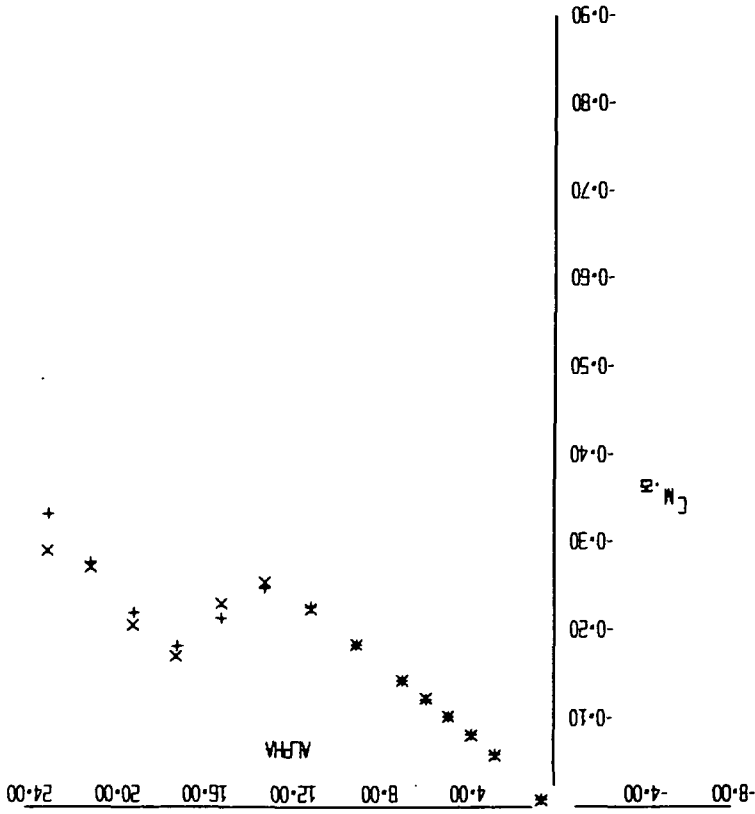


FIGURE 30 (SHEET 4)

10-15-73

LR-101

EFFECT OF CENTER VERTICAL TAIL EXTENSION
FLAPS RETRACTED ORBITER OFF

SYM RUN CONFIGURATION

+	57	s ¹	a ¹⁰	q ¹³	r ²⁷	b ⁸	v ⁹	H ⁸	12,13	z ^{7,8}	v ¹
X	100										

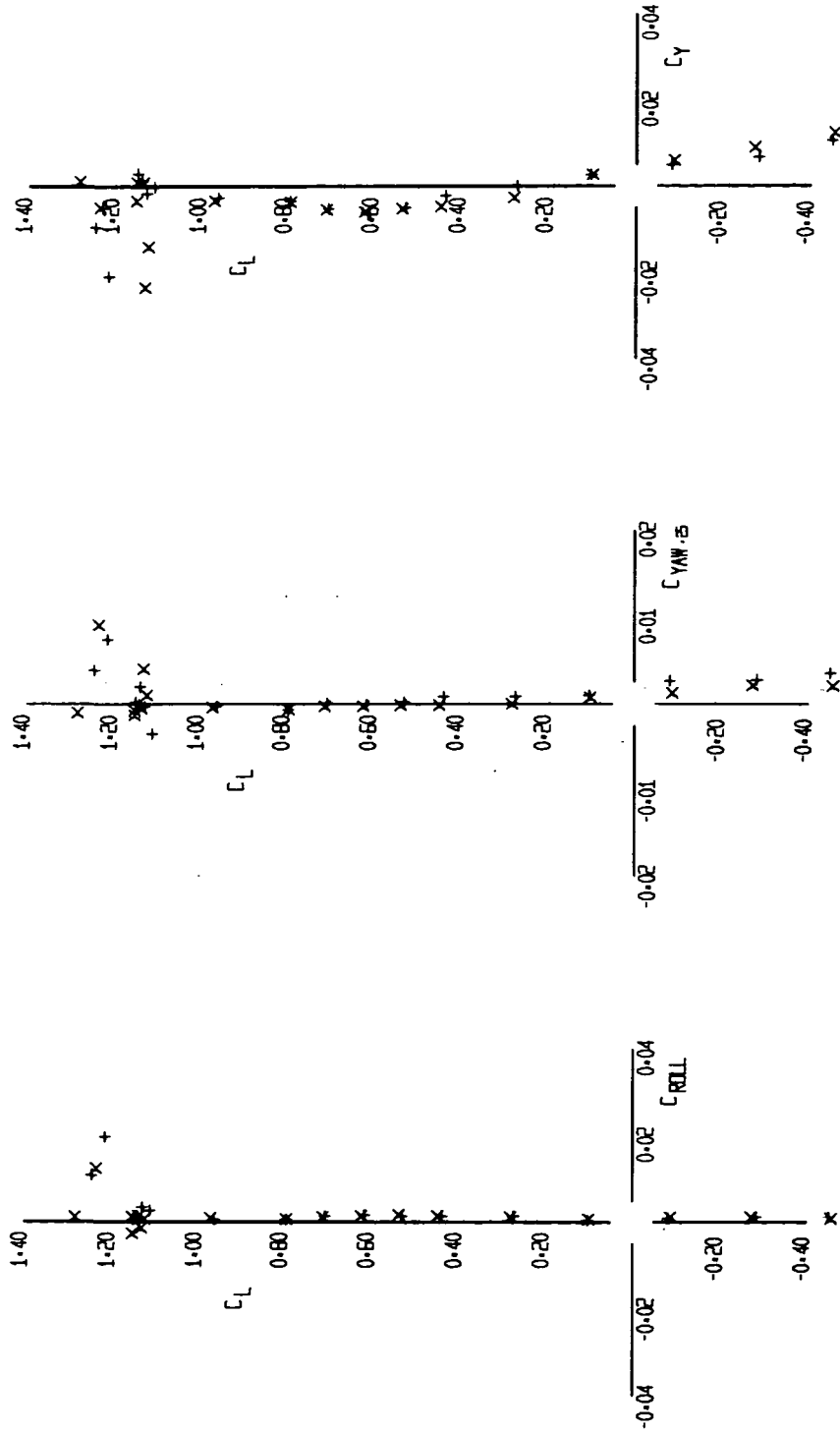


FIGURE 30 (SHEET 5)

57 + X

10-15-73

LR-353

x +

EFFECT OF VERTICAL TAIL ADDITION AT STABILIZER TIPS

SYM	RUN	CONFIGURATION
+	84	s ¹ a ¹⁰ q ¹³ r ³⁷ A ^{5P} b ⁸ 16.9 b ⁸ 12.13 r ^{7.8} v ¹
x	102	0.5 b ¹

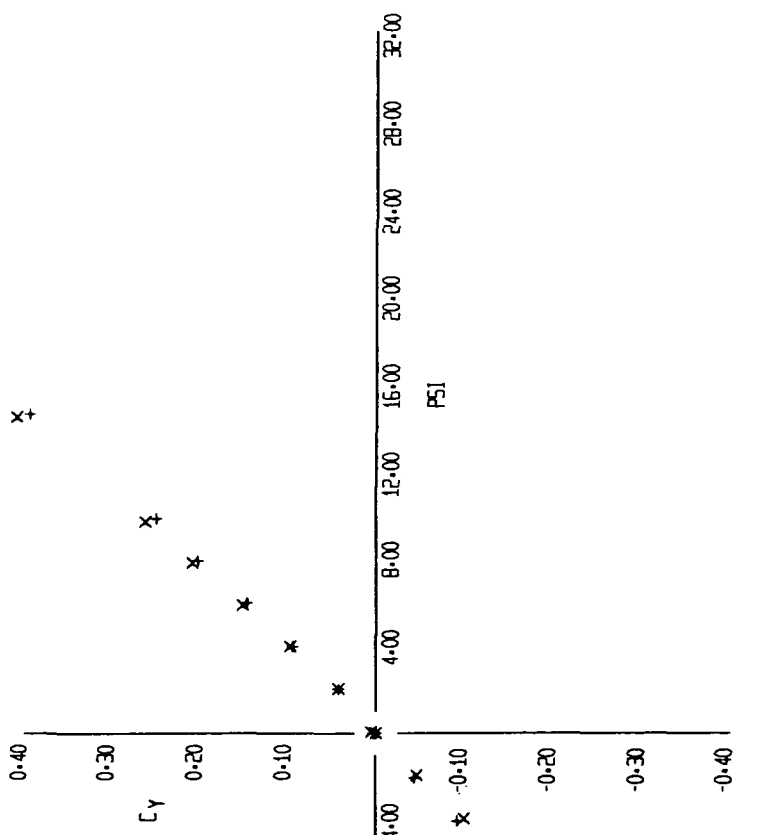


FIGURE 31 (SHEET 1)

LR-
+
10-15-73

11-6E

EFFECT OF VERTICAL TAIL ADDITION AT STABILIZER TIPS

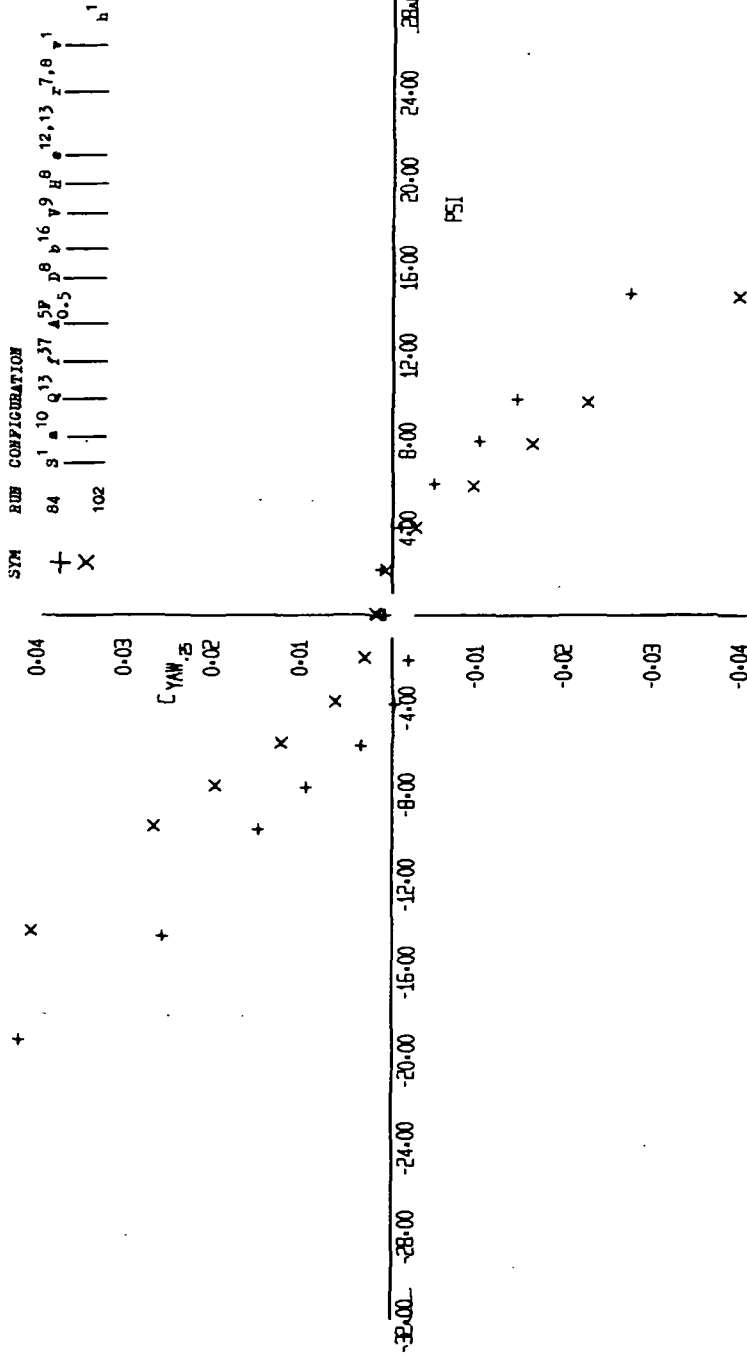


FIGURE 31 (SHEET 2)

LR
+

10-18-73

LR-60

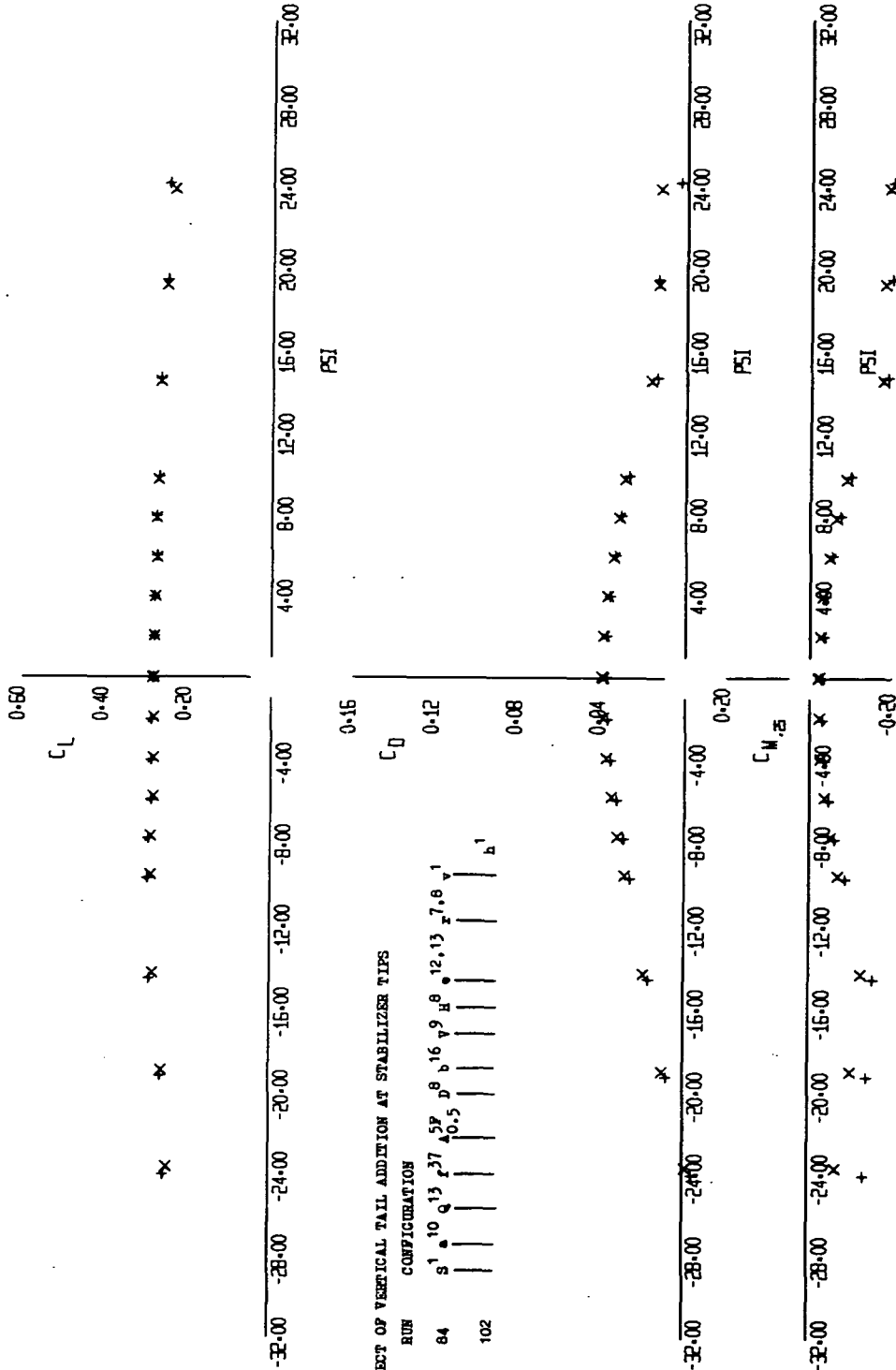


FIGURE 31 (SHEET 4)

U-15-73

U-1-61